IL
NUOVO CIMENTO
ORGANO DELLA SOCIETÀ ITALIANA DI FISICA
SOTTO GLI AUSPICI DEL CONSIGLIO NAZIONALE DELLE RICERCHE

VOL. II, N. 5 *Serie decima* 1° Novembre 1955

Zur quantentheoretischen Begründung der klassischen Physik.

II. – Statistische Mechanik und Thermodynamik.

H. KÜMMEL

Institut für theoretische Physik - Freie Universität Berlin

(ricevuto il 24 Giugno 1955)

Zusammenfassung. — In einer vorhergehenden Arbeit (1) des Verfassers war es gelungen, die makroskopischen Bewegungsgleichungen (als Differenzengleichungen zwischen makroskopischen Observablen) vollständig auf die Quantentheorie zurückzuführen. In der vorliegenden Untersuchung wird nun auch die Statistik und Thermodynamik irreversibler und reversibler Prozesse quantentheoretisch begründet. Es zeigt sich insbesondere, daß sich auch die klassischen Methoden (Phasenraumdichte, Geschwindigkeitsverteilungsfunktion) aus der Mikrostruktur ergeben. Damit ist der Anschluß der gesamten Makrophysik (bei nicht zu tiefer Temperatur) an die Mikrophysik hergestellt.

1. – Einleitung.

Im ersten Teil dieser Arbeit (1) wurde gezeigt, daß ein makroskopisches System ein klassisches mechanisches Verhalten zeigt, obwohl im Kleinen mikroskopische Gesetze gelten. Vorausgesetzt wurde lediglich, daß die Energieeigenwerte des Systems genügend dicht liegen und ungeordnet sind und daß die Wellenfunktionen eine hinreichend vernünftige Form haben. Die gefundenen Gesetze stimmten mit denen der klassischen Hydrodynamik der Form nach überein; wie es aber mit den eingehenden Parametern bzw. den der Thermodynamik zugehörigen Zustandsgrößen und Funktionen steht, blieb noch offen.

(1) H. KÜMMEL: *Nuovo Cimento*, **1**, 1057 (1955); im folgenden als I zitiert.

Der vorliegende II. Teil befaßt sich mit dieser Frage. Während bisher über den Dichteoperator nichts vorausgesetzt wurde (ausser daß er nicht gar zu unvernünftig ist) und die klassischen Gesetze sogar soweit wie möglich für den reinen Fall formuliert wurden, wird jetzt zu untersuchen sein, wie die lokale innere Energie eines Systems den Dichteoperator bestimmt. Da dies im wesentlichen mit der Frage nach der Geschwindigkeitsverteilungsfunktion übereinstimmt, wird eine solche definiert und gezeigt, daß für diese die klassische Bewegungsgleichung gilt. Da nach LUDWIG [2] ferner gesichert ist, daß ein solches physikalisches System einem Gleichgewicht zustrebt, ist auch der Ergodensatz der klassischen Physik bewiesen. Zusammen mit den über die Geschwindigkeitsverteilungsfunktion gefundenen Ergebnissen wird das den Anschluß an die Statistik der Gleichgewichts- und Nichtgleichgewichtszustände ermöglichen.

Dieses Programm wird in Kapitel 2 durchgeführt. Die Rechnungen sind sämtlich im Anhang zusammengefaßt. ((A.3) bedeutet: Anhang, § 3; A.(3) Anhang, Gleichung (3)).

2. – Statistische Mechanik.

2·1. *Energiedichte.* – Neben den in I abgeleiteten makroskopischen Erhaltungssätzen für Masse und Impuls muß auch noch ein Energieerhaltungssatz gelten, der die lokale innere Energie definiert. Es ist klar, daß der Quantentheorie der Begriff einer lokalen Energiedichte $E_g(\mathfrak{R}, t)$ eigentlich fremd ist. Es kann sich also nur um eine passende Definition handeln für eine makroskopische Observable, die man auf Grund der Form des Erhaltungssatzes und wegen $\int E_g(\mathfrak{R}, t)\,\mathrm{d}\mathfrak{R} = \varepsilon$ mit dem Namen der Energiedichte belegt.

Dieselben Prinzipien wie in I führen dann dazu (Rechnungen hierzu s. (A.1)), als Energiedichteoperator für die Gesamtenergiedichte

$$(1)\qquad \underset{mn}{E_g}(\mathfrak{R}, t) = \frac{N}{\Delta V}\int\limits_{\Delta V(\mathfrak{R})} \mathrm{d}r_1 \int\limits_{V} \mathrm{d}r_2 \ldots \mathrm{d}r_N \left\{ \frac{\hbar^2}{2m}\, \underset{1}{\psi^*_{m\nu}}\underset{1}{\psi_{n\nu}} + \left(\sum_{k>1} \frac{1}{2}\, V_{1k} + V_1^{(a)} \right) \psi^*_m \psi_n \right\},$$

und als Energiestromdichte

$$(2)\qquad \underset{mn}{S_\mu}(\mathfrak{R}, t) = \frac{N}{\Delta V}\,\frac{\hbar^2}{i2m}\int\limits_{\Delta V(\mathfrak{R})} \mathrm{d}r_1 \int\limits_{V} \mathrm{d}r_2 \ldots \mathrm{d}r_N \left\{ \frac{\hbar^2}{2m} \left(\underset{1}{\psi^*_{m\mu}}\underset{11}{\psi_{n\nu\nu}} - \underset{11}{\psi^*_{m\nu\nu}}\underset{1}{\psi_{n\mu}} \right) + \right.$$

$$\left. + \left(\frac{1}{2} \sum_{k>1} V_{1k} + V_1^{(a)} \right) \underset{mn}{j_\mu} \right\},$$

einzuführen, damit der Energieerhaltungssatz

$$(3)\qquad \frac{\partial \underset{mn}{E_g}}{\partial t} + \underset{mn}{S_{\mu\mu}} - \dot{R}_{mn} V_1^{(a)} = 0\,,$$

[2] G. LUDWIG: *Zeits. f. Phys.*, **135**. 483 (1953) und: *Grundlagen der Quantenmechanik* (Berlin, Göttingen, Heidelberg, (1954)), Kap. V.

gilt. Zerlegt man E_v in einen makroskopischen Anteil $(m/2)RV_\nu^2$ und die innere (thermische) Energie U:

$$E_v = \frac{m}{2} RV_\nu^2 + U , \tag{4}$$

so erhält man aus dem phänomenologischen Energiesatz unter Verwendung der hydrodynamischen Grundgleichungen (s. I Gl. (50)) als *Definitions*gleichung für den « Wärmestrom » $Q_\nu(\mathfrak{R}, t)$

$$Q_\nu(\mathfrak{R}, t) = S_\nu(\mathfrak{R}, t) - (\delta_{\nu\mu} E_v(\mathfrak{R}, t) - T_{\nu\mu}(\mathfrak{R}, t)) \frac{J_\mu(\mathfrak{R}, t)}{R(\mathfrak{R}, t)} , \tag{5}$$

(wir haben die Indizes mn weglassen müssen, weil $T_{\nu\mu}$ (s. I (51)) Produkte von makroskopischen Observablen enthält). Dagegen wird $U(\mathfrak{R}, t)$ durch (4) definiert.

Es ist uns so gelungen, zwei weitere makroskopische Größen in die Theorie einzuführen, die schon in die Thermodynamik gehören. Da bekanntlich bereits im Gleichgewicht kein Zustand vorliegt, wird man erst recht im allgemeiner vorliegenden Nichtgleichgewichtsfall alle makroskopischen Größen durch ihre mit einem Dichteoperator gebildeten Erwartungswerte ersetzen müssen. Es stellt sich die Aufgabe, diesen so zu bestimmen, daß eine vorliegende Verteilung $U(\mathfrak{R}, t)$ resultiert. Da U sich aus der ungeordneten kinetischen und aus der inneren potentiellen Energie zusammensetzt, muß eine Geschwindigkeitsverteilungsfunktion definiert werden, die wirklich statistischen Charakter hat, d.h. Aussagen über Orts- und Impulsverteilung zuläßt, die nicht vom Typus quantentheoretischer Aussagen sind.

2·2. *Geschwindigkeitsverteilungsfunktion.* – Es gibt nun tatsächlich eine mikroskopische Begründung einer solchen Geschwindigkeitsverteilungsfunktion. Es sei eine Dichtematrix in der Ortsdarstellung $w(\mathfrak{r}_i, \mathfrak{r}_i', t)$ vorgegeben. Deren durch

$$f(\mathfrak{v}_i, \mathfrak{s}, t) = \left(\frac{m}{2\pi\hbar}\right)^{3N} \int \mathrm{d}\bar{\mathfrak{r}}_i \exp\left[-\frac{i}{\hbar} m \sum_{i=1}^{N} \mathfrak{v}_i \bar{\mathfrak{r}}_i\right] w(\bar{\mathfrak{r}}_i, \mathfrak{s}_i; t) , \tag{6}$$

mit

$$\begin{aligned} \bar{\mathfrak{r}}_i &= \mathfrak{r}_i' - \mathfrak{r}_i \\ \mathfrak{s}_i &= \frac{1}{2}(\mathfrak{r}_i + \mathfrak{r}_i'); \qquad \int \mathrm{d}\bar{\mathfrak{r}}_i = \int \mathrm{d}\bar{\mathfrak{r}}_1 \ldots \mathrm{d}\bar{\mathfrak{r}}_N , \end{aligned} \tag{7}$$

definierte Fourierkomponenten sind schon von WIGNER [3] untersucht worden. Wir haben in I.4 darauf hingewiesen, daß diese keine Geschwindigkeitsver-

[3] E. WIGNER: *Phys. Rev.*, **40**, 749 (1932).

teilungsfunktionen darstellen. Der in I entwickelte Formalismus macht es aber leicht, hieraus die richtige Definition einer solchen Funktion zu finden. Untersucht man nämlich (s. (A.2)) den Erwartungswert des Stroms

$$J_\nu(\mathfrak{R}, t) = \int \mathrm{d}\mathfrak{r}_i \, \mathrm{d}\mathfrak{r}_i' (\mathfrak{r}_i | w | \mathfrak{r}_i')(\mathfrak{r}_i' | J_\nu(\mathfrak{R}) | \mathfrak{r}_i) , \tag{8}$$

mit dem in I definierten makroskopischen Stromdichteoperator, so findet man

$$J_\nu(\mathfrak{R}, t) = \frac{N}{\Delta V} \int\limits_{\Delta V(\mathfrak{R})} \mathrm{d}\mathfrak{r}_1 \int\limits_{V} \mathrm{d}\mathfrak{r}_2 \ldots \mathrm{d}\mathfrak{r}_N \int \mathrm{d}\mathfrak{v}_1 \ldots \mathrm{d}\mathfrak{v}_N \, f(\mathfrak{v}_i, \mathfrak{r}_i, t) \mathfrak{v}_\nu^{(1)} , \tag{9}$$

also eine Geschwindigkeitsverteilungsfunktion

$$f_1'(\mathfrak{v}_1, \mathfrak{R}, t) = \frac{N}{\Delta V} \int\limits_{\Delta V(\mathfrak{R})} \mathrm{d}\mathfrak{r}_1 \int \mathrm{d}\mathfrak{r}_2 \ldots \mathrm{d}\mathfrak{r}_N \int \mathrm{d}\mathfrak{v}_2 \ldots \mathrm{d}\mathfrak{v}_N f(\mathfrak{v}_1, \mathfrak{v}_2, \ldots, \mathfrak{v}_N, \mathfrak{r}_i, t) , \tag{10}$$

damit

$$J_\nu(\mathfrak{R}, t) = \int \mathrm{d}\mathfrak{v}_1 \mathfrak{v}_\nu^{(1)} f_1'(\mathfrak{v}_1, \mathfrak{R}, t) , \tag{11}$$

geschrieben werden kann.

Klassische Statistik erfordert jedoch Kenntnis von f_1' und die Gültigkeit der klassischen Bewegungsgleichungen. Auf Grund der Schrödingergleichung

$$\frac{\partial w}{\partial t}(\mathfrak{r}_i, \mathfrak{r}_i', t) + \frac{i}{\hbar}(H - H')w(\mathfrak{r}_i, \mathfrak{r}_i', t) = 0 , \tag{12}$$

kann man dann die Bewegungsgleichung von f_1' nach (10) und (6) untersuchen. Da man makroskopische Bewegungsgleichungen haben will, wird man also nur makroskopisch differenzieren (s. I). Hier zeigt sich nun (s. (A.2)) das einleuchtende Ergebnis: *Klassische Bewegungsgleichungen ergeben sich nur, wenn*

a) f_1' noch über ein « makroskopisches Intervall » im Geschwindigkeitsraum von der Größe $\Delta V(\mathfrak{V}) \geqslant \hbar^3/\Delta V(\mathfrak{R}) m^3$ integriert wird;

b) die Abweichungen vom Gleichgewicht klein sind, d.h. wenn w_{mn} in der Energiedarstellung nur « Fast-Diagonalelemente » enthält.

a) ist der Ausdruck der Gleichberechtigung von Ort und Geschwindigkeit und ist notwendig wegen der Unschärferelation. *b*) bedeutet, daß f_1 makroskopische Observable sein muß, um klassischen Bewegungsgleichungen zu gehorchen. Auf den Zusammenhang mit den Gleichgewichtsfragen werden wir noch zurückkommen.

Man hat also endgültig (mit $\Delta\tau = \Delta V(\mathfrak{R}) \cdot \Delta V(\mathfrak{B})$)

$$f_1(\mathfrak{B}, \mathfrak{R}, t) = \frac{1}{\Delta\tau} \int\limits_{\Delta\tau(\mathfrak{B},\mathfrak{R})} \mathrm{d}\mathfrak{v}_1 \, \mathrm{d}\mathfrak{r}_1 \int\limits_V \mathrm{d}\mathfrak{r}_2 \ldots \mathrm{d}\mathfrak{r}_N \int \mathrm{d}\mathfrak{v}_2 \ldots \mathrm{d}\mathfrak{v}_N f(\mathfrak{v}_i, \mathfrak{r}_i, t) \,, \tag{13}$$

statt (10). Es gilt, wie es sein muß,

$$\int \mathrm{d}\mathfrak{B} f_1(\mathfrak{B}, \mathfrak{R}, t) = R(\mathfrak{R}, t) \,, \tag{14}$$

$$\iint \mathrm{d}\mathfrak{B} \, \mathrm{d}\mathfrak{R} f_1(\mathfrak{B}, \mathfrak{R}, t) = N \,, \tag{15}$$

(makroskopische Integration).

f_1 erfüllt dann die klassische Bewegungsgleichung

$$\frac{\partial f_1}{\partial t}(\mathfrak{B}, \mathfrak{R}, t) = -\mathfrak{B}_\nu f_{1\,\nu}(\mathfrak{B}, \mathfrak{R}, t) + \frac{1}{m} \frac{\Delta f_1}{\Delta \mathfrak{B}_\nu}(\mathfrak{B}, \mathfrak{R}, t) V^{(a)}_\nu(\mathfrak{R}) + \tag{16}$$

$$+ \frac{1}{m} \int \mathrm{d}\mathfrak{B}_2 \mathrm{d}\mathfrak{R}_2 \frac{\Delta f_2}{\Delta \mathfrak{B}_\nu}(\mathfrak{B}, \mathfrak{B}_2, \mathfrak{R}, \mathfrak{R}_2) V_{1\nu}(\mathfrak{R} - \mathfrak{R}_2) \,,$$

wenn man durch

$$f_2(\mathfrak{B}_1, \mathfrak{B}_2, \mathfrak{R}_1, \mathfrak{R}_2, t) = \tag{17}$$

$$= \frac{N(N-1)}{\Delta\tau^2} \int\limits_{\Delta\tau(1)} \mathrm{d}\mathfrak{v}_1 \, \mathrm{d}\mathfrak{r}_1 \int\limits_{\Delta\tau(2)} \mathrm{d}\mathfrak{v}_2 \, \mathrm{d}\mathfrak{r}_2 \int\limits_{-\infty}^{+\infty} \mathrm{d}\mathfrak{v}_3 \ldots \mathrm{d}\mathfrak{v}_N \int\limits_V \mathrm{d}\mathfrak{r}_3 \ldots \mathrm{d}\mathfrak{r}_N f(\mathfrak{v}_i, \mathfrak{r}_i, t) \,,$$

die Geschwindigkeitsverteilungsfunktion für zwei Teilchen einführt.

Mit diesen Funktionen erhält man dann für die Stromdichte

$$J_\nu(\mathfrak{R}, t) = \int \mathrm{d}\mathfrak{B} \mathfrak{B}_\nu f_1(\mathfrak{B}, \mathfrak{R}, t) \,, \tag{18}$$

die kinetische Energiedichte

$$E_{kin}(\mathfrak{R}, t) = \frac{m}{2} \int \mathrm{d}\mathfrak{B} \mathfrak{B}^2 f_1(\mathfrak{B}, \mathfrak{R}, t) \,, \tag{19}$$

und die potentielle Energiedichte

$$E_{pot}(\mathfrak{R}, t) = \frac{1}{2} \int \mathrm{d}\mathfrak{B}_1 \, \mathrm{d}\mathfrak{B}_2 \, \mathrm{d}\mathfrak{R}_2 V_{12}(\mathfrak{R} - \mathfrak{R}_2) f_2(\mathfrak{B}_1, \mathfrak{B}_2, \mathfrak{R}, \mathfrak{R}_2, t) \,. \tag{20}$$

Als Dichte der inneren Energie hat man dann

$$U(\mathfrak{R}, t) = E_{kin}(\mathfrak{R}, t) + E_{pot}(\mathfrak{R}, t) - \frac{m}{2}\frac{J^2(\mathfrak{R}, t)}{R(\mathfrak{R}, t)}. \tag{21}$$

Ganz entsprechend lassen sich alle weiteren makroskopischen Größen ($T_{\nu\mu}$, S_μ, Q_ν) durch f_1 und f_2 ausdrücken. Im Gegensatz zum klassischen Verfahren muß man bei der Ableitung solcher Ausdrücke wie (18) bis (21) die Rechnungen jedesmal neu durchführen und sich überzeugen, daß die quantenmechanischen Operatoren sich gerade so auswirken, daß diese anschaulichen Resultate erhalten werden.

Es ist selbstverständlich, daß die Bewegungsgleichung (16) wieder die klassischen makroskopischen Bewegungsgleichungen für die Observablen liefert, die z.B. in I (42) und I (50) sowie in Gleichung (3) erhalten wurden.

2·3. *Phasenraumdichte.* – In enger Analogie zu dem bisherigen läßt sich eine Phasenraumdichte im ($\mathfrak{V}_i$, $\mathfrak{R}_i$)-Raum durch

$$f_N(\mathfrak{V}_i, \mathfrak{R}_i, t) = \frac{1}{(\Delta\tau)^N}\int\limits_{\Delta\tau_i} \mathrm{d}\mathfrak{v}_i\,\mathrm{d}\mathfrak{r}_i f(\mathfrak{v}_i, \mathfrak{r}_i, t)\,, \tag{22}$$

(integriert über die Zellen $\Delta\tau_i$ an den Stellen $\mathfrak{V}_i$, $\mathfrak{R}_i$) definieren. Die Bewegungsgleichung von f_N (nach denselben Prinzipien wie für f_1 abgeleitet) ist

$$\frac{\partial f_N}{\partial t}(\mathfrak{V}_i, \mathfrak{R}_i, t) + \sum_{i=1}^{N} \mathfrak{V}_\nu^{(i)} f_{N\,|\nu} - \frac{1}{m}\sum_{i=1}^{N}\left(V_{i\,|\nu}^{(a)}(\mathfrak{R}_l) + V_{i\,|\nu}(\mathfrak{R}_i - \mathfrak{R}_l)\right)\frac{\Delta f_N}{\Delta \mathfrak{V}_\nu^{(i)}}(\mathfrak{V}_i, \mathfrak{R}_i, t). \tag{23}$$

Führt man nun die Phasenraumdichte $\varrho(p, q)$ durch

$$\varrho(p_k, q_k, t) = f_N(\mathfrak{V}_i, \mathfrak{R}_i, t)\,, \tag{24}$$

mit $\mathfrak{V}_\nu^{(i)} \to 1/m\; p_k$, $\mathfrak{R}_\nu^{(i)} \to q_k$, $(k = 1 \ldots 3N)$ und $\int \mathrm{d}p\,\mathrm{d}q\varrho = 1$ ein, so wird

$$\frac{\mathrm{d}\varrho}{\mathrm{d}t} \equiv \frac{\partial \varrho}{\partial t} + \sum_{k=1}^{3N}\frac{\partial \varrho}{\mathrm{d}q_k}\dot{q}_k + \sum_{k=1}^{3N}\frac{\partial \varrho}{\partial p_k}\dot{p}_k = 0\,. \tag{25}$$

Dabei haben wir (p, q) *künstlich zeitabhängig* gemacht, indem wir *formal*

Hamilton'sche und Lagrange'sche Funktion durch

$$(26)\qquad \begin{cases} \widetilde{H} = \dfrac{1}{2m}\sum^{3N} p_k^2 + V^{(a)} + V\,, \\ \widetilde{L} = \dfrac{m}{2}\sum^{3N} \dot{q}_k^2 - V^{(a)} - V, \qquad p_k = \dfrac{\partial \widetilde{L}}{\partial \dot{q}_k}, \end{cases}$$

eingeführt haben und als Bewegungsgleichungen für p_k, q_k

$$\dot{p}_k = -\frac{\partial \widetilde{H}}{\partial q_k}, \quad \dot{q}_k = \frac{\partial \widetilde{H}}{\partial p_k},$$

ansetzten. p_k und q_k bleiben also für $V^{(a)} = 0$ immer auf der Energiefläche $\widetilde{H} = \varepsilon = \text{const}$. Die ursprünglich als Zahlen eingeführten Parameter $\mathfrak{B}_i$ und $\mathfrak{R}_i$ werden so durch zeitabhängige Größen ersetzt, (mit dem Wunsch natürlich, eine — wenn auch nur *formale* — Analogie zur klassischen Theorie zu erhalten) daß für ϱ die richtige Bewegungsgleichung resultiert. p und q sind so aneinander gekoppelt, daß der LIOUVILLE'sche Satz $\mathrm{d}q_k\mathrm{d}p_k = \text{const}$ gilt. Ursprünglich war letzterer wegen der Konstanz von $\mathrm{d}\mathfrak{B}_i\mathrm{d}\mathfrak{R}_i$ eine Trivialität und es war natürlich notwendig, die neuen Größen so zu wählen, daß die Invarianz des Volumenelementes im Phasenraum gewahrt bleibt.

Pauliprinzip: Wir wollen hierunter die Forderung der Symmetrie *oder* Antisymmetrie der ψ_n (Bose- bzw. Fermistatistik) verstehen. Die obigen Gleichungen sind alle mit den richtigen Wellenfunktionen abgeleitet, berücksichtigen also das Pauliprinzip in jedem Falle. Die Ausschließung oder Bevorzugung gewisser Gebiete im Phasenraum ist ein spezifisch quantentheoretischer Effekt, der die Bewegungs*gleichungen* nicht berührt. Bei der Lösung derselben hat man Anfangswerte für ϱ (oder f_1, f_2, f_N) einzusetzen; diese aber sind bei richtiger Berücksichtigung des Pauliprinzips nicht willkürlich wählbar. Das erkennt man schon daraus, daß z.B. f_N bzw. ϱ nach ihrer Definition (22), (24) und A.(19) invariant gegen Vertauschung der Teilchenkoordinaten und Impulse sind. Diese Eigenschaft spielt die Rolle einer *Nebenbedingung* für die Bewegunsggleichung und kann aus letzterer natürlich nicht entnommen werden.

Am Beispiel der Fermistatistik kann man dies leicht deutlich machen. Setzt man nämlich z.B. in f_2 $\mathfrak{R}_1 = \mathfrak{R}_2$ und $\mathfrak{B}_1 = \mathfrak{B}_2$ so verschwindet f_2, wie es sein muß:

$$(27)\qquad f_2(\mathfrak{B}, \mathfrak{B}, \mathfrak{R}, \mathfrak{R}, t) \equiv 0\,,$$

mit einer Genauigkeit, die der Orts- bzw. Geschwindigkeitsmeßgenauigkeit entspricht, d.h. z.B. mit $\Delta f_2 \sim (\Delta f_2/\Delta X_\nu)\Delta X_\nu$ (Ausführlicher: s. (A.3)).

Damit wissen wir jetzt, daß wir die klassische *Quanten*statistik [4] formal erhalten haben. Sie ist aber auch physikalisch realisiert: Dies ist dadurch gesichert, daß wir alle vorkommenden makroskopischen Größen A in völliger Analogie zu den Methoden der klassischen Statistik in der Form

$$A = \int a(p_k, q_k)\varrho(p_k, q_k)\,\mathrm{d}p_k\,\mathrm{d}q_k\,, \tag{28}$$

ausdrücken können und daß ferner diese A die klassischen Bewegungsgleichungen erfüllen. Beides zusammen gibt uns das Recht, von einer *Herleitung der Gesetze und Methoden der Gibbs'schen Statistik aus der Quantentheorie* zu sprechen. Die Quantenmechanik ist aber darüber hinaus in der Lage, Aussagen über Nicht-Gleichwichtszustände zu machen. Diesen wollen wir uns daher zuwenden.

2·4. *Das Erreichen des Gleichgewichts.* – Wir nehmen (entsprechend dem Gibbs'schen Standpunkt) an, daß wir eine sehr große Anzahl von Systemen haben, und treiben Statistik mit dieser Systemgesamtheit. Dann ist $\varrho\,\mathrm{d}p_k\,\mathrm{d}q_k$ die Zahl der Systeme an der durch (p_k, q_k) charakterisierten Stelle des $6N$-dimensionalen Phasenraums.

Ludwig [5,6] hat gezeigt, daß für den Erwartungswert eines makroskopischen Operators O gilt

$$\frac{1}{T}\int_0^T \mathrm{d}t\,(Erw(O) - \sum_n w_{nn}O_{nn})^2 \xrightarrow[T\to\infty]{} 0\,. \tag{29}$$

Im Mittel tragen also nur die Diagonalelemente (in der Energiedarstellung) von w und O bei. Wir können auch sagen: Der Gleichgewichtszustand ist durch

$$Erw(O) = \sum_n w_{nn}O_{nn}\,, \tag{30}$$

charakterisiert, und es ist gesichert, daß das Gleichgewicht *praktisch* erreicht wird. Bemerkenswert ist, daß also die Abweichungen vom Gleichgewicht umso größer sind, je größer $|\varepsilon_n - \varepsilon_m|$ in den Matrixelementen O_{nm} bzw. w_{nm} ist, je weiter man sich also von der Diagonale entfernt.

Wir haben oben gesehen, daß f_1 (und daher natürlich auch f_N) nur dann klassische Bewegungsgleichungen erfüllt, wenn f_1 beinahe diagonal ist: *Bei zu*

---

[4] *Quantenstatistik*, weil dem Pauliprinzip automatisch Rechnung getragen ist; natürlich könnte man auch die Boltzmannstatistik erhalten, wenn man an ψ_n keine Symmetrieforderung stellt.

[5] G. Ludwig: loc. cit.

[6] Ähnliche Überlegungen s. bei Van Kampen: *Physica*, **20**, 603 (1954).

großen Abweichungen wird es falsch, der Phasenraumdichte klassische Bewegungsgleichungen zuzuschreiben. Wegen $Erw(O) = \sum_{nm} O_{nm} w_{nm}$ geht allerdings ein solcher sehr von dem Gleichgewicht abweichender Dichteoperator nicht in die Theorie ein, denn es geht $O_{mn} \to 0$ für zu große $|\varepsilon_n - \varepsilon_m|$ (7). *Praktisch* können wir also immer die klassische Bewegungsgleichung der Phasenverteilungsfunktion annehmen (solange, wie die in I formulierten Voraussetzungen über ε_n und ψ_n erfüllt sind, also jedenfalls bei nicht zu niedriger Temperatur).

Kehren wir zur Diskussion der Gleichgewichtszustände zurück. Im Mittel können wir also mit den zeitunabhängigen Gliedern rechnen, d.h. so tun, als ob

$$\frac{\partial \varrho}{\partial t} = 0 = \sum_k \left(\frac{\partial \varrho}{\partial q_k} \dot{q}_k + \frac{\partial \varrho}{\partial p_k} \dot{p}_k \right), \tag{31}$$

wäre. Das bedeutet aber, daß ϱ nur von den $6N$ Konstanten der Bewegungsgleichung abhängen kann. Als eine davon können wir die Energie ε wählen. Man wird ferner annehmen, daß makroskopisch die Energie ε bekannt sei, also ϱ nur auf der Energieschale betrachten. In der klassischen Theorie steht man jetzt vor dem Problem der $6N - 1$ unbekannten Anfangswerte. Die Ergodenhypothese besagt dann, daß jede Verteilung ϱ in die auf der Energiefläche konstante Gleichgewichtsverteilung ϱ_0 « übergeht » (ein einzelnes System kommt im Laufe der Zeit jedem Punkt beliebig nahe, Zeitmittel = = Scharmittel). Das bedeutet, daß es auf diese Anfangswerte nicht ankommt.

Das Problem der $6N - 1$ Anfangswerte ist in der Quantentheorie nur ein Scheinproblem. Sie sind durch die Einführung der Zeitabhängigkeit von p_k und q_k erst künstlich hereingebracht worden, können also in der ursprünglichen Theorie nicht enthalten sein. Die Aussagenlogik der Quantenmechanik sorgt nämlich von selbst dafür, daß alle Stellen auf der Energiefläche im Gleichgewicht (d.h. für die Diagonalelemente der w-Matrix) gleichberechtigt sind. Bekannt ist ja die Energie des Systems mit nur *makroskopischer* Genauigkeit. Also sind nur alle die $w_{nm} \neq 0$, deren $(\varepsilon_n, \varepsilon_m)$ in einem Intervall $(\varepsilon, \varepsilon + \Delta\varepsilon)$ liegen. Betrachten wir nun alle w_{nn} mit solchen ε_n. Das System ist makroskopisch charakterisiert durch eine vorgegebene Verteilung zu Anfang mit einer Gesamtenergie, die auch den Endzustand charakterisiert. Zwischen den ε_n aus dem Intervall ist aber makroskopisch keine Unterscheidung möglich, weil zwischen zugehörigen O_{nn} nach Definition der makroskopischen Observablen eine solche nicht möglich ist; d.h. aber, es müssen alle w_{nn} gleich sein. Ferner wissen wir, daß die Schrödingergleichung kein Raumgebiet vor dem anderen auszeichnet

(7) Große Abweichungen vom Gleichgewicht können auch durch eine passende systematische Auswahl von Matrixelementen w_{nm} verursacht werden. Dann werden die klassischen Gesetze natürlich nicht ungültig.

(Invarianz gegen Translation und Drehungen), wenn wir von Randeffekten absehen. Daraus folgt, daß entweder die Wellenfunktion im Großen kein Raumgebiet auszeichnet (die gemittelte Dichte R_{nn} ist konstant) und daß überall die mittlere Geschwindigkeit verschwindet ($J_{nn} = 0$; an jeder Stelle kommen für jedes Teilchen alle mit dem Energiesatz verträglichen Geschwindigkeiten vor), oder daß mindestens $\sum_{\varepsilon_n < \Delta\varepsilon} R_{nn} = \text{const}$, $\sum_{\varepsilon_n < \Delta\varepsilon} J_{nn} = 0$ ist. Kürzer: die Quantenmechanik zeichnet keine Stelle der Energiefläche aus, weil die Bewegungsgleichung das nicht tut und weil eine makroskopische Unterscheidung zwischen den ε_n aus $(\varepsilon, \varepsilon + \Delta\varepsilon)$ nach Definition ausgeschlossen ist. Damit haben wir aber erkannt, daß die Quantentheorie dafür sorgt, daß

a) ein physikalisches System einem Gleichgewicht (mit konstanten Observablen) zustrebt (LUDWIG'scher Beweis des Ergodensatzes);

b) ein solches Gleichgewicht in der klassischen Formulierung durch eine auf der Energiefläche konstante Phasenraumdichte charakterisiert werden kann.

Damit ist nun klar, daß im Gleichgewicht $J_\nu(\mathfrak{R}, t) = 0$ und $R(\mathfrak{R}, t) = \text{const}$ ist. Irgendeinen Nicht-Gleichgewichtszustand können wir charakterisieren durch Angabe einer Funktion $f_N(\mathfrak{P}_i, \mathfrak{R}, t)$ oder (was meist auf dasselbe hinauskommt) $f_1(\mathfrak{P}, \mathfrak{R}, t)$. Damit stellt sich das Problem, zu einer solchen Funktion die richtige Dichtematrix aus den ψ_n und w_{nm} aufzubauen. Das erfordert aber eine genauere Kenntnis der Eigenfunktionen, ist also im allgemeinen ein zu schwieriges Problem. Wie man in einfachen Fällen vorgehen kann, ist in (A.3) angedeutet. Man muß aber damit rechnen, daß man nicht beliebige Funktionen f angeben kann (man kann ja auch experimentell nicht beliebige Anfangsbedingungen herstellen!), weil die Wellenfunktionen es nicht zulassen. Ein Beispiel dafür haben wir bei der Diskussion des Pauliprinzips erwähnt.

2·5. *Gültigkeitsbereich der Methode.* – In I war die Bewegungsgleichung

$$2m(\varepsilon_n - \sum_{i<k} V_{ik}) = \sum_i^N (W_{n|\nu})^2 , \tag{32}$$

für die Phasenfunktion W_n abgeleitet worden. Diese Gleichung zeigte, daß $V_{|\nu}$ als langsam veränderliche Größe angesehen werden muß, da $W_{n,\nu|\mu}$ als eine solche vorausgesetzt war. Wir konnten dies auch so formulieren: Die kinetische Energie muß groß sein gegenüber der potentiellen. Wir können aber leicht sehen, daß ein sehr steiles und hohes Abstoßungspotential ohne weiteres zulässig ist, solange die kinetische Energie genügend groß ist: Für $|\mathfrak{r}_i - \mathfrak{r}_k| \leqslant R_0$ ($\frac{1}{2}R_0 =$ Radius des abstoßenden Kernes) verschwindet nämlich die Wellenfunktion, was an allen bisherigen Überlegungen nichts ändert. Natürlich

muß man das Volumen $2\cdot(4\pi/3)R_0^3$ als zusätzliches «totes» Volumen in Rechnung stellen. Wenn die Wellenlänge klein ist gegenüber dem Radius R_0, werden zwei Teilchen bekanntlich nach klassischen Gesetzen aneinander gestreut. Das bedeutet, daß die Annahme der Form $\psi_n = A_n \exp[(i/\hbar)W_n]$ für die Wellenfunktion bis dicht an den Rand des abstoßenden Kernes berechtigt bleibt (Fig. 1). Wenn dagegen die Wellenlänge mit R_0 vergleichbar wird, spielen die Interferenzeffekte eine erhebliche Rolle und es gibt nicht zu vernachlässigende Gebiete, in denen ψ_n nicht mehr diese Form (mit *reellen* A_n und W_n) hat. Wie man dann vorgehen kann, wird in einer folgenden Arbeit behandelt werden (8). Diese Frage gehört sinngemäß bereits zu dem Problem der quantenmechanischen Korrekturen des klassischen Verhaltens und wird erst bei niedrigen Temperaturen aktuell.

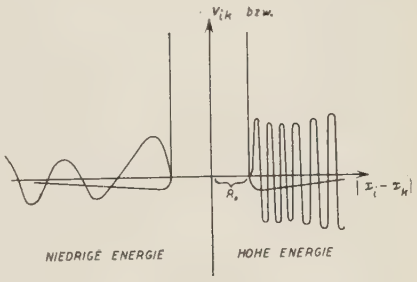

Fig. 1.

2·6. *Thermodynamik.* – Die Entropie lautet (bei unserer Normierung $\int \varrho \, \mathrm{d}p_k \mathrm{d}q_k = 1$)

$$S = -\int \mathrm{d}p_k \mathrm{d}q_k \, \varrho \log \varrho \,. \tag{33}$$

Da S am größten wird, wenn ϱ (bei vorgegebener Energie $\int \varrho \varepsilon' \, \mathrm{d}p_k \mathrm{d}q_k = \varepsilon$) konstant ist, und dort die Form $\varrho_0 = \exp[\lambda - (\varepsilon/\theta)]$ hat, da schließlich angenommen werden kann, daß das Phasenvolumen der Energieschale $\int\limits_{\Delta\varepsilon} \mathrm{d}p_k \mathrm{d}q_k$ mit ε' sehr stark anwächst, erhält man mit den üblichen Überlegungen

$$\lambda = \frac{F}{\theta} = -\log Z \quad \text{mit} \quad Z = \int \exp[-\varepsilon'/\theta]\sigma(\varepsilon')\,\mathrm{d}\varepsilon' = Sp(\exp[-H/\theta]) \,, \tag{34}$$

$$S = \log W \quad \text{mit} \quad W = \text{Zahl der Zustände in } (\varepsilon, \varepsilon + \Delta\varepsilon) \left(= \int\limits_{\Delta\varepsilon} \mathrm{d}p_k \mathrm{d}q_k\right), \tag{35}$$

für F (Freie Energie) und S im Gleichgewicht. Damit ist die Thermodynamik quasistatischer Prozesse gewonnen. Wegen $\varrho_0 \sim \exp[-\varepsilon/\theta]$ erhält man die Form $w_{nn} = \exp[-\varepsilon_n/\theta]/z$ für den klassischen Operator. Die Größen w_{nm} müssen dagegen, wie oben gezeigt, die Nichtgleichgewichtszustände bestimmen.

(8) H. Kümel: *Zeitz. f. Phys.*, im Erscheinen.

Ebenso ist natürlich die Onsager'sche irreversible Thermodynamik [9] enthalten, weil wir den Anschluß an die Methoden der klassischen Statistik gewonnen haben. Konsequenterweise wird man dazu die von PRIGOGINE [10] und anderen durchgeführten Rechnungen heranzuziehen haben, durch welche die «lineare» irreversible Thermodynamik auf der Grundlage der Statistik befriedigend begründet und abgegrenzt wurde. Wir können hier auf Einzelheiten nicht näher eingehen. Außerdem sind dazu die Untersuchungen von VAN KAMPEN [11] zu nennen, die in I bereits erwähnt wurden.

2·7. *Schluss.* – Die vorliegende Untersuchung zeigt, daß es gelungen ist, die klassische Physik vollständig quantentheoretisch zu begründen, und zwar hinsichtlich ihrer *Struktur* und *Methode*. An manchen nicht allgemein zu übersehenden Stellen kann dabei die Quantentheorie noch in die Makrophysik hineinwirken, (Beispiel: Das Pauliprinzip; es äußert sich ja z.B. bei der Metalltheorie in der Makrophysik), sodaß bei der Anwendung der klassischen Gesetze unter Umständen Vorsicht am Platze ist.

Ein solches Beispiel ist die Herleitung der Boltzmann'schen Stoßgleichung: Hier müssen die Symmetrieeigenschaften der ψ_n (und damit der f_1, f_2, f_N) berücksichtigt werden und gehen entscheidend in die Zeitveränderlichkeit ein, weil z.B. f_2 durch f_1 ausgedrückt wird. Bisher hat man immer diese quantentheoretischen Elemente gefühlsmäßig berücksichtigt. Das ist ein Verfahren, daß man in jedem einzelnen Fall exakt begründen kann (und muß), indem man die in der Verteilungsfunktion enthaltene Struktur untersucht.

Ein interessantes Problem wäre die Behandlung der *quantentheoretischen Korrektion* zum klassischen Verhalten. Bei tiefen Temperaturen wird man immer noch klassische Bewegungsgleichungen erwarten, dagegen wird statt des klassischen Wirkungsquerschnitts $4\pi R_0^2$ der quantentheoretische einzusetzen sein. (vgl. 2·5). In einer weiteren Arbeit soll das durchgeführt werden. Interessant wäre auch eine Begründung des statistischen Grundgesetzes $\dot{Q}_j = \sum_{j'} w_{jj'} Q_{j'}$ (j = Phasenzelle) auf der Grundlage der bisherigen Rechnungen. Dies würde eine einfachere Begründung der irreversiblen Thermodynamik ermöglichen [12].

Alle sog. «kinetischen Methoden» (wozu z.B. die Boltzmann'sche Stoßgleichung gehört) bergen übrigens noch eine Reihe von Problemen. Schon bei der klassischen Behandlung führt man dort ja Elemente ein, die die Zeitrichtung auszeichnen; man hat also keine allein klassisch-dynamische Begründung.

[9] S. R. DE GROOT: *Thermodynamics of irreversible processes* (Amsterdam, 1951).
[10] I. PRIGONINE: *Physica*, **15**, 272 (1949); dort weitere Literatur.
[11] N. G. VAN KAMPEN: loc. cit.
[12] N. G. VAN KAMPEN: loc. cit.

Aus der hier dargelegten Arbeit kann eine solche Methode daher offenbar nicht ohne weiteres gewonnen werden. Es ist eine *quantitativere Fassung des Ergodensatzes* notwendig. Diese wird im Zusammenhang mit den obigen Problemen geliefert werden [13].

* * *

Für Diskussionen zu den hier behandelten Fragen habe ich Herrn Professor LUDWIG wiederum sehr zu danken. Für Anregungen danke ich auch Herrn K. JUST und weiteren Mitarbeitern des Institutes.

ANHANG

1. – Energiedichte.

Als Energiedichte der makroskopischen Bewegung haben wir

A.(1) $$E_m(\mathfrak{R}, t) = \frac{m}{2}\frac{J_\nu^2}{R},$$

einzuführen (wir lassen die Energieindizes weg; wegen (I, 2.2) haben wir über alle $\hbar\omega = \varepsilon_m - \varepsilon_n$ zu integrieren und $\varepsilon = \frac{1}{2}(\varepsilon_m + \varepsilon_n)$ näherungsweise festzuhalten. Dann hat J_ν^2/R einen wohldefinierten Sinn). Der Energiesatz lautet auf Grund der Bewegungsgleichung I (50)

A.(2) $$\frac{\partial}{\partial t} E_m(\mathfrak{R}, t) = -\frac{J_\nu}{R} T_{\nu\mu}|_\mu - \frac{m}{2}\left(\frac{J_\nu^2 J_\mu}{R^2}\right)_{|\mu}.$$

Er ist nach den Ergebnissen von I mit dem klassischen identisch. Der phänomenologische Energiesatz für die thermische Energiedichte lautet:

$$R\frac{\mathrm{d}U}{\mathrm{d}t} - \frac{\mathrm{d}R}{\mathrm{d}t}U + RQ_\nu|_\nu - T_{\nu\mu}\left(\frac{J_\nu}{R}\right)_{|\mu} = 0,$$

bzw.

A.(3) $$\frac{\partial U}{\partial t} + \left(U\frac{J_\nu}{R} + Q_\nu\right)_{|\nu} - T_{\nu\mu}\left(\frac{J_\nu}{R}\right)_{|\mu} = 0.$$

---

[13] *Amm. b. d. Korrektur*: Inzwischen sind diese Probleme gelöst. vgl. H. KÜMMEL, *Zeits. Naturf.* (im Erscheinen) und *Zeits. für Physik* (im Erscheinen). Ausserdem hat sich gezeit, daß man sich von der Voraussetzung A.(12), die wegen der tatsächlich vorhandenen Entartung etwas bedenklich ist, befreien kann.

Dabei hat man durch Q_ν den Wärmestromvektor formal eingeführt. Mit (4). A.(2) und A.(3) folgt dann der phänomenologische Energiesatz für die Gesamtenergiedichte (ein äußeres Feld wollen wir nicht in Betracht ziehen)

A.(4) $$\frac{\partial E_g}{\partial t} + S_{\mu|\mu} = 0 ,$$

mit

A.(5) $$S_\mu(\mathfrak{R},t) = (\delta_{\nu\mu} E_g - T_{\nu\mu}) \frac{J_\nu}{R} + Q_\mu .$$

Wenn es uns gelingt, A.(4) quantentheoretisch zu gewinnen, haben wir durch A.(5) den phänomenologisch eingeführten Wärmestromvektor auf die Quantentheorie gegründet.

Die Gleichung A.(4) abzuleiten ist nun im Prinzip nach dem Muster der in I durchgeführten Rechnungen einfach. Nach der Feldtheorie des Elektrons ist nämlich die (mikroskopische) Energiedichte

$$e_g = + \frac{\hbar^2}{2m} \psi^*_{|\nu} \psi_{,\nu} + V \psi^* \psi ;$$

sie steht mit dem (mikroskopischen) Energiestrom

$$s_\mu = \frac{1}{i} \left(\frac{\hbar^2}{2m} \right)^2 [\psi^*_{|\mu} \psi_{|\nu|\nu} - \psi^*_{|\nu|\nu} \psi_{|\mu}] + \frac{1}{i} \frac{\hbar^2}{2m} V j_\mu = \frac{\hbar^2}{2m} [\dot{\psi}^* \psi_{|\mu} + \psi^*_{|\mu} \dot{\psi}] ,$$

in der Beziehung

$$\frac{\partial e_g}{\partial t} + s_{\mu|\mu} = 0 .$$

In Analogie hierzu werden wir [14] für E_g und S_μ die oben angegebenen Gleichungen (1) und (2) ansetzen. Schreibt man noch

A.(6) $$\psi_n = A_n \exp [(i/\hbar) W_r] ,$$

und benutzt die in I über A_n und W_n gemachten Voraussetzungen, so erhält man nach einiger Rechnung in derselben Weise wie dort die gesuchte Relation A.(4).

---

[14] Anders als in I normieren wir $(\psi_n, \psi_m) = \delta_{nm}$.

2. – Geschwindigkeitsverteilungsfunktion.

Der Erwartungswert der Stromdichte an der Stelle R ist definitionsgemäß

A.(7) $$J_\nu(\Re, t) = \sum_{nm} \int \mathrm{d}\mathfrak{r}_i \mathrm{d}\mathfrak{r}_i' (\mathfrak{r}_i | w_t | \mathfrak{r}_i') \psi_m(\mathfrak{r}_i') J_{mn}^\nu(\Re, 0) \psi_n^*(\mathfrak{r}_i) =$$

$$= N \frac{i\hbar}{2mAV} \int_{AV} \mathrm{d}\tilde{\mathfrak{r}}_1 \int \mathrm{d}\tilde{\mathfrak{r}}_i \int \mathrm{d}\mathfrak{r}_i \int \mathrm{d}\mathfrak{r}_i' (\mathfrak{r}_i | w_t | \mathfrak{r}_i') \cdot$$

$$\cdot \left\{ \delta(\tilde{\mathfrak{r}}_i - \mathfrak{r}_i) \frac{\partial}{\partial \tilde{\mathfrak{r}}_\nu^{(i)}} \delta(\mathfrak{r}_i' - \tilde{\mathfrak{r}}_i) - \delta(\mathfrak{r}_i' - \tilde{\mathfrak{r}}_i) \frac{\partial}{\partial \tilde{\mathfrak{r}}_\nu^{(i)}} \delta(\tilde{\mathfrak{r}}_i - \mathfrak{r}_i) \right\} =$$

$$= - N \frac{i\hbar}{2mAV} \int_{AV} \mathrm{d}\tilde{\mathfrak{r}}_1 \int \mathrm{d}\mathfrak{r}_1 \int \mathrm{d}\mathfrak{r}_i \, \delta(\tilde{\mathfrak{r}}_1 - \mathfrak{r}_1) \cdot$$

$$\cdot \left\{ \frac{\partial}{\partial \tilde{\mathfrak{r}}_\nu^{(i)}} (\mathfrak{r}_i | w_t | \tilde{\mathfrak{r}}_1 \mathfrak{r}_2 \dots \mathfrak{r}_N) - \frac{\partial}{\partial \mathfrak{r}_\nu^{(1)}} (\tilde{\mathfrak{r}}_1 \mathfrak{r}_2 \dots \mathfrak{r}_N | w_t | \mathfrak{r}_i) \right\} =$$

$$= \frac{N}{AV} \int_{AV} \mathrm{d}\tilde{\mathfrak{r}}_1 \int \mathrm{d}\mathfrak{r}_1 \dots \mathrm{d}\mathfrak{r}_N \delta(\tilde{\mathfrak{r}}_1 - \mathfrak{r}_1) \mathfrak{v}_\nu^{(1)} f(\mathfrak{v}_i, \mathfrak{r}_i, t) \exp\left[\frac{i}{\hbar} m \mathfrak{v}_1 (\mathfrak{r}_1 - \tilde{\mathfrak{r}}_1) \right].$$

Daraus folgt unmittelbar die Form (9) für $J_\nu(\Re, t)$ mit der durch (10) definierten Geschwindigkeitsverteilungsfunktion f_1'.

Wir untersuchen deren Bewegungsgleichung auf Grund von (12):

A.(8) $$\frac{\partial f_1'}{\partial t}(\mathfrak{v}_1, \Re, t) = \frac{N}{AV} \int_{AV} \mathrm{d}\bar{\mathfrak{s}}_1 \int \mathrm{d}\mathfrak{r}_i \int \mathrm{d}\mathfrak{v}_i \frac{\partial f}{\partial t}(\mathfrak{v}_l, \bar{\mathfrak{s}}_l, t),$$

$$\left(i = 2 \dots N, \; l = 1 \dots N; \quad \int \mathrm{d}\mathfrak{r}_i = \int \mathrm{d}\mathfrak{r}_2 \dots \mathrm{d}\mathfrak{r}_N \text{ u.s.w.} \right).$$

Nach (12) ist

$$\int \mathrm{d}\mathfrak{v}_l \left\{ \frac{\partial f}{\partial t}(\mathfrak{v}_l, \bar{\mathfrak{s}}_l, t) + \sum_{l=1}^{N} \mathfrak{v}_l \frac{\partial f}{\partial \bar{\mathfrak{s}}_l} + \right.$$

$$\left. - \frac{i}{\hbar} \left[V\left(\bar{\mathfrak{s}}_l - \frac{\bar{\mathfrak{r}}_l}{2} \right) - V\left(\bar{\mathfrak{s}}_l + \frac{\bar{\mathfrak{r}}_l}{2} \right) \right] f(\mathfrak{v}_l, \bar{\mathfrak{s}}_l, t) \right\} \cdot \exp\left[\frac{i}{\hbar} m \sum_l \mathfrak{v}_l \bar{\mathfrak{r}}_l \right] = 0 .$$

Mit $\exp\left[- (i/\hbar) m (\mathfrak{v}_1' \bar{\mathfrak{r}}_1 + \sum_{i=2}^{N} \mathfrak{v}_i' \bar{\mathfrak{r}}_i) \right]$ multipliziert, über $\mathfrak{r}_l$ integriert und in A.(8) eingesetzt:

A.(9) $$\frac{\partial f_1'}{\partial t}(\mathfrak{v}_1, \Re, t) = \frac{N}{AV} \int_{AV} \mathrm{d}\bar{\mathfrak{s}}_1 \int \mathrm{d}\bar{\mathfrak{s}}_i \int \mathrm{d}\mathfrak{v}_i \left\{ - \sum_{l=1}^{N} \mathfrak{v}_l \frac{\partial f}{\partial \bar{\mathfrak{s}}_l}(\mathfrak{v}_l, \bar{\mathfrak{s}}_l, t) - \right.$$

$$- \frac{i}{\hbar} \left(\frac{m_i}{2\pi\hbar} \right)^3 \int \mathrm{d}\mathfrak{v}_1' \int \mathrm{d}\bar{\mathfrak{r}}_1 \left[V\left(\bar{\mathfrak{s}}_1 - \frac{\bar{\mathfrak{r}}_1}{2}, \bar{\mathfrak{s}}_i \right) - V\left(\bar{\mathfrak{s}}_1 + \frac{\bar{\mathfrak{r}}_1}{2}, \bar{\mathfrak{s}}_i \right) \right] \cdot$$

$$\left. \cdot \exp\left[\frac{i}{\hbar} m (\mathfrak{v}_1' - \mathfrak{v}_1) \bar{\mathfrak{r}}_1 \right] f(\mathfrak{v}_1', \mathfrak{v}_i, \bar{\mathfrak{s}}_l, t) \right\}.$$

Der Anteil mit $\sum_{i=2}^{N} \mathfrak{v}_i(\partial f/\partial \mathfrak{s}_i)$ verschwindet, weil man ihn durch partielle Integration wegschaffen kann ([15]). Zunächst wollen wir das Glied $\mathfrak{v}_1(\partial f/\partial \mathfrak{s}_1)$ in eine makroskopische Differentiation umformen.

Dazu schreiben wir alles Wesentliche heraus, lassen im Augenblick das Pauliprinzip außeracht (um nicht soviel schreiben zu müssen) und verwenden unsere Form A.(6) für ψ_n:

$$\text{A.(10)} \qquad \frac{1}{\Delta V}\int_{\Delta V} d\mathfrak{s}_1 \int d\bar{\mathfrak{r}}_l \mathfrak{v}_\nu^{(1)} \exp\left[\frac{i}{\hbar} m \sum \mathfrak{v}_l \bar{\mathfrak{r}}_l\right] \frac{\partial}{\partial \mathfrak{r}_\nu^{(1)}} w(\bar{\mathfrak{r}}_l, \mathfrak{s}_l) =$$

$$= \sum_{nm} w_{nm} \int_{\Delta V} d\mathfrak{s}_1 \int d\bar{\mathfrak{r}}_l \mathfrak{v}_\nu^{(1)} \exp\left[\frac{i}{\hbar} m \sum \mathfrak{v}_l \bar{\mathfrak{r}}_l\right] \cdot$$

$$\cdot \frac{\partial}{\partial \mathfrak{s}_\nu^{(1)}} \left\{ A_n\left(\mathfrak{s}_l + \frac{\bar{\mathfrak{r}}_l}{2}\right) A_m\left(\mathfrak{s}_l - \frac{\bar{\mathfrak{r}}_l}{2}\right) \exp\left[\frac{i}{\hbar}\left(W_n\left(\mathfrak{s}_l + \frac{\bar{\mathfrak{r}}_l}{2}\right) - W_m\left(\mathfrak{s}_l - \frac{\bar{\mathfrak{r}}_l}{2}\right)\right)\right]\right\}.$$

Dabei haben wir

$$\text{A.(11)} \qquad w(\bar{\mathfrak{r}}_l, \mathfrak{s}_l) = \sum_{nm} w_{nm} \psi_n\left(\mathfrak{s}_l + \frac{\bar{\mathfrak{r}}_l}{2}\right) \psi_m^*\left(\mathfrak{s}_l - \frac{\bar{\mathfrak{r}}_l}{2}\right),$$

geschrieben. Nun wird $\bar{\mathfrak{r}}_1$ über den ganzen Raum integriert; daher kann man für W_n keine Näherungsannahme machen (vgl. I). Das geht erst, wenn man dafür sorgt, daß $\bar{\mathfrak{r}}_\nu^{(1)} \ll \Delta X_\nu$ bleibt. Wegen des Faktors $\exp[(i/\hbar)m\mathfrak{v}_1\bar{\mathfrak{r}}_l]$ läßt sich das erreichen, indem man $\mathfrak{v}_1$ *über ein Intervall* $\Delta \mathfrak{P}_\nu \gg \hbar/m\Delta X_\nu$ integriert. Dann wird

$$W_n\left(\mathfrak{r}_1 + \frac{\bar{\mathfrak{r}}_1}{2}, \ldots\right) - W_m\left(\mathfrak{r}_1 - \frac{\bar{\mathfrak{r}}_1}{2}, \ldots\right) \approx W_{nm}(\mathfrak{r}_1, \ldots) +$$

$$+ (W_{n|\nu}(\mathfrak{r}_1, \ldots) + W_{m|\nu}(\mathfrak{r}_1, \ldots)) \frac{\bar{\mathfrak{r}}_\nu^{(1)}}{2} + \frac{1}{2} W_{nm|\nu'\mu}(\mathfrak{r}_1, \ldots) \bar{\mathfrak{r}}_\nu^{(1)} \bar{\mathfrak{r}}_\mu^{(1)}.$$

(mit der Abkürzung $W_{nm} = W_n - W_m$).

Alle vorkommenden Größen sind langsam veränderlich, d.h. $\partial/\partial \mathfrak{s}_1$ läßt sich nach der in I entwickelten Methode als $\Delta/\Delta X_\nu$ schreiben. Dabei geht wesentlich ein, daß man die Gleichung I (28) also

$$\text{A.(12)} \qquad \frac{\Delta}{\Delta X_\nu} \int_{\Delta V(\mathfrak{R})} \exp\left[\frac{i}{\hbar} W_{nm}\right] d\mathfrak{r} = \frac{i}{\hbar} W_{nm|\nu} \int_{\Delta V(\mathfrak{R})} \exp\left[\frac{i}{\hbar} W_{nm}\right] d\mathfrak{r},$$

benutzen kann. Dies wiederum gilt nur unter der Voraussetzung $W_{nm|\nu}\Delta X_\nu \ll \hbar$; oder: Die Abweichungen vom Gleichgewicht dürfen nicht zu groß sein (vgl. I, 2·3).

([15]) An der Oberfläche muß ψ_n verschwinden; man drücke f durch die ψ_n aus, um obige Behauptung einzusehen.

Provisional Arrangements for 1956 Meeting of International Commission for Optics and accompanying Optical Symposium on "Frontiers in Physical Optics".

Sponsors: National Academy of Sciences-National Research Council of the USA, National Science Foundation of the U. S. A., American Academy of Arts and Sciences, International Union of Pure and Applied Phvsics, and International Commission for Optics.

Organizing Committee: The planning and conducting of the scientific meetings is the responsibility of the U. S. A. National Committee of the International Commission for Optics.
Further particulars can be obtained from Dr. S. S. Ballard, Visibility Laboratory, Scripps Institution of Oceanography, University of California, San Diego 52, California, U. S. A..

Date: Wednesday, 28th March - Tuesday, 3rd April, 1956.

Place: Cambridge, Massachusetts. Meetings will be held in the Faculty Club and the Kresge Auditorium and Little Theatre of the Massachusetts Institute of Technology.

Programme: One day will be allocated to the meeting of the International Optical Commission, with opportunity for a further meeting if necessary. Four days will be allocated to a symposium on « Frontiers in Physical Optics », with the following selected topics as the main subjects for discussion:

1. New phase contrast and interference microscopic and measuring devices.
2. Thin films and filters.
3. Meteorological optics.
4. Nuclear optics.

Per ulteriori notizie rivolgersi al Prof. PERUCCA - Politecnico di Torino.

In A.(9) steht schließlich noch das Glied mit dem Potential V; unter Weglassung von allem Nebensächlichen schreiben wir dafür ($\Delta\tau = \Delta V(\mathfrak{R})\Delta V(\mathfrak{V})$)

$$\frac{1}{\Delta\tau}\int_{\Delta\tau} d\mathfrak{v}_1\, d\mathfrak{s}_1 \int d\mathfrak{v}_1' \int d\bar{\mathfrak{r}}_1 \left[V\left(\mathfrak{s}_l - \frac{\bar{\mathfrak{r}}_l}{2}\right) - V\left(\mathfrak{s}_l + \frac{\bar{\mathfrak{r}}_l}{2}\right)\right] \exp\left[\frac{im}{\hbar}(\mathfrak{v}_1' - \mathfrak{v}_1)\bar{\mathfrak{r}}_1\right] f(\mathfrak{v}_1', \mathfrak{v}_l, \mathfrak{s}_l, t).$$

Dabei haben wir die Integration über $\mathfrak{v}_1$ bereits hingeschrieben. Wieder können wir nach $\bar{\mathfrak{r}}_1$ entwickeln, weil $|\bar{\mathfrak{r}}_1|$ klein genug bleibt:

$$\text{A.(13)} \quad \frac{1}{\Delta\tau}\left(\frac{m}{2\pi\hbar}\right)^3 \int_{\Delta\tau} d\mathfrak{v}_1\, d\mathfrak{s}_1 \int d\mathfrak{v}_1' \int d\bar{\mathfrak{r}}_1 V_{|\nu}(\mathfrak{s}_1, \mathfrak{s}_l)\bar{\mathfrak{r}}_\nu^{(1)} \exp\left[\frac{i}{\hbar} m(\mathfrak{v}_1' - \mathfrak{v}_1)\bar{\mathfrak{r}}_1\right] f(\mathfrak{v}_1', \mathfrak{v}_l, \mathfrak{s}_l, t) =$$

$$= \frac{1}{\Delta\tau}\left(\frac{m}{2\pi\hbar}\right)^{3(N+1)} \frac{i\hbar}{m} \int d\mathfrak{v}_1\, d\mathfrak{s}_1 \int d\mathfrak{v}_1' \int d\bar{\mathfrak{r}}_1 V_{|\nu}(\mathfrak{s}_1, \mathfrak{s}_l)\bar{\mathfrak{r}}_\nu^{(1)} \int d\bar{\bar{\mathfrak{r}}}_1 \cdot$$

$$\cdot \exp\left[\frac{i}{\hbar} m[(\mathfrak{v}_1' - \mathfrak{v}_1)\bar{\mathfrak{r}}_1 - \mathfrak{v}_1'\bar{\bar{\mathfrak{r}}}_1 - \sum_{i=2}^{N} \mathfrak{v}_i\bar{\bar{\mathfrak{r}}}_i]\right] w(\bar{\bar{\mathfrak{r}}}_l, \mathfrak{s}_l, t) =$$

$$= \frac{1}{\Delta\tau}\frac{i\hbar}{m}\int_{\Delta\tau} d\mathfrak{v}_1\, d\mathfrak{s}_1\, V_{|\nu}(\mathfrak{s}_1, \mathfrak{s}_l)\frac{\partial}{\partial\mathfrak{v}_\nu^{(1)}} f(\mathfrak{v}_1, \mathfrak{v}_l, \mathfrak{s}_l, t).$$

Wir vesuchen nun, auch $\partial/\partial\mathfrak{v}_\nu^{(1)}$ als makroskopische Differentiation zu schreiben. Dazu drücken wir f wieder durch die ψ_n aus; so wird aus A.(13)

$$\text{A.(14)} \quad \frac{i\hbar}{m}\frac{1}{\Delta\tau}\left(\frac{m}{2\pi\hbar}\right)^{3N} \int_{\Delta\tau} d\mathfrak{v}_1\, d\mathfrak{s}_1 \int d\bar{\mathfrak{r}}_1 V_{|\nu}(\mathfrak{s}_1, \mathfrak{s}_l) \cdot$$

$$\cdot \frac{\partial}{\partial\mathfrak{v}_\nu^{(1)}}\left\{\exp\left[-\frac{i}{\hbar} m \sum_{l=1}^{N} \mathfrak{v}_l\bar{\mathfrak{r}}_l\right] \sum_{mn} w_{nm} A_n\left(\mathfrak{s}_l + \frac{\bar{\mathfrak{r}}_l}{2}\right) A_m\left(\mathfrak{s}_l - \frac{\bar{\mathfrak{r}}_l}{2}\right) \cdot \right.$$

$$\left. \cdot \exp\left[\frac{i}{\hbar}\left(W_n\left(\mathfrak{s}_l + \frac{\bar{\mathfrak{r}}_l}{2}\right) - W_m\left(\mathfrak{s}_l - \frac{\bar{\mathfrak{r}}_l}{2}\right)\right)\right]\right\}.$$

$V_{|\nu}$ ist in unserer Näherung klein von erster Ordnung (s. (32) bzw. I (4a) und die dort anschließende Diskussion der Näherungsannahmen). Wir können daher A_n (als Funktion von $\bar{\mathfrak{r}}_1$) als konstant annehmen, da außerdem wegen der Integration über $\mathfrak{v}_1$ für genügende Kleinheit von $|\bar{\mathfrak{V}}_\nu|$ gesorgt wird; aus dem gleichen Grunde sind auch die $W_{n|\nu}$ (und erst recht höhere Ableitungen) praktisch von $\bar{\mathfrak{r}}_1$ unabhängig. Dann wird aus A.(14):

$$\text{A.(15)} \quad \frac{i\hbar}{\Delta\tau m}\left(\frac{m}{2\pi\hbar}\right)^{3N} \int_{\Delta\tau} d\mathfrak{v}_1\, d\mathfrak{s}_1 V_{|\nu}(\mathfrak{s}_1, \mathfrak{s}_l) \frac{\partial}{\partial\mathfrak{v}_\nu^{(1)}} \sum_{nm} w_{nm} A_n(\mathfrak{s}_l) A_m(\mathfrak{s}_l) \exp\left[\frac{i}{\hbar} W_{nm}(\mathfrak{s}_l)\right] \cdot$$

$$\cdot \int_{V} d\bar{\mathfrak{r}}_l \exp\left[\frac{i}{\hbar}\left(\frac{1}{2} W_{n\lambda}(\mathfrak{s}_1) + \frac{1}{2} W_{m|\lambda}(\mathfrak{s}_1) - m\mathfrak{v}_1\right)\bar{\mathfrak{r}}_\lambda^{(1)}\right] \exp\left[-\frac{i}{\hbar} m \sum_{i=2}^{N} \mathfrak{v}_i\bar{\mathfrak{r}}_i\right] =$$

$$= \frac{ih}{\Delta\tau m}\left(\frac{m}{2\pi\hbar}\right)^{3N}(2\pi\hbar)^3\int_{\Delta\tau} d\mathfrak{v}_1\, d\mathfrak{s}_1 V_{|\nu}(\mathfrak{s}_1, \mathfrak{s}_i)\cdot$$

$$\cdot\exp\left[-\frac{i}{\hbar}\, m\sum_i \mathfrak{v}_i\bar{\mathfrak{r}}_i\right]\frac{\partial}{\partial\mathfrak{v}_\nu^{(1)}}\sum_{nm}{}' w_{nm}A_nA_m\exp\left[\frac{i}{\hbar}W_{nm}\right],$$

wobei die Summe über alle ε_n, ε_m zu erstrecken ist, für die

A.(16) $$\tfrac{1}{2}\left(W_{n|\lambda}(\mathfrak{s}_1) + W_{m|\lambda}(\mathfrak{s}_1)\right) = m\mathfrak{V}_1,$$

gilt. Wenn es immer sehr viel benachbarte Energieterme ε_n und ε_m gibt, für die A.(16) erfüllbar ist (was nach den Voraussetzungen über die Terme gesichert ist) ([16]), wirkt $\partial/\partial\mathfrak{v}_1$ auf eine in $\mathfrak{v}_1$ langsam veränderliche Funktion, sodaß wir stattdessen $\Delta/\Delta\mathfrak{V}_\nu$ schreiben können. Damit erhalten wir für A.(13)

A.(17) $$\frac{ih}{m\Delta\tau}\frac{\Delta}{\Delta\mathfrak{V}_\nu}\int_{\Delta\tau(\mathfrak{V},\mathfrak{R})} d\mathfrak{v}_1\, d\mathfrak{s}_1\left(V^{(a)}_{|\nu} + \sum_{i>1} V_{|\nu}(\mathfrak{s}_1 - \mathfrak{s}_i)\right)f(\mathfrak{v}_i, \mathfrak{s}_i, t),$$

wenn wir ein äußeres Feld $V^{(a)}$ neben dem inneren Feld $\sum V_{ik}$ einführen. $V^{(a)}$ wird man innerhalb ΔX als langsam veränderlich fordern; $V_{|\nu}$ ist es nach unseren Näherungsannahmen. Setzt man nun A.(17) in die Bewegungsgleichung A.(9) ein, so folgt:

A.(18) $$\frac{\partial f_1}{\partial t}(\mathfrak{V}, \mathfrak{R}, t) = -\mathfrak{V}_\nu f_{1|\nu}(\mathfrak{V}, \mathfrak{R}, t) - \frac{1}{m}\frac{\Delta}{\Delta\mathfrak{V}_\nu} f_1(\mathfrak{V}, \mathfrak{R}, t)V^{(a)}_{|\nu}(\mathfrak{R}) +$$

$$+ \frac{1}{m}\int d\mathfrak{v}_i\int d\mathfrak{s}_i\,\frac{\Delta}{\Delta\mathfrak{V}_\nu}\int_{\Delta\tau(\mathfrak{V},\mathfrak{R})} d\mathfrak{v}_1\, d\mathfrak{s}_1 f(\mathfrak{v}_i, \mathfrak{s}_i, t)\sum_{i>1} V_{|\nu}(\mathfrak{s}_1 - \mathfrak{s}_i).$$

Wenn alle Teilchen gleich sind, sind alle $V(\mathfrak{s}_1 - \mathfrak{s}_i)$ die gleichen Funktionen. Ferner ist wegen des Pauliprinzips ([17]) (s. unten, (A.3)) f symmetrisch gegen Vertauschung der Teilchenkoordinaten, sodaß das letzte Glied von A.(18) $N-1$ mal dasselbe ergibt. Definiert man daher f_2 nach (17), so resultiert unmittelbar die gesuchte Bewegungsgleichung (16).

Die Gleichungen (19) und (20) für E_{kin} und E_{pot} sind leicht zu beweisen die erste nach demselben Verfahren wie am Anfang dieses Paragraphen, die zweite folgt fast unmittelbar aus der Definition der Energiedichte. Wir übergehen hier diese Rechnungen.

([16]) Natürlich ist auch $w_{nm} \approx w_{n'm'}$ für solche benachbarten Zustände notwendig. Dies ist erfüllt, solange die Zustände mit nur *makroskopischer Meßgenauigkeit* fest gelegt werden können. vgl. S 9.

([17]) Bei der Ableitung der Bewegungsgleichungen war eine Berücksichtigung desselben bis jetzt nicht notwending.

Zur Prüfung der Normierung berechnen wir noch

$$\int \mathrm{d}\mathfrak{B} f_1(\mathfrak{B}, \mathfrak{R}, t) = \frac{N}{\Delta V} \int_{\Delta V} \mathrm{d}\mathfrak{s}_1 \int \mathrm{d}\mathfrak{v}_1 \int \mathrm{d}\mathfrak{s}_1 f(\mathfrak{v}_1, \mathfrak{s}_1, t) =$$

$$= \frac{N}{\Delta V} \int_{\Delta V} \mathrm{d}\mathfrak{s}_1 \int \mathrm{d}\mathfrak{s}_1 (\mathfrak{s}_1, w, \mathfrak{s}_1) = \sum_{nm} \frac{N}{\Delta V} \int_{\Delta V} \mathrm{d}\mathfrak{s}_1 \int \mathrm{d}\mathfrak{s}_1 \psi_n(\mathfrak{s}_1) w_{nm} \psi^*_m(\mathfrak{s}_1) = R(\mathfrak{R}, t);$$

die swar zu zeigen. $\int f_1(\mathfrak{B}, \mathfrak{R}, t)\, \mathfrak{B}\, \mathrm{d}\mathfrak{R} = N$ ist dann eine selbstverständliche Folge.

3. – Eigenschaften der Funktionen f_1 f_2 f_N und ϱ.

Aus der Form

A.(19) $$f_N(\mathfrak{B}_l, \mathfrak{R}_l, t) = \frac{1}{N!} \left(\frac{m}{2\pi\hbar}\right)^{3N} \int_{\Delta \mathfrak{r}_l} \mathrm{d}\mathfrak{v}_l \, \mathrm{d}\mathfrak{r}_l \int \mathrm{d}\bar{\mathfrak{r}}_l \sum_m w_{nm} \exp\left[-\frac{i}{\hbar} \sum_{l=1}^{N} m \mathfrak{v}_l \bar{\mathfrak{r}}_l\right] \cdot$$

$$\cdot \sum_{pp'} (\pm 1)^{p+p'} A^p_n \left(\mathfrak{r}_l + \frac{\bar{\mathfrak{r}}_l}{2}\right) A^{p'}_n \left(\mathfrak{r}_l - \frac{\bar{\mathfrak{r}}_l}{2}\right) \exp\left[\frac{i}{\hbar}\left(W^p_n\left(\mathfrak{r}_l + \frac{\bar{\mathfrak{r}}_l}{2}\right) - W^{p'}_m\left(\mathfrak{r}_l - \frac{\bar{\mathfrak{r}}_l}{2}\right)\right)\right],$$

(p, p' = Permutation; $(\pm 1)^{p+p'}$, je nachdem ob Bose- oder Fermistatistik) leitet man leicht die Gleichung

A.(20) $$f_N(\mathfrak{B}_l, \mathfrak{R}_l, t) \approx \frac{1}{\Delta V^N} \int_{\Delta \mathfrak{r}_l} \mathrm{d}\mathfrak{r}_l \sum_{pp'}{}' (\pm 1)^{p+p'} \sum_{mn}{}' w_{nm} \psi^p_n(\mathfrak{r}_l) \psi^{*p'}_m(\mathfrak{r}_l)$$

ab, wobei die Summation nur über solche $(\varepsilon_n, \varepsilon_m)$ erstreckt wird, für die

A.(21) $$m \mathfrak{B}^{(l)}_\nu = \tfrac{1}{2}\left(W^p_{n|\nu}(\mathfrak{R}_l) + W^{p'}_{m|\nu}(\mathfrak{R}_l)\right),$$

gilt. Dabei sind alle von erster Ordnung kleinen Glieder weggelassen, insbesondere braucht A.(21) nur in dieser Näherung erfüllt zu sein. A.(21) legt also die möglichen Energiewerte fest, die einen vorgegebenen makroskopischen Zustand charakterisieren. Die Energie ε wird, makroskopisch im allgemeinen bekannt sein, also $w_{nm} \neq 0$ nur innerhalb $(\varepsilon, \varepsilon + \Delta\varepsilon)$. Die Bedingungen A.(21) stellen die *Gleichungen der Energieschale* auf quantentheoretischer Grundlage dar. Wenn man also eine vorgegebene « makroskopische » Verteilung f_N herstellen will, muß man

$$w_{nm} \neq 0 \text{ nur für } \begin{cases} 1.\ (\varepsilon_n, \varepsilon_m) \in (\varepsilon, \varepsilon + \Delta\varepsilon), \\ 2.\ (W_n, W_m) \text{ so, daß A.(21) erfüllt ist,} \end{cases}$$

wählen. Das bedeutet schon eine erhebliche Einschränkung für die w_{nm}, weil dies für *alle* $\mathfrak{B}_l$ und $\mathfrak{R}_l$ gelten muß. Andererseits sieht man ein, daß es gerade

deshalb ein sehr kompliziertes Problem ist, w_{nm} im einzelnen zu bestimmen. Würde man alle ψ_n kennen, so könnte man dann weiterhin A.(20) umkehren und zu der *vorgegebenen* Funktion f_N die restlichen w_{nm} durch berechnen [18]. Damit ist diese Aufgabe im Prinzip gelöst, wenn man keine großen Anforderungen an die Genauigkeit stellt.

Es läßt sich schließlich noch zeigen, daß (bei Fermistatistik) $f_N(\mathfrak{V}_1, \mathfrak{R}_1, t) = 0$ wird, wenn z.B. $\mathfrak{V}_1 = \mathfrak{V}_2$ und zugleich $\mathfrak{R}_1 = \mathfrak{R}_2$ ist. Da wir das Wesentliche auch an f_2 erkennen können, zeigen wir es bei dieser Funktion. Zur Abkürzung unterdrücken wir außerdem die Koordinaten aller anderen Teilchen (was offenbar ganz belanglos ist). Dann genügt es zu zeigen, daß

$$\text{A.(22)} \qquad \frac{1}{\Delta\tau^2}\int_{\Delta\tau_1} d\mathfrak{v}_1\, d\mathfrak{s}_1 \int_{\Delta\tau_1} d\mathfrak{v}_2\, d\mathfrak{s}_2 \int d\bar{\mathfrak{r}}_1 \int d\bar{\mathfrak{r}}_2 \sum_{pp'} (-1)^{p+p'} \cdot$$

$$\cdot A_n^p\left(\mathfrak{s}_1 + \frac{\bar{\mathfrak{r}}_1}{2}, \mathfrak{s}_2 + \frac{\bar{\mathfrak{r}}_2}{2}\right) A_m^{p'}\left(\mathfrak{s}_1 - \frac{\bar{\mathfrak{r}}_1}{2}, \mathfrak{s}_2 - \frac{\bar{\mathfrak{r}}_2}{2}\right) \exp\left[-\frac{i}{\hbar} m(\mathfrak{v}_1\bar{\mathfrak{r}}_1 + \mathfrak{v}_2\bar{\mathfrak{r}}_2)\right] \cdot$$

$$\cdot \exp\left[\frac{i}{\hbar}\left\{W_n^p\left(\mathfrak{s}_1 - \frac{\bar{\mathfrak{r}}_1}{2}, \mathfrak{s}_2 - \frac{\bar{\mathfrak{r}}_2}{2}\right) - W_m^{p'}\left(\mathfrak{s}_1 - \frac{\bar{\mathfrak{r}}_1}{2}, \mathfrak{s}_2 - \frac{\bar{\mathfrak{r}}_2}{2}\right)\right\}\right] \approx 0\,.$$

ist. Dies läßt sich nur näherungsweise durchführen; wir werden unten sehen, daß es konsequent ist, bereits die erste Näherung wegzulassen. Tun wir das, so wird die Behauptung

$$\text{A.(23)} \qquad 2\,\frac{(2\pi\hbar)^6}{\Delta\tau^2}\int_{\Delta\tau_1} d\mathfrak{v}_1\, d\mathfrak{s}_1 \int_{\Delta\tau_1} d\mathfrak{v}_2\, d\mathfrak{s}_2 \cdot$$

$$\cdot A_n(\mathfrak{s}_1, \mathfrak{s}_1) A_m(\mathfrak{s}_1, \mathfrak{s}_1) \left\{ \exp\left[\frac{i}{\hbar}[W_{nm} + \underset{1}{W_{nm|\nu}}\mathfrak{S}_\nu^{(1)} + \underset{2}{W_{nm|\nu}}\mathfrak{S}_\nu^{(2)}]\right] \cdot \right.$$

$$\cdot \delta(m\mathfrak{v}_1 - \tfrac{1}{2}(\underset{1}{W_{n\,\nu}} + \underset{1}{W_{m)\,\nu}})\delta(m\mathfrak{v}_2 - \tfrac{1}{2}(\underset{2}{W_{n\,\nu}} + \underset{2}{W_{m)|\nu}}) -$$

$$- \exp\left[\frac{i}{\hbar}[W_{nm} + \underset{1}{W_{n|\nu}}\mathfrak{S}_\nu^{(2)} + \underset{2}{W_{n|\nu}}\mathfrak{S}_\nu^{(1)} - \underset{1}{W_{m|\nu}}\mathfrak{S}_\nu^{(2)} - \underset{2}{W_{m|\nu}}\mathfrak{S}_\nu^{(1)}]\right] \cdot$$

$$\left. \cdot \delta(m\mathfrak{v}_1 - \tfrac{1}{2}(\underset{1}{W_{n|\nu}} + \underset{2}{W_{m|\nu}}))\delta(m\mathfrak{v}_2 - \tfrac{1}{2}(\underset{2}{W_{n|\nu}} + \underset{1}{W_{m|\nu}})) \right\} \approx 0\,,$$

(dabei bedeutet z.B. $\underset{1}{W_{n|\nu}} = (\partial/\partial x_\nu^{(1)}) W_n(1,2)\,|\,\mathfrak{s}_1 = \mathfrak{s}_2 \approx \mathfrak{R}$). $\mathfrak{V}$ ist bis auf die Größenordnung $\Delta\mathfrak{V}_\nu$ bestimmt. Daher kann in den δ-Funktionen $\mathfrak{v}_1$ bzw. $\mathfrak{v}_2$ durch $\mathfrak{V}$ ersetzt werden. Damit wird auch $W_{n|\nu}$ nur mit der Genauigkeit $m\Delta\mathfrak{V}_\nu$ festgelegt; oder: $\Delta W_{n\,\nu} = W_{n,\nu|\lambda}\,\Delta X_\lambda = m\Delta\mathfrak{V}_\nu$; daher war es berechtigt, die zweiten Ableitungen von W_n als klein wegzulassen. Von der gleichen Grös-

---

[18] Für Einzelheiten vgl. H. KÜMMEL, *Zeits. Naturf.*, im Erscheinen.

senordnung ist aber $\Delta_{n\nu}$, sodaß unsere Näherungsannahmen sich als der richtigen Genauigkeit entsprechend herausgestellt haben. Zu ihr gehört eine Unschärfe $\Delta f_N \sim (\Delta f_N / \Delta X_\nu)\Delta X_\nu$ der Verteilungsfunktion, wie es sein muß.

Jetzt ist es aber leicht, unsere Behauptung zu verifizieren. Setzt man überall $\mathfrak{v}_1 = \mathfrak{V}$, so verschwindet nämlich die linke Seite von A.(23), q.e.d.

RIASSUNTO (*)

In un precedente lavoro l'autore è riuscito a ricondurre completamente alla teoria quantistica le equazioni macroscopiche di moto (come equazioni differenziali tra osservabili macroscopiche). Nella presente ricerca si giustificano su basi quantistiche anche la statistica e la termodinamica dei processi irreversibili. Si dimostra, in particolare, che anche i metodi classici (densità dello spazio delle fasi, funzione di ripartizione della velocità) risultano dalla microstruttura. Con ciò è dato il legame della intera macrofisica (a temperature non troppo basse) alla microfisica.

(*) *Traduzione a cura della Redazione.*

Duration of the Diffraction Grating in Relation to the State of the Powders in Suspension.

A. Carrelli and F. S. Gaeta

Istituto di Fisica dell'Università - Napoli

(ricevuto il 30 Giugno 1955)

Summary (*). — It has been observed that the diffraction grating discovered by Carrelli and Porreca in liquid suspensions of powders builds up only after a certain time after the mixing of the two phases. Working with aqueous suspensions of perfectly dryed powders the authors have measured for different substances in water the times necessary for the gradual establishment of the phenomenon and have emphasized a dependence of these times from the nature of the phases in contact and their temperature.

(*) *Editor's Translation.*

Carrelli and Porreca recently studied, with an optical method, the behaviour of disperse systems when crossed by acoustic waves of high frequency. They have shown that, when the acoustic perturbation is rigorously standig the dispersed particles gather in the nodal planes, giving origin in this way, provided some additional conditions to be verified, to a second phase grating, which in turn produces a second diffraction pattern, superimposed to the one generated by the periodical density fluctuations of the dispersing liquid medium.

This second grating, unlike the first one, does not disappear at once after the ceasing of the u. s. perturbation, but dissolves gradually, the corresponding pattern being still visible for some time. This time of permanence, which henceforth we shall call t_p, has been determined by the above mentioned Authors, together with its dependence from the nature and concentration and dimensions of the suspended particles, and with the frequency power and duration of the acoustic perturbation.

We continued these researches employing an arrangement identical to the

one described by the above mentioned Authors [1], except for the disposition of quartz and reflector which in our case are both vertical; the nodal planes are consequently also vertical.

We have introduced this modification in order to render the measure of t_p independent from the falling of the suspended particles under the action of gravity; in our case indeed the movement takes place along the nodal planes themselves, and the perturbation brought about is much reduced. Also the thermal waves due to the heating of the quartz give less disturbance, the temperature gradient being now horizontal. That explains why the values of the time of permanence t_p found by us, are, in the same frequency and power conditions, and for the same couples of substances much higher than those found by CARRELLI and PORRECA. With this experimental arrangement we have studied the behaviour of suspensions which exhibit the permanence effect focusing our attention on the instants which follow immediately the formation of the suspension. We have found in this way that, making use of perfectly dry powders, the permanence of the diffracted orders is not observed at once after the formation of the suspension, but on the contrary the time of permanence increases gradually from zero to a maximum value which is henceforth constant and depends on the nature of the phases in contact and on the experimental conditions. We had care then to ensure the complete dehydration of the powders used drying them each time in an oven before their use, for periods of over an our. Indeed an essication of ten minutes at 60° proved quite satisfactory in nearly all cases, and producing the same effect as a longer drying.

We must note now that in suspensions of the kind used by us the solid particles, being denser than the liquid medium, fall gradually to the bottom of the tank and the number of those remaining in suspension reduces, so that the intensity of the diffracted pattern becomes less and less until at last it disappears completely when all the particles have deposited on the bottom.

To compare properly two determinations of t_p it is necessary to make them both at equal intervals of time after the instant in which the particles were uniformly distributed in the liquid. To these initial conditions one must return after each reading, stirring the liquid again and waiting always a same number of minutes before making the next reading.

Keeping all the other factors constant, namely the power, the duration and the frequency of the ultrasonic waves, and taking great care to ensure the stationarity of the perturbation, we have obtained a regular and general variation of t_p against the time elapsed since the two phases were put in contact, as illustrated in (Fig. 1) for suspension of Fe_2O_3 and (Fig. 2) CaS in water.

---

[1] A. CARRELLI et F. PORRECA: *Nuovo Cimento*, **10**, 98 (1953).

It is worth mentioning the fact that all the substances exhibiting the permanence effect show also an analogous pattern in the variation of t_p: therefore one is led to think that the observed phenomenon is due to an underlying interaction, between the dispersed and the dispersing phases, interaction which

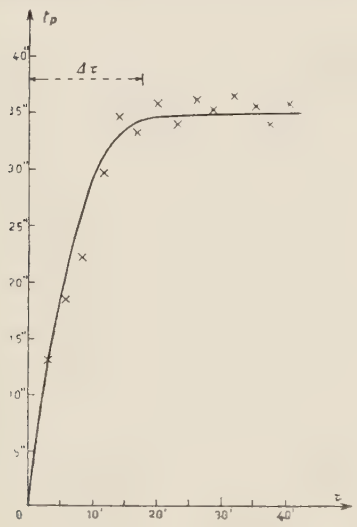

Fig. 1. – Vertical quartz Fe_2O_3 in H_2O; conc. = 0,4 g/l; t = 18 °C 7 orders.

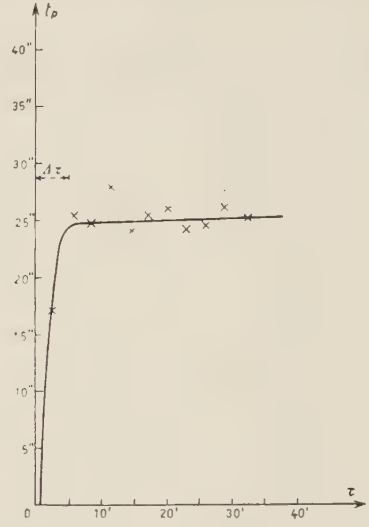

Fig. 2. – Vertical quartz CaS in H_2O; conc. = 0,5 g/l; t = 18 °C 7 orders.

gradually produces the conditions accountable for the diffraction of incident light by the clusters of particles in the nodal planes of the acoustic perturbation.

One must remember indeed that some suspensions do and some others do not exhibit the permanence effect; in particular no one of the experimented substances gave rise to the second diffracted pattern when dispersed in carbon tetrachloride or in benzol, which both, as it is well known, are not-polar substances.

While in every case the general pattern is the same, namely a gradual increase of t_p, with τ until a maximum value of the time of permanence is reached, the value of the period $\Delta\tau$ employed to reach this maximum value depends on the nature of the couple of substances in contact, and $\Delta\tau$ varies from 6 min for the suspension of calcium sulfide in water, to 18 min for the suspension of Fe_2O_3 in water.

Other substances exhibited values between the two ones given above. Namely we obtained a $\Delta\tau$ of 9 min for starch in water, 12 min for $CaSO_4$ in water, $\sim$ 12 min for MnO_2 in water and $\sim$ 15 min for $Fe_2O_3 \cdot 4H_2O$ in water.

We have investigated also whether the value of $\Delta\tau$ depends, for a given couple of substances on the value of t_p: two suspensions of the same kind ob-

tained fractioning by centrifugation a single suspension into two others, one containing the biggest and one the smallest particles, gave widely different t_p's but quite the same $\Delta\tau$.

Moreover some measurements at other frequencies gave the same results as the corresponding ones at 1.8 MHz. The frequencies used were 2.225 MHz. This points to the fact that the process underlying the origin of the second phase grating is intrinsic to the nature of the phases in contact.

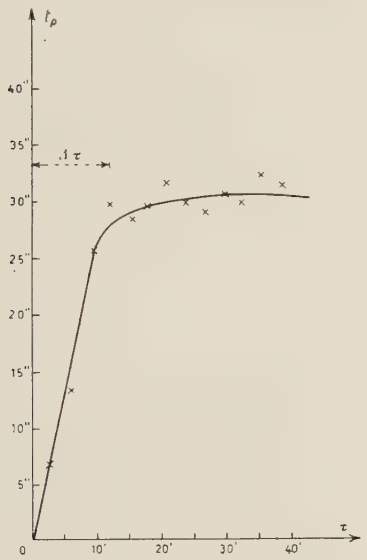

Fig. 3. – Vertical quartz $BaSO_4$ in H_2O; conc. = 0,5 g/l; t = 18 °C 7 orders.

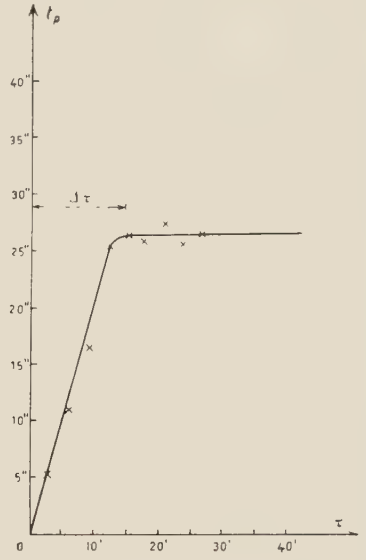

Fig. 4. – Vertical quartz $BaSO_4$ in H_2O; conc. = 0,5 g/l; t = 5 °C 7 orders.

At this point a trial remained to be made, namely to see *if the temperature had an effect* on the time employed to reach the maximum permanence of the second phase grating. While all the preceding experiments were made at room temperature, we obtained the patterns of Figs. 4 and 6 at 5 °C. The difference of the $\Delta\tau$ is evident for the suspension of MgO in water, while for $BaSO_4$ in water such a difference is not detectable.

In conclusion we can say that the contact between the dispersed and the dispersing phase does not always produce the conditions which allow the formation of the second phase grating. Moreover, in the case in which these conditions arise, they do it gradually, and the time $\Delta\tau$ employed to reach their full development depends on the nature of the phases in contact and on their temperature.

The phenomenon bears strong resemblance to a chemical reaction and

suggests an interaction of chemical or electrical nature between the particles of the two phases in contact.

Further investigations on the question will be made also with different methods.

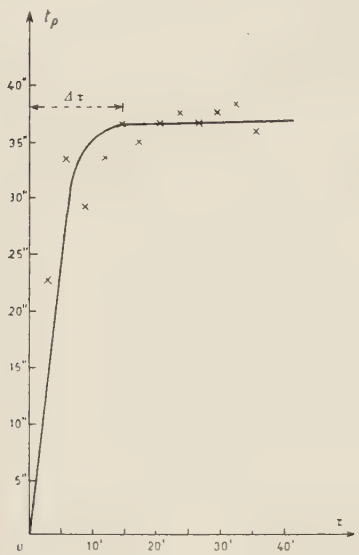

Fig. 5. – Vertical quartz MgO in H_2O; conc. = 0,4 g/l; t = 18 °C 7 orders.

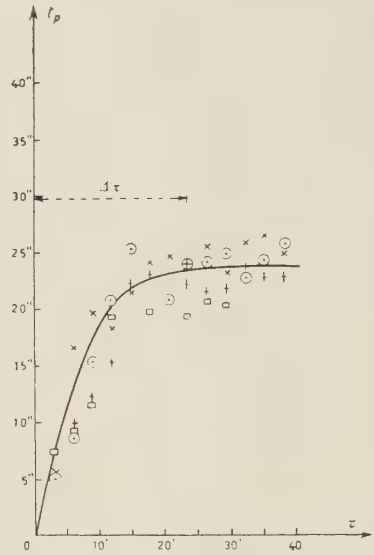

Fig. 6. – Vertical quartz MgO in H_2O; conc. = 0,4 g/l; t = 5 °C 7 orders, four different determinations.

We note here that after the present researches the list of the substances which exhibit the permanence of the second phase grating and of the corresponding t_p's must be integrated as follows:

TABLE I.

Substance	Maximum t_p observed with 10 s duration of the u.s. (ν = 1.8 MHz)	$\Delta\tau$ at room temperature
starch in water	18 s	9 min
$Fe_2O_3 \cdot 4H_2O$ in water	22 s	12 min
CaS »	15 s	6 min
Fe_2O_3 »	normal 16 s	18 min
	centrif. light fraction 42 s	18 min
$BaSO_4$ »	22 s	15 min
MnO_2 »	16 s	12 min
MgO »	18 s	12 min
$CaSO_4 \cdot 2H_2O$ »	13 s	9 min

RIASSUNTO

Si è osservato che il reticolo di diffrazione scoperto da Carrelli e Porreca in sospensioni di polveri solide in liquidi, si forma solo dopo passato un certo tempo dalla miscelazione delle due fasi. Lavorando con sospensioni acquose di polveri perfettamente essiccate si sono misurati i tempi necessari per ottenere il graduale compimento del fenomeno, per varie sostanze in acqua, e si è posta in rilievo una dipendenza di questo tempo dalla natura delle fasi a contatto e dalla loro temperatura.

On the Persistence of a Phase Grating in Some Suspensions when Stopping the Supersonic Waves.

F. Porreca

Istituto di Fisica Sperimentale - Università di Napoli

(ricevuto il 30 Giugno 1955)

Summary (*). – It has been observed that in the substances which present the effect of persistence of the even diffraction lines, when stopping the ultrasonics, for a certain time persists also the trace of the ultrasonic grating built up during the passage of ultrasonics. This trace, consisting in parallel equally luminous lines equally spaced by $\lambda_{u.s.}/2$ is the same which is observed during the action of ultrasonics. This result is identical to that obtained with an artificial phase grating and this gives the direct proof that, after stopping the ultrasonics, in the liquid persists a phase grating of constant $\lambda_{u.s.}/2$.

(*) *Editor's Translation.*

We have experimented in the previous notes [1,2] that some suspensions of powders in liquids, under the action of standing supersonic waves, give, during a few seconds after stopping the ultrasonics, the persistence, of the even order diffracted lines, in the focal plane of a converging lens on which the light beam, emerging from the liquid, falls.

The reason of it has been imputed to the accumulation of the particles suspended in the nodal planes of the standing supersonic waves. This peculiar arrangement in the substances giving the effect causes a periodical variation of the refractive index, with the periodicity of half a wavelength λ of the ultrasonic waves in the liquid under examination. This situation continues even

(1) A. Carrelli and F. Porreca: *Nuovo Cimento*, **9**, 90 (1952).
(2) A. Carrelli and F. Porreca: *Nuovo Cimento*, **10**, 883 (1953).

after having stopped the supersonic action, as long as mechanical and thermic causes do not destroy such a disposition.

Therefore, the effect is to ascribe to the persistence in the medium of a phase grating of a $\lambda/2$ periodicity,.

It is possible to obtain an immediate proof of such an interpretation by the direct observation of the light wave front emerging from the vessel containing the liquid under examination.

A beam of monochromatic light, emerging from a slit S (fig. 1), is made parallel through a collimator lens and sent through an homogeneous liquid medium (water for instance), subjected to ultrasonics, along the OO' direction, parallel to the supersonic wave fronts. On a screen P, placed at right angles with the OO' direction of the light where the image appears most clearly, we see a light pattern made by bright and dark bands, at the same interval from each other [3]. By a magnification optic system L, moving normally to the direction OO' of the light propagation in such a way as to measure its displacement, we can know the periodicity of the observed lines. It is $\lambda/2$.

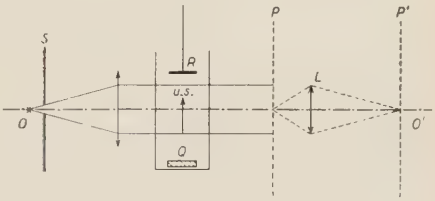

Fig. 1.

Now, if the suspension (starch in water) is put in the vessel we observe the modification of the luminous picture in the plane P, when the ultrasonics are stopped.

Thus we could observe that, during some seconds after stopping the supersonic waves, the same picture remains which we observe when the liquid is crossed by the ultrasonics, i.e. bright and dark lines at $\lambda/2$ intervals. As the supersonic frequency ν is 1.797 MHz, the distance between two consecutive bright lines in starch and water is $0.431 \pm 32 \cdot 10^{-3}$ mm. With the best agreement it coincides with half a wavelength of the examined substance ($\lambda = 0.840$ mm in water).

Then this experiment is the proof that a phase grating of a $\lambda/2$ periodicity remains in the suspension giving the permanence effect, after stopping the standing supersonic waves.

It has been possible to confirm it experimentally by an artificial phase grating, made by slits cut on a transparent thin plexiglass plate with the periodicity of 1 mm.

When the vessel containing the liquid subjected to the ultrasonics is substituted with such a model phase grating we observe bright and dark stripes

---

[3] O. NOMOTO: *Proc. Phys. Math. Soc. Japan*, **18**, 402 (1936).

with the periodicity $0.997 \pm 12 \cdot 10^{-3}$ mm, i.e. exactly the one of the used model grating, with regard to the experimental error.

From this and the fact that, as we noticed, at the stopping of the supersonic waves the same bright stripes remain which one observes during its emission, at $\lambda/2$ intervals, we deduce the most direct proof of the fact that, inside the suspensions giving the persistence effect of the diffracted lines, a phase grating remains with the ultrasonics' half wavelength periodicity.

RIASSUNTO

Si è osservato che nelle sostanze che presentano l'effetto di persistenza delle righe diffratte d'ordine pari, al cessare degli ultrasuoni, rimane per un certo tempo anche la figura del reticolo ultrasonoro formatosi in esso durante il passaggio degli u.s. Questa figura, costituita da righe parallele ugualmente luminose ed equidistanti di $\lambda_{u.s.}/2$, è la stessa di quella che si osserva durante l'azione ultrasonora. Questo risultato è identico a quello ottenuto con un reticolo artificiale di fase e ciò dà una prova diretta della persistenza in seno al liquido di un reticolo di fase, di costante $\lambda_{u.s.}/2$, al cessare degli u.s.

Polarization of High Energy Protons Scattered by Iron.

T. Eriksson

Institute for Mechanics and Mathematical Physics - University of Uppsala

(ricevuto il 1° Luglio 1955)

Summary. — The polarization of protons scattered by iron is calculated at 90, 150, 225 and 400 MeV. The phases are calculated with the so called « optical model ». A similar type and strength of the spin-orbit term is assumed as that used by E. Fermi.

The calculations are similar to those by S. Köhler [1], but for another type of central potential. The phases were calculated by means of the high energy limit of the W.K.B. method, keeping only linear terms of the potential in the expansion. Cf. [2]. The calculations were made for iron, and the nucleus was represented by a spherical, complex potential, with linearly sloping sides [3] and with a spin-orbit coupling term of the type $(1/r)(\mathrm{d}V/\mathrm{d}r)$ [4]. This gives:

$$V = -A - iB\,, \qquad \text{for} \quad r < R_1\,,$$

$$V = -(A + iB)\frac{R_2 - r}{d} - C\frac{\hbar^2}{2M^2c^2}\frac{1}{r}\frac{A}{d}(\boldsymbol{l}\cdot\boldsymbol{s})\,, \qquad \text{for} \quad R_1 < r < R_2\,,$$

$$V = 0\,. \qquad \text{for} \quad r > R_2\,,$$

where $R_1 = 2.18 \cdot 10^{-13}$ cm is the radius for the inner, constant part of the potential and $R_2 = 7.27 \cdot 10^{-13}$ cm is the outer radius. $d = R_2 - R_1 = 5.09 \cdot 10^{-13}$ cm is the surface thickness. A, B and C are constants. C was chosen

---

(1) Report by I. Waller in *Proceedings of the Fifth Rochester Conference on High Energy Nuclear Physics.*

(2) S. Fernbach *et al.*: *Phys. Rev.*, **75**, 1352 (1949).

(3) W. J. Swiatecki: *Phys. Rev.*, **98**, 204 (1955).

(4) S. Fernbach *et al.*: *Phys. Rev.*, **97**, 1059 (1955).

to be 30 (5). A and B were chosen to give total and inelastic scattering cross sections, in the case of neutrons, in accordance with experiments (6) and (7). The calculations were performed for four different energies of the incoming protons 90, 150, 225 and 400 MeV. The corresponding values for A were 26, 15, 15 and 21 MeV and for B 10, 11, 13 and 17.5 MeV. The Coulomb potential was assumed to be the same as that given by a uniform charge distributed within a radius

$$R_c = 4.21 \cdot 10^{-13} \text{ cm}.$$

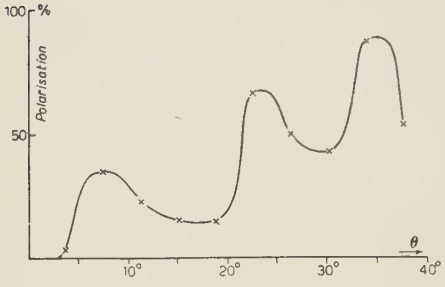

Fig. 1. – The polarization of 90 MeV protons scattered by iron as a function of scattering angle.

In order to make the calculations simpler for heavy nuclei and for high energies, where many phases enter the calculation, the sums over l in the formulae for the scattering amplitudes (see ref. (8)) were replaced by integrals. The Legendre functions were then replaced by Bessel functions of orders zero and one.

The results are shown in figs. 1 and 2, where the polarization is plotted as a function of the scattering angle θ. They show the same general behavior as the earlier calculations by S. Köhler reported in (1). The polarization which vanishes in the forward direction, rises suddenly around 2-5 degrees, depending on the energy. At 90 MeV (fig. 1) it soon decreases again, but at 150 MeV (fig. 2) and higher energies it remains almost constant for a few degrees. The polarization curves at 225 and 400 MeV look very much the same as the curve at 150 MeV except for a contraction of the whole pattern in angular scale and a slight increase of the polarization. The calculated polarization curves may be inaccurate at large angles. This is partly because of the possible inadequacy of

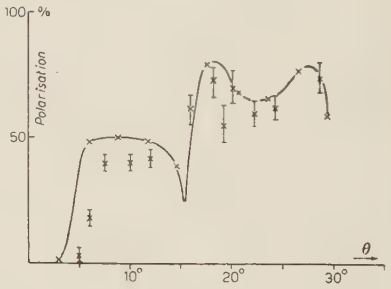

Fig. 2. – The polarization of 150 MeV protons scattered by iron as a function of scattering angle. The crosses with error indications refer to experimental results see ref. (9).

(5) This value is the same as that used by E. Fermi: *Nuovo Cimento*, **11**, 407 (1954).
(6) V. A. Nedzel: *Phys. Rev.*, **94**, 174 (1954).
(7) G. P. Millburn *et al.*: *Phys. Rev.*, **95**, 1268 (1954).
(8) S. Köhler: *Nuovo Cimento*, **2**, 911 (1955).
(9) Report by B. Rose in *Proceedings of the Fifth Rochester Conference on High Energy Nuclear Physics*, and a private communication from B. Rose.

the W.K.B. approximation at high angles and partly because at the highest one or two angles most of the significant figures were lost in the numerical calculation. The difference in the behavior of the polarization curve at 90 MeV (fig. 1) and that obtained by Köhler ref. ([8]) might indicate a greater sensitivity of the results at this energy to the type of central potential chosen. See also Köhler's paper for a discussion. In fig. 2, showing the polarization at 150 MeV, the crosses with indicated errors are experimental values at 130 MeV obtained at Harwell ([9]). A comparison shows, that the calculated values are somewhat higher than the experimental ones, which might in part be due to the difference in energy. Also the calculated curve begins to rise at small angles earlier than the experimental one. An effect of this kind is to be expected from the finite angular resolution of the counters, which is especially important in a region of rapidly varying cross section, as seems to be indicated by the Harwell curves for carbon ([9]). For the general behavior of the curves compare also ref. ([10]).

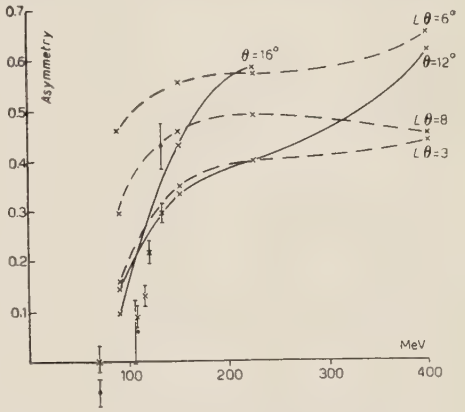

Fig. 3. – The « left and right » asymmetry of protons scattered by iron as a function of energy. The polarization of the incident beam is 70%. The dots and crosses with error indications refer to experimental results at 16 and 12 degrees respectively; see ref. ([9]).

Fig. 3 shows the energy dependence of the polarization. Here it is assumed that the incident beam has a polarization of 70% and the « left and right » asymmetry is plotted as a function of energy. The points and crosses with error indications are the experimental Harwell results at the scattering angles 16 and 12 degrees respectively. The solid curves are the calculated results for these angles. The dotted curves show the variation of polarization with energy for constant L-values, where $L = kR_2$ and k is the wave number of the incident protons. A constant $L\theta$-value means, that one is comparing corresponding parts of the polarization curves for different energies, allowing for the contraction of the angular scale with increasing energy. The calculated curves for constant angle show a marked decrease of the polarization between 150 and 100 MeV, though not as steep as found experimentally.

([10]) R. M. Sternheimer: *Phys. Rev.*, **97**, 1314 (1955).

* * *

I wish to express my gratitude to Professor I. WALLER for suggesting this investigation and for his interest in my work. I am also indebted to Dr. W. J. SWIATECKI for valuable suggestions and many interesting discussions.

RIASSUNTO (*)

Si calcola la polarizzazione dei protoni diffusi dal ferro a 90, 150, 225 e 400 MeV. Le fasi si calcolano col cosidetto « modello ottico ». Si assumono per il termine di accoppiamento spin-orbita tipo e forza simili a quelli usati da E. FERMI.

(*) *Traduzione a cura della Redazione.*

IL NUOVO CIMENTO Vol. II, N. 5 1° Novembre 1955

Polarization of High Energy Nucleons Scattered by Nuclei.

S. KÖHLER

Institute for Mechanics and Mathematical Physics - University of Uppsala

(ricevuto il 1° Luglio 1955)

Summary. — Calculations have been made on the polarisation of protons scattered by nuclei at high energies. With the spin-orbit coupling similar to that used by E. Fermi one appears to get good agreement with experiments at 135 MeV. At 90 MeV phase-shifts were, for comparison, calculated both in the W. K. B. and the Born approximations. An alternative derivation of the explicit formula for the polarisation of neutrons first given by E. Fermi in the Born approximation is outlined briefly.

In the first report on the polarization of nucleons scattered by nuclei at 340 MeV by E. FERMI [1] the nucleon-nucleus interaction was assumed to be given by a potential

$$V = V(r)(1 + i\beta) + \alpha \frac{V'(r)}{r} \boldsymbol{l}\cdot\boldsymbol{s}\,, \tag{1}$$

with

$$\alpha = -\alpha_1 \frac{h^2}{2M^2c^2}\,, \qquad \alpha_1 = 30.$$

Here $\boldsymbol{s}$ and $\boldsymbol{l}$ are the spin and orbital angular momenta in units of h, and M the mass of the nucleon. β is a constant.

If in a partial wave analysis of the Schrödinger equation with a potential

[1] E. FERMI: *Nuovo Cimento*, **11**, 407 (1954).

$V(r)$ the phase-shifts are calculated in the Born approximation one obtains (2):

$$(2) \qquad \delta_l = -\frac{1}{2E}\int_0^\infty V(r)\mathrm{d}z, \qquad z = \sqrt{k^2r^2 - \nu^2}, \qquad \nu = \begin{cases} 0 & \text{for } l = 0, \\ l + \frac{1}{2} & \text{for } l \geqslant 1. \end{cases}$$

Here E is the energy and k the wave number of the incident particle. This approximation for the phase-shifts has been used in the papers published on this subject. It is considered to be a good approximation for cross sections and polarization for small angles (3). In this paper the phases are in one case also calculated by the W.K.B. method.

Preliminary studies showed the coulomb field to be important in calculations of the polarisation at 150 MeV. A report of these has been given (4).

The polarization, as usually defined, is given by

$$(3) \qquad P(\theta) = \frac{2\mathrm{Im}A^*B}{|A|^2 + |B|^2}.$$

With the phase-shifts calculated from (2) the scattering amplitudes for protons are given by (*)

$$(4) \qquad \begin{cases} A(\theta) = f_c(\theta) + \\ + \sum_{l=0}^{\infty} \left((l+1)\exp[2i\delta_{l,\,l+\frac{1}{2}}] + l\exp[2i\delta_{l,\,l-\frac{1}{2}}] - (2l+1)\exp[2i\eta_l]\right) P_l(\cos\theta)\,. \\ B(\theta) = \sum_{l=0}^{\infty} \left(\exp[2i\delta_{l,\,l+\frac{1}{2}}] - \exp[2i\delta_{l,\,l-\frac{1}{2}}]\right) P_l^1(\cos\theta)\,. \end{cases}$$

Here $f_c(\theta)$ is the amplitude for scattering on a point charge Ze, where Ze is the charge of the nucleus. η_l is, in the Born approximation, given by $\eta_l = (Ze^2/\hbar v)\ln(l + \frac{1}{2})$ where v is the velocity of the particle. The phases are calculated from (2) with

$$(5) \qquad V(r) = \begin{cases} V(r)(1 + i\beta) + V_c(r) + \dfrac{l}{2}\alpha\dfrac{V'(r)}{r} & \text{for} \quad \delta_{l+\frac{1}{2}}, \\ V(r)(1 + i\beta) + V_c(r) - \dfrac{l+1}{2}\alpha\dfrac{V'(r)}{r} & \text{for} \quad \delta_{l-\frac{1}{2}}, \end{cases}$$

(2) S. Fernbach, R. Serber and T. B. Taylor: *Phys. Rev.*, **75**, 1352 (1949).

(3) R. J. Glauber: *Phys. Rev.*, **91**, 459 (1953).

(4) Report by I. Waller in *Proc. of the Fifth Rochester Conf. on High Energy Nuclear Physics* (1955).

(*) P_l and P_l^1 are defined as in Schiff: *Quantum Mechanics*, p. 71.

$V_c(r)$ is the electrostatic potential of the charge distribution. Outside the nucleus $V_c(r) = Ze^2/r$.

This paper presents calculations for carbon, aluminium and iron as targets at energies of 135 and 90 MeV. With these elements and in this energy region measurements have been made at HARWELL [5]. The radial dependence of the central potential was taken as parabolic:

$$V(r) = V_0\left(1 - \frac{r^2}{R^2}\right) \qquad r < R,$$

$$V(r) = 0 \qquad r > R,$$

R was taken as $1.6 \cdot A^{-\frac{1}{3}} \cdot 10^{-13}$ cm [6]. The depths of the real and imaginary parts of the central potential were adjusted to reproduce the available neutron and proton absorption (σ_a) and total (σ_t) cross sections [7,8] (*). (The nuclear part of the potential was taken the same for neutrons and protons). The result is given in Table I.

TABLE I.

Target Nucleus	90 MeV: $V_0 = 45$ MeV, $V_0\beta = 25$ MeV				135 MeV: $V_0 = 26$ MeV, $V_0\beta = 26$ MeV			
	σ_a (barns)		σ_t (barns)		σ_a (barns)		σ_t (barns)	
	calc.	obs.	calc.	obs.	calc.	obs.	calc.	obs.
Fe	.801	.76	1.875	1.92	.761	.74	1.430	1.41
Al	.456	.46	1.095	1.10	.426	.43	.772	.79
C (BA)	.238	.23	.545	.52	.219	.23	.379	.37
C (WKB)	.267	.23	.598	.52	—	—	—	—

The nuclear charge was assumed to be uniformly distributed, and the radius of this distribution was taken to be $1.2 \cdot A^{-\frac{1}{3}} \cdot 10^{-13}$ cm (e.g. [9]).

[5] Report by B. ROSE in *Proc. of the Fifth Rochester Conf. on High Energy Nuclear Physics*, and private communication.

[6] W. HECKROTTE: *Phys. Rev.*, **95**, 1279 (1954).

[7] V. A. NEDZEL: *Phys. Rev.*, **94**, 174 (1954).

[8] G. P. MILLBURN, W. BIRNBAUM, W. E. CRANDALL and L. SCHECTER: *Phys. Rev.*, **95**, 1268 (1954).

(*) Cross sections for iron were found by interpolation in a plot of cross sections against A.

[9] D. G. RAVENHALL and D. R. YENNIE: *Phys. Rev.*, **96**, 239 (1954).

Figs. 1-5 show the curves obtained. In fig. 1-3 the lower curve shows the polarization and the upper curves the cross sections corresponding to measurements to the « left » and « right » of a beam with an initial polarization of 70 %. (The conditions in the Harwell experiments). Figs. 4 and 5 give the polarization only. Experimental points, marked with errors, are from the measurements made at HARWELL (5). In fig. 5 the points denote the polarization with phases calculated in the W.K.B. approximation (*).

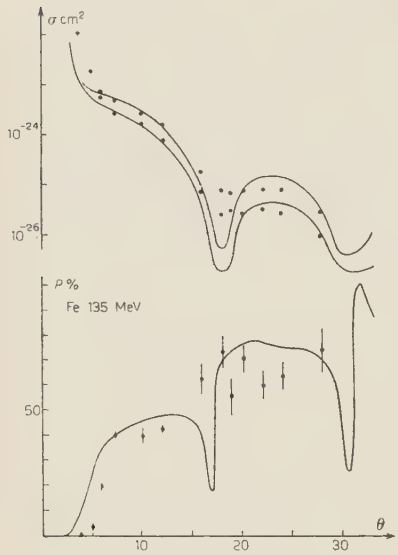

Fig. 1.

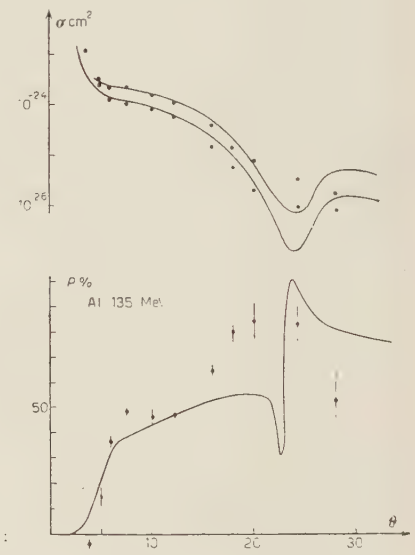

Fig. 2.

At 135 MeV α_1 around 30 gave good overall agreement (1). It is best for iron at 135 MeV. For carbon and aluminium at the same energy the agreement is not so good. Note that the calculations do not show the caracteristic maximum at a small angle that the experiments do. Concerning the general form of the curves compare (10).

At 90 MeV the choice $\alpha_1 = 30$ seems to give a too large polarization, although at this energy only a few experimental points are available. A comparison with calculations by T. ERIKSSON (11), at this energy illustrates the role which may be played by a different choice of the shape of the potential well. The comparison between polarisation calculated by means of the Born and W.K.B. approximations to the phase-shifts for carbon at 90 MeV is shown in fig. 5.

(*) The phases for the highest l were found by extrapolation.

(10) R. M. STERNHEIMER: *Phys. Rev.*, **97**, 1314 (1955).

(11) T. ERIKSSON: *Nuovo Cimento*, **2**, 907 (1955).

The present investigation does not justify the conclusion that the form of the spin-orbit interaction used here is the correct one but it does show that at 135 MeV this form is capable of giving good agreement. Evidence for this form of the interaction, other than the analogy with the Thomas correction, has been discussed ([12]). Experiments with heavier nuclei at 135 MeV would show if also these agree with the value of α used here. It will be of some special interest to see from measurements at higher energies if there is an energy dependence of α. At lower energies a study of the energy dependence of α might be obscured by the greater sensitiveness of the results to the shape of the potential as mentioned above. More calculations in this direction will be made.

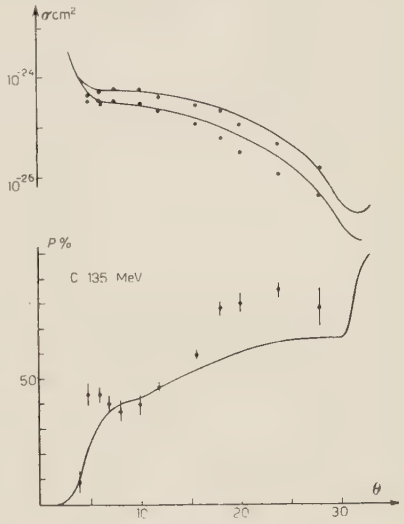

Fig. 3.

The above calculations are for protons. For neutrons an explicit formula for the polarization can be obtained in certain approximations. In the paper by E. Fermi the scattering amplitudes were calculated in the Born approximation. For $V(r)$ in (1) a square well potential was chosen. Then the polarization was given by

$$P(\theta) = \frac{\alpha\beta k^2 \sin\theta}{1 + \beta^2 + \frac{1}{4}\alpha^2 k^4 \sin^2\theta}. \tag{6}$$

It was later shown that (6) is valid for any radial dependence of the central potential if the spin-orbit coupling has the form given by (1) and the phase-

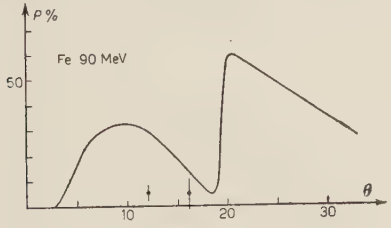

Fig. 4.

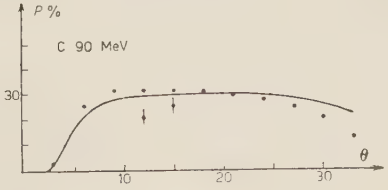

Fig. 5.

([12]) S. Fernbach, W. Heckrotte and J. V. Lepore: *Phys. Rev.*, **97**, 1059 (1955).

shifts are treated as small ([13,14]). It can be shown, however, that the same formula results if only the *change* of the phase-shifts due to the spin-orbit coupling, but not the phase-shifts themselves, are treated as small. (6) will thus hold for neutrons also at lower energies where the Born approximation for the amplitudes is not applicable. Note the energy dependence predicted by (6) if α is regarded as constant. From ([15]) β is found to increase with energy. For this detail compare also Table I.

A more detailed report of the investigation presented here will appear later.

* * *

I wish to express my gratitude to Professor I. WALLER for suggesting this investigation and for many valuable discussions. I also wish to thank Dr. W. J. SWIATECKI for many interesting discussions. Fil. mag. T. BERGGREN and Fil. mag. N. NILSSON have been helpful with some of the numerical computations for which I thank them.

([13]) W. HECKROTTE: *Phys. Rev.*, **94**, 1797 (1954).
([14]) B. J. MALENKA: *Phys. Rev.*, **95**, 522 (1954).
([15]) T. B. TAYLOR: *Phys. Rev.*, **92**, 831 (1953).

RIASSUNTO (*)

Sono stati eseguiti calcoli sulla polarizzazione dei protoni sparpagliati da nuclei ad energie elevate. Col termine di accoppiamento spin-orbita simile a quello usato da E. FERMI sembra si ottenga un buon accordo con l'esperienza a 135 MeV. A 90 MeV gli spostamenti di fase furono, per confronto, calcolati sia nella approssimazione W.K.B., sia in quella di Born. Si indica brevemente un'altra derivazione della formula esplicita per la polarizzazione dei neutroni data per primo da E. FERMI in approssimazione di Born.

(*) *Traduzione a cura della Redazione.*

The Determination of the Scattering Potential from the Spectral Measure Function (*).

I. Continuous Spectrum.

I. Kay and H. E. Moses

Institute of Mathematical Sciences, New York University - New York

(ricevuto il 2 Luglio 1955)

Summary. — It is shown how a generalized form of the Gelfand-Levitan procedure for obtaining scattering potentials from spectral measure functions may be obtained from the theory of operators in a vector space. Part I treats the case where the perturbed and unperturbed Hamiltonians have the same spectrum which is taken to be purely continuous. The vector space in which one works is Hilbert space.

---

1. – Introduction.

For special cases it has been shown by previous workers how the scattering potential can be obtained from the spectral measure function using the equation of Gelfand and Levitan (1). By showing, in addition, how the spectral measure function can be obtained from the scattering phases Jost and Kohn (2) and Levinson (3) have been able to construct the scattering

(*) The research reported in this article was done at The Institute of Mathematical Sciences, New York University, and has been made possible through support and sponsorship extended by Geophysics Research Directorate, Air Force Cambridge Research Center under Contract No. AF 19(122)-463.

(1) I. M. Gelfand and B. M. Levitan: *Izvest. Akad. Nauk SSSR*, Math. Series,, **15**, 309 (1951).

(2) R. Jost and W. Kohn: *Det. Kgl. Danske Vidensk. Selskab, Mat.-fys. Medd.*, **27**, n. 9 (1953).

(3) N. Levinson: *Phys. Rev.*, **89**, 755 (1953).

potential from phases. KAY (1), CORINALDESI (5), and NEWTON and JOST (6) have adapted the method of references (1) and (2) to the one-dimensional wave equation ($-\infty < x < +\infty$), the radial Gordon-Klein-Schrödinger equation, and systems of coupled equations, respectively. In the treatments discussed above the unperturbed Hamiltonian H_0 has been given explicitly as the kinetic energy operator, and it has been assumed that the perturbation is diagonal in the x-representation.

In all of these papers one uses the analytical properties oft he eigenfunctions of the perturbed Hamiltonian H and the special nature of the unperturbed Hamiltonian H_0. In contrast, the approach in the present paper is more abstract and makes use of the « algebraic » relationships between various operators. The advantage of the present viewpoint is that the structure of the inverse problem is seen to be largely independent of the special properties of H and H_0.

We shall now describe the « direct » and « inverse » problems of spectral theory.

In the *direct* problem of spectral theory one is *given*:

a) the Hamiltonian H (which for the while we shall assume has a purely continuous spectrum);

b) the boundary conditions on the eigenfunctions of the continuous spectrum.

One *seeks*:

a) the eigenfunctions of the continuous spectrum;

b) the measure functions (or equivalently weight functions) associated with the eigenfunctions which must be used in the completeness relationship.

The *inverse* problem has a different set of given data. One is *given*:

a) the boundary condition on the eigenfunctions of H;

b) the measure function associated with these eigenfunctions.

One *seeks*:

a) the eigenfunctions of H;

b) the operator H.

The inverse problem is important because in some cases the spectral measure

(1) I. KAY: EM-74, *Inst. of Math. Sci., Div. of Electromagnetic Res.*, New York University.

(5) E. CORINALDESI: *Nuovo Cimento*, **11**, 468 (1954).

(6) R. G. NEWTON and R. JOST: *Nuovo Cimento*, **1**, 590 (1955).

function associated with the eigenfunctions satisfying certain boundary conditions can be obtained simply from the scattering operator. Hence, after obtaining the spectral measure function from the scattering operator, we can obtain the scattering potential $V = H - H_0$ from the measure function. We thereby shall have a method of obtaining the scattering potential from the scattering operator.

The present study is divided into several parts. In Part I we consider the case where H has a purely continuous spectrum. In Part II we shall generalize the results to take into account the case where H has a discrete spectrum in addition to the continuous spectrum. In Part III we show how the one-dimensional Schrödinger equation ($-\infty < x < \infty$), already discussed in reference [1] by means of a special procedure, appears as a case of the more general procedure discussed herein.

We shall sketch the three basic theorems which are proved.

Let there be given a Hamiltonian H_0 with a continuous spectrum whose eigenfunctions corresponding to the eigenvalue E are $|H_0; E\rangle$ and are chosen such that $\langle H_0; E|H_0; E'\rangle = \delta(E - E')$. Let there also be a positive definite Hermitian operator W (the weight operator) which commutes with H_0. We state the first of our theorems as follows:

Theorem 1. Assume that a solution of

$$WU^* = U_0 \tag{1.1}$$

can be found for operators U, U_0 such that

$$U_0 = U^{-1} \tag{1.2}$$

(the asterisk denotes Hermitian adjoint). Then one can construct a Hermitian operator H:

$$H = UH_0U_0 \tag{1.3}$$

whose eigenfunctions $|H; E\rangle$ are given by

$$|H; E\rangle = U|H_0; E\rangle . \tag{1.4}$$

Furthermore, the eigenfunctions $|H, E\rangle$ of H have the normalization

$$\langle H; E'|H; E\rangle = [\omega(E)]^{-1}\delta(E - E') \tag{1.5}$$

where $\omega(E)$ is given by

$$\langle H_0; E|W|H_0; E'\rangle = \delta(E - E')\omega(E) . \tag{1.6}$$

The second and third of our theorems deal with the nature of the solutions of U, U_0, of (1.1).

Theorem 2. Let us write

$$U = I - K, \qquad U_0 = I + K_0 . \tag{1.7}$$

Furthermore, let K, K_0 be triangular in some representation, say x-representation, for example,

$$\begin{cases} \langle x|K|x'\rangle = 0 & x' > x, \\ \langle x|K_0|x'\rangle = 0 & x' > 0. \end{cases} \tag{1.8}$$

Then equation (1) can be solved for *both* U and U_0. Moreover, the solution will be unique. The equation for $\langle x|K|x'\rangle$ will be the Gelfand-Levitan equation. We can motivate the introduction of the triangularity conditions (1.8) by noting that from (1.2), (1.4), (1.7) and (1.8) we have

$$\begin{cases} \langle x|H;E\rangle = \langle x|H_0;E\rangle + \int_{-\infty}^{x} \langle x|K|x'\rangle \,dx' \langle x'|H_0;E\rangle \,d, \\ \langle x|H_0;E\rangle = \langle x|H;E\rangle + \int_{\infty}^{x} \langle x|K_0|x'\rangle \,dx' \langle x'|H_0;E \quad . \end{cases} \tag{1.9}$$

Hence $\langle x|H;E\rangle$ approaches $\langle x|H_0;E\rangle$ as x approaches $-\infty$. That is, the triangularity conditions specify the boundary conditions which $\langle x|H;E\rangle$ are to satisfy.

Theorem 3 is the most surprising of the three theorems.

Theorem 3. If K, K_0 satisfy triangularity conditions (1.8), then the solution U, U_0 of equation (1.1) satisfies the condition (1.2).

The use of the three theorems is the following: one can find an operator H whose eigenfunctions $|H;E\rangle$ are prescribed to have the normalization given by (1.5) and the asymptotic form

$$\lim_{x\to-\infty} \langle x|H;E\rangle = \langle x|H_0;E\rangle, \tag{1.10}$$

where $|H_0;E\rangle$ are prescribed eigenfunctions of a known Hamiltonian H_0. To obtain the operator H and the eigenfunctions $|H;E\rangle$ one need merely construct the operator W and solve equation (1.1) for U, U_0 for the case where K, K_0 have the triangularity properties (1.8). Then H is given by (1.3) and $|H;E\rangle$ by (1.4).

2. – The eigenfunctions of the unperturbed Hamiltonian.

We have assumed that the unperturbed Hamiltonian H_0 has a continuous spectrum only. In most cases the spectrum will be degenerate. It will therefore be convenient to introduce a set of commuting variables, collectively denoted by A_0, each of which also commutes with H_0, such that A_0 and H_0 form a complete set of commuting variables. Using a modification of Dirac's notation we denote the state which is simultaneously an eigenstate of H_0 and A_0 corresponding to the eigenvalues E and a of H_0 and A_0 respectively by $|H_0, A_0; E, a\rangle$. An example of A_0 occurs in the case where H_0 is the kinetic energy operator. A_0 could then be chosen to be the operator whose eigenvalues give the direction of the momentum.

We have

$$H_0 |H_0, A_0; E, a\rangle = E |H_0, A_0; E, a\rangle \,. \tag{2.1}$$

If we assume that the eigenfunctions are normalized, we have

$$\langle H_0, A_0; E, a | H_0, A_0; F, b\rangle = \delta(E - F)\delta(a, b)\,, \tag{2.2}$$

where $\delta(a, b)$ is a generalized δ-function defined by

$$\int f(a)\delta(a, b)\,\mathrm{d}a = f(b) \quad \text{if the range of integration includes } b$$
$$= 0 \quad \text{otherwise.} \tag{2.3}$$

(The integration is to be understood as summation over the values of a in the discrete spectrum.) Since the set of eigenfunctions is to be a complete set, we write

$$\int\int |H_0, A_0; E, a\rangle \,\mathrm{d}E\,\mathrm{d}a \langle H_0, A_0; E, a| = I\,, \tag{2.4}$$

where I is identity operator.

3. – The eigenfunctions of the perturbed Hamiltonian and the transformation operator.

The perturbed Hamiltonian H is given by

$$H = H_0 + \varepsilon V \tag{3.1}$$

where V is the scattering potential and ε is a smallness parameter. We have assumed that the spectrum of H is the same as H_0. Hence the degeneracy of the spectrum of H is the same as that of H_0. Let us introduce a set of commuting operators A, analogous to A_0, which together with H form a complete set of commuting variables. We denote the eigenfunction of H and A which belongs to the eigenvalues E and a of H and A respectively by $|H, A; E, a\rangle$. Hence

$$H|H, A; E, a\rangle = E|H, A; E, a\rangle . \tag{3.2}$$

We also introduce the transformation operator U defined by

$$|H, A; E, a\rangle = U|H_0, A_0; E, a\rangle . \tag{3.3}$$

(This operator is also used, for example, by FRIEDRICHS [7]). We now proceed to develop some relations which U must satisfy. Substituting (3.3) into (3.2), we have

$$\begin{aligned} H|H, A; E, a\rangle &= EU|H_0, A_0; E, a\rangle \\ &= UE|H_0, A_0; E, a\rangle \\ &= UH_0|H_0, A_0; E, a\rangle \end{aligned} \tag{3.4}$$

or

$$HU|H_0, A_0; E, a\rangle = UH_0|H_0, A_0; E, a\rangle . \tag{3.5}$$

Hence on using (2.4),

$$HU = UH_0 . \tag{3.6}$$

For any function $f(H)$ of H we infer

$$f(H)U = Uf(H_0) . \tag{3.7}$$

It will be shown later that U has an inverse, U^{-1}. From (3.6), then,

$$H = UH_0U^{-1} \tag{3.8}$$

and we see that the transformation U is actually a canonical transformation between H and H_0. It is further seen that a relation like (3.8) can hold only when the spectrum of H and H_0 are the same.

---

[7] K. O. FRIEDRICHS: *Comm. on Pure and Applied Math.*, **1**, 361 (1948).

The operator U or equivalently the eigenfunctions $|H, A; E, a\rangle = U|H_0, A_0; E, a\rangle$ are not unique. It can be shown that all possible solutions of (3.6) satisfy the integral equation

$$U = L + \varepsilon \int \frac{P}{E - H_0} V U \delta(E - H_0)\, dE\,, \tag{3.9}$$

where L is an arbitrary operator which commutes with H_0. The symbol P means « principal part » in the integration, the range of integration is the range of the spectrum of E. The operator $\delta(E - H_0)$ is defined by

$$\delta(E - H_0) = \int |H_0, A_0; E, a\rangle\, da \langle H_0, A_0; E, a|\,, \tag{3.10}$$

and has the properties

$$H_0 \delta(E - H_0) = \delta(E - H_0) H_0 = E\,\delta(E - H_0)\,, \tag{3.11}$$

$$\int \delta(E - H_0)\, dE = I\,. \tag{3.12}$$

Equation (3.12) follows from (2.4).

We note that operators which commute with H_0, are in a sense, diagonal in the H_0 representation. Let B be any operator which commutes with H_0; then

$$\langle H_0, A_0; E, a|\, B\, |H_0, A_0; F, b\rangle = \langle a|\beta(E)|b\rangle \delta(E - F)\,, \tag{3.13}$$

where $\langle a|\beta(E)|b\rangle$ is a function of a, b and E (a *proper* function, i.e., not a δ-function, in terms of E) which can be obtained from the operator B.

4. — The outgoing and incoming eigenfunctions; the scattering operator.

There are two transformation operators which play a particularly important role. We denote them by $U_\pm$: The integral equations for these operators are obtained by choosing the operator L properly. The operator U_- is required to satisfy the condition

$$\lim_{t \to -\infty} \exp[iH_0 t] \exp[-iHt] U_- |\varphi\rangle = |\varphi\rangle \tag{4.1}$$

where φ is a state in Hilbert space. The meaning of (4.1) is that if we choose the solution $|\varphi(t)\rangle$ of the perturbed Schrödinger equation

$$H|\varphi(t)\rangle = i \frac{\partial}{\partial t} |\varphi(t)\rangle \tag{4.2}$$

to behave like

$$|\varphi(t)\rangle = \exp[-iH_0t]|\varphi\rangle \qquad \text{when } t \to -\infty, \tag{4.3}$$

then at finite times

$$|\varphi(t)\rangle = \exp[-iHt]U_-|\varphi\rangle\,. \tag{4.4}$$

Since the Schrödinger equation has only a first derivative in time, only one initial condition is required to obtain a unique solution. Equation (4.4) may be regarded as the solution of (4.2) with the initial condition (4.3).

In Appendix I it is shown that condition (4.1) fixes the operator L as

$$L = I - i\pi\varepsilon\int\delta(E - H_0)VU_-\delta(E - H_0)\,\mathrm{d}E\,. \tag{4.5}$$

It is to be noted that L as given by (4.5) commutes with H_0, as required. Substituting (4.5) into (3.9) we find

$$U_- = I + \varepsilon\int\gamma_-(E - H_0)VU_-\delta(E - H_0)\,\mathrm{d}E\,, \tag{4.6}$$

where

$$\gamma_-(x) = -i\pi\delta(x) + \frac{P}{x} = \lim_{\zeta\to+0}\frac{1}{x + i\zeta}\,. \tag{4.7}$$

The eigenfunctions $|H, A; E, a\rangle_-$ of H given by

$$|H, A; E, a\rangle_- = U_-|H_0, A_0; E, a \tag{4.8}$$

are generally called the « outgoing waves ». (Usually, however, the plus subscript is used to denote these eigenfunctions.)

The scattering operator can be conveniently expressed in terms of U_-. It is defined in the following way: If $\varphi(t)$ is a solution of the Schrödinger equation (4.2) such that

$$\lim_{t\to-\infty}\exp[iH_0t]|\varphi(t)\rangle = |\varphi\rangle \tag{4.9}$$

exists, then the scattering operator S is given by

$$\lim_{t\to+\infty}\exp[iH_0t]|\varphi(t)\rangle = S|\varphi\rangle\,. \tag{4.10}$$

If we identify $|\varphi(t)\rangle$ with $\exp[-iHt]U_-|\varphi\rangle$ then the scattering operator is given by

$$\lim_{t\to+\infty}\exp[iH_0t]\exp[-iHt]U_-|\varphi\rangle = S|\varphi\rangle\,. \tag{4.11}$$

In Appendix I, it is shown that

$$S = I - 2\pi i\varepsilon \int \delta(E - H_0) V U_- \delta(E - H_0)\, \mathrm{d}E \,. \tag{4.12}$$

The scattering operator takes a state which behaves like the solution $\exp[-iH_0t]|\varphi\rangle$ of the unperturbed equation at $t = -\infty$ into another $\exp[-iH_0t]S|\varphi\rangle$ of the unperturbed equation when $t = +\infty$.

The operator U_+ is used to solve the final value problem. Specifically, U_+ is defined as that transformation which satisfies

$$\lim_{t\to+\infty} \exp[iH_0t] \exp[-iHt] U_+ |\varphi\rangle = |\varphi\rangle \,. \tag{4.13}$$

The state $|\varphi\rangle$ at finite times is then given by

$$|\varphi(t)\rangle = \exp[-iHt] U_+ |\varphi\rangle \,, \tag{4.14}$$

where $|\varphi(t)\rangle$ behaves like $\exp[-iH_0t]|\varphi\rangle$ for $t = +\infty$. In Appendix I it is shown that in this case the operator L must be taken as

$$L = I + i\pi\varepsilon \int \delta(E - H_0) V U_+ \delta(E - H_0)\, \mathrm{d}E \,. \tag{4.15}$$

Hence U_+ satisfies the equation

$$U_+ = I + \varepsilon \int \gamma_+(E - H_0) V U_+ \delta(E - H_0)\, \mathrm{d}E \,, \tag{4.16}$$

where

$$\gamma_+(x) = i\pi\delta(x) + \frac{P}{x} = \lim_{\zeta\to+0,\, \varepsilon} \frac{1}{x - i\zeta} \,. \tag{4.17}$$

The eigenstates $|H, A; E, a\rangle_+$ of H given by

$$|H, A; E, a\rangle_+ = U_+ |H_0, A_0; E, a\rangle \tag{4.18}$$

are usually called the « incoming waves ». From the definition of the scattering operator it is clear that the inverse scattering operator S^{-1} is given by

$$\lim_{t\to-\infty} \exp[iH_0t] \exp[-iHt] U_+ |\varphi\rangle = S^{-1} |\varphi\rangle \,. \tag{4.19}$$

In Appendix I it is shown that

$$S^{-1} = I + 2\pi i\varepsilon \int \delta(E - H_0) V U_+ \delta(E - H_0)\, \mathrm{d}E \,. \tag{4.20}$$

Generally, the operators U are not unitary. However, the operators $U_{\pm}$ are. In Appendix II it is shown that

$$U_{\pm}^{*}U_{\pm} = I \tag{4.21}$$

where the asterisk mean Hermitian adjoint. Equation (4.21) yields orthonormality relations for $|H, A; E, a\rangle_{+}$, since we have

$$\begin{aligned} {}_{\pm}\langle H, A; E, a | H, A; F, b\rangle_{\pm} &= \langle H_0, A_0; E, a | U_{\pm}^{*}U_{\pm} | H_0, A_0; F, b\rangle \\ &= \langle H_0, A_0; E, a | H_0, A_0; F, b\rangle \\ &= \delta(E - F)\delta(a, b) . \end{aligned} \tag{4.22}$$

Since we have assume the spectrum of H is the same as that of H_0, each set of eigenfunctions, $H, A; E, a_{+}$ and $H, A; E, a_{-}$, is complete. Accordingly, any arbitrary state φ can be expanded in terms of either set. Using (4.22) the coefficients of the expansion can be found and it is seen that

$$|\varphi\rangle = \int\int |H, A; E, a\rangle_{\pm}\, \mathrm{d}E\, \mathrm{d}a\, {}_{\pm}\langle H, A; E, a | \varphi\rangle , \tag{4.23}$$

or

$$\int\int |H, A; E, a\rangle_{\pm}\, \mathrm{d}E\, \mathrm{d}a\, {}_{\pm}\langle H, A; E, a| = \mathrm{I}; \tag{4.24}$$

thus on using (4.8), (4.18), (2.4) we have

$$U_{\pm}U_{\pm}^{*} = I . \tag{4.25}$$

Finally conditions (4.21) and (4.25) imply, by definition of inverse, that

$$U_{\pm}^{*} = U^{-1} \tag{4.26}$$

which is the condition that $U_{\pm}$ be unitary.

5. – The general transformation operator and the spectral weight function.

We shall now consider properties of the general operator U which are analogous to the unitary property of $U_{\pm}$.

From (3.9) we see that we can write U as

$$U = M_{\pm} + \varepsilon \int \gamma_{\pm}(E - H_0) V U \delta(E - H_0)\, \mathrm{d}E , \tag{5.1}$$

where

$$M_{\pm} = L \mp i\pi\varepsilon \int \delta(E - H_0) V U \delta(E - H_0)\, \mathrm{d}E \,. \tag{5.2}$$

In Appendix III we prove that as a consequence of (5.1)

$$U = U_{\pm} M_{\pm} \,. \tag{5.3}$$

(This equation also appears in reference (7)). From equation (5.2) it is clear that the operators $M_{\pm}$ commute with H_0. From (5.3) we can show that the operators $M_{\pm}$ have inverses.

As a special case of (5.3) let, us take the positive sign for the subscripts and identify U with U_-. Then using (4.5) for the operator L associated with U_-, we have

$$M_+ = I - 2i\pi\varepsilon \int \delta(E - H_0) V U_- \delta(E - H_0)\, \mathrm{d}E = S \,. \tag{5.4}$$

Hence (5.3) gives

$$U_- = U_+ S \tag{5.5}$$

or on using (4.26)

$$S = U_+^* U_- \,. \tag{5.6}$$

From (5.3) we have generally

$$U_+ M_+ = U_- M_- \tag{5.7}$$

or

$$M_+ = U_+^* U_- M_- = S M_- \,.$$

Hence

$$S = M_+ M_-^{-1} \,. \tag{5.8}$$

Equation (5.8) shows how one can construct the scattering operator from a general transformation U.

Let us define the weight operator W by

$$W = M_+^{-1} M_+^{*-1} = M_-^{-1} M_-^{*-1} \,. \tag{5.9}$$

It is to be noted that W is a positive definite Hermitian operator which commutes with H_0.

From (5.3), (4.21), (4.25) we have

$$W U^* U = \mathrm{I} \,, \tag{5.10}$$

$$U W U^* = \mathrm{I} \,. \tag{5.11}$$

Equation (5.10) gives the orthogonality relations for $|H, A; E, a\rangle$, and (5.14) gives the completeness relation for these eigenstates. From (5.10) and (5.11) it is clear that

$$U^{-1} = WU^* , \tag{5.12}$$

To justify our calling W a weight operator let us write

$$\langle H_0, A_0; E, a | W | H_0, A_0; F, b\rangle = \langle a | \omega(E) | b\rangle \, \delta(E - F) , \tag{5.13}$$

as is possible from (3.13). Then for any state $|\varphi\rangle$ we have, from (5.11) and (2.4),

$$\begin{aligned} |\varphi\rangle &= UWU^* |\varphi\rangle \\ &= \int\int\int\int U |H_0, A_0; E, a\rangle \, \mathrm{d}E \, \mathrm{d}a \langle H_0, A_0; E, a | W | H_0, A_0; F, b\rangle \, \mathrm{d}F \, \mathrm{d}b \cdot \\ &\cdot \langle H_0, A_0; F, b | U^* |\varphi\rangle \\ &\int\int\int\int |H, A; E, a\rangle \, \mathrm{d}E \, \mathrm{d}a \langle H_0, A_0; E, a | W | H_0, A_0; F, b\rangle \, \mathrm{d}F \, \mathrm{d}b \cdot \\ &\cdot \langle H, A; F, b | \varphi\rangle , \end{aligned} \tag{5.14}$$

or on using (5.13) we have the expansion of $|\varphi\rangle$ in terms of $|H, A; E, a\rangle$, namely

$$|\varphi\rangle = \int \mathrm{d}E \iint |H, A; E, a\rangle \, \mathrm{d}a \langle a | \omega(E) | b\rangle \, \mathrm{d}b \langle H, A; E, b | \varphi\rangle . \tag{5.15}$$

If the spectrum of H had no degeneracy, (5.15) would be written as

$$|\varphi\rangle = \int \mathrm{d}E \, |H; E\rangle \omega(E) \langle H; E | \varphi\rangle , \tag{5.15a}$$

and $\omega(E)$ would play the role of the usual weight function. In the case of degeneracy the weight function must be replaced by the operator $\langle a | \omega(E) | b\rangle$.

To summarize: In the direct problem, if H is given and a set of eigenfunctions (or equivalently a transformation operator U) is specified by choosing the appropriate boundary conditions, we can find the spectral weight operator W corresponding to those eigenfunctions.

6. – The inverse problem.

In the inverse problem we are given an operator W and seek the conditions under which we can solve the equations (cf. (5.10) and (5.11))

$$WU^*U = \mathrm{I} , \tag{6.1}$$

$$UWU^* = \mathrm{I} , \tag{6.2}$$

for U such that $|H, A; E, a\rangle = U|H_0, A_0; E, a\rangle$ is an eigenfunction of a Hamiltonian $H = UH_0U^{-1}$ corresponding to a suitable choice of boundary conditions on $|H, A; E, a\rangle$. Specifically we shall rewrite (6.1) and (6.2) as

$$WU^* = U_0 \tag{6.3}$$

$$U_0 = U^{-1} \tag{6.4}$$

and obtain theorems which will tell us under what conditions we can obtain unique solutions U, U_0 of (6.3) such that (6.4) is satisfied and such that the eigenfunctions $|H, A; E, a\rangle = U|H_0, A_0; E, a\rangle$ approach $|H_0, A_0; E, a\rangle$ asymptotically in some specified representation.

First we shall discuss the necessary conditions on W, independent of the boundary conditions on the eigenfunctions $|H, A; E, a\rangle$.

We shall now show that in order for (6.3) to have a solution for U and U_0 such that (6.4) holds, W *must be a positive definite, Hermitian operator which has an inverse.* Further, in order that H, as given by

$$H = UH_0U_0 = UH_0U^{-1}, \tag{6.5}$$

be Hermitian, W *must commute with* H_0.

Once we have proved this, we shall henceforth assume that W is a positive definite Hermitian operator which commutes with H_0 and has an inverse.

First of all let us show that W must have an inverse. From (6.3) and (6.4),

$$WU^*U = \mathrm{I}, \tag{6.6}$$

from which by multiplication on the right by $U^{-1}U^{*-1}$ we get

$$W = U^{-1}U^{*-1} = (U^*U)^{-1}. \tag{6.7}$$

Clearly W has an inverse W^{-1} given by

$$W^{-1} = U^*U. \tag{6.8}$$

That W must be Hermitian follows immediately from (6.7). We can also show from (6.7) that W is positive definite.

We now show that W must commute with H in order that H as given by (6.5) be Hermitian. From (6.5) and (6.3) we have

$$H = UH_0U_0 = UH_0WU^*, \qquad H^* = U_0^*H_0U^* = UWH_0U^*. \tag{6.9}$$

Then if H is to equal H^* we see from (6.9) that the following equation must hold:

$$UH_0WU^* = UWH_0U^* .$$

On multiplying on the right by U^{*-1} and on the left by U^{-1} we have

$$H_0W = WH_0 . \tag{6.9a}$$

Hence, a necessary condition that H be Hermitian is that W commutes with H_0. This condition is also sufficient as can be easily seen.

The potential V which one would obtain is given by

$$\varepsilon V = H - H_0 = UH_0U^{-1} - H_0 , \tag{6.10}$$

$$\varepsilon VU = UH_0 - H_0U . \tag{6.10a}$$

To show that eigenfunctions $|H, A; E, a\rangle$ of H can be obtained from

$$|H, A; E, a\rangle = U|H_0, A_0; E, a\rangle \tag{6.11}$$

we use (6.5). Then

$$\begin{aligned} H|H, A; E, a\rangle &= HU|H_0, A_0; E, a\rangle = UH_0|H_0, A_0; E, a\rangle \\ &= EU|H_0, A_0; E, a\rangle = E|H, A; E, a\rangle . \end{aligned} \tag{6.12}$$

7. – Boundary conditions on the eigenfunctions and triangularity conditions on operators.

It is clear that for a given operator W which satisfies the conditions discussed in Section 6, there are many operators U_0 and U which satisfy $WU^* = U_0$ and $U^{-1} = U_0$. We wish to introduce additional conditions, understandable from a physical point of view, which will enable us to get essentially unique solutions U, U_0 which satisfy $U^{-1} = U_0$. Toward this end we consider imposing boundary conditions on the eigenfunctions $|H, A; E, a\rangle$ to make them unique.

Let us introduce a Hermitian operator Q which is itself a complete set of commuting variables. Let us denote the eigenvalues of Q by q, whose range is

$$q_0 \leqslant q \leqslant q_1 .$$

In special cases q_0 or q_1 can be 0, or $\mp\infty$. The eigenvector of Q corresponding to the eigenvalue q is denoted by $|q\rangle$.

The boundary condition which can reasonably be imposed on $\langle q|H, A; E, a\rangle$ is

$$\lim_{q\to q_0}[\langle q|H, A; E, a\rangle - \langle q|H_0, A_0; E, a\rangle] = 0\,, \tag{7.1}$$

i.e., that $\langle q|H, A; E, a\rangle$ approach $\langle q|H_0, A_0; E, a\rangle$ asymptotically in the Q-representation. We shall now give conditions on U, U_0 such that (7.1) will often hold and U, U_0 will be unique. These conditions will henceforth be called the *triangularity* conditions. Let us write

$$U = I + \varepsilon K\,, \qquad U_0 = I + \varepsilon K_0\,; \tag{7.2}$$

then

$$\langle q|H, A; E, a\rangle = \langle q|H_0, A_0; E, a\rangle + \varepsilon\int_{q_0}^{q_1}\langle q|K|q'\rangle\,\mathrm{d}q'\langle q'|H_0, A_0; E, a\rangle\,, \tag{7.3}$$

$$\langle q|H_0, A_0; E, a\rangle = \langle q|H, A; E, a\rangle + \varepsilon\int_{q_0}^{q_1}\langle q|K_0|q'\rangle\,\mathrm{d}q'\langle q'|H, A; E, a\rangle\,. \tag{7.4}$$

Let us call any operator P triangular in the Q-representation if

$$\langle q|P|q'\rangle = 0 \qquad q' > q \tag{7.5}$$

and if $\langle q|P|q'\rangle$ is a bounded function for $q' \leq q$. If K and K_0 are triangular and q_0 is finite in the Q-representation, then equations (7.3) and (7.4) become

$$\langle q|H, A; E, a\rangle = \langle q|H_0, A_0; E, a\rangle + \varepsilon\int_{q_0}^{q}\langle q|K|q'\rangle\,\mathrm{d}q'\langle q'|H_0, A_0; E, a\rangle\,, \tag{7.6}$$

$$\langle q|H_0, A_0; E, a\rangle = \langle q|H, A; E, a\rangle + \varepsilon\int_{q_0}^{q}\langle q|K_0|q'\rangle\,\mathrm{d}q'\langle q'|H, A; E, a\rangle\,. \tag{7.7}$$

and (7.1) is clearly satisfied.

If $q_0 = -\infty$, some additional restrictions on $\langle q|K|q'\rangle$ and $\langle q|K_0|q'\rangle$ as $q \to -\infty$ are needed in order that the triangularity condition guarantee the asymptotic form (7.1). An example of such a condition (a rather severe one) is that $\langle q|K|q'\rangle$ and $\langle q|K_0|q'\rangle$ vanish when $q < q_{\min}$, where $q_{\min}$ is finite. In Section **17** we shall discuss sufficient conditions which W must satisfy in order that K and K_0 be such that (7.1) holds.

In our present treatment we have not specified in which representation K, K_0 is to be triangular. Our attitude is that physical reasoning should be used to tell us in which representation the asymptotic relation (7.1) is to hold.

and hence in which representation K, K_0 are to be triangular. In contrast to this attitude, previous authors choose the Q-representation in such a way that the potential V is diagonal in that representation. The emphasis in their papers is on the proof that K and K_0 are triangular in this representation.

Most of the remaining sections of the present paper are devoted to theorems which tell us under what conditions U, U_0 can be obtained uniquely once the Q-representation is given in which K, K_0 is to be triangular.

A summary of the theorems is the following:

1) A necessary condition for a solution is that $\langle q|W-I|q'\rangle$ be a bounded function of q' in the neighborhood of $q'=q$.

2) A sufficient condition for a solution U, U_0 of $WU^*=U_0$ is that the operator $(W-I)$ be bounded less than 1.

3) A sufficient condition for the uniqueness of the solution U, U_0 of $WU^*=U_0$ is that $\langle q|K|q'\rangle$ and $\langle q|K_0|q'\rangle$ be bounded functions in every interval. (This condition is automatically satisfied by the definition of triangularity of K, K_0 in the Q-representation).

4) A sufficient condition that $U^{-1}=U_0$ is that either $\langle q|K|q'\rangle$ or $\langle q|K_0|q'\rangle$ be a bounded continuous function of its arguments.

5) An alternative sufficient condition that U, U_0 are unique and $U^{-1}=U_0$ is that $(W-I)$ be bounded less than 1 and $(W-I)$ have an inverse.

8. Solution of the equation for U, U_0; the Gelfand-Levitan equation.

The triangularity conditions (7.5) as applied to K, K_0 enable us to find a relation between U and W, from which, under suitable conditions on W, we can find U explicitly in terms of W.

Let us write

$$W=I+\varepsilon\Omega\,. \tag{8.1}$$

From (6.3) we have, using the fact that W is Hermitian,

$$UW=U_0^*\,. \tag{8.2}$$

Upon substituting (7.2) and (8.1) into (8.2), we obtain

$$K=K_0^*-\Omega-\varepsilon K\Omega \tag{8.3}$$

or, in terms of the Q-representation,

$$\langle q|K|q'\rangle=\langle q|K_0^*|q'\rangle-\langle q|\Omega|q'\rangle-\varepsilon\int_{q_0}^{q}\langle q|K|q''\rangle\,\mathrm{d}q''\langle q''|\Omega|q'\rangle\,. \tag{8.4}$$

In the integral occuring in (8.4) we have used the triangularity property of K.

Now let us take $q' < q$. Since $\langle q | K_0^* | q' \rangle = 0$, we have

$$\langle q | K | q' \rangle = - \langle q | \Omega | q' \rangle - \varepsilon \int_{q_0}^{q} \langle q | K | q'' \rangle \, dq'' \langle q'' | \Omega | q' \rangle \quad \text{for } q' < q. \tag{8.5}$$

Equation (8.5) is our generalization of the Gelfand-Levitan equation. It is an integral equation of the Fredholm type (if q is considered fixed) which gives K in terms of Ω or equivalently U in terms of W.

One could iterate (8.5) to obtain a solution for $\langle q | K | q' \rangle$. However, we shall proceed in a different way by rewriting equation (8.5) in terms of an operator notation.

Let us define the operator $\delta(q - Q)$ by

$$\delta(q - Q) | q' \rangle = \delta(q - q') | q' \rangle , \tag{8.6}$$

from which it can be seen that on using

$$\int_{q_0}^{q_1} | q \rangle \, dq \langle q | = \mathrm{I} ,$$

we have

$$\delta(q - Q) = | q \rangle \langle q | . \tag{8.7}$$

We define the operator $\eta(q - Q)$ by

$$\eta(q - Q) | q' \rangle = \eta(q - q') | q' \rangle , \tag{8.8}$$

where $\eta(q)$ is the Heaviside step function

$$\begin{aligned} \eta(q) &= 1 , & q > 0, \\ &= 0 , & q < 0. \end{aligned} \tag{8.9}$$

Any operator R, say, which is triangular in the sense

$$\langle q | R | q' \rangle = 0 , \qquad q' > q \tag{8.10}$$

together with the boundedness condition for $q' < q$ can be represented as

$$\langle q | R | q' \rangle = \langle q | P | q' \rangle \, \eta(q - q') , \tag{8.11}$$

where

$$\langle q | P | q' \rangle = \langle q | R | q' \rangle \quad \text{for} \quad q' \leqslant q , \tag{8.12}$$

while

$$\langle q|P|q'\rangle \text{ is arbitrary for } q' > q\,.$$

Relation (8.11) can be written

$$R = \int_{q_0}^{q_1} \delta(q-Q)P\eta(q-Q)\,\mathrm{d}q = \int_{q_0}^{q_1} \eta(Q-q)P\delta(q-Q)\,\mathrm{d}q\,, \tag{8.13}$$

where as before P is an operator such that

$$\langle q|P|q'\rangle = \langle q|R|q'\rangle\,, \qquad \text{for } q < q' \tag{8.14}$$

and

$$\langle q|P|q'\rangle \text{ is arbitrary for } q > q'\,.$$

In particular P can be taken as R. Let us multiply each side of equation (8.5) by $\eta(q-q')$. Since $\langle q|K|q'\rangle\eta(q-q') = \langle q|K|q'\rangle$ we have

$$\langle q|K|q'\rangle = -\langle q|\Omega|q'\rangle\eta(q-q') - \\ -\varepsilon\int_{q_0}^{q_1}\langle q|K|q''\rangle\eta(q-q'')\,\mathrm{d}q''\langle q''|\Omega|q'\rangle\eta(q-q')\,. \tag{8.15}$$

In order that $\langle q|K|q'\rangle$ have a solution it is necessary that $\langle q|\Omega|q'\rangle\eta(q-q')$ exist as the kernel of an integral operator. We shall discuss this point more fully later. From (8.15) we get, in an operator notation,

$$K = -\int_{q_0}^{q_1}\delta(q-Q)\Omega\eta(q-Q)\,\mathrm{d}q - \varepsilon\int_{q_0}^{q_1}\delta(q-Q)K\eta(q-Q)\Omega\eta(q-Q)\,\mathrm{d}q\,. \tag{8.16}$$

We regard (8.16) as our equation for K. We maintain that if the operator $A(q)$ exists, where

$$A(q) = [I+\varepsilon\Omega\eta(q-Q)]^{-1}\,, \qquad A^{-1}(q) = [I+\varepsilon\Omega\eta(q-Q)] \tag{8.17}$$

then a solution of (8.16) is

$$K = -\int_{q_0}^{q_1}\delta(q-Q)A(q)\Omega\eta(q-Q)\,\mathrm{d}q\,. \tag{8.18}$$

This can be shown as follows. If $A(q)$ exists we have from $A(q)A^{-1}(q) = A^{-1}(q)A(q) = I$

$$A(q) = I - \varepsilon\Omega\eta(q-Q)A(q) \\ = I - \varepsilon A(q)\Omega\eta(q-Q)\,. \tag{8.19}$$

On substituting K as given by (8.18) into the right side of (8.16) we obtain

$$(8.20)\quad K = -\int_{q_0}^{q_1}\delta(q-Q)\Omega\eta(q-Q)\,\mathrm{d}q + \varepsilon\int_{q_0}^{q_1}\delta(q-Q)\cdot$$

$$\cdot\left\{\int_{q_0}^{q_1}\delta(q'-Q)A(q')\Omega\eta(q'-Q)\,\mathrm{d}q'\right\}\eta(q-Q)\Omega\eta(q-Q)\,\mathrm{d}q =$$

$$= -\int_{q_1}^{q_1}\delta(q-Q)\Omega\eta(q-Q)\,\mathrm{d}q +$$

$$+\varepsilon\int_{q_0}^{q_1}\delta(q-Q)A(q)\Omega\eta(q-Q)\eta(q-Q)\Omega\eta(q-Q)\,\mathrm{d}q =$$

$$= -\int_{q_0}^{q_1}\delta(q-Q)\Omega\eta(q-Q)\,\mathrm{d}q + \varepsilon\int_{q_0}^{q_1}\delta(q-Q)A(q)\Omega\eta(q-Q)\Omega\eta(q-Q)\,\mathrm{d}q\,.$$

In deriving equation (8.20) we have used the fact that $\delta(q-Q)\delta(q'-Q) = \delta(q-Q)\,\delta(q'-q)$. On using (8.19) we have

$$(8.21)\quad K = -\int_{q_0}^{q_1}\delta(q-Q)\Omega\eta(q-Q)\,\mathrm{d}q + \int_{q_0}^{q_1}\delta(q-Q)\Omega\eta(q-Q)\,\mathrm{d}q -$$

$$-\int_{q_0}^{q_1}\delta(q-Q)A(q)\Omega\eta(q-Q)\,\mathrm{d}q\,,$$

which is just (8.18). Hence (8.18) satisfies (8.16).

Now the operator $A(q) = [I + \varepsilon\Omega\eta(q-Q)]^{-1}$ will always exist (and hence (8.18) will provide a solution for K) if Ω is bounded less than $1/|\varepsilon|$, for in this case $\Omega\eta(q-Q)$ is also bounded less than $1/|\varepsilon|$ (the bound of $\eta(q-Q)$ being less than 1). Then $A(q)$ is given by the series

$$(8.22)\qquad A(q) = \sum_{n=0}^{\infty}\varepsilon^n(-1)^n[\Omega\eta(q-Q)]^n\,.$$

Substitution of (8.22) into (8.18) gives the result for K which one would obtain from iteration.

Incidentally, the condition that Ω is bounded less than $1/|\varepsilon|$ assures us that $W = I + \varepsilon\Omega$ is positive definite.

Having obtained K we can find U, on using (8.19), to be

$$U = \mathrm{I} + \varepsilon K = \mathrm{I} - \varepsilon \int_{q_0}^{q_1} \delta(q-Q) A(q) \Omega \eta(q-Q)\, \mathrm{d}q = \int_{q_0}^{q_1} \delta(q-Q) A(q)\, \mathrm{d}q \,, \tag{8.23}$$

and U_0 to be

$$U_0 = WU^* = (\mathrm{I} + \varepsilon\Omega) \int_{q_0}^{q_1} A^*(q)\delta(q-Q)\, \mathrm{d}q = \tag{8.24}$$

$$= \int_{q_0}^{q_1} \{[\mathrm{I} + \varepsilon\eta(q-Q)\Omega] + \varepsilon\eta(Q-q)\Omega\} A^*(q)\delta(q-Q)\, \mathrm{d}q =$$

$$= \int_{q_0}^{q_1} \{A^{*-1}(q) + \varepsilon\eta(Q-q)\Omega\} A^*(q)\delta(q-Q)\, \mathrm{d}q = \mathrm{I} + \varepsilon \int_{q_0}^{q_1} \eta(Q-q)\Omega A^*(q)\delta(q-Q)\, \mathrm{d}q \,.$$

where the asterisk indicates the Hermitian adjoint, i.e.

$$A^*(q) = [I + \varepsilon\eta(q-Q)\Omega]^{-1}, \qquad A^{*-1}(q) = [I + \varepsilon\eta(q-Q)\Omega] \,. \tag{8.17a}$$

Hence K is given by

$$K_0 = \frac{1}{\varepsilon}[U_0 - \mathrm{I}] = \int_{q_0}^{q_1} \eta(Q-q)\Omega A^*(q)\delta(q-Q)\, \mathrm{d}q \,. \tag{8.25}$$

An alternative expression for K_0 will prove useful later. It arises from the identity

$$\Omega[I + \varepsilon\eta(q-Q)\Omega]^{-1} = [I + \varepsilon\Omega\eta(q-Q)]^{-1}\Omega \,, \tag{8.26}$$

or

$$\Omega A^*(q) = A(q)\Omega \,.$$

The identity (8.26) can be proved by multiplying on the right by $[I + \varepsilon\eta(q-Q)\Omega]$ and on the left by $[I + \varepsilon\Omega\eta(q-Q)]$. The alternative form K_0 is then

$$K_0 = \int_{q_0}^{q_1} \eta(Q-q) A(q)\Omega\delta(q-Q)\, \mathrm{d}q \,. \tag{8.27}$$

On comparing (8.27) with (8.13) it is clear that K_0 has the desired triangularity properties.

9. – Uniqueness theorems.

In this section we prove the uniqueness of the solutions (8.18) and (8.27) for K and K_0. The proof presented here depends on the positive definite character of W.

Theorem: If there is a solution U, U_0 of $WU^* = U_0$ such that

$$\langle q|\, U\,|q'\rangle = \delta(q-q') + \varepsilon\langle q|\, K\,|q'$$

and

$$\langle q|\, U_0\,|q'\rangle = \delta(q-q') + \varepsilon\langle q|\, K_0\,|q'\rangle\,,$$

where $\langle q|\, K\,|q'\rangle$ and $\langle q|\, K_0\,|q'\rangle$ are bounded functions of q and q' and are triangular in the sense that they vanish when $q' > q$, then this solution is the only solution of this character.

Proof: Assume that there is another such solution $U^{(1)} = I + K^{(1)}$ and $U_0^{(1)} = I + \varepsilon K_0^{(1)}$. Then in addition to having the relation

$$WU^* = U_0 \tag{9.1}$$

we should have

$$WU^{*(1)} = U_0^{(1)}\,. \tag{9.2}$$

On subtracting we find

$$W(K^* - K^{*(1)}) = (K_0 - K_0^{(1)})\,. \tag{9.3}$$

Let us define R and R_0 by

$$R = K - K^{(1)}\,, \qquad R_0 = K_0 - K_0^{(1)}\,. \tag{9.4}$$

From the properties of K, $K^{(1)}$, K_0, $K_0^{(1)}$ we find that $\langle q|\, R\,|q'\rangle$ and $\langle q|\, R_0\,|q'\rangle$ vanish for $q' > q$ and that they are bounded functions of q and q'. Equation (9.3) can be written as

$$\int_{q_0}^{q'} \langle q|\, W\,|q''\rangle\, \mathrm{d}q''\langle q''|\, R^*\,|q'\rangle = \langle q|\, R_0\,|q'\rangle\,, \tag{9.5}$$

from which

$$\int_{q_0}^{r} \mathrm{d}q \int_{q_0}^{q'} \mathrm{d}q''\langle r|\, R\,|q\rangle\langle q|\, W\,|q''\rangle\langle q''|\, R^*\,|q'\rangle = \int_{q'}^{r} \langle r|\, R\,|q\rangle\, \mathrm{d}q\langle q|\, R_0\,|q'\rangle\,, \tag{9.6}$$

where $r > q'$. Let us now let r approach q'. Under the boundedness conditions assumed for R and R_0, the integral on the right of (9.6) vanishes. Hence

$$\int_{q_0}^{q'} dq \int_{q_0}^{q'} dq'' \langle q'|R|q\rangle\langle q|W|q''\rangle\langle q''|R^*|q'\rangle = 0 . \tag{9.7}$$

If we regard $\langle q|R^*|q'\rangle$ as a vector, say $|\varphi\rangle$, insofar as it is a function of q, and if we regard q' as a fixed parameter, then equation (9.7) has the form

$$\langle\varphi|W|\varphi\rangle = 0 . \tag{9.8}$$

Since W is positive definite, it follows that $|\varphi\rangle = 0$, or, equivalently $R = 0$. Hence $U = U^{(1)}$, $U_0 = U_0^{(1)}$ and the solution is unique.

In Appendix IV we present an alternative proof of the uniqueness. However, it is not quite so useful as the present proof, because instead of using the positive definite character of W, it assumes that $\varepsilon\Omega = W - I$ has an inverse.

10. – Proof that $U^{-1} = U_0$.

Thus far we have discussed only equation

$$WU^* = U_0 \tag{10.1}$$

and have shown that under quite general conditions, this equation has a unique solution if we specify that $\varepsilon K_0 = U_0 - I$ and $\varepsilon K = U - I$ are to be triangular in a specified representation. We have not yet discussed our other requirement on U and U_0, namely

$$U^{-1} = U_0 . \tag{10.2}$$

It might be expected that the solutions U and U_0 which are obtained from (10.1) using the triangularity conditions of K and K_0 would satisfy (10.2) only under rather exceptional conditions on the weight operator W, since equations (10.1) and (10.2) appear to be quite independent of one another. Surprisingly, however, it turns out that rather general conditions on W are sufficient to insure (10.2).

We give two proofs that $U^{-1} = U_0$. One is an abstract proof (using only the equation (10.1)) and the other makes use of the explicit solutions (8.23) and (8.24) for U and U_0. We present the abstract proof here because of its simplicity. The second proof is given in Appendix V.

Theorem: If $\langle q|K|q'\rangle$ and $\langle q|K_0|q'\rangle$ vanish when $q' > q$ and are bounded continuous functions of q and q' for $q < q'$, then $U^{-1} = U_0$.

Proof: We shall prove this theorem in two parts. First we shall prove $UU_0 = I$ (i.e., U_0 is the right inverse of U); then we shall show that U^{-1} exists, from which it follows that $U_0 = U^{-1}$.

Let us first prove $UU_0 = I$ for the case where $\langle q|K|q'\rangle$ and $\langle q|K_0|q'$ are matrices (i.e., where Q has a discrete spectrum) (*). Our requirements on K and K_0 are then

$$\begin{cases} \langle q|K|q'\rangle = 0\,, & q' \geqslant q, \\ \langle q|K_0|q'\rangle = 0\,, & q' \geqslant q. \end{cases} \tag{10.3}$$

Now from (10.1) we have

$$UW = U_0^* \tag{10.4}$$

or

$$UWU^* = U_0^* U^* = UU_0\,. \tag{10.5}$$

The second equation follows from (10.1). From (10.5) we have, on using $U = I + \varepsilon K$, $U_0 = I + \varepsilon K_0$,

$$K + K_0 + \varepsilon K K_0 = K^* + K_0^* + \varepsilon K_0^* K^*\,, \tag{10.6}$$

or, in terms of the Q-representation,

$$\begin{aligned} \langle q|K|q'\rangle + \langle q|K_0|q'\rangle + \varepsilon\langle q|KK_0|q'\rangle = \\ = \langle q|K^*|q'\rangle + \langle q|K_0^*|q'\rangle + \varepsilon\langle q|K_0^*K^*|q'\rangle\,. \end{aligned} \tag{10.7}$$

Now from (10.3) it can be shown that $\langle q|KK_0|q'\rangle = 0$ for $q' \geqslant q$. Hence the left-hand side of (10.7) vanishes when $q' \geqslant q$. But since

$$\langle q|K^*|q'\rangle = \langle q|K_0^*|q'\rangle = \langle q|K_0^*K^*|q'\rangle = 0\,, \qquad q' \leqslant q,$$

it follows that the right-hand side vanishes when $q' < q$. Hence the right and left members of (10.7) vanish identically, i.e.,

$$K + K_0 + \varepsilon K K_0 = 0 = K^* + K_0^* + \varepsilon K_0^* K^*\,. \tag{10.8}$$

(*) This proof was suggested to the authors by Professors J. B. Keller and B. Friedman.

Hence

$$UU_0 = I + \varepsilon K + \varepsilon K_0 + \varepsilon K K_0 = I\,, \tag{10.9}$$

as required.

We shall now indicate the generalization of this proof to the case where Q has a continuous spectrum. The sole difference is that we do not want or need to require that $\langle q|K|q\rangle = \langle q|K_0|q\rangle = 0$, that is, that K and K_0 be zero on the diagonal. In this case our previous considerations lead us to the conclusion that

$$\langle q|K|q'\rangle + \langle q|K_0|q'\rangle + \varepsilon\langle q|KK_0|q'\rangle = 0 \tag{10.10}$$

for $q < q'$ or $q > q'$,

and

$$\langle q|K|q\rangle + \langle q|K_0|q\rangle + \varepsilon\langle q|KK_0|q\rangle \neq 0 \tag{10.10a}$$

generally.

This expression (10.10a) will under our conditions be finite, however, for all q. Let $K + K_0 + \varepsilon + KK_0$ operate on a state $|\varphi\rangle$ in Hilbert space whose Q-representative $\langle q|\varphi\rangle$ is a continuous function of q. Then the Q-representative of $(K + K_0 + \varepsilon KK_0)|\varphi\rangle$ is given by

$$\int_{q_-}^{q} [\langle q|K|q'\rangle + \langle q|K_0|q'\rangle + \varepsilon\langle q|KK_0|q'\rangle]\,\mathrm{d}q'\langle q'|\varphi\rangle \quad .$$

Clearly this integral equals zero, since, for fixed q, the integrand is zero for all q' except possibly for $q' = q$, where it is finite. Hence

$$(K + K_0 + \varepsilon KK_0)|\varphi\rangle = 0 \tag{10.11}$$

for that set of states $|\varphi\rangle$ whose Q-representatives $\langle q|\varphi\rangle$ are continuous. Since this set of states is dense in Hilbert space, one can extend the definition of $K + K_0 + \varepsilon KK_0$ to the whole Hilbert space, in which case (10.11) holds for all states $|\varphi\rangle$ in the Hilbert space. Hence, by definition, (10.8) holds, and, finally so does (10.9).

We proceed now to the second part of the proof. We shall show that under the conditions of the theorem U has an inverse. The inverse $U^{-1} = (I + \varepsilon K)^{-1}$ obviously exists if the bound of K is less than $1/|\varepsilon|$. However, this condition is too restrictive and does not make use of the triangularity properties of K. A necessary and sufficient condition for U to have an inverse is that the equation $U|\varphi\rangle = 0$, when applied to any state $|\varphi\rangle$ in Hilbert space, implies that $|\varphi\rangle = 0$.

We shall now appeal to the theory of the Volterra integral equation to show that U satisfies this condition if U acts on the set of states $|\varphi\rangle$ whose Q-representatives $\langle q|\varphi\rangle$ are continuous functions of q. $U|\varphi\rangle = 0$ can be written as

$$\langle q|\varphi\rangle + \varepsilon\int_{q_0}^{q}\langle q|K|q'\rangle\,\mathrm{d}q'\langle q'|\varphi\rangle = 0\,. \tag{10.12}$$

According to the Volterra theory ([8]) the only continuous function $\langle q|\varphi\rangle$ which can satisfy this equation if $\langle q|K|q'\rangle$ is a continuous, bounded function of q and q' is $\langle q|\varphi\rangle = 0$.

Hence U^{-1} exists when applied to the set of states $|\varphi\rangle$ which have continuous Q-representatives. It follows from (10.4) that $U_0U = I$ when applied to any state in this set. Since the set of continuous representatives is dense in the whole Hilbert space, the extension of U_0U into the rest of Hilbert space must also be I. Finally, therefore,

$$U_0U = I \tag{10.13}$$

over the whole Hilbert space.

In the case where q_0 equals $-\infty$, our reasoning has to be modified slightly, for the Volterra theory cannot be applied directly to this case. Instead of considering all states whose representatives $\langle q|\varphi\rangle$ are continuous, we restrict ourselves to those continuous states for which a $q_{\min}$ exists such that $\langle q|\varphi\rangle = 0$ when $q < q_{\min}$. The value of $q_{\min}$ may be arbitrarily small so long as it is finite. It may also be different for different states. Hence the equation (10.12) is replaced by

$$\langle q|\varphi\rangle + \int_{q_{\min}}^{q}\langle q|K|q'\rangle\,\mathrm{d}q'\langle q'|\varphi\rangle = 0\,. \tag{10.12a}$$

Then the Volterra theory may be applied to show that the only solution in this set is $\langle q|\varphi\rangle = 0$, and a reasoning similar to that used earlies shows that $U_0U = I$ when U_0U is applied to any state in this set. Since this set is dense in the whole Hilbert space, $U_0U = I$ in the whole Hilbert space as before.

The condition that $\langle q'|K|q''\rangle$ be continuous is a little more severe than we should like; we should prefer the condition that $\langle q|K|q'\rangle$ be bounded, so that we might include the case where there are a finite umber of point dis-

---

([8]) W. SCHMEIDLER: *Integralgleichungen mit Anwendungen in Physik und Technik*, I, *Lineare Integralgleichung* (Leipzig, 1950), p. 243.

continuities. The Volterra theory can be extended to include such cases. The proof in Appendix V is also valid for such operators, provided we assume that (8.23) and (8.24) give the solutions for U and U_0 and that the operators W^{-1} and Ω^{-1} exist.

11. – Generalizations.

Up to now we have assumed that Q by itself forms a complete set of commuting variables and looked for a triangular K in terms of this representation. Let us now assume that $Q_1, Q_2, ..., Q_n$ form a complete set of commuting variables. Then K and K_0, in terms of this representation, are given by

$$\langle q_1, q_2, ..., q_n | K | q_1', q_2', ..., q_n' \rangle$$

and

$$\langle q_1, q_2, ..., q_n | K_0 | q_1', q_2', ..., q_n' \rangle .$$

If we assume that K and K_0 are triangular in only one of the variables, q_1, say, i.e., if

$$\langle q_1, q_2, ..., q_n | K | q_1', q_2', ..., q_n' \rangle = 0 , \qquad q_1' > q_1$$

$$\langle q_1, q_2, ..., q_n | K_0 | q_1', q_2', ..., q_n' \rangle = 0 , \qquad q_1' > q_1$$

and if these operators obey the appropriate boundedness and continuity conditions in terms of the variables q_1 and q_1', the previous theory applies without any essential alteration.

In fact, if one writes operators, say P, and vectors $|\varphi\rangle$ in the $Q_1 ... Q_n$ representation as

$$\langle q_1, q_2, ..., q_n | P | q_1', q_2', ..., q_n' \rangle = \langle q_1 | P | q_1' \rangle$$

and

$$\langle q_1, q_2, ..., q_n | \varphi \rangle = \langle q_1 | \varphi \rangle ,$$

and regards $\langle q_1 | P | q_1' \rangle$ as an operator and $\langle q_1 | \varphi \rangle$ as a vector in terms of the remaining variables, one can go through the previous discussion and see that the formulas remain unaltered. One need merely interpret continuity and boundedness in a somewhat more general fashion to preserve the various theorems. We refrain from doing so explicitly, since the procedure is almost obvious.

The following much greater generalization appears possible. If we require that K and K_0 have the same invariant subspace in Hilbert space, and that K^* and K_0^* have invariant subspaces orthogonal to those of K, K_0, the theory appears to be valid. If one works in a proper representation one can generalize

the concept of triangularity in terms of a suitable Q-representation and carry out the previous procedure. Perhaps the writers will sketch this method in later papers.

12. – Relation to the Wiener-Hopf integral equation.

The Wiener-Hopf integral equation for *two* unknown functions $f(z)$ and $g(z)$ is written

$$f(z) = g(z) + \gamma(z) + \int_{-\infty}^{z} f(z-\tau)\beta(\tau)\,\mathrm{d}\tau\,. \tag{12.1}$$

Here z ranges from $-\infty$ to $+\infty$. The functions $\gamma(z)$ and $\beta(z)$ are given, and $f(z)$ and $g(z)$, the unknown functions, satisfy the boundary conditions

$$\begin{cases} f(z) = 0 & z < 0\,, \\ g(z) = 0 & z > 0\,. \end{cases} \tag{12.2}$$

It has been shown (e.g., ref. [9]) that with certain restrictions of $\gamma(z)$ and $\beta(z)$ one may solve for both unknown functions explicitly. The usual procedure makes use of the analytic properties of these functions. Now we shall show that our equations for K and K_0 reduce in special cases to the standard Wiener-Hopf equation (12.1). In terms of the Q-representation, we have (cf. (8.4))

$$\langle q|K|q'\rangle = \langle q|K_0^*|q'\rangle - \langle q|\Omega|q'\rangle - \varepsilon\int_{q_0}^{q} \langle q|K|q''\rangle\,\mathrm{d}q''\langle q''|\Omega|q'\rangle\,. \tag{13.2}$$

This is an equation for both K and K_0^*. Let us now take q_0 and q_1 as being $-\infty$ and $+\infty$ respectively. Furthermore, let us assume $\langle q|\Omega|q'\rangle$, $\langle q|K|q'\rangle$ and $\langle q|K_0^*|q'\rangle$ are functions of the difference $q-q'$ only. We shall write

$$\begin{aligned} \langle q|K|q'\rangle &= K(q-q') \\ \langle q|K_0^*|q'\rangle &= K_0^*(q-q') \\ \langle q|\Omega|q'\rangle &= \Omega(q-q') \end{aligned}$$

---

[9] R. E. A. C. Paley and N. Wiener: *Fourier Transforms in the complex domain* (New York, 1934), Chapter IV.

for the extended operators H and H_0 it is possible that operators U, $U_0 = U^{-1}$ exist such that

$$\tilde{H} = U\tilde{H}_0 U^{-1} . \tag{13.3}$$

Generally, one is required to work in a vector space larger than Hilbert space. The way of extending the space is discussed in Part II where H is taken to have a point spectrum in addition to the continuous spectrum.

14. – A necessary condition for the triangularity of K, K_0.

For many weight operators W there are generally many representations such that we can find unique operators $U = I + \varepsilon K$ and $U_0 = I + \varepsilon K_0$ and such that K and K_0 are triangular in these representations. To get unique solutions for U and U_0, one must specify which of these representations one wishes to use; one should choose from physical considerations the one in which the perturbed eigenfunctions approach the unperturbed eigenfunctions asymptotically.

It should not be assumed, however, that once a positive definite operator $W = I + \varepsilon\Omega$ has been given it is possible to choose *any* representation for triangularity of K, K_0. Generally, once W has been given, there is a restricted class of representations in which K, K_0 can be triangular.

A useful necessary condition, which we have discussed earlier, for the triangularity of K and K_0 is the following: In order that K, K_0 be triangular in the Q-representation, the operator

$$\int_{q_0}^{q_1} \delta(q - Q)\Omega\eta(q - Q)\,\mathrm{d}q ,$$

must exist.

This condition, which follows from equation (8.16), enables us to discard representations in which K, K_0 cannot be triangular. For example, if Ω is a constant, then we have

$$\int_{q_0}^{q_1} \delta(q - Q)\Omega\eta(q - Q)\,\mathrm{d}q = \Omega\int_{q_0}^{q} \delta(q - Q)\eta(q - Q)\,\mathrm{d}q .$$

But the operator $\int_{q_0}^{q} \delta(q - Q)\,\eta(q - Q)\,\mathrm{d}q$ is not defined for *any* Q-representation. Hence if Ω, or equivalently W, is a constant, K, K_0 cannot be triangular in *any* representation. At most we can require that K, K_0 be diagonal in the

Q-representation, i.e., singular along the diagonal. In this case it can be shown that the most general solution for U and U_0 which satisfies $WU^* = U_0$, $U_0 = U^{-1}$ is

$$U = (W)^{-\frac{1}{2}} \exp[i\theta(Q)], \qquad U_0 = (W)^{\frac{1}{2}} \exp[-i\theta(Q)], \tag{14.1}$$

where $\theta(Q)$ is an arbitrary real function of Q. In the case, for example, where H_0 in the Q-representation is given by $-i(\partial/\partial q)(-\infty < q < \infty)$, we have

$$H = -i\frac{\partial}{\partial q} + \theta'(q), \tag{14.2}$$

where the prime indicates the derivative.

An example of a representation in which K, K_0 cannot be triangular for *any* Ω is the H_0-representation, for in this case, since Ω always commutes with H_0, we have

$$\int_{q_0}^{q_1} \delta(q - H_0)\Omega\eta(q - H_0)\,dq = \Omega\int_{q_0}^{q_1} \delta(q - H_0)\eta(q - H_0)\,dq, \tag{14.3}$$

which again is undefined. In (14.3) we have labelled the eigenvalues of H_0 by q instead of E, as in earlier sections of the paper. As before, the requirement nearest to triangularity which we can impose is that K, K_0 be diagonal in the H_0 representation. In this case the general solution for U, U_0 is similar to that obtained for the previous case, namely

$$U = (W)^{-\frac{1}{2}} \exp[i\theta(H_0)], \qquad U_0 = (W)^{\frac{1}{2}} \exp[-i\theta(H_0)], \tag{14.4}$$

where $\theta(H_0)$ is an arbitrary real function of H_0. Now we have

$$H = H_0 \tag{14.5}$$

and the effect of the transformation U is merely to change the normalization of the eigenfunctions of H_0.

15. – A simple example.

An example which provides us with exact, unique solutions U, U_0 of $WU^* = U_0$ such that $U = U_0^{-1}$ and K, K_0 are triangular in a specific representation will now be given. Let us take the Q-representation to be the usual x-representation, i.e., let the eigenvalues q lie in a continuum between $-\infty$

and $+\infty$. Further let H_0 be

$$H_0^Q = -i\frac{\mathrm{d}}{\mathrm{d}q}, \tag{15.1}$$

where the superscript Q denotes that H_0 is expressed in the Q-representation. The eigenfunctions in the Q-representation are given by

$$\langle q|H_0; E\rangle = \frac{1}{\sqrt{2\pi}}\exp[iEq]. \qquad -\infty < E < +\infty \tag{15.2}$$

Let us choose an Ω such that $W = I + \varepsilon\Omega$ is positive definite and $\int \delta(q-Q)\cdot \cdot \Omega\eta(q-Q)\,\mathrm{d}q$ exists. Such an Ω is given by

$$\Omega = \frac{2\alpha}{H_0^2 + \alpha^2}, \qquad \alpha > 0, \tag{15.3}$$

and

$$W = I + 2\varepsilon\frac{\alpha}{H_0^2 + \alpha^2}. \tag{15.4}$$

It is clear that W is positive definite for $\varepsilon \geqslant -\alpha/2$. We shall restrict ourselves to such values of ε. It is easy to show that

$$\langle q|\Omega|q'\rangle = 2\alpha\int_{-\infty}^{+\infty}\langle q|H_0; E\rangle\frac{1}{E^2+\alpha^2}\langle H_0; E|q'\rangle\,\mathrm{d}E = \exp[-\alpha|q-q'|]. \tag{15.5}$$

To show that $\int \delta(q-Q)\,\Omega\eta(q-Q)\,\mathrm{d}q$ exists we write it in the Q-representation:

$$\langle q|\int \delta(q''-Q)\Omega\eta(q''-Q)|q'\rangle = \langle q|\Omega|q'\rangle\eta(q-q') = \tag{15.6}$$

$$= \exp[-\alpha(q-q')]\eta(q-q').$$

The integral equation for $\langle q|K|q'\rangle$ is

$$\langle q|K|q'\rangle = -\exp[-\alpha(q-q')] - \varepsilon\int_{-\infty}^{q}\langle q|K|q''\rangle\exp[-\alpha|q''-q'|]\mathrm{d}q''. \tag{15.7}$$

A solution of this equation is

$$\langle q|K|q'\rangle = \frac{1}{\varepsilon}(\alpha-\gamma)\exp[-\gamma(q-q')]\eta(q-q'), \tag{15.8}$$

where

$$\gamma = \sqrt{\alpha^2 + 2\alpha\varepsilon}\,, \tag{15.8a}$$

or

$$\langle q|\,U\,|q'\rangle = \delta(q-q') + (\alpha-\gamma)\exp\left[-\alpha(q-q')\right]\eta(q-q')\,. \tag{15.9}$$

Hence

$$\langle q|\,U_0\,|q'\rangle = \delta(q-q') + (\gamma-\alpha)\exp\left[-\alpha(q-q')\right]\eta(q-q')\,. \tag{15.10}$$

K, K_0 satisfy the conditions for the uniqueness theorem of Section 9. Hence (15.9) and (15.10) are the only solutions of $WU^*=U_0$ in which K and K_0 have the desired triangularity properties.

Actually, (15.7) has another solution for $\varepsilon<0$. It is

$$\langle q|\,K\,|q'\rangle = \frac{1}{\varepsilon}(\alpha+\gamma)\exp\left[\gamma(q-q')\right]\eta(q-q')\,. \tag{15.11}$$

However, it can be shown that this solution has the property

$$\int_{-\infty}^{q'}\int_{-\infty}^{q'}\langle q'|\,K\,|q\rangle\,dq\langle q|\,W\,|q''\rangle\,dq''\langle q''|\,K^*\,|q'\rangle = \frac{1}{\varepsilon}\frac{(\alpha+\gamma)}{(\alpha-\gamma)} < 0\,, \tag{15.12}$$

since $\varepsilon<0$, and $\alpha>\gamma$. Hence $\langle q|\,K^*\,|q'\rangle$ considered as a function of q, with q' fixed, is outside the domain where W is positive definite. But since we prescribed W to be positive definite, we reject this solution. On the other hand, the first-mentioned solutions for K and K_0 are in the domain where W is positive definite. This example illustrates how the positive definite character of W is used to select unique solutions for K.

It is easy to show that $U^{-1}=U_0$ by using the explicit forms (15.9) and (15.10).

The example that we have discussed here has the virtue of illustrating the theorems discussed earlier. However, it is somewhat trivial in the sense that

$$H = UH_0U_0 = H_0\,, \tag{15.13}$$

as follows from the fact that U commutes with H_0. In fact, with our choice of H_0 and q, U will always commute with H_0 for any W which is such that U, U_0 can be obtained uniquely. This result is a consequence of the fact that $\langle q'|\,U\,|q'\rangle$ will always be a function of the difference $q-q'$ and from this it follows that $\langle H_0; E|\,U\,|H_0; E'\rangle$ is diagonal and thus commutes with H_0. We refrain from giving details. With these choices of W, however, the perturbation $V=0$ is unique.

16. Triangularity of operators and asymptotic conditions on eigenfunctions when $q_0 = -\infty$.

In Section 7 it was indicated that triangularity of the operators K and K_0 is not sufficient to guarantee that $\langle q|H, A; E, a\rangle$ approaches $\langle q|H_0, A_0; E, a\rangle$ as $q \to q_0$ in the case where $q_0 = -\infty$ (or $+\infty$). The triangularity conditions are usually sufficient, however, to permit one to obtain unique solutions U, U_0, and hence a potential V, from a given weight operator W, as seen from the previous work.

In particular, the problem of Section **15** provides us with an example where the triangularity conditions yield unique operators U, U_0 and V, but where the asymptotic conditions fail. To show how the conditions fail we note that on using K as obtained from Section **15** we have

$$\int_{-\infty}^{q} \langle q|K|q'\rangle \, dq' \langle q'|H_0; E\rangle = \frac{(\alpha-\gamma)}{\varepsilon}(\gamma + iE)^{-1} \exp[iEq] , \tag{16.1}$$

Hence the expression $\int_{-\infty}^{q} \langle q|K|q'\rangle \, dq' \langle q'|H_0; E\rangle$ clearly does not approach zero as $q \to -\infty$. We have in fact for finite q:

$$\langle q|H; E\rangle = \langle q|H_0; E\rangle[1 + (\alpha-\gamma)(\gamma + iE)^{-1}] . \tag{16.2}$$

Hence the eigenfunctions $\langle q|H; E\rangle$ are also eigenfunctions of H_0, which was to be expected, since $H = H_0$.

We shall now give two sets of sufficient conditions on W (or equivalently Ω) to guarantee that the triangularity condition implies the asymptotic condition (7.1).

The first sufficient condition is based on the observation that if there is a $q_{\min}$ such that $\langle q|K|q'\rangle$ vanishes when $q < q_{\min}$, then

$$\lim_{q\to-\infty} \int_{-\infty}^{q} \langle q|K|q'\rangle \, dq' \langle q'|H_0, A_0; E, a\rangle = 0 . \tag{16.3}$$

Theorem: If there is a $q_{\min}$ such that $\langle q|\Omega|q'\rangle$ vanishes when $q < q_{\min}$, then

$$\lim_{q\to-\infty} [\langle q|H, A; E, a\rangle - \langle q|H_0, A_0; E, a\rangle] = 0 .$$

Proof: Since Ω is Hermitian, the condition

$$\langle q|\Omega|q'\rangle = 0 \qquad q < q_{\min} , \tag{16.4}$$

implies

$$\langle q|\Omega|q'\rangle = 0 \qquad q' < q_{\min} . \tag{16.5}$$

The equation for $\langle q|K|q'\rangle$ is

$$\langle q|K|q'\rangle = -\langle q|\Omega|q'\rangle - \varepsilon \int_{q_{\min}}^{q} \langle q|K|q''\rangle \,\mathrm{d}q'' \langle q''|\Omega|q'\rangle , \qquad (q' < q). \tag{16.6}$$

Now when $q < q_{\min}$ and $q' < q$,

$$\langle q|K|q'\rangle = 0 , \tag{16.7}$$

as follows from (16.4), (16.5) and (16.6). Hence (16.3) is valid and the asymptotic condition holds.

The sufficient condition which we have stated is somewhat severe in that we may expect (16.3) to hold even if $q_{\min}$ does not exist, provided that $\langle q|\Omega|q'\rangle$ approaches zero sufficiently rapidly as $q \to -\infty$. This leads us to our second sufficient condition which we shall state without proof.

Theorem: Let $\langle q|H_0, A_0; E, a\rangle$ be a bounded function of q for sufficiently small q, and let $\langle q|K|q'\rangle$ be an absolutely integrable function of q'; further, let $|\langle q|\Omega|q'\rangle| \leqslant r(q')$ for all q, where $r(q')$ is a function such that

$$\int_{-\infty}^{q} r(q')\,\mathrm{d}q' < \infty .$$

Then

$$\lim_{q\to-\infty} \int_{-\infty}^{q} \langle q|K|q'\rangle \,\mathrm{d}q' \langle q'|H_0, A_0; E, a\rangle = 0 ,$$

and hence

$$\lim_{q\to-\infty} [\langle q|H, A; E, a\rangle - \langle q|H_0, A_0; E, a\rangle] = 0 .$$

Appendix I

Expressions for $U_{\mp}$, S, S^{-1}.

Using equation (3.7) we have

$$\exp[iH_0 t] \exp[-iHt] U_- = \exp[iH_0 t] U_- \exp[-iH_0 t] . \tag{I.1}$$

Using (3.9) with $U = U_-$, and using the fact that L commutes with H_0, we

obtain

$$\text{(I.2)}\quad \exp[iH_0t]U_-\exp[-iH_0t] = L + \varepsilon\int\frac{P}{E-H_0}\exp[-i(E-H_0)t]VU_-\delta(E-H_0)\,\mathrm{d}E\,.$$

Now it can be shown that

$$\text{(I.3)}\qquad \lim_{t\to\pm\infty}\frac{P}{E-H_0}\exp[-i(E-H_0)t] = \mp i\pi\delta(E-H_0)\,,$$

when both sides of the equation are applied to appropriate states in Hilbert space. Hence

$$\text{(I.4)}\quad \lim_{t\to-\infty}\exp[iH_0t]\exp[-iHt]U_-|\varphi\rangle = L|\varphi\rangle + i\pi\int\delta(E-H_0)VU_-\delta(E-H_0)\,\mathrm{d}E\,|\varphi\rangle = |\varphi\rangle\,,$$

from which (4.5) follows. Equation (4.15) is obtained similarly. To get the expression for S one shows, using (I.3) and (4.5), that

$$\text{(I.5)}\quad \lim_{t\to+\infty}\exp[iH_0t]\exp[-iHt]U_-|\varphi\rangle = L|\varphi\rangle - i\pi\int\delta(E-H_0)VU_-\delta(E-H_0)\,\mathrm{d}E\,|\varphi\rangle =$$

$$= \left[I - 2i\pi\int\delta(E-H_0)VU_-\delta(E-H_0)\,\mathrm{d}E\right]|\varphi\rangle = S|\varphi\rangle\,.$$

The expression for S^{-1} is obtained similarly.

Appendix II

Proof of $U_\pm^*U_\pm = I$.

Let us consider the equation with the negative subscript. From (4.6) we have

$$\text{(II.1)}\quad U_-^*U_- = I + \varepsilon\int\gamma_-(E-H_0)VU_-\delta(E-H_0)\,\mathrm{d}E + \varepsilon\int\delta(E-H_0)U_-^*V\gamma_-^*(E-H_0)\,\mathrm{d}E + \varepsilon^2\int\int\delta(E-H_0)U_-^*V\gamma_-^*(E-H_0)\gamma_-(E'-H_0)VU_-\delta(E'-H_0)\,\mathrm{d}E\,\mathrm{d}E'\,,$$

where

$$\gamma_{\pm}^{*}(E-H_0) = +i\pi\delta(E-H_0) + \frac{P}{E-H_0} = -\gamma_{-}(H_0-E)\,. \tag{II.2}$$

Now, it can be shown that the functions $\gamma_{\pm}(x)$ satisfy the identity

$$\gamma_{\pm}(x)\gamma_{\pm}(y) = \gamma_{\pm}(x+y)[\gamma_{\pm}(x)+\gamma_{\pm}(y)]\,. \tag{II.3}$$

Hence

$$\begin{aligned}\gamma_{\pm}^{*}(E-H_0)\gamma_{-}(E'-H_0) &= -\gamma_{-}(H_0-E)\gamma_{-}(E'-H_0)\\ &= -\gamma_{-}(E'-E)[\gamma_{-}(H_0-E)+\gamma_{-}(E'-H_0)]\\ &= \gamma_{-}(E'-E)[\gamma_{\pm}^{*}(E-H_0)-\gamma_{-}(E'-H_0)]\,.\end{aligned} \tag{II.4}$$

Then the fourth term on the right of (II.1) is given by

$$\begin{aligned}&\varepsilon^2\iint\delta(E-H_0)U_{\pm}^{*}V\gamma_{\pm}^{*}(E-H_0)\gamma_{-}(E'-H_0)VU_{-}\delta(E'-H_0)\,\mathrm{d}E\,\mathrm{d}E' =\\ &= \varepsilon^2\iint\gamma_{-}(E'-E)\delta(E-H_0)U_{\pm}^{*}V\gamma_{\pm}^{*}(E-H_0)VU_{-}\delta(E'-H_0)\,\mathrm{d}E\,\mathrm{d}E' -\\ &-\varepsilon^2\iint\gamma_{-}(E'-E)\delta(E-H_0)U_{\pm}^{*}V\gamma_{-}(E'-H_0)VU_{-}\delta(E'-H_0)\,\mathrm{d}E\,\mathrm{d}E' =\\ &= \varepsilon^2\int\gamma_{-}(E'-H_0)\left[\int\delta(E-H_0)U_{\pm}^{*}V\gamma_{\pm}^{*}(E-H_0)\,\mathrm{d}E\right]VU_{-}\delta(E'-H_0)\,\mathrm{d}E' -\\ &-\varepsilon^2\int\delta(E-H_0)U_{\pm}^{*}V\left[\int\gamma_{-}(E'-H_0)VU_{-}\delta(E'-H_0)\,\mathrm{d}E'\right]\gamma_{-}(H_0-E)\,\mathrm{d}E\,.\end{aligned} \tag{II.5}$$

In equation (II.5) we have used the fact that

$$f(E)\delta(E-H_0) = f(H_0)\delta(E-H_0)\,, \tag{II.6}$$

where $f(E)$ is any function of E. In the last equation of (II.5), we write

$$\left[\varepsilon\int\delta(E-H_0)U_{\pm}^{*}V\gamma_{\pm}^{*}(E-H_0)\,\mathrm{d}E\right] = U_{\pm}^{*}-I\,,$$

$$\left[\varepsilon\int\gamma_{-}(E-H_0)VU_{-}\delta(E-H_0)\,\mathrm{d}E\right] = U_{-}-I\,,$$

so that after rearrangement of terms the fourth term on the right of (II.1) becomes

$$\begin{aligned}&\varepsilon^2\iint\delta(E-H_0)U_{\pm}^{*}V\gamma_{\pm}^{*}(E-H_0)\gamma_{-}(E'-H_0)VU_{-}\delta(E'-H_0)\,\mathrm{d}E\,\mathrm{d}E' -\\ &= -\varepsilon\int\gamma_{-}(E-H_0)VU_{-}\delta(E-H_0)\,\mathrm{d}E - \varepsilon\int\delta(E-H_0)U_{\pm}^{*}V\gamma_{\pm}^{*}(E-H_0)\,\mathrm{d}E +\\ &+\varepsilon\int\gamma_{-}(E-H_0)U_{\pm}^{*}VU_{-}\delta(E-H_0)\,\mathrm{d}E - \varepsilon\int\delta(E-H_0)U_{\pm}^{*}VU_{-}\gamma_{-}(H_0-E)\,\mathrm{d}E\,.\end{aligned} \tag{II.7}$$

The first two terms on the right of (II.6) cancel the second and third terms on the right of (II.1).

We can write the last two terms on the right on (II.7) as

$$\text{(II.8)}\quad \varepsilon\int_{\gamma}(E'-H_0)U_-^*VU\,\delta(E'-H_0)\,\mathrm{d}E'-\varepsilon\int\delta(E-H_0)U_-^*VU\,\gamma_-(H_0-E)\,\mathrm{d}E=$$

$$=\varepsilon\iint\gamma_-(E'-E)\delta(E-H_0)U_-^*VU_-\delta(E'-H_0)\,\mathrm{d}E\,\mathrm{d}E'-$$

$$-\varepsilon\iint\delta(E-H_0)U_-^*VU_-\gamma_-(E'-E)\delta(E'-H_0)\,\mathrm{d}E\,\mathrm{d}E'=0\,.$$

Hence the fourth term on the right of (II.1) merely cancels the second and third terms and we are left with our desired result

$$U_-^*U_-=I\,.$$

The relation $U_+^*U_+=I$ is proved similarly.

Appendix III

Proof of $U=U_-M_-$.

Let us prove $U=U_-M_-$. From equations (4.6) and (5.1) we have

$$\text{(III.1)}\quad U_-^*U=M_-+\varepsilon\int\gamma_-(E-H_0)VU\delta(E-H_0)\,\mathrm{d}E+$$

$$+\varepsilon\int\delta(E-H_0)U_-^*V\gamma_-^*(E-H_0)\,\mathrm{d}EM_-+$$

$$+\varepsilon^2\iint\delta(E-H_0)U_-^*V\gamma_-^*(E-H_0)\gamma_-(E'-H_0)VU\delta(E'-H_0)\,\mathrm{d}E\,\mathrm{d}E'\,.$$

By a procedure similar to that used in Appendix II, one can show that the fourth term on the right of (III.1) cancels the second and third term. Hence

$$\text{(III.2)}\qquad U_-^*U=M_-\,.$$

Finally, on using the completeness relation (4.25) we have the desired result. The relation $U=U_+M_+$ is proved similarly.

Appendix IV

Alternative uniqueness theorem.

Theorem: If the inverse of $[I + \varepsilon\Omega\eta(q-Q)]$, namely $A(q)$, exists and is unique and if the inverse of Ω exists, then the only possible solution of (8.16) for K is given by (8.18).

Proof: From the triangularity properties of K we may write

$$K = \int_{q_0}^{q_1} \delta(q-Q) K \eta(q-Q)\,\mathrm{d}q\,. \tag{IV.1}$$

Equation (8.16) may then be written

$$\int_{q_0}^{q_1} \delta(q-Q) K \eta(q-Q)[I + \varepsilon\Omega\eta(q-Q)]\,\mathrm{d}q = -\int_{q_0}^{q_1} \delta(q-Q)\Omega\eta(q-Q)\,\mathrm{d}q\,. \tag{IV.2}$$

Now K is to be a triangular operator such that $\langle q|K|q'\rangle = 0$ for $q' > q$. Accordingly it must always be possible to represent K in the form (see (8.13))

$$K = \int_{q_0}^{q_1} \delta(q-Q) P \eta(q-Q)\,\mathrm{d}q\,, \tag{IV.3}$$

where $\langle q|P|q'\rangle = \langle q|K|q'\rangle$ for $q' < q$. If Ω has an inverse we can always find an operator T such that

$$T = P\Omega\,. \tag{IV.4}$$

Hence the general expression for a triangular operator K can be written

$$K = \int_{q_0}^{q_1} \delta(q-Q) T\Omega\eta(q-Q)\,\mathrm{d}q\,. \tag{IV.5}$$

It is our objective to obtain the most general operator T which will allow K to satisfy (IV.2). Having obtained this operator we shall obtain from (IV.5) the most general K which can satisfy this equation. Let us substitute (IV.5) into (IV.2) to obtain an equation for T. The left-hand side becomes

$$\int_{q_0}^{q_1} \delta(q-Q)\left[\int_{q_0}^{q_1} \delta(q'-Q) T\Omega\eta(q'-Q)\,\mathrm{d}q'\right]\eta(q-Q)[I + \varepsilon\Omega\eta(q-Q)]\,\mathrm{d}q = \tag{IV.6}$$

$$= \int_{q_0}^{q_1} \delta(q-Q) T\Omega\eta(q-Q)\eta(q-Q)[I + \varepsilon\Omega\eta(q-Q)]\,\mathrm{d}q =$$

$$= \int_{q_0}^{q_1} \delta(q-Q) T \Omega \eta(q-Q) [I + \varepsilon \Omega \eta(q-Q)] \, \mathrm{d}q =$$

$$= \int_{q_0}^{q_1} \delta(q-Q) T [I + \varepsilon \Omega \eta(q-Q)] \Omega \eta(q-Q) \, \mathrm{d}q \, .$$

In (IV.6) we have used the relations

$$\delta(q-Q)\delta(q'-Q) = \delta(q-Q)\delta(q-q') \, , \tag{IV.7}$$

$$\eta(q-Q)\eta(q-Q) = \eta(q-Q) \, . \tag{IV.8}$$

Hence we have from (IV.2) an equation for T, namely

$$\int_{q_0}^{q_1} \delta(q-Q) T [I + \varepsilon \Omega \eta(q-Q)] \Omega \eta(q-Q) \, \mathrm{d}q = -\int_{q_0}^{q_1} \delta(q-Q) \Omega \eta(q-Q) \, \mathrm{d}q \, . \tag{IV.9}$$

Equation (IV.9) is of the form

$$\int_{q_0}^{q_1} \delta(q-Q) A \eta(q-Q) \, \mathrm{d}q = \int_{q_0}^{q_1} \delta(q-Q) B \eta(q-Q) \, \mathrm{d}q \, , \tag{IV.10}$$

where A and B are two operators. In terms of the Q-representation (IV.10) reads

$$\langle q | A | q' \rangle \eta(q-q') = \langle q | B | q' \rangle \eta(q-q') \, , \tag{IV.11}$$

which means

$$\langle q | A | q' \rangle = \langle q | B | q' \rangle \, , \qquad \text{for } q' < q; \tag{IV.12}$$

$$\langle q | A | q' \rangle = \langle q | C | q' \rangle \, , \qquad \text{for } q' > q, \tag{IV.13}$$

where C is an arbitrary integrable operator. Let us take $C = B + D$ where D is arbitrary; then

$$\langle q | A | q' \rangle = \langle q | B | q' \rangle + \langle q | D | q' \rangle \eta(q'-q) \, , \tag{IV.14}$$

or

$$A = B + \int_{q_0}^{q_1} \delta(q-Q) D \eta(Q-q) \, \mathrm{d}q \, . \tag{IV.15}$$

Equation (IV.15) is the most general solution of (IV.10) for A in terms of B. Let us identify A with $T[I + \varepsilon \Omega \eta(q-Q)]\Omega$ of equation (IV.9) and B with $-\Omega$. Then we have

$$T[I + \varepsilon \Omega \eta(q-Q)]\Omega = -\Omega + \int_{q_0}^{q_1} \delta(q-Q) D \eta(Q-q) \, \mathrm{d}q \, , \tag{IV.16}$$

from which

$$T = -A(q) + \int_{q_0}^{q_1} \delta(q'-Q) D\eta(Q-q')\,\mathrm{d}q'\,\Omega^{-1}A(q)\,. \tag{IV.17}$$

This is the most general solution one can obtain for T. With this T one obtains the most general solution for K, on using (IV.5), namely

$$K = \int_{q_0}^{q_1} \delta(q-Q)T\Omega\eta(q-Q)\,\mathrm{d}q = -\int_{q_0}^{q_1} \delta(q-Q)A(q)\Omega\eta(q-Q)\,\mathrm{d}q + \tag{IV.18}$$

$$+\int_{q_0}^{q_1} \delta(q-Q)\left[\int_{q_0}^{q_1} \delta(q'-Q)D\eta(Q-q')\,\mathrm{d}q'\right]\Omega^{-1}A(q)\Omega\eta(q-Q)\,\mathrm{d}q\,.$$

Now the first term on the right is the solution which we have obtained previously. The second term will be shown to be zero: it becomes

$$\int_{q_0}^{q_1} \delta(q-Q)D\eta(Q-q)\Omega^{-1}\Omega\eta(q-Q)A(q)\,\mathrm{d}q = \tag{IV.19}$$

$$= \int_{q_0}^{q_1} \delta(q-Q)D\eta(Q-q)\eta(q-Q)A(q)\,\mathrm{d}q = 0\,,$$

since

$$\eta(Q-q)\eta(q-Q) = 0\,. \tag{IV.20}$$

In (IV.19) we have used the fact that $\Omega\eta(q-Q)$ commutes with $A(q)$, a result obtained from equation (8.19).

We have thus shown that under our assumptions $A(q)$ and Ω^{-1} exist and are unique, and that hence the only solution for K is given by (8.18).

Appendix V

Alternative proof that $U^{-1} = U_0$.

Theorem: If the conditions on Ω are such that the equation $WU^* = U_0$ has the solutions U and U_0 given by (8.23) and (8.24), and such that Ω^{-1} exists, then $U^{-1} = U_0$.

We shall first prove that

$$UU_0 = I\,, \tag{V.1}$$

or, what is the same, that

$$K + K_0 = -\varepsilon K K_0\,. \tag{V.2}$$

We write (8.18) and (8.27)

$$K = -\int_{q_0}^{q_1} \delta(q - Q) A(q) \Omega \eta(q - Q)\, \mathrm{d}q\,, \tag{V.3}$$

$$K_0 = \int_{q_0}^{q_1} \eta(Q - q) A(q) \Omega \delta(q - Q)\, \mathrm{d}q\,. \tag{V.4}$$

Hence

$$KK_0 = -\int_{q_0}^{q_1}\int_{q_0}^{q_1} \mathrm{d}q\, \mathrm{d}q'\, \delta(q - Q) A(q) \Omega \eta(q - Q) \eta(Q - q') A(q') \Omega \delta(q' - Q)\,. \tag{V.5}$$

Now using the facts that

$$\int_{q_0}^{q_1} \delta(q - Q)\, \mathrm{d}q = I\,, \tag{V.6}$$

and

$$\begin{cases} \delta(q - Q)\eta(q' - Q) = \eta(q' - q)\delta(q - Q)\,, \\ \delta(q - Q)\eta(Q - q') = \eta(q - q')\delta(q - Q)\,, \end{cases} \tag{V.7}$$

we see that from (V.3) and (V.4) we can write

$$K = -\int_{q_0}^{q_1}\int_{q_0}^{q_1} \mathrm{d}q\, \mathrm{d}q'\, \delta(q - Q) \eta(q - q') A(q) \Omega \delta(q' - Q)\,, \tag{V.8}$$

$$K_0 = \int_{q_0}^{q_1}\int_{q_0}^{q_1} \mathrm{d}q\, \mathrm{d}q'\, \delta(q - Q) \eta(q - q') A(q') \Omega \delta(q' - Q)\,. \tag{V.9}$$

Hence

$$K + K_0 = \int_{q_0}^{q_1}\int_{q_0}^{q_1} \mathrm{d}q\, \mathrm{d}q'\, \delta(q - Q) \eta\,(q - q')[A(q') - A(q)] \Omega \delta(q' - Q)\,. \tag{V.10}$$

Now

$$\begin{aligned} A(q') - A(q) &= A(q)[A^{-1}(q)A(q') - I] \\ &= A(q)[A(q') - I + \varepsilon \Omega \eta(q - Q) A(q')]\,. \end{aligned} \tag{V.11}$$

From (8.19)

$$A(q') - I = -\varepsilon \Omega \eta(q' - Q) A(q')\,. \tag{V.12}$$

Hence

$$A(q') - A(q) = \varepsilon A(q) \Omega [\eta(q - Q) - \eta(q' - Q)] A(q')\,. \tag{V.11a}$$

Furthermore,

$$\eta(q-q')[\eta(q-Q)-\eta(q'-Q)] = \eta(q-Q)\eta(Q-q') \,. \tag{V.13}$$

Hence, after some obvious rearrangements we have

$$\eta(q-q')[A(q')-A(q)] = \varepsilon A(q)\Omega\eta(q-Q)\eta(Q-q')A(q') \,. \tag{V.14}$$

Substituting this expression in (V.10) we have, on comparing with (V.5),

$$K + K_0 = \tag{V.15}$$

$$= \varepsilon \int_{q_0}^{q_1}\int_{q_0}^{q_1} \mathrm{d}q\,\mathrm{d}q'\,\delta(q-Q)A(q)\Omega\eta(q-Q)\eta(Q-q')A(q')\Omega\delta(q'-Q) = -\varepsilon K K_0 \,,$$

as required.

We shall now prove

$$U_0 U = I \,. \tag{V.16}$$

Equation (V.16) is equivalent to

$$W U^* U = I \,. \tag{V.17}$$

Since we are assuming that W has an inverse W^{-1} equation (V.17) is equivalent to

$$W^{-1} = U^* U \,. \tag{V.18}$$

From equation (8.23) we have

$$U = \int_{q_0}^{q_1} \delta(q-Q)A(q)\,\mathrm{d}q, \qquad U^* = \int_{q_0}^{q_1} A^*(q')\delta(q'-Q)\,\mathrm{d}q' \,. \tag{V.19}$$

Thus, on using $\delta(q-Q)\delta(q'-Q) = \delta(q-Q)\delta(q-q')$ we obtain

$$U^* U = \int_{q_0}^{q_1} A^*(q)\delta(q-Q)A(q)\,\mathrm{d}q \,. \tag{V.20}$$

At this point it will be convenient to introduce derivatives of operators. We shall do so formally, although undoubtedly it is possible to justify the steps rigorously. On taking the derivative with respect to q of

$$A(q)A^{-1}(q) = I \,, \tag{V.21}$$

one obtains

$$\left[\frac{\mathrm{d}}{\mathrm{d}q}A(q)\right]A^{-1}(q) + A(q)\left[\frac{\mathrm{d}}{\mathrm{d}q}A^{-1}(q)\right] = 0 \,, \tag{V.22}$$

or

$$\frac{\mathrm{d}}{\mathrm{d}q} A(q) = -A(q)\left[\frac{\mathrm{d}}{\mathrm{d}q} A^{-1}(q)\right] A(q) . \tag{V.23}$$

But from (8.17)

$$\frac{\mathrm{d}}{\mathrm{d}q} A^{-1}(q) = \varepsilon\Omega \frac{\mathrm{d}}{\mathrm{d}q}\eta(q-Q) = \varepsilon\Omega\delta(q-Q) . \tag{V.24}$$

Thus on substituting (V.24) into (V.23) and integrating we get

$$A(q) = C - \varepsilon\int_{q_0}^{q} A(q')\Omega\delta(q'-Q)A(q')\,\mathrm{d}q' , \tag{V.25}$$

where C is an operator to be determined by boundary conditions on $A(q)$. We note that

$$\eta(q_1-Q) = 1 , \qquad \eta(q_0-Q) = 0 , \tag{V.26}$$

which follows from the fact that

$$\eta(q_1-Q)|\varphi\rangle = \int_{q_0}^{q_1} |q\rangle\eta(q_1-q)\,\mathrm{d}q\langle q|\varphi\rangle ,$$

for any state $|\varphi\rangle$. Since $q_0 \leqslant q \leqslant q_1$, $\eta(q_1-q) = 1$. Hence $\eta(q_1-Q)|\varphi\rangle = \int_{q_0}^{q_1}|q\rangle\,\mathrm{d}q\langle q|\varphi\rangle = |\varphi\rangle$, from which the first of equations (V.26) follows. The second is obtained similarly. Therefore,

$$A^{-1}(q_1) = W, \qquad A^{-1}(q_0) = I , \tag{V.27}$$

from which it follows that

$$A(q_1) = W^{-1}, \qquad A(q_0) = I . \tag{V.28}$$

Using the second boundary condition of (V.28) in (V.25), we have

$$A(q) = I - \varepsilon\int_{q_0}^{q} A(q')\Omega\delta(q'-Q)A(q')\,\mathrm{d}q' , \tag{V.29}$$

and on using the first of equations (V.28) we get

$$W^{-1} = I - \varepsilon\int_{q_1}^{q_1} A(q)\Omega\delta(q-Q)A(q)\,\mathrm{d}q . \tag{V.30}$$

Bur from (8.26)

$$A(q)\Omega = \Omega A^*(q) \,. \tag{V.31}$$

Hence on using (V.30) and (V.20) we have

$$W^{-1} = I - \varepsilon\Omega \int_{q_0}^{q_1} A^*(q)\delta(q-Q)A(q)\,dq = I - \varepsilon\Omega U^*U \,. \tag{V.32}$$

Now

$$WW^{-1} = (I + \varepsilon\Omega)W^{-1} = I \,, \tag{V.33}$$

or

$$W^{-1} = I - \varepsilon\Omega W^{-1} \,. \tag{V.34}$$

Comparing (V.34) and (V.32), we see that

$$\Omega W^{-1} = \Omega U^*U \,, \tag{V.35}$$

or, if Ω has an inverse,

$$W^{-1} = U^*U, \tag{V.36}$$

or finally

$$WU^*U = U_0U = I \,, \tag{V.37}$$

which was to be shown.

RIASSUNTO (*)

Si mostra come dalla teoria degli operatori in uno spazio vettoriale si possa derivare una forma generalizzata del procedimento di Gelfand-Levitan per ottenere i potenziali di scattering dalle funzioni di misura spettrale. La Parte I tratta il caso in cui le Hamiltoniane perturbate e imperturbate hanno lo stesso spettro che si considera puramente continuo. Lo spazio vettoriale che si considera è lo spazio di Hilbert.

(*) *Traduzione a cura della Redazione.*

Particules de très grandes vitesses en mécanique spinorielle.

A. Proca

Institut Henri Poincaré - Paris

(ricevuto il 4 Luglio 1955)

Resumé. — En prenant comme point de départ la mécanique spinorielle du point matériel, l'auteur étudie le cas où la vitesse tri-dimensionnelle de ce dernier est égale à celle de la lumière. Cette condition n'est naturellement réalisable que si la masse au repos est nulle. Dans ce cas on obtient la description de toute une classe de particules parmi lesquelles le photon, et pour lesquelles on écrit certaines de leurs caractéristiques importantes.

1. – Au moyen d'un simple passage à la limite, toute mécanique relativiste peut fournir la description des propriétés d'une particule qui se meut avec la vitesse de la lumière et qui, par conséquent, présente des caractéristiques assez proches de celles d'un photon. Il en est ainsi, par exemple, de la mécanique spinorielle des particules que nous avons développée ailleurs [1].

Notons qu'il ne suffit pas de faire tendre la vitesse d'une particule vers c, pour obtenir automatiquement la description d'un photon et cela pour plusieurs raisons, à savoir:

A priori, il peut y avoir *plusieurs* types de particules se mouvant avec la vitesse de la lumière mais différant par d'autres propriétés (liées, par exemple, à leur spin); et la comparaison est malaisée, parce que les informations que nous possédons sur le photon s'expriment en termes des grandeurs ondulatoires (ondes électromagnétiques) qui lui sont attachées, alors que la description mécanique envisagée fait appel à des notions corpusculaires. Toute conciliation de ces deux points de vue suppose nécessairement l'introduction de nouvelles hypothèses.

Toutefois, l'étude du cas limite est intéressante en elle-même et nous allons

[1] *Journ. Phys.*, **15**, 65 (1954).

l'esquisser ci-après. Comme dans l'article cité, nous nous limiterons à la forme « classique » de la théorie, cela non seulement pour laisser ouverte toute question d'interprétation, mais aussi et surtout pour obtenir des résultats indépendants de la quantification et soumettre ainsi à un test notre hypothèse fondamentale.

Pour faciliter la lecture, nous résumerons dans le paragraphe suivant les résultats déjà acquis.

2. – Notations, équations fondamentales, etc.

L'hypothèse fondamentale consiste à admettre que le mouvement d'un point est essentiellement décrit par des variables spinorielles, au lieu de l'être par des vecteurs x^ϱ comme en mécanique relativiste classique.

Pour la commodité du formalisme, nous adoptons la technique employée dans la théorie de l'électron de Dirac. Nous désignerons par ξ une matrice à une colonne d'éléments ξ_1, ξ_2, ξ_3, ξ_4 qui se transforme comme le Ψ de la théorie de Dirac et que nous appellerons spineur pour abréger. La matrice adjointe sera définie par:

$$\xi^+ = i\tilde{\xi}^* \gamma^4 ,$$

où $\tilde{\xi}^*$ est la matrice transposée et conjuguée de ξ. γ_2, γ_2, γ_3, γ_4 sont des matrices 4×4 satisfaisant à

$$\gamma^\varrho \gamma^\sigma + \gamma^\sigma \gamma^\varrho = 2\delta^{\varrho\sigma} .$$

En général, les résultats sont indépendants de la représentation des γ^ϱ; lorsque nous en aurons besoin, nous choisirons la représentation usuelle:

$$\gamma^1 = \begin{pmatrix} . & . & . & -i \\ . & . & -i & . \\ . & i & . & . \\ i & . & . & . \end{pmatrix}, \qquad \gamma^2 = \begin{pmatrix} . & . & . & -1 \\ . & . & 1 & . \\ . & 1 & . & . \\ -1 & . & . & . \end{pmatrix},$$

$$\gamma^3 = \begin{pmatrix} . & . & -i & . \\ . & . & . & i \\ i & . & . & . \\ . & -i & . & . \end{pmatrix}, \qquad \gamma^4 = \begin{pmatrix} 1 & . & . & . \\ . & 1 & . & . \\ . & . & -1 & . \\ . & . & . & -1 \end{pmatrix}.$$

Les spineurs ξ, ξ^+ définissent la particule et son mouvement. Les équations auxquelles ils obéissent (voir plus loin) sont établies à partir d'un Lagrangien choisi pour des raisons de simplicité et d'invariance. Il en est de même en théorie de Dirac et comme les éléments simples sont les mêmes dans les deux

cas, il n'est pas étonnant que certains résultats des deux théories soient formellement identiques.

A partir des spineurs ξ, ξ^+ on peut calculer les grandeurs caractérisant la particule dans l'espace-temps. Le lien entre l'espace spinoriel des ξ et l'espace-temps est donné par la relation

$$\frac{dx^\varrho}{d\tau} = \xi^+\gamma^\varrho\xi\,, \tag{1}$$

où τ est le paramètre invariant par rapport auquel on définit le mouvement.

Soit λ_ϱ le vecteur quantité de mouvement, du genre temps; définissons l'invariant

$$\lambda = m_0 c = \sqrt{-\lambda_\varrho\lambda^\varrho}\,, \tag{2}$$

m_0 étant la « masse au repos » de la particule.

Avec $x^4 = ict = ix^0$ et $\gamma^5 = \gamma^1\gamma^2\gamma^3\gamma^4$, nous posons pour les grandeurs quadratiques réelles d'espace-temps:

$$\Omega_1 = -i\xi^+\xi \qquad \Omega_2 = \xi^+\gamma^5\xi$$

$$u^\varrho = \xi^+\gamma^\varrho\xi \qquad w^\varrho = i\xi^+i\gamma^5\gamma^\varrho\xi$$

$$m^{\varrho\sigma} = i\xi^+\frac{i}{2}(\gamma^\varrho\gamma^\sigma - \gamma^\sigma\gamma^\varrho)\xi\,.$$

Entre ces grandeurs existent un certain nombre d'identités algébriques parmi lesquelles nous aurons besoin des suivantes:

$$\begin{cases} w_q u_r - w_r u_q = -m_{qr}\Omega_2 - im_{p4}\Omega_1 \\ -iw_p u_4 + iw_4 u_p = -m_{qr}\Omega_1 + im_{p4}\Omega_2 \end{cases} \qquad (p\,q,\,r = 1,2,3) \tag{3}$$

$$\begin{cases} (m_{23})^2 + (m_{31})^2 + (m_{12})^2 = -(u_4)^2 - (w_4)^2 - \Omega_2^2 \\ (m_{14})^2 + (m_{24})^2 + (m_{34})^2 = +(u_4)^2 + (w_4)^2 + \Omega_1^2 \\ \sum (m_{23})(m_{14}) = i\Omega_1\Omega_2 \end{cases} \tag{4}$$

$$\begin{cases} \sum (m_{23})u_1 = +i\Omega_1 w_4 \\ \sum (m_{14})u_1 = -\Omega_2 w_4\,. \end{cases} \tag{5}$$

Enfin, la relation entre le temps propre ds de la particule et $d\tau$ est donnée

par (*loc. cit.* éq. (5))

$$-c^2\,\mathrm{d}s^2 = \sum(\mathrm{d}x^\varrho)^2 = -(\Omega_1^2 + \Omega_2^2)\,\mathrm{d}\tau^2\,. \tag{6}$$

Cela étant, les équations fondamentales s'écrivent en l'absence de champ:

$$\begin{cases} \dfrac{\mathrm{d}\xi}{\mathrm{d}\tau} = -\lambda_\varrho\gamma^\varrho\xi & \dfrac{\mathrm{d}\xi^+}{\mathrm{d}\tau} = +\lambda_\varrho\xi^+\gamma^\varrho\,, \\ \dfrac{\mathrm{d}x^\varrho}{\mathrm{d}\tau} = \xi^+\gamma^\varrho\xi & \dfrac{\mathrm{d}\lambda_\varrho}{\mathrm{d}\tau} = 0\,. \end{cases} \tag{7}$$

a) *Pour* $\lambda \neq 0$, la solution générale est

$$\xi = a\exp[i\lambda\tau] + b\exp[-i\lambda\tau] \qquad \xi^+ = b^+\exp[i\lambda\tau] + a^+\exp[-i\lambda\tau] \tag{8}$$

où λ_ϱ, a, b sont des constantes satisfaisant à

$$\begin{cases} (i\lambda + \lambda_\varrho\gamma^\varrho)a = 0 & (-i\lambda + \lambda_\varrho\gamma^\varrho)b = 0 \\ a^+(i\lambda + \lambda_\varrho\gamma^\varrho) = 0 & b^+(-i\lambda + \lambda_\varrho\gamma^\varrho) = 0 \\ \lambda^2 + \lambda_\varrho\lambda^\varrho = 0\,. \end{cases} \tag{9}$$

Si l'on prend quatre constantes complexes *arbitraires* et qu'on les arrange en une colonne φ, on peut écrire

$$\begin{cases} a = (-i\lambda + \lambda_\varrho\lambda^\varrho)\varphi & b = (i\lambda + \lambda_\varrho\gamma^\varrho)\varphi \\ a^+ = \varphi^+(-i\lambda + \lambda_\varrho\gamma^\varrho) & b^+ = \varphi^+(i\lambda + \lambda_\varrho\gamma^\varrho)\,. \end{cases} \tag{10}$$

b) *Pour* $\lambda = 0$, on a comme solution générale en fonction de quatre constantes arbitraires, arrangées sous forme de colonne g:

$$\xi = (1 - \lambda_\varrho\gamma^\varrho\cdot\tau)g \qquad \xi^+ = g^+(1 + \lambda_\varrho\gamma^\varrho\cdot\tau)\,. \tag{11}$$

3. – Particules se mouvant avec la vitesse de la lumière.

Imposons à la particule précédente la seule condition que sa vitesse tridimensionnelle soit égale à celle de la lumière. On peut voir immédiatement que cette condition entraîne cette autre que *la masse au repos de la particule*, m_0 donc $\lambda = m_0 c$, *doit être nulle.*

Examinons cette question en détail, puisque nous aurons besoin des ré-

sultats correspondants à plusieurs autres reprises. On a (6)

$$\sum (\mathrm{d}x)^2 = -(\Omega_1^2 + \Omega_2^2)\,\mathrm{d}\tau^2 ,$$

donc si la vitesse est égale à c on devra avoir

(12) $$\boxed{\Omega_1 = -i\xi^+\xi = 0 \qquad \Omega_2 = \xi^+\gamma^5\xi = 0}\ .$$

En fonction des quatre composantes λ de la quantité de mouvement et des quatre constantes arbitraires que contient la solution (10), ces conditions se traduisent par

(13) $$\lambda^2\varphi^+\varphi = 0 , \qquad \lambda^2\varphi^+\gamma^5\varphi = 0$$

et

$$\lambda\cdot\lambda_\varrho(\varphi^+\gamma^5\gamma^\varrho\varphi) = 0 .$$

Deux cas sont possibles:

a) $\varphi^+\varphi = \varphi^+\gamma^5\varphi = \lambda_\varrho\cdot\varphi^+\gamma^5\gamma^\varrho\varphi = 0$ avec $\lambda \neq 0$ et

b) $\lambda = \sqrt{-\lambda_\varrho\lambda^\varrho} = m_0 c = 0$.

Considérons le cas *a*). Puisque $\varphi^+\varphi = \varphi^+\gamma^5\varphi = 0$ les identités mentionnées (3) permettent d'écrire la proportionnalité

$$\frac{\varphi^+\gamma^\varrho\varphi}{\varphi^+\gamma^5\gamma^\varrho\varphi} = \frac{\varphi^+\gamma^\sigma\varphi}{\varphi^+\gamma^5\gamma^\sigma\varphi} = \dots .$$

On n'a donc pas seulement $\lambda_\varrho\cdot\varphi^+\gamma^5\gamma^\varrho\varphi = 0$, mais aussi

$$\lambda_\varrho\cdot\varphi^+\gamma^\varrho\varphi = 0 .$$

D'autre part,

$$\sum \lambda_\varrho^2 = -\lambda^2 \qquad \text{et} \qquad \sum (\varphi^+\gamma^\varrho\varphi)^2 = -(\Omega_1^2 + \Omega_2^2) = 0 .$$

Ces relations permettent d'écrire une identité de Lagrange d'où l'on déduit la proportionnalité

$$\frac{\varphi^+\gamma^\varrho\varphi}{\lambda_\varrho} = \frac{\varphi^+\gamma^\sigma\varphi}{\lambda_\sigma} = \dots .$$

Par conséquent, puisque $\sum (\varphi^+\gamma^\varrho\varphi)^2 = 0$, la somme

$$\sum \lambda_\varrho^2 = -\lambda^2 = 0$$

sera également nulle.

Donc le cas *a*) se ramène au cas *b*) et l'on peut conclure que, en mécanique spinorielle, seules les particules de masse au repos nulle peuvent atteindre la vitesse de la lumière. « *Masse au repos nulle* » *ne veut rien dire de plus que ceci*: entre les composantes de la quantité de mouvement $\lambda_k = p_k$ et l'énergie $\lambda_4 = i\lambda_0 = i(w/c)$, on a toujours dans ce cas la relation

$$p_1^2 + p_2^2 + p_3^2 = \left(\frac{w}{c}\right)^2 .$$

4. – Particules de masse au repos nulle.

Remarquons toutefois que si $\lambda = 0$, c'est la relation (11) et non pas (10) qui convient et à laquelle il faut appliquer nos conditions $\Omega_1 = \Omega_2 = 0$. De (11) on déduit

$$\Omega_1 = -i\xi^+\xi = -ig^+g, \qquad \Omega_2 = \xi^-\gamma^5\xi = g^+\gamma^5 g - 2\lambda_\varrho \cdot g^+\gamma^5\gamma^\varrho g \cdot \tau .$$

Donc, nos conditions reviennent à restreindre la généralité de la constante g en lui imposant les conditions

$$g^+g = 0, \quad g^+\gamma^5 g = 0 \qquad \text{et} \qquad \lambda_\varrho \cdot g^+\gamma^5\gamma^\varrho g = 0 . \tag{14}$$

On satisfait à ces conditions (14) en prenant pour g les solutions des équations:

$$\lambda_\varrho \gamma^\varrho g = 0 , \tag{15}$$

comme on s'en assure aisément.

[Remarquons que ces équations peuvent s'écrire sous une forme présentant une analogie avec celle du cas $\lambda \neq 0$, à savoir

$$\begin{cases} \lambda_0 g = \lambda_K \alpha^K g \\ \lambda_0 \widetilde{g^*} = \lambda_K \widetilde{g^*} \alpha^K \end{cases} \tag{16}$$

où $\widetilde{g^*}$ est la matrice transposée et conjuguée de g, $i\lambda_0 = \lambda_4$ et α^K les matrices de Dirac

$$\alpha^K = i\gamma^4\gamma^K \qquad (K = 1, 2, 3) \qquad \alpha^4 = \gamma^4].$$

Avec cette solution, compte tenu de (11), on a $\xi = g$.

Tous les ξ, *donc toutes les grandeurs d'espace temps d'une particule de vitesse c* (parmi lesquelles il faudra compter le photon), *sont des constantes*. Cette

solution se déduit de la solution générale, valable pour n'importe quel λ.

$$\xi = a \exp [i\lambda\tau] + \exp [-i\lambda\tau] ,$$

en y faisant $\lambda = 0$. Dans ce cas on peut prendre $g = a + b$ et l'on a

$$\lambda_\varrho \gamma^\varrho g = 0 .$$

Remarquons toutefois que les g satisfaisant à ces équations

$$\lambda_\varrho \gamma^\varrho g = 0$$

ne dépendent que de *deux* constantes arbitraires complexes, au lieu de quatre comme dans le cas $\lambda \neq 0$. Deux des quatre composantes, g_1, g_2, étant quelconques, les deux autres s'en déduisent, par exemple, par l'opération

$$\begin{vmatrix} g_3 \\ g_4 \end{vmatrix} = S \begin{vmatrix} g_1 \\ g_2 \end{vmatrix} , \tag{17}$$

avec $S = (1/\lambda_0)(\lambda_1\sigma_1 + \lambda_2\sigma_2 + \lambda_3\sigma_3)$ où les σ sont les matrices 2×2 de Pauli; l'existence de

$$\lambda_0^2 = \lambda_1^2 + \lambda_2^2 + \lambda_3^2$$

introduit deux signes.

5. – Disposition dans l'espace des diverses grandeurs mesurables attachées à la particule.

Considérons dans l'espace les diverses grandeurs d'espace temps

$$\xi^+ A \xi = g^+ A g$$

attachées à une particule de masse au repos nulle.

En vertu de (14) et du paragraphe 3 nous pouvons dire que:

a) la vitesse $u^\varrho = g^+ \gamma^\varrho g$ est proportionnelle à λ_ϱ et au vecteur

$$w^\varrho = i g^+ i\gamma^5 \gamma^\varrho g ,$$

et dans l'espace, les vecteurs u^K, λ^K et w^K ont même support.

b) Considérons le spin de la particule (*loc. cit.* § 11)

$$\tfrac{1}{2} m_{\varrho\sigma} = -\tfrac{1}{2}\xi^+ \cdot \tfrac{1}{2}(\gamma^\varrho\gamma^\sigma - \gamma^\sigma\gamma^\varrho) \cdot \xi ,$$

tenseur antisymétrique et, comme d'habitude, séparons la « partie d'espace » et la « partie de temps » que nous appellerons respectivement

$$\mu_i = -\tfrac{1}{2}m_{jK}, \qquad i\pi_K = \tfrac{1}{2}m_{K4} \qquad (i, j, K = 1, 2, 3). \tag{18}$$

Puisque $g^+g = g^+\gamma^5 g = 0$, les identités (4) et (5) donnent

$$\begin{cases} \sum \mu_K^2 = \sum \pi^2, & \sum \mu_K \pi_K = 0 \\ \sum u_K \mu_K = \sum u_K \pi_K = 0 . \end{cases} \tag{19}$$

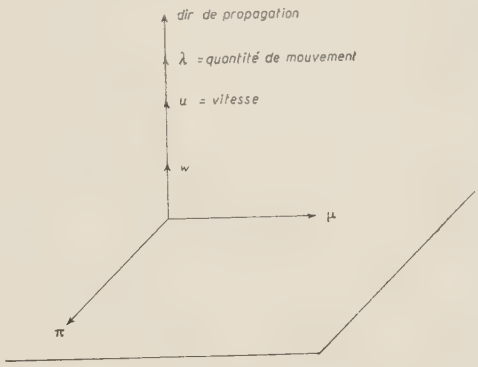

Les deux « vecteurs » π et μ sont égaux, perpendiculaires entre eux et perpendiculaires à la direction de la vitesse.

On peut donc tracer la figure ci-contre des vecteurs qui accompagnent dans son mouvement une particule ayant la vitesse de la lumière, figure qui reproduit la disposition générale des champs électromagnétiques d'un photon.

6. – Expressions simples.

Nous ne restreignons pas la généralité en choisissant un repère tel que la propagation se fasse le long de l'axe des z, donc $u_1 = u_2 = 0$, ce qui entraine $\lambda_1 = \lambda_2 = 0$.

Les grandeurs attachées au photon ont les valeurs suivantes en fonction de deux grandeurs complexes arbitraires ξ_1 et ξ_2:

vitesse (dérivée par rapport à τ):

$$u_1 = 0 \qquad u_2 = 0 \qquad u_3 = \pm 2(\xi_1^*\xi_1 + \xi_2^*\xi_2) \qquad u_4 = 2i(\xi_1^*\xi_1 + \xi_2^*\xi_2) ,$$

vitesse dans l'espace ordinaire:

$$V_1 = 0 \qquad V_2 = 0 \qquad V_3 = \pm c .$$

Vecteur w proportionnel à la vitesse:

$$w_1 = 0 \qquad w_2 = 0 \qquad w_3 = -2(\xi_1^*\xi_1 - \xi_2^*\xi_2) \qquad w_4 = \mp 2i(\xi_1^*\xi_1 - \xi_2^*\xi_2) .$$

Composantes du spin:

$$\tfrac{1}{2}m_{23} = (\xi_1^*\xi_2 + \xi_2^*\xi_1) \qquad \tfrac{1}{2}m_{31} = \tfrac{1}{2}(\xi_1^*\xi_2 - \xi_2^*\xi_1) \qquad \tfrac{1}{2}m_{12} = 0 ,$$

$$\tfrac{1}{2}m_{14} = \mp (1/i)(\xi_1^*\xi_2 - \xi_2^*\xi_1) \qquad \tfrac{1}{2}m_{24} = \pm (\xi_1^*\xi_2 + \xi_2^*\xi_1) \qquad \tfrac{1}{2}m_{34} = 0 ,$$

soit avec les notations (18)

$$\mu_1 = \xi_1^*\xi_2 + \xi_2^*\xi_1 \qquad \mu_2 = (1/i)(\xi_1^*\xi_2 - \xi_2^*\xi_1) \qquad \mu_3 = 0\,,$$

$$\pi_1 = \mp\,(1/i)(\xi_1^*\xi_2 - \xi_2^*\xi_1) \qquad \pi_2 = \pm\,(\xi_1^*\xi_2 + \xi_2^*\xi_1) \qquad \pi_3 = 0\,.$$

Les longueurs correspondantes sont

$$\sum \mu_K^2 = \sum \pi_K^2 = 4\xi_1^*\xi_1 \cdot \xi_2^*\xi_2\,.$$

7. – Quelques remarques.

a) D'une façon générale les équations de base ne fournissent les ξ qu'à un facteur près et une normalisation est nécessaire. On peut poser comme d'habitude par exemple

$$\xi_1^*\xi_1 + \xi_2^*\xi_2 = 1\,.$$

b) Même un corpuscule ayant la vitesse de la lumière reste encore caractérisé par le vecteur w_K. On voit aisément qu'un cas particulier intéressant est celui où

$$w_K = 0 \qquad (K = 1, 2, 3),$$

pour la raison suivante. On a *en général* (vitesse quelconque)

$$u_\varrho m^{\varrho K} = -\,w_K \Omega_2\,,$$

donc si $w_K = 0$, $u_\varrho m^{\varrho K} = 0$. Considérons le repère dans lequel la particule est au repos $u_1 = u_2 = u_3 = 0$; dans ce repère donc $m^{4K} = 0$ comme il est bien connu. Donc une particule avec $w^K = 0$ est telle que son spin se réduit à ses composantes d'espace, à un seul « vecteur », dans le système au repos.

Il n'est pas impossible que ce cas soit exclusivement réalisé dans la nature, la théorie avec $w^K = 0$ donnant le cas idéal général. Quoiqu'il en soit nous retiendrons que $w^K = 0$ représente un cas particulier intéressant et nous l'envisagerons même pour le cas limite qui nous intéresse ici et où l'on ne peut plus parler de « système au repos ».

Dans ce cas, $w^K = 0$ signifie $\xi_1^*\xi_1 = \xi_2^*\xi_2$, la condition de normalisation devient $\xi_1^*\xi_1 = \frac{1}{2}$ et l'on a simplement

$$\sum \mu_K^2 = \sum \pi_K^2 = 1\,.$$

Les « longueurs » d'espace et de temps du spin sont égales à l'unité.

c) Dans ce même cas, les valeurs des grandeurs d'espace temps se déduisent de ξ_1, ξ_2 c'est-à-dire en fin de compte de deux angles φ_1 et φ_2 qui représentent les phases de ξ_1, ξ_2.

Les vecteurs $\boldsymbol{\mu}$ et $\boldsymbol{\pi}$ sont perpendiculaires l'un à l'autre et l'azimut de leur ensemble autour de la direction du mouvement mesuré par l'angle que fait, par exemple, $\boldsymbol{\mu}$ avec l'axe Ox, est égal à $\varphi_2 - \varphi_1$.

On définit ainsi une sorte de *direction de polarisation*, comme pour les photons, mais qui ne dépend pas d'une onde.

Nous avons appelé « spin » le tenseur de composantes $\frac{1}{2}m^{\rho\sigma}$. Sa longueur est nulle $\sum m_{\rho\sigma}m^{\rho\sigma} = 0$. *La longueur du spin des particules de vitesse c est nulle.*

Parmi ces particules on doit compter également le photon. Cependant une comparaison à ce stade n'est pas possible, attendu que l'étude du photon n'a été faite qu'en fonction des champs électromagnétiques qui constituent la lumière et que nous n'avons pas encore étudié ces champs en mécanique spinorielle.

Il nous faut examiner comment cette mécanique attache normalement des champs aux particules, ce que nous allons faire dans l'article suivant.

RIASSUNTO (*)

Partendo dalla meccanica spinoriale del punto materiale, l'autore studia il caso in cui la velocità tridimensionale di questo è uguale a quella della luce. Questa condizione, naturalmente, è realizzabile soltanto se la massa a riposo è nulla. Si ottiene così la descrizione di tutta una classe di particelle, fra cui il fotone, per le quali si scrivono alcune delle loro più importanti caratteristiche.

(*) *Traduzione a cura della Redazione.*

IL NUOVO CIMENTO Vol. II, N. 5 1° Novembre 1955

Interférences en mécanique spinorielle.

A. Proca

Institut Henri Poincaré - Paris

(ricevuto il 4 Luglio 1955)

Resumé. — Après avoir étudié qualitativement les phénomènes d'interférence en se plaçant à un point de vue différent du point de vue habituel, l'auteur montre comment les intégrales premières de la mécanique spinorielle du point matériel permettent d'écrire tout naturellement l'expression d'un champ périodique qu'on peut supposer attaché à la particule et qui intervient dans les termes d'interaction pour rendre compte des phénomènes d'interférences. Ce champ représente l'onde attachée à la particule et la manière dont il a été calculé montre quelles sont ses relations avec les trajectoires et les autres grandeurs corpusculaires. Lorsque la masse au repos est nulle, l'arbitraire dans le choix de ce champ est plus grand. On peut alors trouver aisément parmi toutes les possibilités, une solution qui présente les caractéristiques essentielles des champs électromagnétiques attachés au photon.

1. – Les grandeurs qui caractérisent une particule en mécanique classique, la vitesse, la quantité de mouvement, etc. ne suffisent pas pour expliquer les phénomènes d'interférences; il faut en introduire de nouvelles, qui serviront à préciser les détails de cette explication.

Le progrès initial et essentiel de la mécanique ondulatoire — on l'oublie trop souvent, — a été précisément l'introduction d'une nouvelle caractéristique de la particule, l'*onde* ψ; celle-ci a permis d'ailleurs non seulement la prévision des phénomènes d'interférences, mais aussi le traitement satisfaisant des problèmes quantiques.

En laissant provisoirement ces derniers de coté, la question se pose de savoir si l'introduction des variables spinorielles n'est pas susceptible de faciliter, en mécanique classique, le choix d'une telle grandeur, caractéristique des interférences. Nous verrons qu'il en est bien ainsi, mais auparavant il importe de bien préciser le point de vue adopté dans ce qui suit.

2. – Conditions générales.

Soit X la nouvelle grandeur caractérisant la production des interférences. Lorsque la particule interagit convenablement avec un dispositif expérimental approprié, des interférences apparaissent. Du point de vue théorique cela signifie, en théorie corpusculaire, qu'un terme d'interaction s'ajoutera au Lagrangien et que les nouvelles trajectoires qui en résultent aboutiront toutes exclusivement sur des franges brillantes.

Ce terme d'interaction contiendra d'une part X, qui caractérise le corpuscule et d'autre part, certains éléments caractérisant l'appareil.

En ce qui concerne X, celui-ci doit évidemment présenter une périodicité dans l'espace-temps: cela n'est qu'une autre façon d'énoncer l'hypothèse fondamentale qu'une *onde* est attachée au corpuscule. Le corpuscule est ainsi caractérisé par une période, mais celle-ci ne semble pas décelable directement dans des expériences simples, à cause de sa petitesse. Remarquons alors que toutes les expériences d'interférences mettent en jeu des dispositifs destinés à la mettre en évidence *au moyen de battements*. Le rôle de l'appareil consiste à introduire une « différence de marche » entre les rayons qui interfèrent de façon à permettre l'apparition de battements observables. Dans l'interaction, la période du corpuscule se combine avec un élément caractéristique de l'appareil pour réaliser la différence de marche mentionnée.

Cet élément qui caractérise l'appareil peut être lui-même une période, mais cela n'est pas indispensable. En effet, il peut être simplement une distance spatiale caractéristique, qui se combine avec la période spatiale du corpuscule et donne des battements. Prenons un exemple. Dans l'expérience des trous d'Young (supposés pour le moments infiniment petits pour éliminer les effets de la diffraction) l'appareil est évidemment caractérisé par *la distance finie entre les deux trous*. C'est cette longueur qui apparaît dans le terme d'interaction et se combine avec la période pour fournir une différence de marche convenable et des franges observables.

Cette manière de parler peut sembler oiseuse à première vue. En réalité elle est avantageuse parce qu'elle déplace le problème vers l'étude des termes d'interaction, tout en conservant au mobile son caractère corpusculaire essentiel.

Reprenons l'expérience des trous d'Young et supposons qu'on bouche l'un des trous, par exemple après le départ des corpuscules de la source. Les franges disparaissent et l'explication corpusculaire qu'on donne d'habitude de ce fait se heurte à de grosses difficultés.

En fait, lorsque le corpuscule entre en interaction avec l'écran et fixe ainsi sa trajectoire ultérieure, deux cas peuvent se présenter: ou bien l'écran possède deux trous ou bien il n'en a qu'un seul. S'il est percé de deux trous, *cela signifie qu'il est caractérisé par une distance finie*, celle qui les sépare, précisément.

L'interaction combine cette distance avec la période de la particule pour donner un système de franges. *Si l'on bouche l'un des trous, il n'y a plus de distance spatiale qui caractérise l'appareil*; il n'y a plus de possibilité de combinaison avec la période, il n'y a plus de franges. En d'autres termes, les franges disparaissent non pas parce qu'en bouchant le trou on empêche les corpuscules d'y passer, *mais parce que cela fait disparaître la longueur finie caractéristique de l'écran*, et annule le terme d'interaction correspondant.

Dans l'exemple précédent, l'appareil était caractérisé par une distance finie, unique qui se combine avec X dans le terme d'interaction. Cela n'est pas le seul cas possible. Tout d'abord, la longueur caractéristique peut être non seulement spatiale, mais spatio-temporelle, et l'appareil peut aussi être caractérisé par son équivalent en termes d'angle, etc. Ensuite, l'appareil peut être caractérisé par *plusieurs* de ces longueurs, c'est à dire par tout un spectre discret de longueurs. Enfin, si l'on veut tout grouper en une explication unique, on doit aussi envisager l'éventualité où l'appareil est caractérisé par un spectre *continu* de longueurs. Les phénomènes physiques qui correspondent à cette éventualité sont les phénomènes de diffraction, comme on s'en rend compte aisément en considérant les différences de marche classiques.

Considérons encore une fois des trous d'Young de dimensions normales: lorsqu'on bouche l'un des trous les franges d'interférences disparaissent parceque la distance entre les centres des trous n'existe plus. Mais l'appareil est caractérisé par le trou restant, de diamètre petit mais fini et qui peut être considéré comme une suite continue de longueurs actives. Ces longueurs continuent à se combiner dans le terme d'interaction avec la période du corpuscule et à donner des plages noires ou brillantes: ce sont les figures de diffraction.

En résumé, les appareils interviennent de diverses manières pour interagir avec le corpuscule, dont la grandeur caractéristique qui entre en jeu, X, est essentiellement une grandeur périodique dans l'espace-temps.

Le problème essentiel reste alors le suivant: que devons-nous choisir (en mécanique spinorielle classique), comme grandeur X?

3. – Intégrales premières.

Reprenons les équations générales.

Que λ soit nul ou non, le mouvement libre possède une intégrale première [*loc. cit.* éq. (20)]

$$\lambda_\varrho u^\varrho = \lambda_\varrho \xi^+ \gamma^\varrho \xi_\varrho = \lambda_\varrho \frac{\mathrm{d}x^\varrho}{\mathrm{d}\tau} = \text{constante}\,. \tag{1}$$

a) Si $\lambda = 0$, on déduit des équations fondamentales que *la constante est*

liée à l'action; elle peut s'écrire:

$$\lambda_\varrho \xi^+ \gamma^\varrho \xi = \frac{1}{2}\left(\frac{\mathrm{d}\xi^+}{\mathrm{d}\tau}\,\xi - \dot{\xi}^+\frac{\mathrm{d}\xi}{\mathrm{d}\tau}\right) = I_0 .$$

En fonction des constantes a et b de la solution générale elle a pour valeur

$$\lambda_\varrho \frac{\mathrm{d}x^\varrho}{\mathrm{d}\tau} = i\lambda(b^+b - a^+a) ,$$

de sorte qu'en intégrant une fois on peut écrire

$$\lambda_\varrho x^\varrho = i\lambda\tau(b^+b - a^+a) + C , \tag{2}$$

la nouvelle constante réelle C étant égale par exemple à $\lambda_\varrho r_0^\varrho$ où r_0^ϱ est la position de la particule matérielle à « l'instant » $\tau = 0$.

b) Si $\lambda = 0$, on a la même intégrale première mais avec une constante nulle:

$$\lambda_\varrho u^\varrho = \lambda_\varrho \frac{\mathrm{d}x^\varrho}{\mathrm{d}\tau} = 0 .$$

En intégrant, on aura simplement:

$$\lambda_\varrho x^\varrho = C = \lambda_\varrho r_0^\varrho .$$

4. – Champs spinoriels.

Revenons au cas $\lambda \neq 0$.

Pour un corpuscule donné de moments λ_ϱ et de masse au repos λ/c on aura

$$\xi = a \exp\left[i\lambda\tau\right] + b \exp\left[-i\lambda\tau\right] ,$$

où a et b, définis à une constante multiplicative près, satisfont aux équations

$$(i\lambda + \lambda_\varrho\gamma^\varrho)a = 0 , \qquad (-i\lambda + \lambda_\varrho\gamma^\varrho)b = 0 .$$

Cela peut encore s'écrire

$$\boxed{\xi = a_1 \exp\left[ir_\varrho x^\varrho\right] + b_1 \exp\left[-ir_\varrho x^\varrho\right]} , \tag{3}$$

avec

$$a_1 = a \exp\left[\frac{-C}{(b^+b - a^+a)}\right] , \qquad b_1 = b \exp\left[\frac{+C}{(b^+b - a^+a)}\right] , \qquad r = \frac{\lambda}{i(b^+b - a^+a)} ;$$

a_1, b_1 satisfont aux mêmes conditions que les a, b et l'on a

$$b_1^+ b_1 - a_1^+ a_1 = b^+ b - a^+ a \,. \tag{4}$$

Le sens de (3) est clair. Le premier membre ξ s'obtient en remplaçant dans le second x^ϱ par leurs valeurs en fonction de τ, c'est-à-dire *en suivant la trajectoire de la particule. ξ est une fonction de τ.*

Considérons maintenant une particule définie à la manière habituelle (par les λ_ϱ, a, b et les diverses constantes) et soit x^ϱ un point *quelconque variable* de l'espace temps. Nous pouvons attacher à cette particule la grandeur (spinorielle)

$$\boxed{X = a_1 \exp\left[i r_\varrho x^\varrho\right] + b_1 \exp\left[-i r_\varrho x^\varrho\right]} \,. \tag{5}$$

(5) est formellement identique à (3); la différence consiste dans le fait que ξ est une fonction de τ [par l'intermédiaire de la trajectoire $x(\tau)$], tandis que *X est une fonction des quatre variables indépendantes x^ϱ*, c'est-à-dire fonction d'un point d'univers.

Pour une particule donnée, *X est un champ dont la valeur est égale au ξ de cette particule le long des trajectoires de celle-ci. X présente le caractère périodique cherché*; en fait, c'est une onde et l'on voit bien quel est le mécanisme qui le lie au corpuscule envisagé.

Son intérêt réside dans l'énoncé suivant: pour former un terme d'interaction dont la présence dans le Lagrangien rende compte des phénomènes d'interférences, il faudra tenir compte aussi de X (et des éléments qui en dérivent, par exemple X^+). Il n'est pas difficile de former de pareils termes si nous nous laissons guider par le fait qu'au fond c'est une différence de marche qui doit apparaître pour que les battements soient réalisés.

5. – Champs d'espace-temps, $\lambda \neq 0$.

Il existe un lieu indubitable, quoique de nature assez spéciale, entre les corpuscules et les champs X que nous leur avons fait correspondre; cela justifie un examen plus approfondi de la question. Dès l'abord, cependant, il convient de remarquer qu'en raison de leur caractère spinoriel, les champs X ne peuvent être immédiatement accessibles à l'expérience et ne sont en fait que des intermédiaires de calcul.

Cependant à partir des X nous pouvons former des grandeurs d'espace-temps, de la forme $X^+ A X$ avec des opérateurs A convenables, lesquels sont accessibles aux mesures et susceptibles éventuellement d'interprétation physique.

Pour avoir un exemple, prenons $A = \gamma^\sigma$. Nous attachons ainsi au corpu-

seule un champ vectoriel $J^\sigma = X^+\gamma^\sigma X$ qui s'écrira:

$$(6) \quad J^\sigma = a_1^+\gamma^\sigma a_1 + b_1^+\gamma^\sigma b_1 + (b_1^+\gamma^\sigma a_1)\exp[2ir_\varrho x^\varrho] + (a_1^+\gamma^\sigma b_1)\exp[-2ir_\varrho x^\varrho].$$

En tout point, ce champ a une valeur déterminée. *Le long d'une trajectoire du corpuscule*, on aura, puisque X se réduit à ξ:

$$(7) \quad J^\sigma_{\text{traj}} = \xi^+\gamma^\sigma\xi .$$

Donc le long de la trajectoire, le champ vectoriel J^σ a la valeur de la vitesse du corpuscule.

Remarquons qu'en vertu de $\lambda_\varrho(a^+\gamma^\varrho b) = 0$, on a aussi $\partial_\sigma J^\sigma = 0$.

Un autre exemple s'obtient en prenant comme opérateur $A = \partial/\partial x^\sigma$. Le champ ainsi obtenu est $X^+(\partial X/\partial x^\sigma)$ et a la valeur $-\lambda_\sigma$ quelle que soit la trajectoire.

On peut former ainsi toute une série de champs d'espace-temps, tensoriels donc observables, sans que cela signifie naturellement qu'ils aient été réellement observés.

Considérons enfin l'opérateur $A = \mu^{\varrho\sigma} = -\frac{1}{2}(\gamma^\varrho\gamma^\sigma - \gamma^\sigma\gamma^\varrho)$. En tenant compte que l'on a pour $\lambda \neq 0$ d'après les équations fondamentales:

$$\lambda_\varrho(b^+\mu^{\varrho\sigma}a) = -i\lambda(b^+\gamma^\sigma a)$$

$$\lambda_\varrho(a^+\mu^{\varrho\sigma}b) = +i\lambda(a^+\gamma^\sigma b)$$

$$i\lambda(b^+\gamma^\sigma b + a^+\gamma^\sigma a) = \lambda_\sigma(b^+b - a^+a)$$

on pourra écrire

$$(8) \quad \lambda_\sigma = rJ^\sigma + \tfrac{1}{2}\partial_\varrho(X^+\mu^{\varrho\sigma}X) ,$$

avec $r^2 = -r_\varrho r^\varrho$, soit encore sous une autre forme

$$(9) \quad \partial(X^+\mu^{\varrho\sigma}X) = -X^+\left(2\frac{\partial}{\partial x^\sigma} + \frac{i\lambda\gamma^\sigma}{(b^+b - a^+a)}\right)X .$$

λ_σ est la quantité de mouvement le long d'une trajectoire, J_σ est lié à la vitesse, $X^+\mu^{\varrho\sigma}X$ au spin. (8) donne l'équivalent d'une décomposition bien connue en mécanique ondulatoire, mais remarquons aussi que (9) sont *des équations du type de Maxwell*, ce qui pourra avoir son importance lorsqu'on introduira la notion de «charge électrique» dans la théorie.

6. – Cas limite $\lambda = 0$.

Lorsque $\lambda \neq 0$, le processus par lequel on peut rattacher l'onde à la particule est arbitraire, mais il existe une manière, pour ainsi dire « naturelle » de le faire, celle que nous avons indiquée. Lorsque $\lambda = 0$, cet arbitraire est beaucoup plus grand et le raisonnement utilisé au paragraphe 4, ainsi que l'équation (2) ne nous sont plus d'aucun secours. Ce cas est, entre autres, celui du photon.

Il est tentant d'adopter la même solution que dans le cas $\lambda \neq 0$, à savoir:

$$X = a \exp [ir_\varrho x^\varrho] + b \exp [-ir_\varrho x^\varrho] ,$$

avec les r_ϱ proportionnels aux λ_ϱ, $\lambda = 0$, et

$$\lambda_\varrho \gamma^\varrho a = \lambda_\varrho \gamma^\varrho b = 0 .$$

Mais les a et b sont indépendants et introduisent deux arbitraires au lieu d'un seul. On peut restreindre cet arbitraire en admettant a priori une relation entre a et b; celle qui vient la première à l'esprit est $a = b$, mais la relation $a = \gamma^5 b$ semble plus avantageuse.

En effet dans ce cas, on a pour le champ d'espace-temps $X^+ \mu^{\varrho\sigma} X = F^{\varrho\sigma}$ une expression particulièrement simple:

$$F^{\varrho\sigma} = X^+ \mu^{\varrho\sigma} X = 2(b^+ i\mu^{\varrho\sigma} \gamma^5 b) \cdot \sin 2r_\varrho x^\varrho . \tag{10}$$

Il est donc possible d'attacher à un corpuscule se mouvant avec la vitesse de la lumière un champ purement sinusoïdal dont la fréquence est proportionnelle à λ_1 donc à l'énergie. L'amplitude des diverses composantes est donnée par

$$- b^+ i(\gamma^\varrho \gamma^\sigma - \gamma^\varrho \gamma^\sigma) \cdot \gamma^5 b .$$

Il suffit de comparer cette expression à l'expression $\frac{1}{2} m_{\varrho\sigma}$ étudiée au paragraphe 5 de l'article précédent pour voir que les mêmes conclusions s'appliquent en interchangeant seulement les parties d'espace et de temps. Donc le champ $F^{\varrho\sigma}$ attaché à ces particules $\lambda = 0$ est sinusoïdal et présente, dans l'espace, la même disposition bien connue du champ électromagnétique de la lumière. De plus on voit aisément qu'en vertu des équations de base

$$\frac{\partial}{\partial x^\varrho} F^{\varrho\sigma} = 0 ,$$

comme pour la lumière dans le vide.

Parmi les particules $\lambda = 0$ on doit également compter le photon. On peut donc en partant de la définition spinorielle d'une particule de vitesse c, lui attacher un champ observable analogue à celui qui accompagne le photon.

Cela n'implique pas nécessairement l'identité de ces deux champs. Le champ de la lumière a un caractère électromagnétique, lequel n'apparait pas en mécanique spinorielle.

Le problème ne pourra être efficacement abordé que lorsqu'on introduira dans cette mécanique les notions de charge et de champ électromagnétique.

RIASSUNTO (*)

Dopo aver studiato qualitativamente i fenomeni d'interferenza mettendosi da un punto di vista differente da quello abituale, l'autore mostra come gli integrali primi della meccanica spinoriale del punto materiale permettano di scrivere in modo del tutto naturale l'espressione di un campo periodico che può supporsi collegato alla particella e che interviene nei termini d'interazione per render conto dei fenomeni d'interferenza. Questo campo rappresenta l'onda collegata alla particella e il modo con cui è stato calcolato mostra quali siano le sue relazioni con le traiettorie e le altre grandezze corpuscolari. Quando la massa a riposo è nulla, l'arbitrarietà nella scelta di questo campo è maggiore. Si può allora trovare facilmente, fra tutte le possibili, una soluzione che presenti le caratteristiche essenziali dei campi elettromagnetici collegati al fotone.

(*) *Traduzione a cura della Redazione.*

Energy Estimation of Photon Induced Cascade Showers (*).

P. A. Bender (**)

Washington University, St. Louis, Mo.

(ricevuto il 18 Luglio 1955)

Summary. — In order to find the best method by which an experimenter can estimate the energy of a cascade shower seen in a multiplate cloud chamber, a study has been carried out testing various estimation formulae involving different parameters of a shower. Cloud chamber pictures were scanned for cascade showers resulting from the decay photons of π^0-mesons. The energies of these two photons are related to the angle between them by $\sqrt{E_1 E_2} = mc^2/2 \sin(\theta/2)$. The estimation procedures were tested for consistency with this consequence of the conservation of energy-momentum, the product of the estimated energies being compared with the value calculated from the measured angle between the cores. When the entire shower development takes place in the chamber, our best energy estimate is given by E_0 (MeV) $= 33.8P$, where P is the total number of track segments in all the compartments times the thickness of a plate in radiation lengths in the direction of the shower. The constant applies to 0.63 cm Pb plates. This expression applies to the range 100-1 000 MeV with an estimated standard error of $\pm$ 20-25%. When only the number, N_{max} of tracks in the compartment in which the shower has its maximum development can be determined, our best estimate is $E_0 = 87.4 N_{max}$, with an estimated standard error of $\pm$ 30-35%. Another parameter considered for the case when P can be determined was $\sqrt{PN_{max}}$. $E_0 = 54.5\sqrt{PN_{max}}$ is at least as good an estimate, and perhaps slightly better than, $E_0 = 33.8P$ in the range 200-1000 MeV. The results are compared with shower theory and with R. R. Wilson's « Monte Carlo » results. Excellent agreement is found with the later, using a cutoff of 8 MeV, as regards fluctuations as well as average behavior. It follows that the uncertainties in energy estimation by the above formulae are due mainly to physical fluctuations in the shower development.

(*) This work was supported in part by the joint program of the Office of Naval Research and the Atomic Energy Commission.

(**) This paper is based on a thesis submitted in partial fulfillment of the requirements for the degree of Master of Arts, Washington University.

In previous work [1-5] a number of different methods have been used to estimate the energy of electron-photon cascade showers. We have undertaken a calibration of these and other methods using a suggestion of DESTAEBLER's [2], which takes advantage of the chief mode of decay of a π^0-meson ($\pi^0 \to \gamma_1 + \gamma_2$) in the following manner. The energies of the photons are related by the expression,

$$\sqrt{E_1 E_2} = \frac{m_\pi c^2}{2 \sin \theta/2},$$

which is a consequence of the laws of conservation of energy and momentum. The angle θ, easily measured in a cloud chamber for $E_1 - E_2 < \sim 1$ GeV gives us $\sqrt{E_1 E_2}$. On the same picture the product $\sqrt{X_1 X_2}$, where X is any shower parameter, can be found readily by examining the two showers produced by the decay photons of the neutral meson. The plot of $\sqrt{E_1 E_2}$ against $\sqrt{X_1 X_2}$ gives us

a) a relation between the energy E and the parameter X for an average shower;

b) an idea of the fluctuations from the average;

c) a means of comparison with various shower theories.

The photographs viewed for this study were taken by M. ANNIS and N. HARMON at Berthoud Pass, Colorado (altitude 3 400 m) in a cloud chamber designed by E. J. ALTHAUS [6]. Three thousand technically acceptable pictures were obtained during the summer of 1952. Throughout this period the chamber contained eleven 0.63 cm thick lead plates [7]. Fifteen hundred pictures obtained the following summer were also examined. In this latter run the second and third plates from the top were removed. Other details, as they pertain to this experiment, were essentially the same as during the 1952 run.

A π^0-meson shows itself in a multiple plate cloud chamber as two photon-initiated showers whose axes intersect at the point of the decay of the π^0-meson. Since its lifetime is so short ($\sim 5 \cdot 10^{-15}$ s) [8], we can assume the point of decay

(1) F. SALVINI and Y. B. KIM: *Phys. Rev.*, **88**, 40 (1952).

(2) H. S. BRIDGE, H. COURANT, H. DESTAEBLER and B. ROSSI: *Phys. Rev.*, **95**, 110 (1954).

(3) J. C. STREET: *Journ. Franklin Inst.*, **227**, 765 (1939).

(4) W. B. FRETTER: *Phys. Rev.*, **76**, 511 (1949).

(5) W. E. HAZEN: Private communication.

(6) E. J. ALTHAUS: *Study of Stopped-Meson Neutrons* (Ph. D. thesis, Washington University, St. Louis, Mo., 1950); E. J. ALTHAUS and R. D. SARD: *Phys. Rev.*, **91**, 373 (1953).

(7) Operating details will be given by N. HARMON: *Ph. D. thesis* (Washington University, St. Louis, in preparation).

(8) B. M. ANAND: *Proc. Roy. Soc.*, A **220**, 183 (1953).

to be identical with the point of production. This point is a nuclear interaction, which can be recognized in most cases by the non-electronic tracks emerging from the plate. Thus we establish the following criteria. We require:

a) at least two showers, each of which points back to the intersection in a plate of two or more non-electronic tracks;

b) that both showers pass their maximum in the illuminated region of the chamber;

c) that the two showers be resolvable one from the other;

d) that the number of tracks in each shower be greater than two, yet small enough so that they can be counted.

Under these criteria eighteen examples of π^0-decay were found. Several pictures contained three or four showers whose axes intersected at a single nuclear interaction. These could not be examples of the rarer modes of decay of the π^0-meson

$$(\pi^0 \to \gamma + e^+ + e^-, \qquad \pi^0 \to e^+ + e^- + e^+ + e^-),$$

since in these pictures all the showers had a « missing link » between the event and the shower, and thus had to be photon-induced. The interpretation is that there were two neutral mesons produced, (one photon leaving the chamber in the three-shower pictures). If the above criteria led to ambiguous pairing of showers for two π^0-events, then the whole event was eliminated from the statistics.

The angle θ between the two photons was found by measuring the spatial coordinates of the nuclear event and of a convenient point on the axis of each shower. These were then combined in the simple geometric formula to ca - culate the angle.

When counting the numbers of electron tracks in a shower, it is necessary to eliminate background tracks due to unrelated, low energy electrons. This was done by counting only those tracks in a shower which were straight and within 50° of the shower axis ([9]).

N_{max} ([1]) is the first parameter to be considered. It is defined as the number of track segments between two successive plates at the maximum development of a shower. The data obtained are plotted in Fig. 1. Another parameter is the tracklength P ([2]), here defined as the total number of track segments of the shower times the thickness of one plate in radiation lengths in the direction of the shower. Fig. 2 shows the data. Another parameter considered was

([9]) R. R. Wilson: *Phys. Rev.*, **86**, 261 (1952).

at which the number of electrons reaches a maximum. Another is Z, the depth of the « center of gravity » of the shower. The angular spread of each the geometric mean of these two quantities $\sqrt{PN_{max}}$ which is plotted in Fig. 3.

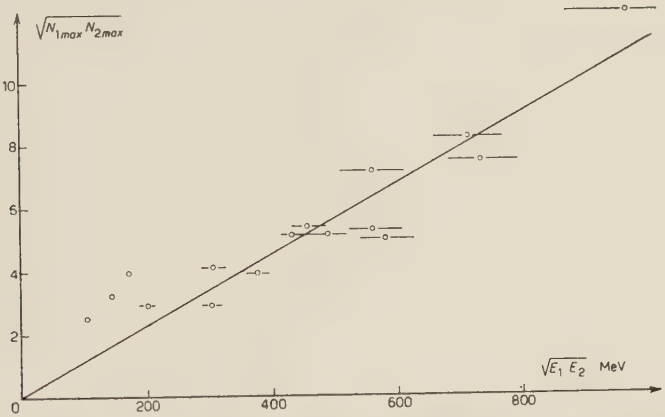

Fig. 1. – Number of tracks at the maximum developement of the shower vs. the energy product determined by the angle between the π^0 disintegration photons. The best straight line through the points is shown.

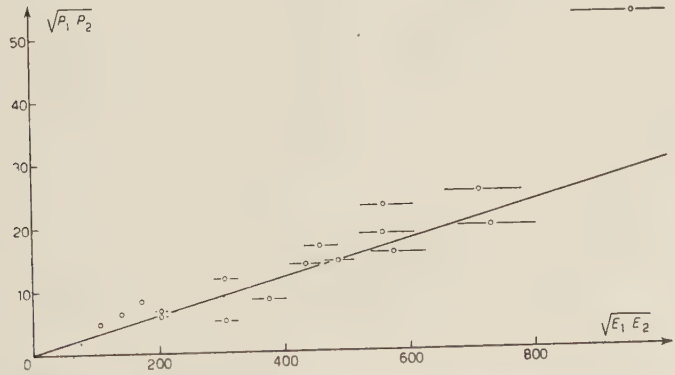

Fig. 2. – The track length (the total number of track segments in all the compartments times the thickness of the plate in the direction of the shower) vs. the energy product. The best straight line through the points is shown.

Among the other parameters which were tested is T, the depth in lead shower was also examined. In all these cases no correlation with the energy of the photon could be found.

The results have been compared to conventional shower theory ([10]). The theoretical expressions for N_{max} and for the track length give values which

([10]) B. Rossi and K. Greisen: *Rev. Mod. Phys.*, **13**, 240 (1941).

are considerably higher than the data indicate. However the assumptions made in the theory are not entirely justified in the energy regions studied and in the material used in this experiment.

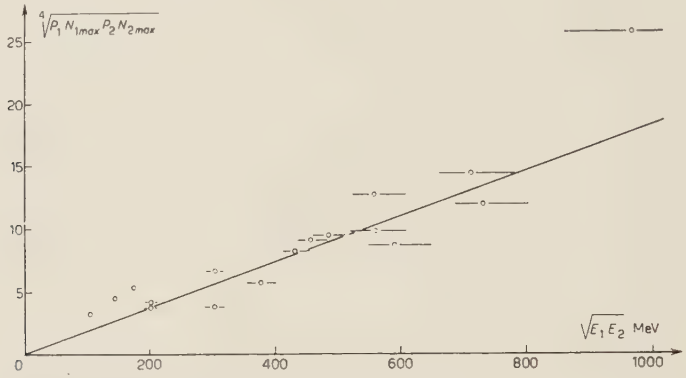

Fig. 3. – The geometric mean of the maximum number and the track length vs. the energy product. The best straight line through the points is shown.

The form of the Monte Carlo calculations carried out by R. R. Wilson [9] has a natural advantage over the other calculations since it provides individual shower histories instead of only an average-shower curve. Thus we can not only compare the average relationships between the energy of the shower and any particular parameter but also the fluctuations from the average. This is easily done using the Monte Carlo histories by counting the number of electrons whose energy is greater than a cutoff energy of order of magnitude 7.3 MeV [9], occurring at depths corresponding to the thickness of the lead plates in the cloud chamber (1.1 radiation length). We used histories generously lent to us by R. R. Wilson. The average values obtained from 100 histories at $E_0 = 100$, 200 and 300 MeV using a cutoff of 8 MeV, are indicated by the solid lines on Figg. 1, 2 and 3. This cutoff energy was chosen to fit our data and selection criteria. These curves can be represented by the equations:

$$E_0 = 87.4 N_{\max} ,$$

$$E_0 = 33.8 P ,$$

$$E_0 = 54.5 \sqrt{N_{\max} P} .$$

The straight line given by the least squares fit of the cloud chamber data lies well within the statistical spread of the Monte Carlo results which are discussed below. Our results are in excellent agreement with those obtained recently by Hazen working with showers produced by electrons of known energy.

The deviation of each experimental point from the Monte Carlo line was calculated and is shown in the upper histograms (Fig. 4, 5, 6). The deviations of the Monte Carlo histories about the same average are shown in the lower

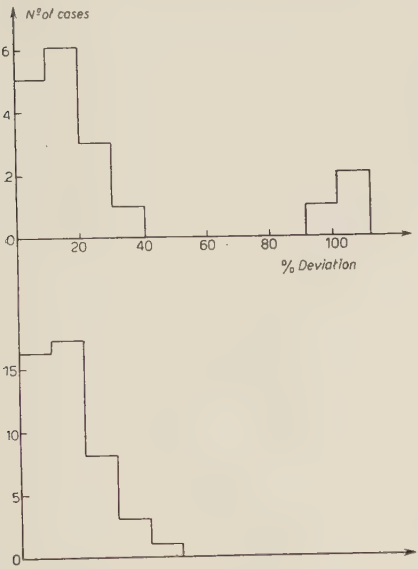

Fig. 4. – Number of tracks at maximum. *Upper*: Distribution of experimental data about the straight line of fig. 1. *Lower*: Distribution of Monte Carlo history data about the same straight line.

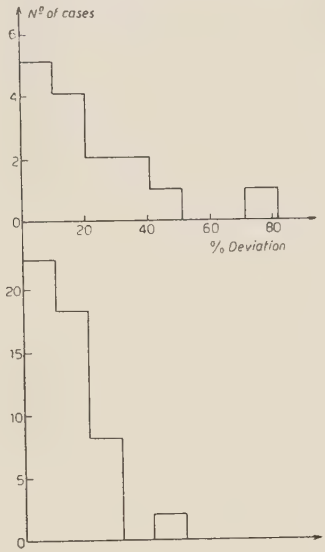

Fig. 5. – The track length. *Upper*: Distribution of experimental data about the straight line of fig. 2. *Lower*: Distribution of Monte Carlo history data about the same straight line.

histograms. It should be noted that in order for the comparison to be more realistic, Monte Carlo histories of the same energy (300 MeV) were randomly paired in order to give us $\sqrt{X_1 X_2}$. Since it is most probable for a π^0-meson to share its energy equally between its photons, the choice of equal energy showers is justified. The three points separated from the rest of the data (Figg. 4 and 6) represent the data for showers whose energy is below 200 MeV.

The Monte Carlo histograms show an r.m.s. deviation of approximately 20% in the first case, 15% in the second, and 15% in the third, with some indication that the third histogram is narrower than the second. However, we must expect somewhat larger relative deviations, a factor of approximately 1.4, in the energy estimation of individual showers, since here we have used the geometric mean of two showers for each point.

Although there are too few experimental cases to permit us to draw a smooth curve, we see that the experimental histograms have roughly the same

distribution as the Monte Carlo histories; and therefore deviations are due mainly to the inherent fluctuations in shower development. It appears that there would be little point in further refinement of the estimation procedure.

Our data provide additional evidence for the view that most of the high-energy photons produced in nuclear interactions result from the decay in flight of π^0-mesons. They also confirm R. R. WILSON's Monte Carlo shower histories when cut off at about 8 MeV.

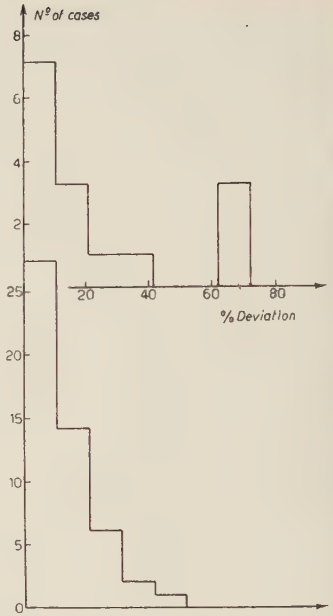

Fig. 6. – The geometric mean. *Upper*: Distribution of experimental data about the straight line of fig. 3. *Lower*: Distribution of Monte Carlo history data about the same straight line.

* * *

The author is deeply indebted to Professor R. D. SARD for aid and encouragement. Thanks are due N. HARMON for his invaluable help.

RIASSUNTO (*)

Per determinare il metodo migliore col quale uno sperimentatore possa stimare l'energia di uno sciame in cascata osservato in una camera a nebbia a setti multipli è stato condotto uno studio saggiando diverse formole approssimate contenenti differenti parametri di uno sciame. Furono esaminate fotografie prese alla camera di Wilson ricercandovi sciami in cascata originati dai fotoni di decadimento di mesoni π^0. Le energie di questi due fotoni sono proporzionali all'angolo che formano fra di loro secondo $\sqrt{E_1 E_2} = mc^2/2 \sin(\theta/2)$. La compatibilità dei sistemi di stima con questa conseguenza della conservazione dell'impulso energetico, fu esaminata confrontando il prodotto delle energie stimate col valore calcolato dall'angolo misurato fra gli assi degli sciami. Quando l'intero sviluppo dello sciame avviene entro la camera, il nostro miglior risul-

(*) *Traduzione a cura della Redazione.*

tato è dato da E_0 (MeV) $= 33.8P$, dove P è il numero totale di segmenti di traccia in tutti gli scomparti per lo spessore di una placca in lunghezze di radiazione nella direzione dello sciame. La costante è calcolata per setti di 0.63 cm Pb. Quest'espressione è valida per l'intervallo 100-1 000 MeV con un errore di $\pm$ 20-25%. Quando si può determinare soltanto il numero N_{max} di tracce nello scomparto in cui lo sciame ha il massimo sviluppo, la nostra miglior stima è $E_0 = 87.4N_{max}$; con un error medio stimato di $\pm$ 30-35%. Un altro parametro, considerato per il caso che P possa essere determinato, è stato $\sqrt{PN_{max}}$; $E_0 = 54.5\sqrt{PN_{max}}$ è un valore almeno altrettanto buono, forse un po' migliore di $E_0 = 33.8P$ nell'intervallo 200-1 000 MeV. I risultati si confrontano con la teoria degli sciami e coi risultati ottenuti da R. R. Wilson col « Monte Carlo ». Si trova un ottimo accordo con quest'ultimi, applicando un taglio di 8 MeV, per quanto riguarda sia le fluttuazioni sia la media. Ne segue che le incertezze nella stima dell'energia per mezzo delle formole di cui sopra sono principalmente dovute a fluttuazioni fisiche nello sviluppo degli sciami.

Statistical Spread in Pulse Size of the Proportional Counter Spectrometer.

A. Bisi and L. Zappa

Istituto di Fisica Sperimentale del Politecnico - Milano

(ricevuto il 29 Luglio 1955)

Summary. — The pulse size distribution from monoenergetic radiations in a proportional counter was analyzed in the energy range between 2 and 70 keV. It is shown that the experimental data on total relative variances fit strictly to the relation: $\sigma_P/\overline{P} = 0.138/E^{0.395}$ The obtained spreads are smaller than would be according to Poisson's distribution. An attempt is made to deduce the relative variance in the number of initial electrons produced when the total energy of the primary particle is available for useful ionization.

1. – Introduction.

The output pulse size of a proportional counter, arising from full energy of a monoenergetic radiation absorbed in the counter gas, is subject to statistical fluctuations. Actually there are fluctuations in the initial number of ionizations and fluctuations introduced by the statistics of the multiplication process in the counter.

According to a theoretical treatment given by Frisch [1] and to the experimental results of Hanna, Kirkwood and Pontecorvo [2], the relative variance (mean square relative standard deviation) of the output pulse size is practically independent from the multiplication factor. Then it can be written:

$$\left(\frac{\sigma_P}{\overline{P}}\right)^2 = \frac{1}{N}\left(\frac{\sigma_A}{\overline{A}}\right)^2 + \left(\frac{\sigma_N}{\overline{N}}\right)^2$$

[1] O. R. Frisch: *Statistics of Multiplicative Processes.* Unpublished Lectures 1948.

[2] G. C. Hanna, D. H. W. Kirkwood and B. Pontecorvo: *Phys. Rev.*, **75**, 985 (1949).

where: $(\sigma_P/\bar{P})^2$ is the relative variance of the output pulse size;

$(\sigma_A/\bar{A})^2$ gives the relative variance in the number of ions produced in an avalanche by a single ionization electron;

$(\sigma_N/\bar{N})^2$ gives the relative variance in the number of initial electrons.

The contribution to the relative variance due to the multiplication process was evaluated by SNYDER [3] and FRISCH [1] and found to be equal to $1/N$. The calculation was based on the assumption that the instantaneous probability for an electron to make an ionizing collision is merely a function of the electric field and not of the previous history of the electron. That is obviously a rough approximation. CURRAN, COCKCROFT and ANGUS [4] were able to detect the pulse distribution due to individual photoelectrons released at the cathode of a proportional counter filled with argon (50%) and methane (50%). Actually their results show that the relative variance is:

$$\frac{1}{\bar{N}}\left(\frac{\sigma_A}{\bar{A}}\right)^2 = \frac{0.68}{N}\,. \tag{1}$$

The fluctuation of the number of primary ions for a given initial energy was theoretically investigated by FANO [5]. The relative variance is due to the fact that some collisions are ionizing while others are not, and to statistical fluctuations of energy loss in the ionizing and in the exciting collisions. According to the estimates of FANO the relative variance $(\sigma_N/\bar{N})^2$ becomes $1/\bar{N}k$, with k between 2 and 3: that is, it is smaller than that obtained with a Poisson distribution. The results of FANO were partially supported by measurements of the total fluctuation in pulse size made by HANNA *et al.* [2] and by CURRAN *et al.* [4]. The counters were filled with argon and methane (CURRAN *et al.*) and with xenon and methane, argon and methane (HANNA *et al.*). No significant differences were observed in the pulse size distributions obtained with these mixtures. The energy of the investigated radiations were: ~ 0.250, 2.8, and 17.4 keV (HANNA *et al.*), 8.0 and 17.4 keV (CURRAN *et al.*). In this energy range the total relative standard deviation was found to vary approximately like $1/\sqrt{\bar{N}}$. There is at present no theoretical explanation of the very small spreads observed.

Up to date no experimental data are available between 20 and 50 keV; at higher energies (60 and 190 keV), as indicated by WEST [6], the relative

---

[3] H. S. SNYDER: *Phys. Rev.*, **72**, 181 (1947).
[4] S. C. CURRAN, A. L. COCKROFT and J. ANGUS: *Phil. Mag.*, **40**, 929 (1949).
[5] U. FANO: *Phys. Rev.*, **70**, 44 (1946); **72**, 26 (1947).
[6] D. WEST: *Progress in Nuclear Physics*, **30**, 18 (1953).

spreads are larger than would be expected from an extrapolation of the results quoted above. As may be seen no definite conclusions can therefore be drawn about the dependence on the energy of the total relative variance of the pulse size distribution given by a proportional counter.

The present work has been intended as an investigation of the energy dependence of the total relative variance of the pulse size distribution in a proportional counter filled with argon and methane in the energy range between 2 and 70 keV.

2. – Measuring Techniques.

Two counters were employed in these measurements. The counters consist of aluminium cylinders of an inner diameter of 7 cm and effective lengths of 33 cm and 28 cm. The center wire is of high tempered steel, 0.1 mm in diameter. The counters were filled with argon (90%, 70%) and methane (10%, 30%) mixtures (between 1 and 2 atm total pressure). The pulses are taken off the wire and fed through a mod. 220 linear amplifier or a mod. 100 linear amplifier ([7]), into a stable, high speed, twenty channel electronic pulse analyzer ([8]).

The spread of a pulse size distribution is caused not only by statistical fluctuations but also by additional fluctuations arising from experimental apparatus. The causes of additional fluctuations are listed below together with the steps taken to minimize them.

a) Inequalities in the diameter and eccentricity of the wire. The uniformity of the wire diameter was strictly controlled through microscopical examination. The wire was carefully cleaned. The spread in gas multiplication caused by an eccentricity of the wire, according to the calculations of ROSSI and STAUB ([9]) is negligible in our counters.

b) End and wall effect. A sufficient thickening of the wire at the two ends avoids the multiplication process but does not distort much the radial character of the field. The wall effect affecting the detection of high energy radiation ([10]) reduces the number of pulses in the peaks of the distribution, but does not reduce practically the energy resolution ([11]).

([7]) W. C. ELMORE and M. SANDS: *Electronic Experimental Techniques* (New York, 1949), pp. 166, 170.

([8]) E. GATTI: *Nuovo Cimento*, **11**, 153 (1954).

([9]) B. ROSSI and H. STAUB: *Ionization Chambers and Counters* (New York, 1949), p. 91.

([10]) A. BISI and L. ZAPPA: *Nuovo Cimento*, **12**, 211 (1954).

([11]) D. WEST, J. K. DAWSON and C. J. MANDLEBERG: *Phil. Mag.*, **43**, 875 (1952).

c) Negative ion formation. The counter is attached to a gas purifier containing Ca-Mg alloy turnings, heated electrically.

d) Instability of the high voltage supply. The counter was operated by a +5000 regulated supply. This high voltage power supply shows a drift of not more than 0.01 percent for a period of some hours in continuous operation ([12]).

e) Radial extension of the track. The length of the track of the initial ionization has been kept always small compared with the counter radius, and the collection time of the electrons has been kept as short as possible.

f) Drift in amplifier and pulse analyzer. The drift in the counter and in the electronic apparatus checked by a calibrating X-ray line was found to be negligible.

g) Amplifier noise. The input tube noise, in our case, does not contribute to the spread of the pulse size distribution.

h) Variations in the channel width of the analyzer. No spread arises from the pulse analyzer, owing to the fact that the width is constant for all channels ([8]) and owing to the shortness of the counting time (< 10 min).

Finally it was found that the spread is independent from the multiplication factor.

3. – Energy Resolution.

Soft γ-rays and X-rays following K-capture and K-internal conversion were used as ionizing radiations to study the output pulse size distribution of the proportional counter. The energies of the electromagnetic radiations, together with the radioactive isotopes employed, are listed in Table I. For K_α energy we have used the weighed mean of the K_{α_1}, and K_{α_2} energies derived from the table of HILL, CHURCH and MIHELICH ([13]).

The pulse size distributions produced by the investigated radiations can be fitted with gaussian curves, at least in an interval of about ± 3 standard deviations, in the energy range between 2 and about 40 keV. The standard deviation (σ) can therefore be obtained by measuring the width of the peak at half maximum (Δ). We have in fact:

$$\Delta = 2.36 \cdot \sigma \,.$$

([12]) W. A. HIGHIMBOTHAM: *Rev. Sci. Instr.*, **22**, 429 (1951).

([13]) R. D. HILL, E. L. CHURCH and J. W. MIHELICH: *Rev. Sci. Instr.*, **23**, 523 (1952).

TABLE I.

Isotope	Mode of decay	K_α energy (keV)	γ energy (keV)
^{51}Cr	E.C., γ	2.00 (escape peak)	—
»	»	4.95	—
^{55}Fe	E.C.	5.86	—
^{71}Ge	E.C.	9.25	—
^{85}Sr	E.C., γ	13.75	—
^{109}Cd	E.C., γ	22.10	—
^{137}Cs	β^-, γ	32.05	—
^{210}Pb (RaD)	β^-, γ	—	46.7
^{181}W	E.C.	57.15	—
^{195}Au	E.C., γ	66.20	—

Two matters have to be considered in the determination of the width of a peak:

a) Complexity of the K X-ray spectrum. At low energies (less than 20 keV) the K_α and K_β radiations are not resolved. Owing to the fact that the peak separation is about 3σ, any additional spreads can be neglected. At higher energies the K_α and K_β radiations are clearly resolved, but at these energies the complexity of the K_α radiation becomes apparent. No serious error however arises from the K_α complexity, at least not in our energy range: in fact the width of a peak at about 60 keV undergoes an increase not greater than 5%.

b) Finite channel width of the pulse analyzer. For low energy radiations the resolution is little affected owing to the fact that the analyzer allots four or more window widths to a peak between points at half counting rate. At high energy this is not generally possible; the contribution to the smearing can be easily evaluated for a gaussian peak. In our measurements the correction made to the width of a peak at 60 keV is not greater than 10%.

The results of our measurements are listed in Table II and plotted in Fig. 1. The widths of the peaks were corrected only for the effect discussed at *b*). The accuracy of the quoted values is better than 5%.

TABLE II.

Energy (keV)	2.00	4.95	5.86	9.25	13.75	22.10	32.05	46.7	57.15	66.20
$\sigma_P/\overline{P}$ (%)	10.5	7.3	6.9	5.9	5.1	4.10	3.50	2.94	2.92	2.70

4. – Conclusions.

As may be seen from Fig. 1 the total relative variances are smaller than would be according to Poisson distributions. In the investigated energy range

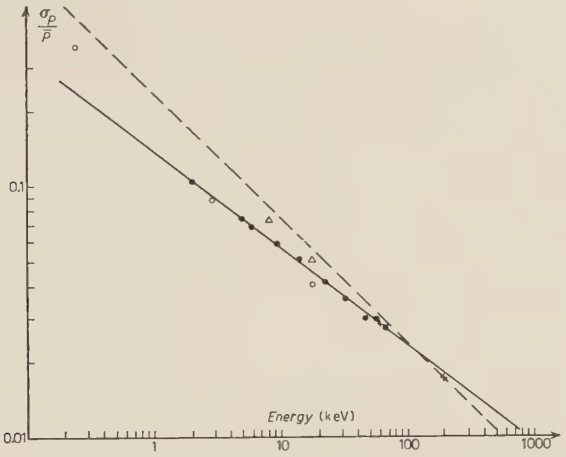

Fig. 1. – Total relative standard deviation of pulse size distribution from a proportional counter as a function of the energy (full line). Broken line: Poisson distribution. (● our measurements, ○ HANNA *et al.* [2], △ CURRAN *et al.* [4], + WEST [6]).

the total relative variance is found to be connected to the energy in agreement with the relation:

$$\frac{\sigma_P}{\bar{P}} = \frac{0.138}{E^{0.395}}. \tag{2}$$

Eq. (2) at high energy fits also rather closely the experimental data of WEST [6] and of NEWTON and ROSE [6]. Only at very low energy [2] (~ 0.250 keV) the spread is definitely greater than would be expected from eq. (2).

From eq. (2) and on the basis of the results of CURRAN *et al.* [4] about the relative variance in the number of ions of a single avalanche [eq. (1)], we shall attempt now to deduce the

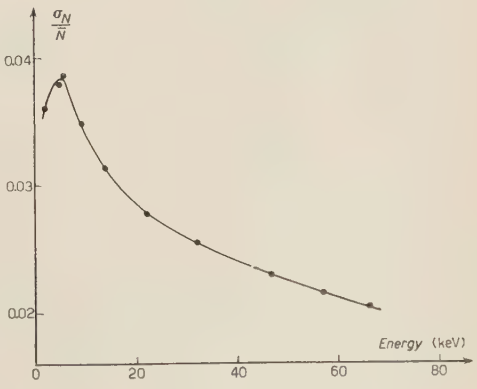

Fig. 2. – Relative standard deviation in the number of initial electrons as a function of the energy.

relative variance in the number of initial electrons. Fig. 2 shows the result of such calculation. For the purpose of this calculation we have assumed that the average energy loss E_i is 28.6 eV per ion pair ([14]).

A characteristic feature of these results is a well defined maximum shown by the curve of Fig. 2. By considering that the K-shell of argon is primarily responsible for the absorption of the low energy quanta, it may be seen that the maximum corresponds to the production of a photoelectron with an energy nearly equal to the K-shell binding energy. The shape of the curve of Fig. 2 is rather surprising. No doubt, of course, that at energies lower than 2 keV the relative variance will increase with the decreasing E.

* * *

We wish to express our thanks to Prof. G. BOLLA for his kind interest.

([14]) S. C. CURRAN, A. L. COCKROFT and G. M. INSCH: *Phil. Mag.*, **41**, 517 (1950).

RIASSUNTO

Si studia la distribuzione in altezza degli impulsi di un contatore proporzionale per radiazioni monoenergetiche nell'intervallo di energia compreso tra 2 e 70 keV. Si dimostra che gli scarti quadratici medi percentuali variano con l'energia secondo la relazione $\sigma_P/\overline{P} = 0.138/E^{0.395}$. Tali scarti sono inferiori a quelli calcolabili in base alla formula di Poisson. Si esamina infine la fluttuazione della ionizzazione primaria prodotta da una particella assorbita nel gas del contatore.

IL NUOVO CIMENTO Vol. II, N. 5 1° Novembre 1955

Virtual Oscillators in the Metallic Model of Luminescent Molecules.

A. Jabłoński

Physics Department, Nicholas Copernicus University - Toruń, Poland

(ricevuto l'8 Agosto 1955)

Summary. — The character of virtual oscillators connected with electronic transitions responsible for absorption and fluorescence bands of some luminescent molecules (fluorescein, rhodamine B, euchrisine, trypaflavine and acridine yellow) is determined by using the transition moments, calculated by Mlle Laffitte on basis of the metallic model of molecules. Contrary to the hitherto prevailing views, according to which these oscillators should be linear, the metallic model yields non-linear oscillators for above molecules, viz. very anisotropic flat oscillators. Hence it follows that the theoretical values of the principal polarization of fluorescence P_p of these molecules are lesser than they would be in the case of linear oscillators, viz. $P_p < 0.5$. The calculated values of P_p are: 0.47 for fluorescein, 0.49 for rhodamin B and 0.485 for euchrisine, trypaflavine and acridine yellow. The differences between these values and those actually observed are believed to be due, at least partially, to the depolarizing effect of torsional vibrations of luminescent molecules. Assuming the whole difference to be due to torsional vibrations, the upper limit is estimated of the dependence of this effect on temperature. The dependence appears to be rather feeble (since the whole effect is small), but seems to be detectable. One of the aims of the present paper is to show the usefulness of the notion of the « spatial virtual oscillator », of which the « flat oscillator » and the « linear oscillator » are particular cases.

The notion of a « spatial virtual oscillator » as well as those of a « flat virtual oscillator » and of a « linear virtual oscillator » are often used in papers dealing with polarization of photoluminescence of solutions, and especially in those papers, in which the problem of the so called « fundamental polariz-

ation » [1] and that of « principal polarization » [2] is considered. The character of the virtual oscillators, or, more strictly, their anisotropy, is made directly responsible for the actual value of fundamental (or principal) polarization of different luminescent solutions.

In order to avoid any misunderstandings it is advisable to state the exact meaning in which the terms « spatial », « flat » and « linear » oscillators were used in earlier papers of the present writer [3], and in which they will be used here.

We consider a virtual oscillator responsible for a particular absorption or emission band to be linear, if there is only one direction with respect to molecular axes, which the corresponding transition moment (the dipole moment) can assume. The oscillator is spatial (or flat) in cases, in which the transition moments responsible for one band, can assume different directions with respect to molecular axes. Such an oscillator possesses in general three principal transition probabilities Γ_1, Γ_2 and Γ_3 for three mutually perpendicular directions, where, say Γ_1, may have the direction, in which the transition probability assumes its maximum. Let us chose the axes so as $\Gamma_1 \geqslant \Gamma_2 \geqslant \Gamma_3$. If $\Gamma_3 = 0$ and $\Gamma_1 \neq 0$, $\Gamma_2 \neq 0$, the oscillator is flat. If only $\Gamma_1 \neq 0$, the oscillator is linear.

The notions of spatial and flat oscillators are reasonable and useful in cases, in which the probability distribution of directions (with respect to molecular axes) of transition moments in emission is practically independent of the manner of excitation (as in condensed media, in which this independence is due to disturbances of the luminescent molecule by surrounding molecules of solvent). Clearly, a set of linear oscillators connected with the same band, and, besides, fulfilling the above condition of independence, is to be treated as one single spatial (or flat, if the set is plane) oscillator. The notion of the « spatial » or « flat » oscillator is purely statistical — it does not concern a single event, which may be due to a linear (or e.g. a circular) transition moment.

If the oscillators connected with absorption band (in which photoluminescence is excited) and with photoluminescence band are known, the fundamental (or principal) polarization can be calculated theoretically [4].

---

[1] The rate of polarization of photoluminescence of an isotropic solution, in which there are no depolarizing factors, provided the photoluminescence be excited by polarized primary light.

[2] The fundamental polarization in cases in which the excitation occurs in the absorption band involving transition between the same pair of electronic levels, between which the transition responsible for emission of fluorescence band occurs.

[3] A. JABŁOŃSKI: *Zeits. f. Phys.*, **96**, 236 (1935); *Acta Phys. Pol.*, **4**, 371 and 389 (1935); **5**, 271 (1936); **10**, 193 (1950). Cfr. also P. PRINGSHEIM: *Fluorescence and Phosphorescence* (New York, 1949), p. 368.

[4] Cfr. A. JABŁOŃSKI: l. c.

There are cases, in which there is no doubt that the virtual must be considered as non-linear (as e.g. the case of the benzene molecule, in which absorption and fluorescence is connected with symmetrical flat oscillator: $\Gamma_1 = \Gamma_2 \neq 0$, and $\Gamma_3 = 0$).

It seems, however, to be a generally accepted view that in the case of molecules lacking of any centre or axis of symmetry the virtual oscillators must be considered as linear (totally anisotropic) oscillators. The theoretical value of principal polarization P_p of such molecules would be 0.5.

Recently Mlle LAFFITTE has published [5] results of her investigations, of which the most interesting for us are the calculations of transition moments (dipole moments) for different luminescent molecules on the basis of the metallic model of molecules. She has shown that the transition moments giving rise to the same band, have in general different directions with respect to molecular axes. Thus, e.g., in the case of the well known fluorescence band (and the, reverse absorption band) of fluorescein there are two transition moments parallel to one of the molecular axes (x-axis), and two other moments making angles $+ 12^\circ 30'$ and $- 12^\circ 30'$ with it, all the transition moments lying in the plane of the molecule. If we assume that the probability distribution of these transition moments in emission does not depend on the manner of excitation (as it seems to be actually the case), we here have obviously the case of a flat oscillator. The oscillator is lying in the plane of the molecule, $\Gamma_1 = \Gamma_x$ being parallel to the x-axis, and $\Gamma_2 = \Gamma_y$ parallel to the y-axis (perpendicular to the former). The components A_x and A_y of the four transition moments, calculated by Mlle LAFFITTE, are given in the table I. The relative principal transition probabilities are obtained by adding the squares of the corresponding components of transition moments (see Table I).

TABLE I.

No of trans. mom.	A_x	A_x^2	A_y	A_y^2
1	— 1.506	2.27	0	0
2	— 1.159	1.34	0	0
3	— 1.334	1.78	— 0.295	0.087
4	— 1.334	1.78	+ 0.295	0.087
	$\Gamma_x = 7.17$		$\Gamma_y = 0.174$	

[5] E. LAFFITTE: *Ann. de Phys.*, **10**, 71 (1955).

The result is: $\Gamma_1 = \Gamma_x = 7.17$, $\Gamma_2 = \Gamma_y = 0.174$ ($\Gamma_3 = 0$).

The principal polarization P_p has to be calculated by means of [6]

$$P_p = \frac{3\sum_{i=1}^{3}\Gamma_i^2 - (\sum_{j=1}^{3}\Gamma_j)^2}{\sum_{i=1}^{3}\Gamma_i^2 + 3(\sum_{j=1}^{3}\Gamma_j)^2}, \tag{1}$$

the rate of depolarization by means of

$$\varrho_p = \frac{2(\sum_{j=1}^{3}\Gamma_j)^2 - \sum_{i}^{3}\Gamma_i^2}{(\sum_{j=1}^{3}\Gamma_j)^2 + 2\sum_{i=1}^{3}\Gamma_i^2}. \tag{2}$$

The values calculated for fluorescence of fluorescein are: $P_p = 0.47$ and $\varrho_p = 0.36$. The experimental value is $P_p' = 0.45$.

The other dye molecules investigated by Mlle LAFFITTE [7] are: rhodamin B euchrisine, trypaflavine and acridine yellow.

The relative principal transition probabilities and the resulting principal polarizations of fluorescence of these molecules are compiled in the Table II. In the last column the Mlle LAFFITTE's experimental values of P_p' are given.

TABLE II.

	Γ_x	Γ_y	P_p	P_p' [7]
Rhodamine B	7.582	0.054	0.49	0.46
Euchrysine	7.519	0.065	0.485	0.45$_+$
Trypaflavine	7.451	0.078	0.405	0.45$_+$
Acridine Yellow				

The experimental values of principal polarization P_p' are smaller than the theoretical values. The difference between theoretical and experimental values $P_p - P_p'$ is believed to be, at least partially, due to the depolarizing effect of torsional vibrations of luminescent molecules. Since the metallic model yields a smaller value of principal polarization P_p of fluorescence of fluorescein than that adopted in the earlier papers ($P_p = 0.5$), the resulting difference

---

[6] Cfr. A. JABŁOŃSKI: l. c.

[7] E. LAFFITTE: l. c.

$P_p - P'_p$ becomes also smaller: $P_p - P'_p = 0.02$, compared with 0.06 formerly adopted.

In general case, the knowledge of P_p and P'_p does not suffice for getting exact information on torsional vibrations of luminescent molecules. Nevertheless, as shown in earlier papers ([5]), a very rough estimate can yet be made of the standard deviation $\sqrt{\overline{\varepsilon^2}}$ of the angles of turn ε of molecular axes (ε means the angle made by a molecular axis with its equilibrium direction). The expression by means of which $\sqrt{\overline{\varepsilon^2}} = \sqrt{\delta}$ is calculated reads ([8]):

$$3\delta^2 - 2\delta + \frac{P_p - P'_p}{P_p(3 - P'_p)} = 0 , \tag{3}$$

or, for $\delta \ll 1$,

$$\delta = \frac{P_p - P'_p}{2P_p(3 - P'_p)} . \tag{4}$$

Assuming the whole difference $P_p - P'_p$ to be due to torsional vibrations, we obtain for the fluorescein molecule (in plexiglass) $\sqrt{\overline{\varepsilon^2}} \approx 5^\circ\,13'$, compared with 9 or even 10° given in earlier papers (for fluorescein molecule in glyceric solution). Obviously, the true standard deviation may be lower indeed — the experimental value of P'_p being possibly affected by some errors unaccounted for, as e.g. by unperfect geometry of the experimental arrangement, and, besides, the metallic model being a rather rough approximation.

From (3) we have for $\delta \ll 1$

$$P'_p \approx P_p[1 - (6 - 2P_p)\delta] . \tag{5}$$

On the other hand ([5])

$$\delta = \overline{\varepsilon^2} = \frac{\hbar}{I\omega}\left(\frac{1}{2} + \frac{1}{\exp[\hbar\omega/kT] - 1}\right), \tag{6}$$

where I denotes the relevant moment of inertia of the molecule, ω the angular frequency of its torsional vibrations about the corresponding axis of inertia, and the other notations are the usual ones. For $\hbar\omega \ll kT$ (6) becomes approximately

$$\delta = \frac{\hbar}{I\omega}\left(\frac{1}{2} + \frac{kT}{\hbar\omega}\right). \tag{7}$$

([8]) The simplification made by deriving the expression (3) rest on the assumption $\sqrt{\varepsilon^2}$ to be the same for all molecular axes.

Putting (7) into (5) we obtain

$$P_p' = P_p\left[1-(6-2P_p)\frac{\hbar}{I\omega}\left(\frac{1}{2}+\frac{kT}{\hbar\omega}\right)\right], \tag{8}$$

an expression enabling us to estimate roughly the effect of temperature on P_p'. For $P_p = 0.47$, $I = 10^{-38}$ g cm^2 and $\omega = 1.88\cdot 10^{13}$ s^{-1} (wave number 100 cm^{-1}), we obtain the following values of P_p' for three different (absolute) temperatures

T °K	P_p'
0	45.9
100	45.5
300	43.7

Thus, the estimated dependence of P_p' on temperature is very weak indeed but, presumably, still possible to be detected experimentally.

In the above considerations extensive use is made of the notion of non linear virtual oscillators. One of the chief aims of the present paper is to show its usefulne·.

RIASSUNTO (*)

Si determina per mezzo dei momenti di transizione, calcolati da M.lle Laffitte sulla base del modello metallico delle molecole, il carattere di oscillatore virtuale connesso alle transizioni elettroniche che provocano le bande di assorbimento e di fluorescenza di alcune molecole luminescenti (fluoresceina, rodamina B, eucrisina, tripaflavina e giallo acridina). Contrariamente alle vedute finora generalmente ammesse, secondo le quali questi oscillatori dovrebbero essere lineari, il modello metallico porta per le suddette molecole ad oscillatori non lineari, cioè ad oscillatori piani fortemente asimmetrici. Ne consegue che i valori teorici della polarizzazione principale della fluorescenza P_p di queste molecole sono minori dei corrispondenti valori nel caso di oscillatori lineari, cioè $P_p < 0.5$. I valori calcolati di P_p sono: 0.47 per la fluoresceina, 0.49 per la rodamina B e 0.485 per l'eucrisina, la tripaflavina e il giallo acridina. Si ritiene che le differenze tra questi valori e quelli realmente osservati siano dovute, almeno parzialmente, all'effetto depolarizzante di vibrazioni torsionali delle molecole luminescenti. Ammettendo che l'intera differenza sia dovuta a vibrazioni torsionali, si stima il limite superiore della dipendenza di questo effetto dalla temperatura. Tale dipendenza appare assai debole (poichè l'intero effetto è modesto), ma sembra ancora misurabile. Uno degli scopi del presente lavoro è di mostrare l'utilità della nozione di « oscillatore spaziale virtuale » di cui l'« oscillatore piano » e l'« oscillatore lineare » sono casi particolari.

(*) *Traduzione a cura della Redazione.*

IL NUOVO CIMENTO Vol. II, N. 5 1° Novembre 1955

Asymptotic Expansions of Phase Shifts at High Energies.

M. VERDE (*)

Institute for Advanced Study - Princeton (New Jersey)

(ricevuto l'8 Agosto 1955)

Summary. — One gives asymptotic expansions of the phase shifts for large values of the momentum, considering central static potentials only. For non-singular potentials a recurrence relation which allows the calculation of terms of every order in $1/p$ is established. For potentials which are singular as $1/r$ at the origin, or regular for all angular momenta, the expansions are explicitly written neglecting terms of the order $1/p^5$.

The production of high energy particles in the laboratory is adding considerable new experimental information to our knowledge of nuclear fields. Nucleons of several hundreds MeV, for instance, have been observed in collision with nuclei and new interesting features, like the polarization of nucleon beams, have been discovered. At these high energies, the nuclei no longer constitute small obstacles, their linear dimensions becomes indeed many times the wave lengths of the incoming particles. This opens the interesting possibility of investigating nuclear form factors under conditions which may be considered simpler for theoretical interpretation, in the sense that geometrical optics becomes valid. This particular circumstance and the general trend of obtaining experimental data in these limit conditions raises the question of evaluating the phase shifts asymptotically for large values of the momentum involved in the collision.

It is well known that the scattering matrix, even for relative simple radial dependence of the corresponding potential, is a rather complicated function of the momentum, which can not be expressed, with the exception of a very few cases, in terms of known transcendental functions. Its behavior for small

---

(*) On leave from Turin University, Italy.

momenta has been satisfactorily studied as it is possible to express the phase shifts as a power series of the energy ([1]). Extensive studies have been made in order to establish the potential corresponding to a given scattering matrix ([2,3]) and great attention has been recently dedicated to the behavior of the phase shifts as a power series of the potential strength ([4,5]). At high energies one commonly has recourse to the Born expansions or to the JWKB method. These two approximations besides the fact that they lead to closed form expressions for the phase shifts in very few cases, can not be regarded as giving asymptotic expansions for large values of the momentum p.

The leading term of the desired expansion which falls off as $1/p$ for central static potentials everywhere regular and finite, is well known ([6,7]) and the following term in $1/p^3$ has been given recently ([8]). Under such restriction one excludes from the very beginning the centrifugal barrier (*).

We will present in Section 1 simple recurrence relations which allow us to calculate terms of any order, for the same class of regular potentials.

An expansion in inverse powers of the momentum does not exist for singular potentials as the phase shifts in this case have a logarithmic branch point at $p = \infty$. Yet, it is possible to establish also in these cases analogous asymptotic expansions, as shown in Section 2 for singular S wave scattering. We take into account the centrifugal barrier in Section 3.

We could not maintain in Sections 2 and 3 the same degree of generality as in Section 1, and the method followed there is essentially different. The presence of the logarithmic singularity is connected with the appearance of turning points, because of which the wave function changes from an oscillating into an exponential function. This is also the reason for the failure of a direct applicability of the same method used for regular potentials. As briefly mentioned in the concluding remarks, this method can be extended to take care of the presence of turning points, it does, however, not lead to formulas useful for practical calculations.

([1]) I. M. Blatt and V. F. Weisskopf: *Theoretical Nuclear Physics* (New York, 1952).

([2]) V. Bargmann: *Phys. Rev.*, **75**, 301 (1949); *Rev. Mod. Phys.*, **21**, 488 (1949).

([3]) R. Jost and W. Kohn: *Phys. Rev.*, **87**, 977 (1952); **88**, 382 (1952); R. G. Newton and R. Jost: *Nuovo Cimento*, **1**, 590 (1955).

([4]) R. Jost and A. Pais: *Phys. Rev.*, **82**, 840 (1952).

([5]) W. Kohn: *Rev. Mod. Phys.*, **26**, 292 (1954).

([6]) G. Parzen: *Phys. Rev.*, **80**, 261 (1950).

([7]) D. S. Carter: *Ph. D. Thesis at Princeton University* (1952), unpublished.

([8]) E. Corinaldesi: *Nuovo Cimento*, **12**, 438 (1954).

(*) In the mentioned paper ([8]) the first two terms of the asymptotic expansions are presented for an arbitrary angular momentum, yet they are only valid for the S scattering by a regular and finite potential.

1. – We will begin by dealing in this section with the case of potentials non singular at the origin and falling off for large distances r, faster than $1/r$.

The equation of motion, more conveniently written as a Riccati differential equations is

$$\varphi^2 + \varphi' + (p^2 - U) = 0 \,, \tag{1}$$

φ being the logarithmic derivative of the wave function ψ: $\varphi = \psi'/\psi$.

$p^2 = (2\mu E/\hbar^2) r_0^2$ can be chosen dimensionsless, introducing the range r_0 of the potential. We consider the solution φ which for large values of p goes as $+ip = -ip = i\sqrt{(2\mu E/\hbar^2) r_0^2}$. Putting

$$\varphi(r) = ip + f(p, r) \,,$$

the term in p^2 is eliminated from (1). f obeys the equation:

$$f^2 + f' + 2ipf = U \tag{2}$$

which suggests an ansatz of the form

$$2ipf = U + \sum_1^\infty{}_n \left(\frac{1}{2ip}\right)^n f_n(r) \,. \tag{3}$$

Substituting (3) in (2) and equating the coefficients of the same power of $1/2ip$, one obtains the following recurrence relation:

$$f_{n+1}(r) + f_n'(r) + \sum_0^{n-1}{}_s f_s(r) f_{n-1-s}(r) = 0 \tag{4}$$

valid for $n = 0, 1, 2, \ldots$ with $f_0 = U$, $f_{-1} = 0$. This is sufficient to evaluate every function $f_n(r)$.

In particular:

$$\begin{cases} f_0 = U \,, \qquad f_1 = -U' \,, \qquad f_2 = U'' - U^2 \,, \qquad f_3 = -U'' + 2(U^2)' \\ f_4 = U^{(\mathrm{IV})} - 3(U^2)'' + (U')^2 + 2U^3 \qquad \text{and so on.} \end{cases} \tag{5}$$

Neglecting all the derivatives of the potential, all f with n odd vanish, and

$$f_{2n} = 2^{2n+1} \binom{\frac{1}{2}}{1+n} U^{n+1} \,. \tag{6}$$

If on the other hand one restricts oneself to terms linear in f, one has

$$f_n = (-1)^n U^{(n)} \,. \tag{7}$$

One solution of (1) normalized to one for $r = 0$ is:

$$\psi_1 = \exp\left[\int_0^r \varphi(r)\,\mathrm{d}r\right] = \exp\left[ipr + \sum_0^\infty{}_n \left(\frac{1}{2ip}\right)^n \int_0^r f_n(r)\,\mathrm{d}r\right].$$

One needs to change sign to p for a second independent solution, so that the boundary condition at $r = 0$ is satisfied by

$$\psi = \exp\left[-\int_0^r \varphi(p, r)\,\mathrm{d}r\right] - \exp\left[-\int_0^r \varphi(-p, r)\,\mathrm{d}r\right],$$

which gives for the phase shifts the expansion:

$$\delta_0(p) \cong -\sum_0^\infty{}_n (-1)^n \left(\frac{1}{2p}\right)^{2n+1} \int_0^\infty f_{2n}(r)\,\mathrm{d}r\,. \tag{8}$$

It is not difficult to prove that (3) is an asymptotic solution of (2) for large values of p in the sense of H. Poincaré. This means that

$$\lim_{p\to\infty}\left\{f(p, r) - \sum_0^N{}_n \left(\frac{1}{2ip}\right)^n f_n(p, r)\right\} p^N = 0\,,$$

if $f(p, r)$ is the exact solution. The series (3) and (8) will in general not be convergent; nevertheless, the first terms may represent good approximations as is usual with asymptotic expansions.

We wish now to remark that the values of f_n given in (6) and (7) furnish the well known JWKB and first Born approximation of $\delta_0(p)$ respectively.

Inserting (6) in (8) one has indeed

$$\delta_0(p) \cong \lim_{r\to\infty} \int_0^r \sqrt{(p^2 - U} - p)\,\mathrm{d}r\,.$$

The value (7) gives instead

$$\delta_0(p) \cong (-1)^{n+1} \sum \left(\frac{1}{2ip}\right)^{2n+1} \int_0^\infty U^{(2n)}(r)\,\mathrm{d}r = -\frac{1}{p}\int_0^\infty U(r)\,\sin^2 pr\,\mathrm{d}r,$$

which is the well known formula of the first Born approximation.

The JWKB and the Born methods correspond therefore to a particular choice of terms in the expansion (8), and this may represent a worse approximation of δ_0 than the consideration of the first few terms in (8). This circumstance is well known in the use of asymptotic expansions, where the

consideration of terms of higher orders does not necessarily give an improvement of the result.

The explicit form assumed by (8), which shows functional dependence of δ_0 from the potential U, is

$$(9) \quad \delta_0(p) \cong -\frac{1}{2p}\int_0^\infty U\,\mathrm{d}r - \left(\frac{1}{2p}\right)^3\left(U'(0) + \int_0^\infty U^2\,\mathrm{d}r\right) - \\ - \left(\frac{1}{2p}\right)^5\left(-U'''(0) + 3(U^2)'_0 + \int_0^\infty U'^2\,\mathrm{d}r + 2\int_0^\infty U^3\,\mathrm{d}r\right) + O\left(\frac{1}{p^7}\right).$$

The coefficients of the expansion depend upon the properties in large of the potential through the integrals, and also are sensitive to the analytical behavior of the potential near the origin through the values of the derivatives of the potential at this point.

With potentials singular at the origin the coefficients become infinite and the expansion meaningless. This indicates that in such cases a simple expansion in inverse powers of the momentum does not exist. With singular repulsive potentials the largeness of p^2 is offset at the turning point where $p^2 - U = 0$ and because of which ψ''/ψ changes its sign. Even for regular potentials one has to expect that the approximations (8) and (9) become poor, if the momentum is not large enough to exclude the presence of a turning point.

The expansion (9), as is apparent from the recurrence relations (4) is also an expansion in powers of the potential strength. This is to bring in connection with the well known result that the successive Born approximations contain the factor $1/p$.

We will, therefore, for the more difficult case of singular potentials, deduce the corresponding expansions starting from the Liouville-Neumann solution of the integral equation equivalent to (1) (*).

2. – S-Wave Scattering by Potentials Singular as $1/r$ at the Origin.

The integral corresponding to (1) for a solution zero at the origin, is:

$$(10) \quad \psi = \sin pr + \frac{1}{p}\int_0^r \sin p(r - r')U(r')\psi(r')\,\mathrm{d}r' .$$

(*) This is the method which has been used in (8) for regular potentials. Our version of the method is greatly simplified and allows the consideration of singular potentials and of the centrifugal barrier.

(9) G. N. WATSON: *Theory of Bessel Functions* (Cambridge, 1948), p. 389.

It is more convenient to work with an equivalent system of coupled differential equations of the first order, and for this purpose we put

$$2i\psi = \exp[ipr]v_1 - \exp[-ipr]v_2\,, \qquad v_1(0) = v_2(0) = 1\,.$$

The system of the two coupled integral equations for the v's is:

$$v_1 = 1 + \frac{1}{2ip}\int_0^r U(r')\{v_1 - \exp[-2ipr']v_2\}\,dr'\,,$$

$$v_2 = 1 + \frac{1}{2ip}\int_0^r U(r')\{v_1 \exp[+2ipr'] - v_2\}\,dr'\,.$$

Differentiating this with respect to r one has:

$$\frac{\partial \boldsymbol{v}}{\partial r} = \frac{1}{2ip}\boldsymbol{H}(r)\cdot\boldsymbol{v}\,, \tag{11}$$

where $\boldsymbol{v}$ is a column matrix:

$$\boldsymbol{v} = \begin{pmatrix} v_1 \\ v_2 \end{pmatrix},$$

and $\boldsymbol{H}$ the square matrix:

$$H = U(r)\begin{pmatrix} 1 & -\exp[-2ipr] \\ \exp[2ipr] & -1 \end{pmatrix}. \tag{12}$$

The Liouville-Neumann solution of (11) normalized to one when $r = 0$ is

$$\boldsymbol{v} = \exp\left[\frac{1}{2ip}P\left\{\int_0^r \boldsymbol{H}\,dr\right\}\right]\cdot\boldsymbol{v}_0 = \sum\left(\frac{1}{2ip}\right)^n P\cdot\int_0^r \{\boldsymbol{H}(r_1)\ldots\boldsymbol{H}(r_n)\}\,dr_1\ldots dr_n\cdot\boldsymbol{v}_0\,. \tag{13}$$

$\boldsymbol{v}_0$ is the unit vector $\begin{pmatrix}1\\1\end{pmatrix}$ and the symbol P has the same meaning of ordered product in space, as the corresponding symbol used for the time in quantum electrodynamics. Here the products $\boldsymbol{H}(r_h)\cdot\boldsymbol{H}(r_k)$ do not commute, as $\boldsymbol{H}$ is the matrix defined in (12). The integration with respect to r takes place in the domain defined by the inequalities $r_1 > r_2 \ldots > r_n$.

A symbolic expression for the phase shifts may be derived from (13). It is also possible here to establish for regular potentials recurrence relations for the successive terms of (13). Since we are interested in the case of singular potentials, for which it is not possible to do this, we will limit ourselves to the consideration of the first two terms.

The knowledge of v_1 is sufficient to give δ_0, indeed

$$\delta_0(p) = \frac{1}{2i} \ln \frac{v_1}{v_2} = \operatorname{arctg} \left(\frac{\operatorname{Im} v_1}{\operatorname{Re} v_1} \right)_{r=\infty},$$

where

$$v_{1,2} = \operatorname{Re} v_1 \pm i \operatorname{Im} v_1 .$$

Therefore

$$(14) \quad \operatorname{tg} \delta_0 = -\frac{1}{p} \int_0^\infty U(r) \sin^2 pr \, dr + \frac{1}{p^2} \int_0^\infty U(r) \sin 2pr \int_0^r U(r') \sin^2 pr' \, dr' + O\left(\frac{1}{p^5}\right).$$

It now remains to pick out the coefficients of the terms in $1/p$ and $1/p^3$. The pole of first order of U in $r = 0$ can be eliminated in the integral $\int_0^\infty U(r) \sin^2 pr \, dr$ subtracting the known integral:

$$U_{-1} \int_0^\infty \frac{\exp[-\alpha r]}{r} \sin^2 pr \, dr .$$

Therefore

$$(15) \quad \int_0^\infty U \sin^2 pr \, dr = \frac{U_{-1}}{4} \ln \left(1 + \frac{4p^2}{\alpha^2}\right) + \int_0^\infty \left(U - U_{-1} \frac{\exp[-\alpha r]}{r}\right) \sin^2 pr \, dr \cong$$

$$\cong \frac{U_{-1}}{4} \ln \left(1 + \frac{4p^2}{\alpha^2}\right) + \frac{1}{2} \int_0^\infty \left(U - U_{-1} \frac{\exp[-\alpha r]}{r}\right) dr + \frac{1}{8p^2} \left(U - U_{-1} \frac{\exp[-\alpha r]}{r}\right)'_{r=0} .$$

Here use has been made of the asymptotic expansions

$$(16) \quad \int_0^\infty f(r) \cos 2pr \, dr \cong \sum_1^n (-1)^n \left(\frac{1}{2p}\right)^{2n} f^{(2n-1)}(0) ,$$

where $f(r)$ is regular in $r = 0$.

We have now to evaluate the term of the order $1/p$ in the double integral

$$J(p) = \int_0^\infty U(r) \sin 2pr \int_0^\infty U(r') \sin^2 pr' \, dr' .$$

It is easy, integrating by parts, to express the derivative of $J(p)$ with

respect to p, by single integrals. One has

$$-p\frac{dJ}{dp} = \int_0^\infty U \sin 2pr \int_0^r (r'U') \sin^2 pr' \, dr' + \int_0^\infty U \sin^2 pr \int_r^\infty (rU)' \sin 2pr' \, dr' =$$

$$= \frac{1}{2}\int_0^\infty U\cdot(rU - U_{-1}) \sin 2pr \, dr - \frac{1}{2p}\int_0^\infty U(rU)' \sin^2 pr \, dr .$$

Having recourse to the same device of subtracting the singularities at the origin, and using the expansion (16) together with the analogous

$$\int_0^\infty f(r) \sin 2pr \, dr \cong \sum_0^n (-1)^n \frac{f^{(2n)}(0)}{(2p)^{2n+1}}, \tag{17}$$

one finds:

$$\frac{dJ}{dp} \cong -\frac{U_{-1}U_0}{4p^2} + \frac{1}{8p^2} U_{-1}U_0 \ln\left(1 + \frac{4p^2}{\alpha^2}\right) +$$

$$+ \frac{1}{4p^2}\int_0^\infty \left(U(rU)' - U_{-1}U_0 \frac{\exp[-\alpha r]}{r}\right) dr + O\left(\frac{1}{p^4}\right).$$

Integrating term by term with respect to p, which is known to be allowed with asymptotic expansions, one gets

$$J(p) \cong -\frac{U_{-1}U_0}{4p} \ln\frac{2p}{\alpha} - \frac{1}{4p}\int_0^\infty \left(U(rU)' - U_{-1}U_0 \frac{\exp[-\alpha r]}{r}\right) dr + O\left(\frac{1}{p^3}\right). \tag{18}$$

The constant of integration has been put equal to zero, because J is an odd function of p.

The final expression for δ_0, using relations (14), (15), (18) is:

$$\operatorname{tg}\delta_0(p) \cong -\frac{1}{2p}\left[\int_0^\infty \left(U - U_{-1}\frac{\exp[-\alpha r]}{r}\right) dr + U_{-1}\ln\frac{2p}{\alpha}\right] + \tag{19}$$

$$-\left(\frac{1}{2p}\right)^3 \left[\left(U - U_{-1}\frac{\exp[-\alpha r]}{r}\right)'_{r=0} + \right.$$

$$\left. + 2U_{-1}U_0 \ln\frac{2p}{\alpha} + 2\int_0^\infty \left(U(rU)' - \frac{U_{-1}U_0}{r}\exp[-\alpha r]\right) dr + O\left(\frac{1}{p^5}\right)\right].$$

This formula contains (9) as a particular case for $U_{-1} = 0$.

It is in principle possible to apply the same methods to evaluate terms of higher orders. Yet, as the formulas become clumsy, the work involved is rather tedious.

We will illustrate the use of (19) in two simple cases, namely for the Yukawa and the Hulthen's potentials $U_{-1}\exp[-r]/r$, $U_{-1}\exp[-r]/(1-\exp[-r])$ respectively.

In the first case putting $\alpha = 1$ in (19) we have

$$\delta_0(p) \cong -\frac{U_{-1}}{2p}\ln 2p + \frac{U_{-1}^2}{4p^3}\ln p + O\left(\frac{1}{p^5}\right).$$

For the Hulthen's potential, the exact expression for δ_0 is known [1] and can be written in term of $\ln \Gamma(p)$. One has

$$\delta_0 = \frac{1}{2i}\ln\left\{\frac{\Gamma(1+2ip)}{\Gamma(1-2ip)}\cdot\frac{\Gamma(1-iU_{-1}/2p)}{\Gamma(1+iU_{-1}/2p)}\cdot\frac{\Gamma(1-2ip-iU_{-1}/2p)}{\Gamma(1+2ip+iU_{-1}/2p)}\right\}.$$

Using the Stirling formula for $\ln\Gamma(1+z)$, one deduces for the leading term in $1/p$

$$\delta_0(p) = -\frac{U_{-1}}{2p}\ln 2p + \frac{U_{-1}}{2p}\Gamma'(1).$$

This result is contained in (19), remembering that:

$$\Gamma'(1) = \int_0^\infty\left(\frac{\exp[-r]}{r} - \frac{\exp[-r]}{1-\exp[-r]}\right)\mathrm{d}r.$$

3. – Scattering for $l \neq 0$.

The presence of a centrifugal barrier introduces a singularity of the type $1/r^2$ and this again excludes simple expansions in inverse powers of the momentum. It is advisable therefore to follow closely the method of last section.

With the following notation

$$j_l(pr) = \left(\frac{\pi pr}{2}\right)^{\frac{1}{2}} J_{l+\frac{1}{2}}(pr), \qquad n_l(pr) = (-1)^l\left(\frac{\pi pr}{2}\right)^{\frac{1}{2}} J_{-l-\frac{1}{2}}(pr),$$

$$h_l^{\pm}(pr) = n_l(pr) \pm ij_l(pr),$$

the integral equation corresponding to (10) reads:

$$(10') \qquad \psi = j_l(pr) + \frac{1}{p}\int_0^r [j_l(pr)n_l(pr') - n_l(pr)j_l(pr')]U(r')\psi(r')\,\mathrm{d}r',$$

and with

$$2i\psi = h_l^+ v_1 - h_l^- v_2 , \qquad v_1(0) = v_2(0) = 1$$

the corresponding system for the $\boldsymbol{v}$'s is:

$$\frac{\partial \boldsymbol{v}}{\partial r} = \frac{1}{2ip} \boldsymbol{H}(r) \cdot \boldsymbol{v}, \tag{11'}$$

where

$$\boldsymbol{H}(r) = U(r) \begin{pmatrix} (j_l^2 + n_l^2) & -(h_l^-)^2 \\ (h_l^+)^2 & -(j_l^2 + n_l^2) \end{pmatrix}.$$

The leading term of the expansion for $\delta_l(p)$ is readily obtained if $U(r)$ is non singular. For $p \to \infty$, $\boldsymbol{H}(r)$ becomes diagonal $\boldsymbol{H}(r) \cong U(r) \begin{pmatrix} 1 & 0 \\ 0 & -1 \end{pmatrix}$ the matrix elements off the diagonal being rapidly oscillating functions of r do not give contribution to the first order. From

$$\boldsymbol{v}(\infty) = \exp \frac{1}{2ip} \int_0^\infty \boldsymbol{H} \mathrm{d}r \; \boldsymbol{v}_0 ,$$

one deduces the well known result:

$$\delta_0(p) = \frac{1}{2i} \ln \frac{v_1}{v_2} = -\frac{1}{2p} \int_0^\infty U(r) \, \mathrm{d}r ,$$

which is independent of l. The expression analogous to (14) is

$$\delta(p) \simeq -\frac{1}{p} \int_0^\infty U(r) j_l^2(pr) \, \mathrm{d}r + \frac{2}{p^2} \int_0^\infty U(r) j_l(pr) n_l(pr) \int_0^r U(r') j_l^2(pr') \, \mathrm{d}r' + O\left(\frac{1}{p^5}\right). \tag{14'}$$

We will allow also for $l \neq 0$ potentials $U(r)$ which may have a pole of the first order at the origin.

It is easy to find that

$$j_l^2(pr) = \frac{1 - (-1)^l \cos^2 pr}{2} + (-1)^l \frac{\sin 2pr}{2pr} l(l+1) + \frac{1}{p^2 r^2} l(l+1) + O\left(\frac{1}{p^4}\right),$$

where $O(1/p^4)$ means that the neglected terms will first contribute in the asymptotic expansion of the coefficients of (14') in the order $1/p^5$.

We have now to evaluate the first two terms of the integral:

$$J(p) = \int_0^\infty U(r) j_l^2(pr)\,\mathrm{d}r\,. \tag{20}$$

If $U(r)$ has a zero $\sim r^2$ at the origin, no logarithmic terms will arise in the first two orders. We have therefore to subtract from (20) an integral

$$J_k(p) = \int_0^\infty f(r) j_l^2(pr)\,\mathrm{d}r\,,$$

whose asymptotic behaviour is known and to choose $f(r)$ so that $U(r) - f(r)$ has a zero of the second order at the origin. For $f(r)$ we take:

$$f(r) = \left\{\frac{U_{-1}}{r} + (\alpha U_{-1} + U_0) + r[U'(0) + \alpha[\alpha U_{-1} + U(0)] - \frac{\alpha^2}{2} U_{-1}]\right\} \exp[-\alpha r]. \tag{21}$$

The asymptotic expansion of (20) remembering (16) and (17) becomes:

$$J(p) \simeq \frac{1}{2}\int_0^\infty [U(r) - f(r)]\,\mathrm{d}r - \frac{l(l-1)}{4p^2}\int_0^\infty \frac{1}{r^2}[U(r) - f(r)]\,\mathrm{d}r + J_k(p) + O\left(\frac{1}{p^4}\right). \tag{22}$$

For the calculation of the first two terms of $J_k(p)$ we refer to the Appendix.

Our last task is now to find the leading term of the double integral

$$L_l(p) = \int_0^\infty U(r) j_l(pr) n_l(pr) \int_0^r U(r') j_l^2(pr')\,\mathrm{d}r'\,. \tag{23}$$

If $U(r)$ is regular at the origin, this is simply given by: $-(1/16)\int_0^\infty U^2\,\mathrm{d}r$, because we can put $j_l^2(pr)$ equal to $(1 - (-1)^l \cos 2pr)/2$, and $j_l(pr)n_l(pr)$ equal to $((-1)^l/2)\sin 2pr$.

One obtains the same results as for $l = 0$ and this remains true in every order.

If $U(r)$ has a pole at the origin it is convenient to proceed as for the S-wave scattering. Differentiating (23) with respect to p and integrating by parts, one has:

$$-p\frac{\mathrm{d}L_l}{\mathrm{d}p} = \int_0^\infty U j_l n_l \int_0^r (r'U)' j_l^2\,\mathrm{d}r' + \int_0^\infty U j_l^2 \int_r^\infty (r'U)' j_l n_l\,\mathrm{d}r'\,.$$

Here it is again necessary to evaluate the term in $1/p$ and to integrate back. Although it is not difficult to prove that the coefficient of the logarithmic term is the same as for $l = 0$, it remains still an open question to establish the general dependence on l, of the additional $1/p$ term.

We will therefore limit ourselves, for a general expression of the phase shifts, to the case of regular potentials. One obtains, remembering (14'), (22) and the appendix:

$$\operatorname{tg}\,\delta_l(p) = -\frac{1}{2p}\left[\int_0^\infty (U(r) - f(r))\,\mathrm{d}r + \frac{1}{\alpha}\left(2U(0) + \frac{U'(0)}{\alpha}\right)\right] -$$
$$- \left(\frac{1}{2p}\right)^3 \left[\int_0^\infty U^2\,\mathrm{d}r + 2l(l+1)\left(\int_0^\infty \frac{1}{r^2}(U-f)\,\mathrm{d}r - \alpha U(0)\right) + \right.$$
$$\left. + 2l(l+1)U'(0)\left(\ln\frac{2p}{\alpha} - \frac{1}{2} + \sum_1^l \frac{1}{n}\right)\right] + O\left(\frac{1}{p^5}\right),$$

where

$$f(r) = [U(0) + r\cdot(U'(0) - \alpha U(0))]\exp[-\alpha r].$$

4. – Concluding remarks.

The main question which arises with every kind of approximation of unknown functions is concerned with the range of its validity, or with the estimate of the error introduced by neglecting terms of higher orders. Since the general term of the expansion has a rather complicated nature, it is hard to believe that this question can be answered in its full generality. We may guess that besides the requirement of small wave lengths in comparison with the dimensions of the obstacle, it is essential that either no turning point should exist or that they should be near to the origin, as is always realized at sufficiently high energies. If the turning points happen to be distant from the origin it is more advisable to use approximations of JWKB type, which correspond to an expansion in inverse powers of $p^2 - U$. It is also possible to improve the form commonly used of the JWKB method, with an iteration procedure that takes into account the derivatives of the potential and therefore correctly describes terms of order higher than $1/p$. It is even possible to give formally the expression of the general term of the expansion with recurrence relations. These expressions, however, are extremely involved, containing multiple integrations which cannot be performed even for very simple potentials. The complications here again are due to the necessity of correctly describing the analytical behavior of the wave function near the turning point.

The main advantage of the expansions given in this paper lies in the fact that they provide a simple functional dependence of the phase shift on the potential. It is noteworthy that the behavior of $\delta_l(p)$ is very sensitive to the nature of the singularity at the origin. For potentials singular as $1/r^\lambda$ ($\lambda < 2$) one does not have expansions in inverses of entire powers of p.

Another question which arises is the necessity of taking into consideration the relativistic kinematical corrections which are important especially for light particles at high energies. The method followed here can be extended to cover such cases. We hope to enlarge in the near future the present work, to include spin and velocity dependent potentials as well as to take care of relativistic collisions.

* * *

The author wishes to acknowledge his indebtedness to Professor ROBERT OPPENHEIMER for a grant-in-aid and the hospitality at the Institute for Advanced Study, to the FOA and to the NRC for a fellowship, to the Turin University for a leave for research.

APPENDIX

For the calculation of the first two terms of the expansion in $1/p$ of the integral

$$J_k(p) = \int_0^\infty \frac{\exp[-\alpha r]}{r} j_l^2(pr)\,\mathrm{d}r\,,$$

we have to use the well known result

$$J_k(p) = \frac{1}{2} Q_l\left(1 + \frac{\alpha^2}{2p^2}\right),$$

where $Q_l(z)$ is a Legendre function of the second kind [10]

$$Q_l(z) = \frac{1}{2} P_l(z) \ln\frac{z+1}{z-1} - \sum_1^l{}_n \frac{1}{n} P_{n-1}(z) P_{l-n}(z)\,.$$

---

[10] MAGNUS and OBERHETTINGER: *Formeln und Sätze* (Berlin, 1948), p. 76.

One has:

$$Q_l\left(1+\frac{\alpha^2}{2p^2}\right)\cong\left(\ln\frac{2p}{\alpha}-\sum_1^l{}_n\frac{1}{n}\right)+\frac{\alpha^2}{4p^2}\,l(l+1)\left[\ln\frac{2p}{\alpha}-\sum_1^l{}_n\frac{1}{n}\right]+O\left(\frac{1}{p^4}\right).$$

The only other integrals required in (22) are:

$$-\frac{\partial Q_l}{\partial\alpha}\cong\frac{1}{\alpha}-\frac{\alpha}{2p^2}\,l(l+1)\left[\ln\frac{2p}{\alpha}+\frac{1}{2}-\sum_1^l{}_n\frac{1}{n}\right]+O\left(\frac{1}{p^4}\right)$$

$$\frac{\partial^2 Q_l}{\partial\alpha^2}\cong\frac{1}{\alpha^2}+\frac{1}{2p^2}\,l(l+1)\left[\ln\frac{2p}{\alpha}-\frac{1}{2}+\sum_1^l{}_n\frac{1}{n}\right]+O\left(\frac{1}{p^4}\right).$$

RIASSUNTO

Si derivano alcuni sviluppi asintotici, per grandi valori dell'energia, degli sfasamenti relativi ad urti in campi statici e centrali. Nel caso di potenziali ovunque regolari, si stabilisce una formula ricorrente che permette il calcolo dei coefficienti dello sviluppo di un ordine qualunque. Per potenziali singolari come $1/r$ nell'origine, o regolari con una barriera centrifuga, gli sviluppi sono scritti esplicitamente trascurando termini di ordine $1/p^5$.

A New Multiple Scattering Parameter.

H. J. Lipkin, S. Rosendorff and G. Yekutieli

Physics Department, Weizmann Institute of Science - Rehovoth (Israel)

(ricevuto il 16 Agosto 1955)

Summary. — A new parameter is proposed for the characterization of the multiple scattering observed in tracks of charged particles. This parameter is the mean value of the cosine of a constant times the projected scattering angle. The theoretical relation between the mean value of the cosine parameter and the momentum-velocity product $p\beta$ of the particle can be calculated analytically in a simple way. A theoretical dispersion is also calculable, thereby giving an estimate of the error. This is in contrast to the parameter usually used in track measurements; namely, the mean absolute value of the projected scattering angle where the mean value calculation is complicated and the dispersion is excessively sensitive to the form of the scattering law at large angles. Theoretical results for the mean value and dispersion of the cosine parameter are given for two cases: 1) angles between successive tangents at intervals along the track; 2) angles between successive chords. The effect of the correlation between successive measurements is considered in the latter case.

1. – Introduction.

It is common practice to use measurements of the multiple scattering of charged particles in cloud chambers and photographic plates to estimate the value of the product $p\beta$ of the particle momentum and its velocity. The usual procedure is to calculate from the experimental data the mean value of a convenient parameter characterizing the multiple scattering, such as the projected angle between successive chords or tangents drawn at certain intervals along the track. If a single scattering law is assumed, a theoretical value for the mean value of this parameter can be calculated which is a function of $p\beta$. The value of $p\beta$ giving agreement between the theoretical and the experimental values of the scattering parameter is assumed to be the best value for

the particle. If the mean square value of the parameter is calculated from the theory, this gives an indication of the breadth of the distribution and makes possible an estimate of the error in the value of $p\beta$.

Several very detailed calculations of multiple scattering theory have been made ([1-3]). In all cases it is assumed that the desired parameter is the angle between successive chords or tangents. In the use of this parameter, the following difficulties are encountered:

1) An exact analytic calculation of the mean absolute value of this parameter is very difficult.

2) Because the scattering drops off slowly at large angles, an unreasonably large contribution to the result comes from large angle scattering. Unless some form of cut-off is introduced, the theoretical mean square angle is very large, and it is impossible to give a theoretical estimate of error. OLBERT ([2]) avoids this difficulty by introducing a cut-off on the single scattering distribution, based upon considerations of finite nuclear size. SCOTT ([3]) introduces an arbitrary cut-off on the multiple scattering distribution at four times the mean angle. The results obtained naturally depend upon the form of cut-off assumed.

The purpose of this work is to suggest a new parameter to characterize the multiple scattering which does not suffer from the two difficulties mentioned above. This parameter is $\cos(\eta\varphi)$, where φ is the projected scattering angle and η is a constant multiplier whose value is chosen according to conditions discussed below. The mean value of this cosine parameter is simply the appropriate component of the Fourier transform of the multiple scattering distribution function. As has been shown ([1,4]) the Fourier transforms of the single and multiple scattering distributions are very simply related, although the relation between the distribution functions themselves is complicated. It is therefore possible to calculate the mean and mean square values of the cosine parameter with relative ease. Since all powers of the cosine are expressible in terms of Fourier components of different arguments, the higher moments of the distribution of the cosine parameter can be obtained directly once the mean value is known for all values of the multiplier η.

If the value of the multiplier η is properly chosen, the use of the cosine parameter is equivalent to the use of the mean square angle with an effective cut-off at large angles. This follows from the fact that $1 - \cos(\eta\varphi)$ is approx-

([1]) G. MOLIÈRE: *Zeits. f. Naturf.*, **2a**, 133 (1947); **3a**, 78 (1948).
([2]) S. OLBERT: *Phys. Rev.*, **87**, 319 (1952).
([3]) W. T. SCOTT: *Phys. Rev.*, **85**, 245 (1952).
([4]) H. A. BETHE: *Phys. Rev.*, **89**, 1256 (1953).

imately equal to $(\eta\varphi)^2/2$ for small values of $\eta\varphi$ but is much less than $(\eta\varphi)^2/2$ for large values of $\eta\varphi$ and remains bounded. The contribution of large angle scattering is thus drastically reduced, and the mean value of the cosine parameter is very insensitive to the form of the single scattering law at large angles. It is thus permissible to use Molière's simple approximate formula for projected single scattering, even though it is accurate only for small angles, and to neglect effects due to the finite size of the nucleus.

2. – Calculation of the cosine parameter for the tangent case.

Consider the track of a particle divided into a number of segments of length t. At the end of each segment a tangent is drawn to the track, and the projected angles between successive tangents are measured. Each angle depends only upon the scattering which has occured within the particular segment intercepted between the tangents. Each angle measurement is therefore independent of the others, and the distribution function for these angles is simply the multiple scattering distribution function for particles which have traversed a thickness t of the scattering substance. The mean value of any parameter can therefore be calculated from the multiple scattering distribution function, and the mean square as well, which gives the dispersion.

It is desirable to have an estimate of the error in an experimental value of $p\beta$ which is obtained by using the mean value of the cosine parameter. This estimate can be calculated if the distribution function for the mean value of the cosine parameter is known. As this distribution function is not easily obtained explicitly, it will be assumed to be normal if the number of measurements is large. For this case an estimate of the error is given by dividing the dispersion of a single measurement by the square root of the number of measurements [5].

The calculations for the cosine parameter can be made without requiring the explicit form of the angular distribution function for multiple scattering. All that is necessary is its Fourier transform. A convenient point of departure for the calculation is the expression relating the Fourier transforms of the single scattering and the multiple scattering distributions. This relation appears in various forms in the literature [6] and is derived in a different

---

[5] The error in assuming a normal distribution can be determined from calculations of the higher moments of the cosine parameter. These moments are easily calculated from the results given for the mean value of $\cos\eta\varphi$ for all values of the multiplier η. Once the higher moments are known, standard statistical methods can be used. (Cf. CRAMER: *Methods of Mathematical Statistics* (Princeton, 1946).

[6] See in particular BETHE, equation (7) and MOLIÈRE, equation (8.3). Since

manner in section 4, equation (4.6) below for the general case in which there are correlations. This relation can be written:

$$(2.1)\qquad \int_0^\infty f(q,t)\cos\eta q\,\mathrm{d}q = \exp\left[-Nt\int_0^\infty W(\chi)\,\mathrm{d}\chi\{1-\cos(\eta\chi)\}\right] = \exp\left[\Omega(\eta)-\Omega_0\right].$$

Where $W(\chi)\,\mathrm{d}\chi$ is the single scattering differential cross-section into the projected angle interval $\mathrm{d}\chi$, and $f(\varphi, t)\mathrm{d}\varphi$ is the multiple scattering distribution in the projected angular interval $\mathrm{d}\varphi$ after traversing a thickness t. N is the number of scattering atoms per unit volume, and $\Omega(\eta)$ and Ω_0 are defined as

$$(2.2)\qquad \Omega(\eta) = Nt\int_0^\infty W(\chi)\,\mathrm{d}\chi\cos(\eta\chi)\,,$$

$$(2.2')\qquad \Omega_0 = \Omega(0)\,.$$

Thus Ω_0 is the mean number of single scattering processes occurring in the thickness t of scattering substance.

From equation (2.1) the mean and mean square values of the cosine parameter can immediately be written:

$$(2.3)\qquad \langle\cos(\eta\varphi)\rangle = \exp\left[\Omega(\eta)-\Omega_0\right]$$

$$(2.3')\qquad \langle\cos^2(\eta\varphi)\rangle = (1/2)[1+\exp\{\Omega(2\eta)-\Omega_0\}]\,.$$

If Molière's [1] expression for $W(\chi)$ is introduced into (2.2) and $\eta \ll 1/\chi_a$ the functions $\Omega(\eta)$ and Ω_0 are given explicitly by the relation:

$$(2.4)\qquad \Omega_0-\Omega(\eta) = (1/2)(\sigma\eta)^2[1-(1/B)\ln(\tfrac{1}{2}\sigma^2\eta^2)]$$

$$(2.4')\qquad \Omega_0 = (\chi_c/\chi_a)^2\,,$$

where $\sigma^2 = \chi_c^2 B/2$, and B is Molière's parameter defined by the transcendental equation:

$$(2.5)\qquad B-\ln B = \ln(\chi_c/\chi_a)^2 + 1 - 2C = \ln(e\chi_c^2/\gamma^2\chi_a^2)\,.$$

projected angles only are treated here, the cosine transform is used in all cases rather than the Bessel transformation.

$C = \ln \gamma = 0.577 \ldots$ is Euler's constant. χ_c and χ_a are defined by the relation:

$$\chi_c^2 = 4\pi N t (zZe^2/pc\beta)^2 \tag{2.6}$$

$$\chi_a = (\hbar/ap)[1.13 + 3.76(zZ/137\beta)^2]^{\frac{1}{2}} \tag{2.6'}$$

z is the charge of the particle, Z the charge of the scattering atoms, p the particle momentum, c the velocity of light, β the particle velocity in units of c, e the electronic charge, and a the Thomas-Fermi radius of the atom.

From equation (2.4),

$$\Omega_0 - \Omega(2\eta) = 4[\Omega_0 - \Omega(\eta)] - 2(\sigma^2\eta^2/B) \ln 4 \,. \tag{2.7}$$

Substituting equation (2.7) into (2.3') and writing $\Omega = \Omega_0 - \Omega(\eta)$

$$\langle \cos^2 (\eta\varphi) \rangle = (1/2)\{1 + \exp [-4\bar{\Omega} + 2(\sigma^2\eta^2/B) \ln 4]\} \tag{2.8}$$

$$\langle \cos^2 (\eta\varphi) \rangle - \langle \cos (\eta\varphi) \rangle^2 = \tag{2.9}$$
$$= 2 \exp [-2\bar{\Omega}(\sinh^2 \bar{\Omega} + (1/4) \exp (-2\Omega)\{\exp (2\sigma^2\eta^2/B) \ln 4 - 1\})] \,.$$

The mean square deviation of the cosine parameter, which is given by equation (2.9), does not give directly the estimated error in the determination of the value of $p\beta$ for the particle, since the functional relation between $\cos (\eta\varphi)$ and $p\beta$ is not linear. If a Gaussian distribution is assumed for $\langle \cos (\eta\varphi) \rangle$, the square root of equation (2.9) divided by the square root of the number of measurements, n, gives the dispersion $D[\cos (\eta\varphi)]$, and therefore defines limiting values of $\cos (\eta\varphi)$ such that only 32 % of the cases lie outside these limits. Using these limiting values of $\cos (\eta\varphi)$ and equations (2.3), (2.4) and (2.6), corresponding limits in $p\beta$ can be obtained, and an effective dispersion $D(p\beta)$ for $p\beta$ can be defined. Since the parameter σ is proportional to $p\beta$,

$$\frac{D(p\beta)}{p\beta} = -\frac{D(\sigma)}{\sigma} = \frac{D[\cos (\eta\varphi)]}{\sigma(\mathrm{d}/\mathrm{d}\sigma)\langle \cos (\eta\varphi) \rangle} = \tag{2.10}$$
$$= \frac{[\sinh^2 \bar{\Omega} + (\tfrac{1}{4}) \exp [-2\bar{\Omega}] \{\exp [2\sigma^2\eta^2/B] \ln 4 - 1\}]^{\frac{1}{2}}}{\sqrt{2n}\,(\bar{\Omega} - \sigma^2\eta^2/2B)} \,.$$

The result of (2.10) can be interpreted as follows: The multiple scattering distribution is approximately gaussian at small angles, with a single-scattering « tail » present at large angles. Since the Fourier transform of a gaussian is also a gaussian, the first term in equation (2.4) represents a gaussian, and

therefore the term proportional to $1/B$ can be interpreted as the contribution of the single scattering tail. Calculations for the case of a pure gaussian distribution have been made by one of us (G.Y.) [7] showing that a value of $D(p\beta)/p\beta$ of $1/\sqrt{2}$ is obtained if the mean square angle is used as the parameter, and that this is the optimum value possible. Since the cosine parameter is equivalent to the mean square angle if η is small, the same case is obtainable from equation (2.10) by setting $\eta\sigma \ll 1$, and discarding the effect of the « tail » by setting $1/B = 0$. The result $1/\sqrt{2}$ is obtained, as expected.

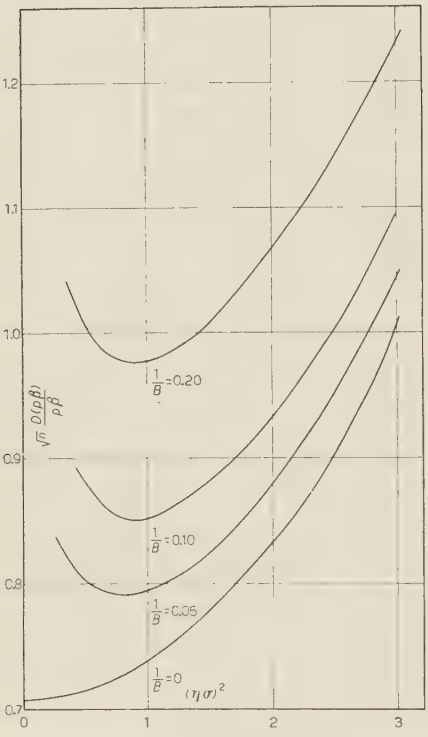

Fig. 1. – The dispersion vs. $(\eta\sigma)^2$ in the tangent case.

For finite values of B, equation (2.10) diverges as $\eta \to 0$, as is to be expected since the mean square also diverges when the single scattering tail is taken into account. For $\eta \neq 0$, a cut-off is effectively introduced by the deviation of the cosine from the square at large angles, and a finite result is obtained. The choice of the exact value of η is thus equivalent to choosing the location of the cut-off. For optimum results η must be large enough to cut down the contribution from the « tail », as given by the terms proportional to $1/B$ in (2.10), but it must not be so large that the desired part of the distribution is also cut off. This latter effect is given by the deviation of $\sinh \bar{\Omega}$ from $\bar{\Omega}$ in the gaussian part of (2.10) as a result of the effective cut-off. Numerical values for equation (2.10) are plotted in Fig. 1. The optimum value of η is that which minimizes $D(p\beta)/p\beta$, and is about $1/\sigma$, giving a value of $D(p\beta)/p\beta \sim 0.9$, depending upon the value of B. This is not much greater than the value 0.707 for the gaussian case and is in reasonable agreement with values given by SCOTT for the mean absolute angle with a cut-off. The minimum is rather broad, as is indicated by the curves of Fig. 1.

[7] G. YEKUTIELI: CERN report BS-7.

3. – The effect of a single scattering cut-off.

OLBERT (2) has treated the effect of the finite size of the nucleus upon the multiple scattering distribution function and has calculated the mean square projected angle of scattering. This has been achieved by assuming that the projected single scattering cross-section $W(\chi)\mathrm{d}\chi$ is zero for all angles greater than a cut-off angle φ_0, and that for smaller angles it is given by Molière's small angle approximation formula:

$$NtW(\chi)\,\mathrm{d}\chi = \tfrac{1}{2}\,\chi_c^2\,\frac{\mathrm{d}\chi}{(\chi^2+\chi_a^2)^{\frac{3}{2}}}. \tag{3.1}$$

Using Olbert's assumption, it is also possible to calculate the mean value and dispersion of the cosine parameter. All the results of the preceding section are valid; it is merely necessary to replace the quantity $\bar{\Omega}$ by the corresponding quantity $\bar{\Omega}_c$, calculated by introducing equation (3.1) with the cut-off into the definition (2.2) of $\Omega(\eta)$. Thus:

$$\bar{\Omega}_c = \chi_c^2 \int_0^{\varphi_0} \frac{(1-\cos\eta\chi)\,\mathrm{d}\chi}{(\chi^2+\chi_a^2)^{\frac{3}{2}}}. \tag{3.2}$$

Note that if $\varphi_0 = \infty$, equation (3.2) reduces to the case without cut-off, and $\bar{\Omega}_c = \bar{\Omega}$. If $\varphi_0 \gg \chi_a$, equation (3.2) can be written:

$$\bar{\Omega}_c = \bar{\Omega} - \chi_c^2 \int_{\varphi_0}^{\infty} \frac{(1-\cos\eta\chi)\,\mathrm{d}\chi}{\chi^3} = \bar{\Omega} - \frac{\sigma^2(1-\cos\eta\varphi_0)}{B\varphi_0^2} - \tag{3.3}$$

$$- \frac{\sigma^2\eta^2}{B}\left[\frac{\sin\eta\varphi_0}{\eta\varphi_0} - Ci(\eta\varphi_0)\right],$$

where $Ci(u) = -\int_u^{\infty} t^{-1}\cos t\,\mathrm{d}t$ is the cosine integral. If η is sufficiently large so that $\eta\varphi_0 \gg 1$, the asymptotic form for $Ci(\eta\varphi_0)$ can be used and equation (3.3) becomes:

$$\bar{\Omega}_c = \bar{\Omega}\left[1 - \frac{2}{\eta^2\varphi_0^2[B + \ln(4/\chi_c^2\eta^2B^2)]} - O(\eta\varphi_0)^{-3}\right]. \tag{3.3'}$$

The terms depending on the cut-off angle φ_0 can be neglected if $2/\eta^2\varphi_0^2 B \ll 1$. In the preceding section it was shown that optimum results for the cosine parameter are obtained when $1/\eta \sim \sigma = \chi_c\sqrt{B/2}$. For this case $2/\eta^2\varphi_0^2 B$ is of

order $(\chi_c/\varphi_0)^2$ which is clearly negligible. It is therefore permissible to neglect the effect of cut-off in equation (3.3). The cosine parameter is therefore insensitive to effects of finite nuclear size which produce a cut-off on the single scattering law.

Equation (3.3) can also be used in the limit $\eta \to 0$ to give a value for the mean square projected angle. In this case, $Ci(u)$ is replaced by the approximation for small values of u, namely $\ln(\gamma u)$. This compensates the term in $\ln \eta$ in equation (2.4) so that a finite result is obtained:

$$\bar{\Omega}_{c0} = (1/2)(\sigma\eta)^2[1 - (1/B)\{\ln(\tfrac{1}{2}\sigma^2/\gamma^2\varphi_0^2) - 3\}] \tag{3.4}$$

and

$$\langle\varphi^2\rangle = 2[1 - \langle\cos(\eta\varphi)\rangle]/\eta^2 = \sigma^2[1 + (1/B)\{\ln(2\gamma^2\varphi_0^2/\sigma^2) - 3\}] \tag{3.4'}$$

in agreement with Olbert's result.

4. – The case of the angle measured between successive chords.

If the angles measured along a track are those between successive chords rather than between successive tangents, the problem is no longer described simply in terms of the multiple scattering of particles passing through a thickness t of matter. There are two new complications: 1) the contribution of each individual single scattering to the measured angle depends upon the position along the track where the scattering occurs; 2) each single scattering contributes to two measured angles; namely the angles between the segment where the scattering occurs and the preceding and following segments. The two measurements are therefore not independent and the correlation between them must be taken into account. This is illustrated in the simple example shown in Fig. 2. A particle is incident along the line of OP and suffers only one single scattering within the two segments shown. The particle paths and the associated chords are drawn for four cases in which the single scattering occurs at four different points A, B, C, and D along the path. It is evident that the angles θ_A, θ_B, θ_C, and θ_D drawn between the corresponding chords are all different and that only in the case of θ_C, where the scattering occurs exactly at the boundary between two segments is the measured angle equal to the angle

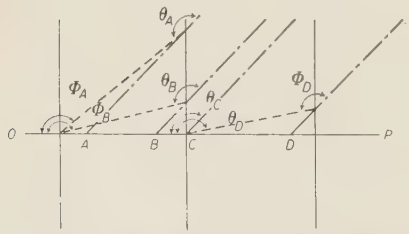

Fig. 2. – The dependence of the angle between successive chords upon the position of each single scattering.

of scattering. The angles φ_A, φ_B, and φ_D illustrate the contribution of this single scattering to adjacent measurements.

This problem has been considered by MOLIÈRE [8] who obtains expressions for the distribution function for the angle between successive chords. The same method can be used to calculate the cosine parameter. The dependence of the contribution of each single scattering upon the position where it occurs is considered by defining a weight function $a_m(y)$. This function describes the weight to be given to a single scattering occurring at a point y along the track in the calculation of its contribution to the angle measured at the end of the m-th segment. If the angles are all small, the tangent of the angle can be taken as equal to the angle. The relation between the angle φ_m measured between successive chords at the end of the m-th segment and the individual single scattering angles χ_i occurring along the track at points y_i is therefore:

$$\varphi_m = \sum_i a_m(y_i)\chi_i \,. \tag{4.1}$$

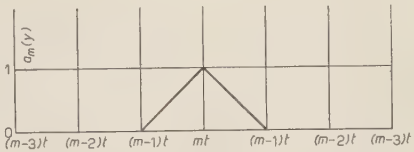

Fig. 3. – The weight function $a_m(y)$.

It is evident from Fig. 2 that the weight function $a_m(y_i)$ for the angle θ is a maximum when the scattering occurs at the point C, and that it decreases linearly in both directions. Thus $a_m(y_i)$ has the form shown in Fig. 3 and is given by:

$$\begin{cases} a_m(y_i) = 1 - |y_i/t - m| & \text{for} \quad |y_i - mt| \leqslant t \\ a_m(y_i) = 0 & \text{for} \quad |y_i - mt| > t \end{cases} \tag{4.2}$$

where t is the length of each segment.

Because of the correlation between adjacent measurements, it is not sufficient to calculate the distribution function for a given angle φ_m. It is necessary to consider the whole set of values $(\varphi_1, \varphi_2 \ldots, \varphi_n)$, where n is the number of angles measured (the number of segments is therefore $n+1$) and to define a distribution function $P(\varphi_1, \varphi_2, \ldots, \varphi_n)\,\mathrm{d}\varphi_1\,\mathrm{d}\varphi_2 \ldots \mathrm{d}\varphi_n$ representing the probability of finding simultaneously φ_1 between φ_1 and $\varphi_1 + \mathrm{d}\varphi_1$, φ_2 between φ_2 and $\varphi_2 + \mathrm{d}\varphi_2$, etc. To obtain an expression for this distribution function consider first the probability for a particle to suffer k single scatterings by angles $\chi_1, \chi_2, \ldots, \chi_k$ at the point $y_1, y_2, \ldots, y_k$ respectively in traversing the $n+1$ segments of thickness t:

$$P(\chi_1, \chi_2, \ldots, \chi_k;\ y_1, y_2, \ldots, y_k) = \{\exp[-(n+1)\Omega_0]/k!\} \prod_{i=1}^{k} [W(\chi_i)N]\,, \tag{4.3}$$

---

[8] G. MOLIÈRE: *Zeits. f. Naturf.*, **10a**, 177 (1955).

where the exponential factor represents the probability of traversing the distance $(n+1)t$ without suffering single scattering, and the factor $k!$ is introduced because without it each set of values is counted $k!$ times. The probability that a particle suffers k single scatterings and that the set of values $(\varphi_1, \varphi_2, ..., \varphi_n)$ is obtained for angles between successive chords is obtained by integrating the distribution (4.3) over all values of (χ_i, y_i) consistent with the conditions (4.1). If this is now summed over k from 1 to ∞, the desired distribution function is obtained:

$$(4.4)\quad P(\varphi_1, \varphi_2, \dots \varphi_n) = \sum_{k=1}^{\infty} \{\exp[-(n+1)\Omega_0]/k!\} \int d\chi_1 \int dy_1, \dots \int d\chi_k \int dy_k \cdot$$
$$\cdot \prod_{i=1}^{k} \{NW(\chi_i) \prod_{m=1}^{n} \delta[\varphi_m - \sum_j a_m(y_j)\chi_j]\} .$$

Although the distribution function (4.4) is quite complicated, its Fourier transform, as in the tangent case, is much simpler, and the cosine parameter is readily calculated. Consider first the mean value of a generalized Fourier component having the form $\exp i[\sum_m \eta_m \varphi_m]$. The integration over φ_m is trivial because of the delta functions, giving:

$$(4.5)\quad \exp[i\sum_m \eta_m \varphi_m]_{\text{av}} = \exp[-(n+1)\Omega_0] \sum_k \int d\chi_1 \int dy_1 \dots \int d\chi_k \int dy_k \prod_{i=1}^{k} [NW(\chi_i)] \cdot$$
$$\cdot \exp[i \sum_{m=1}^{n} \eta_m \sum_{j=1}^{k} a_m(y_j)\chi_j]/k! .$$

This can be written more simply:

$$(4.5')\quad \langle \exp i[\sum_m \eta_m \varphi_m] \rangle =$$
$$= \exp[-(n+1)\Omega_0] \sum_k \left\{ N \int d\chi_i \int dy_i W(\chi_i) \exp[i \sum_m \eta_m a_m(y_i)\chi_i] \right\}^k \Big/ k! =$$
$$= \exp[-(n+1)\Omega_0] + N \int d\chi \int dy W(\chi) \exp[i \sum_m \eta_m a_m(y)\chi] .$$

Since $W(\chi)$ is an even function of (χ), the imaginary exponential can be replaced by a cosine. The integrand is thus simply $\Omega[\sum_m \eta_m a_m(y)]/t$ by the definition (2.2) of $\Omega(\eta)$. Noting also that $\int \Omega_0 dy/t = (n+1)\Omega_0$, equation (4.5) can be written:

$$(4.6)\qquad \langle \exp[i \sum_m \eta_m \varphi_m] \rangle = \exp\left[\int \{\Omega[\sum \eta_m a_m(y)] - \Omega_0\} dy/t \right] .$$

The integration with respect to y is straightforward although tedious after the explicit expression (2.4) for Ω is introduced into equation (4.6). The following special cases are of interest for the calculation of the mean value and dispersion of the cosine parameter:

Case I. $\eta_p = \eta,\ \eta_m = 0\ (m \neq p)$.
Introducing the explicit expressions for Ω and a_p,

$$\bar{\Omega}_1 = -\ln\langle\exp[i\eta\varphi_p]\rangle = (1/3)(\sigma\eta)^2[1 + 2/3B - (1/B)\ln(\sigma^2\eta^2/2)]\,. \tag{4.7}$$

Case II. $|p-q| > 1,\ \eta_p = \pm\eta_q = \eta,\ \eta_m = 0\ \ (m \neq p,\ m \neq q)$.

$$\bar{\Omega}_2 = -\ln\langle\exp[i\eta(\varphi_p \pm \varphi_q)]\rangle = 2\,\bar{\Omega}_1\,. \tag{4.7'}$$

Case III. $\eta_p = \eta_{p+1} = \eta,\ \ \eta_m = 0\ \ (m \neq p,\ m \neq p+1)$.

$$\bar{\Omega}_{2+} = -\ln\langle\exp[i\eta(\varphi_p + \varphi_{p+1})]\rangle = (5/2)\bar{\Omega}_1 - \sigma^2\eta^2/3B\,. \tag{4.7''}$$

Case IV. $\eta_p = -\eta_{p+1} = \eta,\ \ \eta_m = 0\ \ (m \neq p,\ m \neq p+1)$.

$$\bar{\Omega}_{2-} = -\ln\langle\exp[i\eta(\varphi_p - \varphi_{p+1})]\rangle = (3/2)\bar{\Omega}_1\,. \tag{4.7'''}$$

The mean value of the cosine parameter is then given by:

$$\langle(1/n)\sum_{m=1}^{n}\cos\eta\varphi_m\rangle = \exp[-\bar{\Omega}_1]\,. \tag{4.8}$$

The mean square value is given by:

$$\begin{aligned}
\langle[(1/n)\sum_{m=1}^{n}\cos\eta\varphi_m]^2\rangle &= \left\langle\left(\frac{1}{2n}\right)^2\sum_{p=1}^{n}\sum_{q=1}^{n}\exp[i\eta(\varphi_p+\varphi_q)] + \right.\\
&\left. + 2\exp[i\eta(\varphi_p-\varphi_q)] + \exp[-i\eta(\varphi_p+\varphi_q)]\right\rangle =\\
&= \frac{1}{2n}\{\exp[-\bar{\Omega}_1(2\eta)] + 1\} + \{[n(n-3)+2]/n^2\}\exp[-\bar{\Omega}_2] +\\
&+ [(n-1)/n^2]\{\exp[-\bar{\Omega}_{2+}] + \exp[-\bar{\Omega}_{2-}]\} =\\
&= \exp[-\bar{\Omega}_2]\left(1 + \frac{2}{n}\left\{\sinh^2\bar{\Omega}_1 + 2\sinh^2\left(\frac{\bar{\Omega}_1}{4}\right) + \right.\right.\\
&+ \frac{\exp[-\bar{\Omega}_2]}{4}\{\exp[2\bar{\Omega}_2 - \bar{\Omega}_1(2\eta)] - 1\} +\\
&\left.\left. + \frac{\exp[-\bar{\Omega}_1/2]}{2}\{\exp[(5/2)\bar{\Omega}_1 - \bar{\Omega}_{2+}] - 1\}\right\} -\right.\\
&\left. - \frac{4}{n^2}\left\{\sinh^2\left(\frac{\bar{\Omega}_1}{4}\right) + \frac{\exp[-\bar{\Omega}_1]/2}{4}\{\exp[(5/2)\bar{\Omega}_1 - \bar{\Omega}_{2+}] - 1\}\right\}\right).
\end{aligned} \tag{4.8'}$$

The mean square deviation of the cosine parameter is therefore given by:

$$(4.9)\quad \frac{1}{n^2}\left\{\left\langle\left[\sum_{m=1}^{n}\cos\eta\varphi_m\right]^2\right\rangle - \left\langle\sum_{m=1}^{n}\cos\eta\varphi_m\right\rangle^2\right\} = \exp\left[-2\bar{\Omega}_1\right]\left(\frac{2}{n}\left\{\sinh^2\bar{\Omega}_1 + \right.\right.$$

$$+ 2\sinh^2\left(\frac{\bar{\Omega}_1}{4}\right) + \frac{\exp\left[-2\bar{\Omega}_1\right]}{4}\left\{\exp\left[4\sigma^2\eta^2\ln 4/3B\right] - 1\right\} +$$

$$\left. + \frac{\exp\left[-\bar{\Omega}_1/2\right]}{2}\left\{\exp\left[\sigma^2\eta^2/3B\right] - 1\right\}\right\} -$$

$$\left. - \frac{4}{n^2}\left\{\sinh^2\frac{\bar{\Omega}_1}{4} + \frac{\exp\left[-\bar{\Omega}_1/2\right]}{4}\left\{\exp\left[\sigma^2\eta^2/3B\right] - 1\right\}\right\}\right).$$

If n is large the terms proportional to $1/n^2$ can be neglected. Then, as in the simple tangent case, the effective dispersion of $p\beta$ is given by:

$$(4.10)\quad \frac{D(p\beta)}{p\beta} = \frac{D(\sum\cos\eta\varphi_m)}{\sigma(\mathrm{d}/\mathrm{d}\sigma)\left\langle\sum\cos(\eta\varphi_m)\right\rangle} =$$

$$\frac{\left\{\sinh^2\bar{\Omega}_1 + 2\sinh^2\left(\frac{\bar{\Omega}_1}{4}\right) + \frac{e^{-2\bar{\Omega}_1}}{4}\left\{e^{4\sigma^2\eta^2\ln 4/3B} - 1\right\} + \frac{e^{-\bar{\Omega}_1|2}}{2}\left[e^{\sigma^2\eta^2/3B} - 1\right]\right\}^{\frac{1}{2}}}{\sqrt{2n}(\bar{\Omega}_1 - \sigma^2\eta^2/3B)}.$$

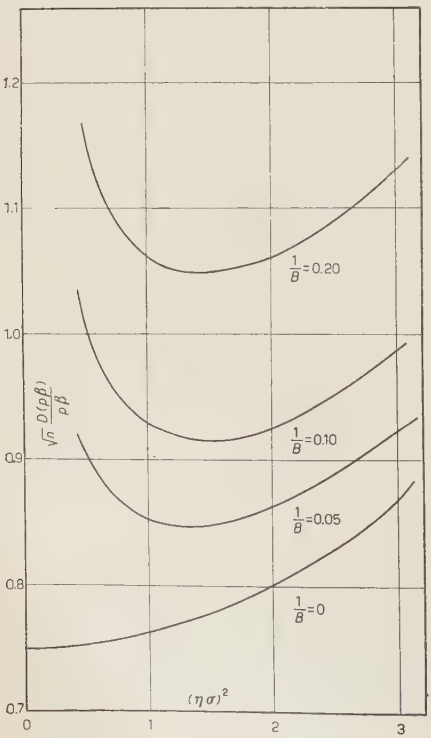

Fig. 4. – The dispersion vs. $(\sigma\eta)^2$ in the chord case.

Equation (4.10) is similar in form to equation (2.10) for the tangent case. The first two terms in the numerator are from the gaussian, the next two from the tail. Of each pair there is one term which resembles the tangent case and an additional term which can be interpreted as the effect of the correlation.

For the gaussian portion with $\eta = 0$, the result $D(p\beta)/p\beta = 3/4\sqrt{n}$ is obtained which is the result obtained for the mean square angle in the gaussian case. When the effect of the tail is considered, the behaviour of $D(p\beta)/p\beta$ as a function of η is similar to the tangent case, and is shown in Fig. 4. A

minimum is obtained for $\eta \sim 1.2/\sigma$, giving a value of $D(p\beta)/p\beta \sim 0.96$. The effect of the correlation is thus to increase the error by about 7%.

5. – Application of the cosine parameter.

The calculation of the value of $p\beta$ from experimental data by the use of the cosine parameter is somewhat more complicated than the conventional method using the mean absolute value of the projected scattering angle. This is because the optimum value of the multiplier η depends upon the value of $p\beta$. It is therefore necessary to assume a trial value for $p\beta$ in order to obtain a value for η. Using this value for η, the values of σ and of $p\beta$ can be calculated, as well as the dispersion of $p\beta$. If the value of $\eta\sigma$ obtained is reasonably close to the value giving minimum dispersion, the calculation can be terminated at this point. Otherwise the new value of $p\beta$ can be used to determine η and the process repeated. Because of the insensivity of the dispersion with variations in η, it should be possible to find a good value of η without many iterations.

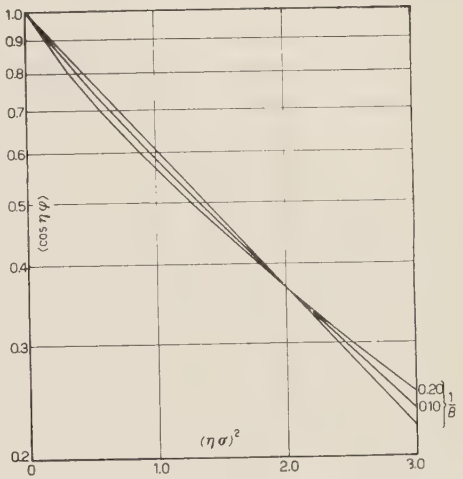

Fig. 5. – $\langle\cos\eta\varphi\rangle$ vs. $(\eta\sigma)^2$ for the tangent case.

To aid in the calculations, Figs. 1, 4, 5, 6, have been prepared giving the values of the cosine parameter and the dispersion as function of $(\eta\sigma)^2$ for several values of the parameter B. A curve of Molière's parameter B as a function

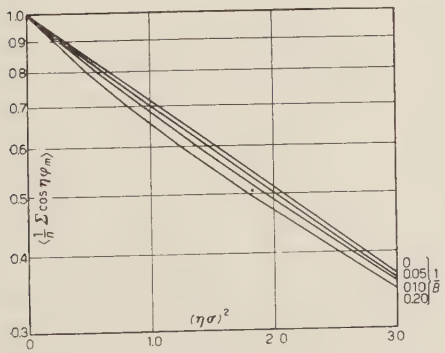

Fig. 6. – $\langle(1/n)\sum\cos\eta\varphi\rangle$ vs. $(\eta\sigma)^2$ for the chord case.

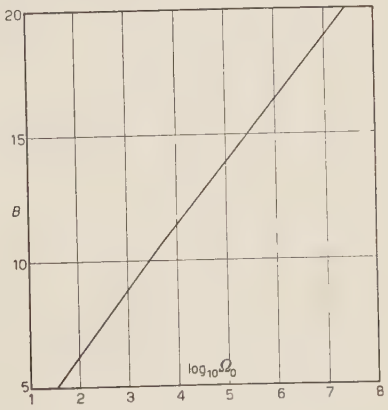

Fig. 7. – Molière's parameter B vs. $\log_{10}\ \Omega_0$.

of $\log_{10} \Omega_0$ is given in Fig. 7. Curves for Ω_0 can be found in the literature (9).

Experimental results on the use of the cosine parameter will be reported at a later date.

(9) W. HEISENBERG: *Kosmische Strahlung* (Berlin, Göttingen, Heidelberg, 1953), p. 512.

RIASSUNTO (*)

Si propone un nuovo parametro per la caratterizzazione dello scattering multiplo osservato nelle tracce delle particelle cariche. Tale parametro è il valor medio del coseno di una costante per la proiezione dell'angolo di scattering. La relazione teorica tra il valor medio del parametro coseno e il prodotto $p\beta$ della quantità di moto per la velocità della particella può agevolmente essere calcolato analiticamente. Si può calcolare anche una dispersione teorica dando così una stima dell'errore. Questo è in contrasto col parametro comunemente usato nelle misure delle tracce; cioè il valor medio assoluto della proiezione dell'angolo di scattering per il quale il calcolo del valor medio è complicato e la dispersione è sensibilissima alla forma della legge di scattering sotto grandi angoli. Risultati teorici per il valor medio e la dispersione del parametro coseno sono dati per due casi: 1) angoli fra tangenti successive ad intervalli lungo la traccia; 2) angoli tra corde successive. In quest'ultimo caso si considera l'effetto della correlazione tra le successive misure.

(*) *Traduzione a cura della Redazione.*

On the Energy Determination of Electron Pairs.

E. Lohrmann

Physikalisches Institut der Universität Bern
Hochspannungslaboratorium - Hechingen, Germany

(ricevuto il 28 Agosto 1955)

Summary. — The limitations of determining the energy of electron pairs by means of their angular divergence are investigated by considering in detail the influence of multiple scattering. It is shown that at energies of the order of 1 GeV and higher the divergence of pair electrons is essentially determined by multiple scattering.

1. – Introduction.

The aim of this investigation is to discuss the influence of multiple scattering on the determination of the energy of electron pairs by means of their angle of divergence using the generally accepted formula of Borsellino [1]

$$\omega_p = \frac{4mc^2 \cdot \Phi_a}{k}, \tag{1}$$

ω_p is the most probable angle of separation,
$\Phi_a \approx 1$ is a factor describing the energy distribution of the electrons,
m is the electron mass, k the photon energy.

2. – Basic scattering formulas.

We start by deriving an expression for the probability $W(x, y, \eta)\,\mathrm{d}y\,\mathrm{d}\eta$, that an electron after traversing a distance x in a scattering material suffers

[1] G. Baroni, A. Borsellino, L. Scarsi and G. Vanderhaeghe: *Nuovo Cimento*, **10**, 1653 (1953).

a lateral displacement between y and $y+\mathrm{d}y$ and a net change of direction between η and $\eta+\mathrm{d}\eta$ projected in a plane of observation containing the x-axis We will take into account the energy loss by bremsstrahlung.

The probability $W(x, y, \eta)$ can be shown (cf. SCOTT [2]) to follow the differential equation

$$\left(\frac{\partial}{\partial x}+\eta\frac{\partial}{\partial y}\right)\cdot W(x, y, \eta)=\frac{1}{\lambda}\cdot\frac{\partial^2 W(x, y, \eta)}{\partial\eta^2} \tag{2}$$

for small values of y and η.

For high energies of the electron $E\gg mc^2$ λ is given by

$$\lambda = K^2E^2\,, \tag{3}$$

K depends only little on E.

If λ is independent of x, a solution of equ. (2) is according to FERMI [3]

$$W(x, y, \eta)\,\mathrm{d}y\,\mathrm{d}\eta=\frac{\lambda\sqrt{3}}{2\pi x^2}\exp\left[-\frac{\lambda}{x}\left\{\eta^2-\frac{3\eta y}{x}+\frac{3y^2}{x^2}\right\}\right]\mathrm{d}y\,\mathrm{d}\eta \tag{4}$$

satisfying the boundary condition

$$W(0, y, \eta)=\delta(y)\cdot\delta(\eta)\,. \tag{5}$$

If we assume λ to be a function of x, it can easily be verified by substitution, that the following function $P(x, y, \eta, c, g)$ is a solution of equ. (2):

$$P(x, y, \eta, c, g)=A(c)\cdot B(g)\exp\left[c^2\varphi_1+cy-2cg\varphi_2-c\eta x+g\eta+g^2\varphi_3\right], \tag{6}$$

c and g are arbitrary complex parameters.

$\varphi_1(x)$, $\varphi_2(x)$ and $\varphi_3(x)$ are given by

$$\left\{\begin{aligned}\varphi_1(x)&=\int_0^x\frac{t^2}{\lambda(t)}\,\mathrm{d}t\,,\\ \varphi_2(x)&=\int_0^x\frac{t}{\lambda(t)}\,\mathrm{d}t\,,\\ \varphi_3(x)&=\int_0^x\frac{1}{\lambda(t)}\,\mathrm{d}t\,.\end{aligned}\right. \tag{7}$$

---

[2] W. T. SCOTT: *Phys. Rev.*, **76**, 212 (1948).

[3] B. ROSSI and K. GREISEN: *Rev., Mod. Phys.*, **13**, 240 (1941).

Setting $A(c) = B(g) = \text{const.}$, integrating over c and g from $-i\infty$ to $+i\infty$ and normalizing, one gets the distribution function sought for

$$(8)\quad W(x, y, \eta)\,\mathrm{d}y\,\mathrm{d}\eta = \\ = \frac{1}{4\pi(\varphi_1\varphi_3 - \varphi_2^2)^{\frac{1}{2}}} \exp\left[-\frac{\eta^2(\varphi_1 - 2x\varphi_2 + x^2\varphi_3) + 2y\eta(\varphi_2 - x\varphi_3) + y^2\varphi_3}{4(\varphi_1\varphi_3 - \varphi_2^2)}\right]\mathrm{d}y\,\mathrm{d}\eta\,.$$

On putting $\lambda = \text{const.}$, equ. (8) of course reduces to equ. (4).

For the energy loss by bremsstrahlung we have approximately

$$(9)\qquad E = E_0 \exp\left[-lx\right],$$

E_0 is the initial energy of the electron and l^{-1} is the radiation length. It follows

$$(10)\qquad \lambda(x) = K^2E_0^2 \exp\left[-2l\cdot x\right].$$

With this function equ. (8) can be shown to fulfill the boundary condition equ. (5) and to represent gaussian distributions in y and η. On integrating over η we get the probability $W_1(x, y)\,\mathrm{d}y$ of a lateral displacement between y and $y+\mathrm{d}y$ after a distance x:

$$(11)\quad W_1(x, y)\,\mathrm{d}y = \frac{1}{[4\pi(\varphi_1 - 2x\varphi_2 + x^2\varphi_3]^{\frac{1}{2}}} \exp\left[-\frac{y^2}{4(\varphi_1 - 2x\varphi_2 + x^2\varphi_3)}\right]\mathrm{d}y\,.$$

In the same way we get for the probability $W_2(x, \eta)\,\mathrm{d}\eta$ of observing a net change of direction between η and $\eta+\mathrm{d}\eta$ after a distance x

$$(12)\qquad W_2(x, \eta)\,\mathrm{d}\eta = \frac{1}{\sqrt{4\pi\varphi_3}} \exp\left(-\frac{\eta^2}{4\varphi_3}\right)\mathrm{d}\eta\,.$$

Inserting the functions equ. (7) determined according to equ. (10) we get in the case of energy loss by bremsstrahlung for the r.m.s. displacement in the plane of observation

$$(13)\qquad \bar{y} = \frac{1}{E_0\cdot K(2l^3)^{\frac{1}{2}}}\cdot(\exp\left[2lx\right] - 2x^2l^2 - 2lx - 1)^{\frac{1}{2}}.$$

Taking a pair the electrons of which have the same initial energy E_0 resulting in a photon energy of $2E_0$ we have for their r.m.s. spatial distance neglecting an initial divergence of the pair

$$(14)\qquad y_0 = \frac{2^{\frac{1}{2}}}{E_0K\cdot l^{\frac{3}{2}}}\,(\exp\left[2lx\right] - 2x^2l^2 - 2lx - 1)^{\frac{1}{2}}$$

(one factor of $2^{\frac{1}{2}}$ takes account of the mutual scattering between both electrons, the other one comes from the transition to a spatial distribution for the case of small displacements.)

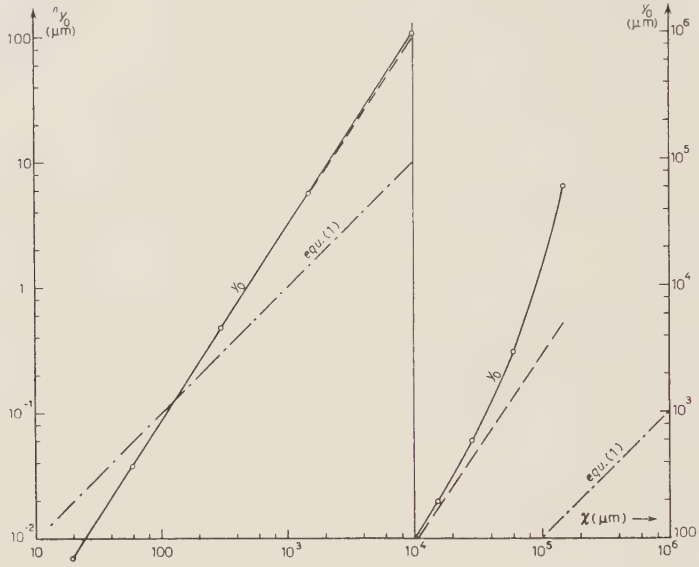

Fig. 1. – Separation of an electron pair of 1 GeV each. —— y_0: r.m.s. separation due to multiple scattering equ. (14); ----- the same without consideration of bremsstrahlung. –·–· separation according to equ. (1).

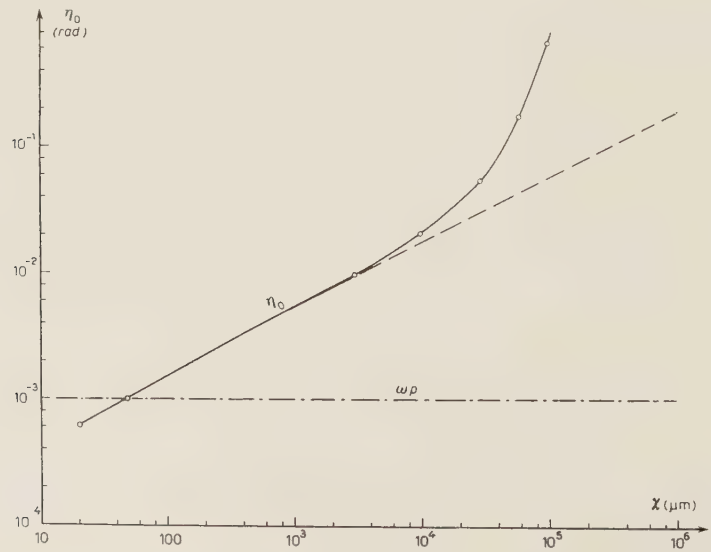

Fig. 2. – Angle between pair electrons of 1 GeV each. —— η_0: r.m.s. angle due to multiple scattering equ. (15). ---- the same without consideration of bremsstrahlung. –·–· ω_p: angle according to equ. (1).

In a similar way we get for the r.m.s. angle in space between the two electrons at a distance x from the origin of the pair

$$\eta_0 = \frac{2}{E_0 \cdot K l^{\frac{1}{2}}} (\exp [2lx] - 1)^{\frac{1}{2}}. \tag{15}$$

The functions $y_0(x)$ and $\eta_0(x)$ are plotted in Fig. 1 and Fig. 2 for nuclear emulsion for an electron energy $E_0 = 1$ GeV, putting $l^{-1} = 29$ mm. K was determined by fitting the distribution in η equ. (12) to the theory of Molière. The variation of the scattering constant at small distances was taken into account. For distances > 500 μ a value of 30 MeV/(100 μm)$^{\frac{1}{2}}$·degree was used. For comparison the most probable angle and the most probable separation according to equ. (1) are given also. They are equal to η_0 and to y_0 at 50 μm and 130 μm respectively independently of electron energy.

3. – Influence of the energy distribution of the electrons.

We are now going to derive the distribution $W_5(y)$ of the distance y between the electrons of pairs produced by photons of energy $k = 2E_0$ by integrating over the energy distribution of the electrons. We will again neglect an initial divergence of the pair. The distribution of the displacement of one electron of energy E in space is according to equs. (11) and (13)

$$W_3(y)\,\mathrm{d}y = \frac{1}{(\pi)^{\frac{1}{2}}} \cdot \frac{E}{2\varphi} \exp\left[-\frac{y^2 E^2}{4\varphi^2}\right] \mathrm{d}y \tag{16}$$

putting

$$\varphi(x) = (\exp [2lx] - 2x^2 l^2 - 2lx - 1)^{\frac{1}{2}} \cdot (2K^2 l^3)^{-\frac{1}{2}}. \tag{17}$$

The distribution of the distance y between two electrons of energy E and $k - E$ produced by a photon of energy k is

$$W_4(y)\,\mathrm{d}y = \left[4\varphi^2 \cdot \pi \left(\frac{1}{E^2} + \frac{1}{(k-E)^2}\right)\right]^{\frac{1}{2}} \exp\left[-\frac{y^2}{4\varphi^2} \cdot \frac{1}{1/E^2 + 1/(k-E)^2}\right] \mathrm{d}y \tag{18}$$

introducing $u = E/k$ and y_0, the r.m.s. separation one gets in case of equipartition of energy on both electrons, we have

$$W_4(y)\,\mathrm{d}y = \frac{2u(1-u)}{[\pi y_0^2 (u^2 + (1-u)^2)]^{\frac{1}{2}}} \exp\left[-\left(\frac{2y}{y_0}\right)^2 \frac{u^2(1-u)^2}{u^2 + (1-u)^2}\right] \mathrm{d}y\,. \tag{19}$$

Multiplying equ. (19) by $P(k, u)\,\mathrm{d}u$, the probability that one of the pair

electrons has an energy between E and $E+\mathrm{d}E$ and integrating over the energy distribution we get the probability $W_5(y)\,\mathrm{d}y$ that the distance between the two electrons of the pair is between y and $y+\mathrm{d}y$.

Restricting ourselves to energies $k > 1$ GeV, we can approximately choose for $P(k, u)$ the probability calculated by BETHE and HEITLER [4] for complete screening. $P(k, u)$ may then be approximated with an accuracy of about 5% by

$$P(k, u) \approx C\cdot[u^2 + (1-u)^2]^{\frac{1}{2}}\,. \tag{20}$$

We thus have with the abbreviation $p = 2y/y_0$

$$W_5(y)\,\mathrm{d}y = C'\int_0^1 u(1-u)\exp\left[-p^2\frac{u^2(1-u)^2}{u^2+(1-u)^2}\right]\mathrm{d}u\,\mathrm{d}y\,. \tag{21}$$

The normalization may be carried out by reversing the order of integration. It follows

$$W_5(y)\,\mathrm{d}y = \frac{2}{y_0\pi^{\frac{1}{2}}[\frac{1}{2}+(1/4\sqrt{2})\cdot\ln((1+\sqrt{2})/(1-\sqrt{2}))]}\cdot F(p)\,. \tag{22}$$

The function

$$F(p) = \int_0^1 u(1-u)\exp\left[-p^2\frac{u^2(1-u)^2}{u^2+(1-u)^2}\right]\mathrm{d}u\,, \tag{23}$$

is plotted in Fig. 3. The distribution $\exp[-y^2/2y_0^2)$ corresponding to the equipartition of energy between both electrons is drawn in for comparison (normalized to the same area). $F(p)$ may be shown by expanding p into a series to be represented by

$$F(p) = 0.67 - 0.013p^2 + 0.0007p^4 \qquad p \leqslant 2 \tag{24}$$

and by expanding the exponent in powers of u and confining the range of integration to $p\cdot u = 2$ we have

$$F(p) = p^{-2} - 0.8p^{-3} \qquad \text{for } p \geqslant 4. \tag{25}$$

Both approximations equs. (24) and (25) are true to about 5% within the limits given for p.

The probability

$$W_6(y) = \int_0^p W_5(p)\,\mathrm{d}p \tag{26}$$

---

[4] H. BETHE and W. HEITLER: *Proc. Roy, Soc.*, A **146**, 83 (1934).

of a pair to have a separation $< 2y/y_0$ is plotted in Fig. 4. We have applied a cut-off for calculating $W_6(y)$ at $\rho = 30$, which however affects $W_6(y)$ to less than 5%.

It may be noted that equs. (22)-(26) can easily be extended to the distribution of the angles η. If the distribution of the angles for equipartition of energy is

$$W_7(\eta)\,\mathrm{d}\eta = (2\pi\bar{\eta}^2)^{-\frac{1}{2}} \exp\left[-\eta^2/2\bar{\eta}^2\right]\mathrm{d}\eta \tag{27}$$

the distribution integrated over the energy distribution of the electrons will be

$$W_8(\eta)\,\mathrm{d}\eta = \frac{2}{\bar{\eta}\pi^{\frac{1}{2}}\left(\frac{1}{2} + 1/4\sqrt{2}\cdot\ln\left((1+\sqrt{2})/(1-\sqrt{2})\right)\right)} \cdot F\left(\frac{2\eta}{\bar{\eta}}\right)\mathrm{d}\eta\,. \tag{28}$$

Denoting by s the most probable distance between the electrons according to equ. (1) if follows from equ. (7) and Fig. 1 that at $x = 130$ μm the separation due to multiple scattering is $> s$ in 55% of all cases. There exists a 70% probability that the separation due to scattering is $> 2s$ at a distance of 1 mm. This result might suggest that equ. (1) determines the separation of the pair up to distances of the order of 100 μm, whereas the separation at distances > 1000 μm from the origin of the pair should be essentially determined by multiple scattering. Demanding a minimum separation of the tracks of 0.5 μm to be distinguishable, the limits given above correspond to photon energies of 560 MeV and 4 GeV respectively. For higher energies a rough estimate of the upper and lower limit for photon energy can be made by neglecting an initial divergence of the pair at high energies, noting that a photon of energy $2E_0$ should give a separation between $\frac{1}{5}\,y_0$ and $5y_0$ with a probability of 90%, y_0 being connected with E_0 by equ. (14) or Fig. 1. For a single event this does

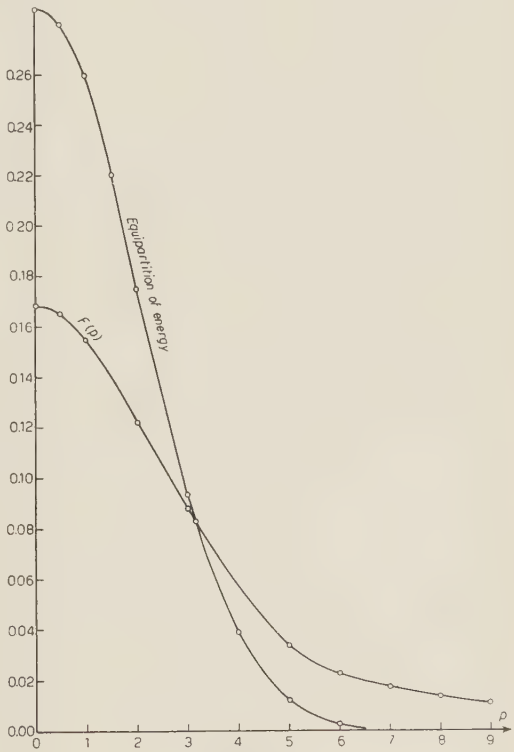

Fig. 3.

not mean very much, however, as the probability of a separation exceeding the limits given above does not decrease very rapidly.

The influence of the emission of bremsstrahlung on the divergence of the pair by the impulses transmitted by the quants was shown to be negligible by EULER and WERGELAND ([5]).

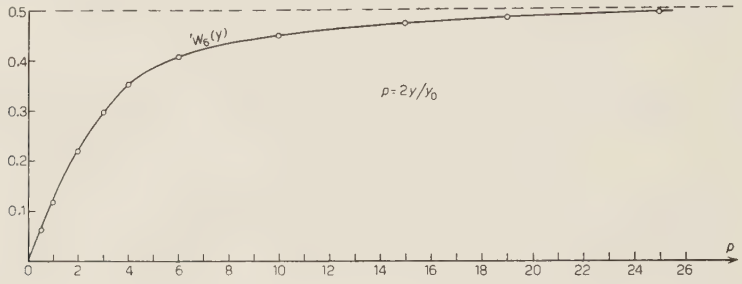

Fig. 4.

Conclusion: Equ. (1) can be applied for estimating photon energies up to 0.5 GeV, if the angle is measured at a distance $\leqslant 100$ μm from the origin of the pair. For higher energies scattering measurements should be made to determine the energy.

4. – Root mean square values.

It is clear that one should take the most probable separation given by equ. (1) for estimating the energy of a single pair of low energy. The r.m.s. value of this angle derived from the Borsellino formula is considerably greater and is not far from the expression given by STEARNS ([6]), if one applies the same cut-off. The r.m.s. value of the separation due to multiple scattering according to equ. (22) would still be higher for high energies; it is not given however, as its exact value depends rather critically on the angle of cut-off used because of the asymptotic form of $F(p)$ equ. (25).

* * *

The author wishes to express his thanks to Prof. Dr. F. G. HOUTERMANS for the hospitality he enjoyed in his institute, to Prof. Dr. E. SCHOPPER for

([5]) H. EULER and H. WERGELAND: *Astrophysica Norvegica*, **3**, 165 (1940).
([6]) M. STEARNS: *Phys. Rev.*, **76**, 836 (1949).

granting a leave of absence and above all to Dr. M. TEUCHER for many stimulating discussions. A grant from the Deutsche Forschungsgemeinschaft is gratefully acknowledged.

RIASSUNTO (*)

Si esaminano le possibilità di determinare l'energia delle coppie di elettroni per mezzo del loro angolo di divergenza, considerando in dettaglio lo scattering multiplo. Si dimostra che ad energie dell'ordine di 1 GeV e maggiori la divergenza delle coppie di elettroni è essenzialmente determinata dallo scattering multiplo.

(*) *Traduzione a cura della Redazione.*

The Formation of ^{32}P from Atmospheric Argon by Cosmic Rays.

L. Marquez and N. L. Costa

Centro Brasileiro de Pesquisas Fisicas - Rio de Janeiro, Brasil

(ricevuto il 7 Settembre 1955)

Summary. — It is shown by experiments that radioactive ^{32}P is formed as a spallation product of argon by cosmic rays. This ^{32}P is found in the rain water, and its average activity in fresh rain water of Rio de Janeiro is 0.20 dpm/liter.

1. – Introduction.

It is known that the interaction of the cosmic rays with the nuclei of nitrogen and oxygen of the air produces a substantial number of neutrons which are captured after being slowed down by the reaction $^{14}N(n, p)^{14}C$. This radioactive ^{14}C was discovered by Libby and co-workers, and it has been and is being used for dating archeological samples. Details of the work are found in a book by Libby ([1]). It is also expected that as spallation products of nitrogen and oxygen, all the isotopes lighter than ^{18}O will be formed, and of these tritium was found by Kaufman and Libby ([2]), and ^{7}Be was found by Arnold and Al-Salih ([3]) in rain water.

There is also in the atmosphere a substantial amount of argon, namely 0.93 percent by volume, and therefore one would expect that as spallation products of argon all the nuclides lighter than ^{40}A would be formed. Of these nuclides, ^{32}P is probably the easiest one to detect. We looked for and found ^{32}P as a spallation product of argon by cosmic rays.

From cosmic ray data ([4]) it is estimated that the maximum rate of formation of ^{32}P lies between 10 and 20 km height, and this rate decreases for

([1]) W. F. Libby: *Radiocarbon Dating* (Chicago, 1952).
([2]) S. Kaufman and W. F. Libby: *Phys. Rev.*, **93**, 1337 (1954).
([3]) J. R. Arnold and H. L. Al-Salih: *Science*, **121**, 451 (1955).
([4]) M. A. Pomerantz: *Phys. Rev.*, **95**, 531 (1954).

lower and higher altitudes, being much smaller at sea level. From thermodynamic considerations one would expect that the ^{32}P formed by cosmic rays would be oxidized to H_3PO_4 and also that if the water in the atmosphere condenses, the H_3PO_4 would concentrate in the water phase. We would expect then to find the ^{32}P in the rain water or in the water condensed from the air by any process.

We decided to look for it in the rain water and for this purpose we collected the water from the roof of our laboratory in an area of about 50 m^2 and this water was lead through pipes into tanks of 200 liters capacity. There were two unexpected difficulties in the chemical procedure. The rain water carried always a large amount of silica from the tile roof, and this made necessary the separation of silica. The rain water also carried some 5 mg of P per tank from the decomposition of leaves and other organic materials that fell on the roof between rains. This made impossible to prepare thin samples of P.

2. – Experimental Method.

The chemical procedure adopted was as follows. To each tank with 200 liters of rain water was added 5 mg of P as phosphate, 15 ml of concentrated HNO_3 and one g of Fe as ferric ion. The water was stirred and allowed to stand for one hour; after that some base was added to bring the solution to pH of 10 or greater to precipitate the ferric hydroxide which would carry the phosphate. The solution was allowed to stand until the precipitate settled in the bottom and the supernatant was clear. This took several hours and sometimes it was necessary to add a solution of K_2SO_4 to help the coagulation of the ferric hydroxide. The supernatant was siphoned and the residue was filtered.

The hydroxide was dissolved by boiling it with 500 ml of 4 N HCl for 15 min. At this point it was necessary to filter insoluble leftovers from the tiles and the leaves. The filtrate was oxidized with bromine water, evaporated to dryness and dehydrated for one hour at 110 °C. The residue was taken up with some 12 N HCl, diluted with water and the silica filtered. The filtrate was evaporated to near dryness, boiled with concentrated HNO_3 to expel HCl, diluted with a 10 percent solution of ammonium nitrate, and the phosphate precipitated with ammonium molibdate reagent.

The ammonium phosphomolibdate was centrifuged, washed with dilute HNO_3, and dissolved in NH_4OH containing some citric acid. The solution was made faintly acid, magnesium chloride was added and then made basic with NH_4OH to precipitate the magnesium ammonium phosphate. This precipitate was centrifuged, washed with dilute NH_4OH, dissolved in HCl, evaporated to dryness, and dehydrated as before to eliminate the silica. The residue was taken with HCl, diluted and the silica filtered. The filtrate was diluted to 0.3 N in HCl and passed through a cation exchange column. For

the preparation and use of the column we followed SAMUELSON (5). The effluent and washings were evaporated to a small volume and the phosphate precipitated as the magnesium ammonium phosphate. It was filtered through a circular paper filter of 2.5 cm diameter, washed, dried, weighed, and mounted for counting.

The samples were counted at 3 mm from the end window of a Geiger counter. The mica window had a diameter of 2.5 cm and it was 2 mg/cm^2 thick. Initial activities ranged from 10 to 40 cpm. The background in a lead shield was 27 cpm. The counts were recorded in a scaler of conventional type.

Once we found that the ^{32}P appeared consistently in the rain water, we made a test to find out whether part or all of this ^{32}P could come from a nuclear explosion. A nuclear explosion produces neutrons in the MeV region. These neutrons can make ^{32}P by three processes; ^{31}P(n, γ)^{32}P, ^{32}S(n, p)^{32}P and ^{35}Cl(n, α)^{32}P. The first reaction is more rapid with slow neutrons, and the two others go only with neutrons in the MeV region. For that test we made a separation of Ba, with the idea of observing ^{140}Ba, which has a large fission yield and its half-life is almost the same as the half-life of ^{32}P. We added 5 mg of Ba per tank of 200 liters of rain water. The ferric hydroxide was precipitated with a mixture of sodium hydroxide and sodium carbonate to precipitate the Ba also. The rest of the procedure was the same as before and the Ba was precipitated as $BaSO_4$ from the supernatant of the ammonium phosphomolibdate. We could not observe any ^{140}Ba, but from the activity observed we could estimate that the activity of ^{140}Ba is at least four times smaller than the activity of ^{32}P in the same amount of rain water. This shows that the ^{32}P that we found is not formed in a nuclear explosion, since it seems that much more ^{140}Ba would be formed in a nuclear explosion than ^{32}P.

3. – Results and Discussion.

The results of six experiments are shown in Table I. The activities were followed until they got lost in the background; this was from three to five half-lives and no other activity was seen throughout this period, which shows that the chemistry was satisfactory. The maximum energy of the β-particles was found by measuring the absorption coefficient at the initial part of the absorption curve with Al; and it was in agreement with the maximum energy of the β-particles from ^{32}P. In order to convert initial activities into desintegration rates we had to apply correction factors for geometry, absorption, self-absorption, back-scattering and chemical yield. For these corrections we estimate that the absolute activities might be in error as much as 30 percent.

---

(5) O. SAMUELSON: *Ion Exchangers in Analytical Chemistry* (New York, 1953).

TABLE I. – *The activity of* ^{32}P *in rain water of Rio de Janeiro and related data.*

Date 1955	Amount of rain water liters	Observed half-life days	Initial activity dpm/liter
May 30	500	12	0.09
May 31	600	17	0.23
June 9	300	15	0.30
June 21	600	15	0.26
June 23	800	15	0.23
July 8	800	14	0.10

There is a spread of a factor of three between the smallest and the largest activity of ^{32}P found; this is similar to the spread of values found by ARNOLD and AL-SALIH [3] in the case of ^{7}Be. The average value of the activity of ^{32}P in the rain water of Rio de Janeiro is 0.20 dpm/liter. This is compatible with what one would estimate from the activity of ^{7}Be found by ARNOLD and AL-SALIH, taking into account the amount of A in the air, plausible yields for ^{32}P from A and of ^{7}Be from N and O, and the decay from the time of the formation to the time of the rainfall. We do not attempt to calculate the formation rate of ^{32}P, since this involves meteorological times which are uncertain.

We could not detect the activity of ^{33}P, although it should be there. This was due to the fact that our samples had thickness of about 30 mg/cm^2. Taking into account the absorption in the sample, window, etc., and estimating the yield of ^{33}P from the empirical relation for spallation reactions used by RUDSTAM [6], we calculate that the ^{33}P could not appear neatly in our decay curves. It could shift the half-life of ^{32}P towards a larger value, and there seems to be some indication of that, but we can not consider that as a definite proof that ^{33}P is there.

* * *

We are indebted to Prof. U. CAMERINI for his continued interest and help during this work.

---

[6] S. G. RUDSTAM: *Phil. Mag.*, **46**, 344 (1955).

RIASSUNTO (*)

Si dimostra per mezzo di esperimenti che il ^{32}P radioattivo si forma come prodotto di scissione dell'argon sotto l'azione dei raggi cosmici. Lo si trova nell'acqua piovana e la sua attività media nell'acqua piovana recente è a Rio de Janerio 0,20 dpm/litro.

(*) *Traduzione a cura della Redazione.*

High Sensitivity and Accuracy Pulse Trigger Circuit.

S. Barabaschi, C. Cottini and E. Gatti

Laboratori CISE - Milano

(ricevuto il 23 Settembre 1955)

Summary. — A high sensitivity pulse height selector is described obtained using a retarding field diode and a differential negative resistance of high stability obtained by means of a multi-electrode electronic tube using the current division between screen grid and anode. The threshold of the discriminator can be set in the range of 1 to 30 mV its stability being in this range better than 1%.

1. – Introduction.

The described circuit is a discriminator which allows the extension of the results obtained through the Kandiah circuit [1] from the region of a few tens millivolts to that of a few millivolts.

Fundamentally, the instrument described may be considered a parallel of a negative differential resistance of the N [2,3] type and of a positive resistance whose value can be driven by the input pulse amplitude fed to the discriminator.

On a normal condition the system is in itself stable: input pulses of sufficient amplitude affect the driven resistance (retarding field diode) in such a way as its value exceeds the threshold value at which such resistance becomes equal in absolute value to the negative resistance.

Under these conditions the system is unstable and performs a transition of its own, which indicates the arrival of an input pulse superior to the threshold.

---

[1] K. Kandiah: *PIEE II*, **101**, 239 (1954).
[2] N. Carrara: *Alta Freq.*, **8**, 683 (1939).
[3] S. Malatesta: *Alta Freq.*, **16**, 87 (1947).

The driven resistance is an indirectly heated thermoionic diode in which a constant current I_0 flows in the normal condition.

If I_0 is chosen sufficiently small (smaller than the current $I_\infty = 245 \cdot 10^{-9} \cdot (T/1000)^{\frac{1}{2}}(A/d^2)$ as defined by W. R. FERRIS [4] for a plane geometry diode, where A is the area of the electrodes and d their distance from each other) the anode is negative by some tenths of a volt with respect to the cathode: the diode is in the retarding field region. As is well known, the diode current in this region is:

$$I = I_s \exp\left[\frac{eE}{kT}\right]$$

and consequently the differential conductance is

$$G = I\frac{e}{kT}.$$

In the normal condition a steady current I_0 flows through the diode which therefore presents a differential conductance

$$G_0 = \frac{e}{kT} I_0$$

depending only on the steady current I_0 and from the temperature T of the cathode.

The factor e/kT of a diode with an oxide cathode is nearly 11 V^{-1} and its value is found to be well reproducible. The diode therefore is an almost ideal standard of differential conductance driven by the current which crosses it.

In the circuit which we are describing as well as in that of K. KANDIAH, the input pulse modifies the steady current in the diode and consequently also its differential conductance.

2. – Description of the Instrument (*).

While KANDIAH chooses a cathode-coupled multivibrator type of a circuit to obtain a negative resistance we have chosen the negative resistance existing between screen grid and cathode of a multi-grid tube using the current division between screen grid and anode [5-8].

(*) Patent pending.

(4) W. R. FERRIS: *RCA Review*, **10**, 134 (1947).

(5) E. W. HEROLD: *P.I.R.E.*, **23**, 1201 (1935).

(6) A. PINCIROLI: *AEI*, **3**, 232 (1937).

(7) A. PINCIROLI: *Alta Freq.*, **9**, 581 (1940).

(8) A. PINCIROLI: *Alta Freq.*, **10**, 644 (1941).

Such choice has been made after sorting out the simple known methods for obtaining negative resistance in view of the opportunities offered by the selected arrangement to achieve a high stability of negative resistance through the use of stabilized voltage sources and two feed-back circuits (scheme in Fig. 1) that stabilize the steady currents.

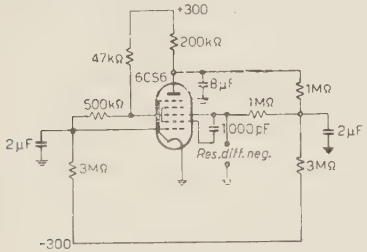

Fig. 1. – Circuit to obtain a stable negative resistance with a 6CS6 tube.

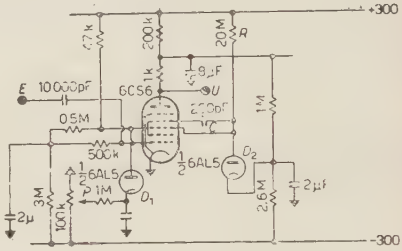

Fig. 2. – Discriminator scheme for positive input pulses.

Thus the screen grid potential and current, the anode potential and current, and the cathode current are stabilized. The multi-grid tube therefore has the virtual cathode fed by a constant current I_K and a control grid potential V_{03} such as will maintain pre-fixed ratio between the screen and anode currents.

For the circuit shown in Fig. 1 the differential negative resistance has the value of 1650 ohm.

The complete scheme of the discriminator is shown in Fig. 2.

Two retarding field diodes D_1 and D_2 are paralleled to the negative resistance, D_1 being connected between g_2 and ground and D_2 between g_3 and ground (through condensers).

A steady current which can be set at will through the potentiometer P is impressed on D_1, while in D_2 flows a fixed steady current of 15 μA.

The two diodes are in fact in parallel with respect to pulses and their differential conductances are summed.

We can consider the diodes, for the moment as really in parallel since their doubling is due to considerations involved in the return to the initial condition of the circuit after a transition.

The input signal (positive in the case of Fig. 2) is applied to g_1 and it determines through the transconductance S between g_1 and g_2 a diminution of the circulating current in the diodes. As has been said, if the input pulse is of sufficient amplitude, their differential conductance is diminished to below the absolute value of the negative conductance and the circuit becomes unstable. g_2 and g_3 then drop by about 3 V in a time of 10^{-7} s. The output pulse is picked up at the anode of the multi-grid tube where the transition causes the complete interdiction of the current.

The drop of g_2 and g_3 at the transition is limited to about 3 V because the potential of g_2 influences substantially the electronic current and such drop is sufficient to counterbalance completely the 1 mA current which is switched by g_3 from the anode to the screen grid, during the transition itself.

The circuit remains in the new condition until g_3, rising linearly in potential, due to the discharge of condenser C through the resistance R, controls again the division of current between g_2 and the anode and starts the reverting transition which is limited in amplitude by the clamping of D_1 and D_2 diodes.

The duration between the initial and the reverting transition is the « dead time » of the discriminator and is determined by I_{D_2}, C and by the amplitude of the g_3 drop. For the circuit of Fig. 2 its value is 30 μs.

The reason for using two diodes D_1 and D_2 is now evident. It has enabled us to obtain a constant dead time for every value of the threshold that can be varied by varying the current in diode D_1 but leaving that of diode D_2, which influences the dead time, unchanged.

3. – Analisis of the Circuit and Experimental Results.

The formula which connects the threshold value for the input pulses to the parameters of the circuit is the following:

$$E = \frac{kT}{e}\,\frac{Y_{\text{neg}}}{S}\left(\frac{I_0 - I_0^*}{I_0^*} - \log\frac{I_0}{I_0^*}\right), \tag{3}$$

$$I_0^* = \frac{kE}{e}\,Y_{\text{neg}}, \tag{3'}$$

where Y_{neg} is the negative differential conductance presented by the multigrid tube between g_2 and ground (where the contribution of the positive resistance presented by the various resistors in the circuit is included), S the transconductance between grids g_1 and g_2, I_0^* the critical steady current in the retarding field which makes the circuit unstable without external pulses being applied, I_0 the actual normal current in the diodes. (By I_0 and I_0^* is understood the sum of the currents in the two diodes).

On Fig. 3 the experimental results are compared with the theoretical expectation of formula (3).

By comparing our formula (3) with that relative to the circuit of Kandiah which is

$$E = \frac{kT}{e}\left(\times\,\frac{I_0 - I_0^*}{I_0^*} - \log\frac{I_0}{I_0^*}\right),$$

it is inferred that the sensitivity of our circuit, for equal ratio I_0/I_0^*, is larger by the factor S/Y_{neg} which in our working conditions is 9.4.

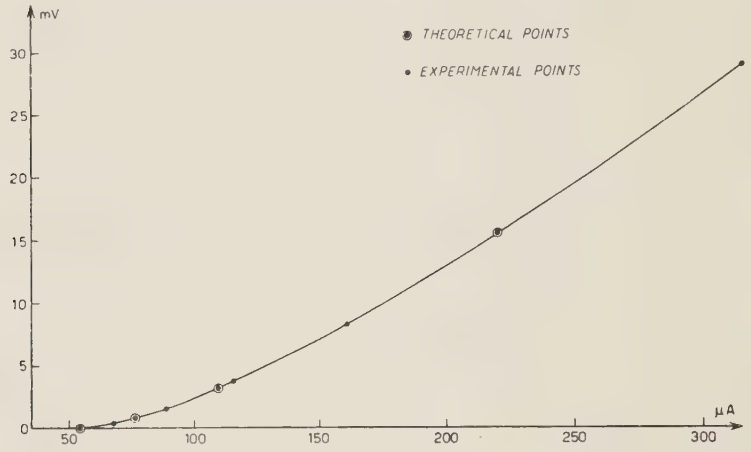

Fig. 3. – Experimental and theoretical values of the threshold voltage as function of I_0/I_0^*.

It is further to be noted that the variations of S influence the value of the threshold with the weight of their percentage variation for any level of the threshold, while the zero stability is dependent on the stability of I_0^* or in fact (considering the relation (6) of the Appendix) on the stability of both the negative conductance and the positive conductance of the retarding field diode.

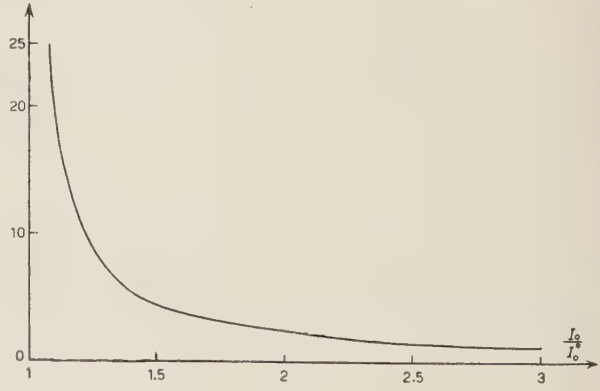

Fig. 4. – Weight function relating percentage variations of threshold value to percentage variations of temperature in diodes and negative resistance.

From formula (3) the percentage variation of the threshold value caused by a given percentage variation of the cathode temperature of the diodes and of the negative resistance Y_{neg}, is easily deduced: we have

$$\frac{\mathrm{d}(ES)/(ES)}{(\mathrm{d}T/T) + (\mathrm{d}Y_{neg}/Y_{neg})} = \frac{1}{\dfrac{(I_0/I_0^*) - 1}{\log (I_0/I_0^*)} - 1},$$

the function of I_0/I_0^* appearing at the second member is plotted in Fig. 4.

The following bench tests have been made to ascertain the reliability of the circuit.

1) In order to ascertain the stability of the negative resistance, the heating voltage of the retarding field diode was maintained constant while the heating voltage of the 6CS6 tube was variated from 5.7 to 6.6 V; the current I_0^* (current at which the circuit is unstable without external signal being applied) was measured and found unchanged within instrumentation accuracy, i.e. variation less than .5 %.

2) The steady current I_0 having been fixed at 77 μA corresponding to $I_0/I_0^* = 1.4$, a 1 % variation was found in the amplitude of the pulses which were capable of triggering the circuit when the heating voltage of 6CS6 tube was variated from 5.7 to 6.3 V.

Thus taking into account the ratio of about 5, in this case, for the percentage variation of the threshold with respect to the percentage variation of the negative resistance, we can conclude that the stability of negative resistance is at least of 1/500.

The same variation of 1 % in the threshold value, caused by the 10 % variation in the heating voltage, was observed when working with the ratio $I_0/I_0^* = 5$. For this ratio the weight of the percentage variation of the negative resistance on the percentage variation in the threshold is only 0.7, which drives one to conclude that the observed 1 % variation in the threshold value is not due to a negative resistance variation but to a variation of the transconductance S which, as has been already said, has always the same weight for every value of the threshold.

3) Three samples of 6SC7 tube have been inserted in the circuit and the values of I_0 have shown the following spread:

67 μA

65 μA

61 μA.

The differences observed are believed to be due to small differences in the geometry of the tubes.

4) The heating voltage of the 6CS6 tube was maintained constant while that of the 6AL5 tube, i.e. of the two retarding field diodes, was variated and the corresponding variation of the critical current I_0^* observed: the experimental results are shown in Fig. 5. Taking formula (3′) into account we can

conclude that the 10% variation in the heating voltage of the diodes corresponds to a 4% variation in the absolute temperature of their cathodes.

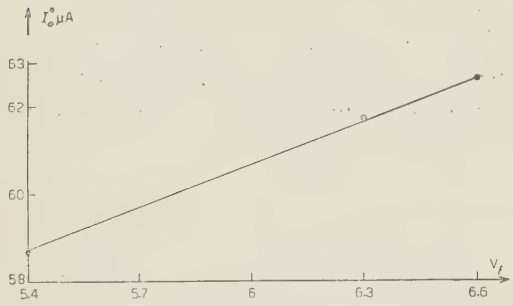

Fig. 5. – Variation of differential resistance of 6AL5 diode in the retarding field region against variation of heating voltage.

This experimental result is in complete agreement with the results of SUKETOSHI and IKEHARA (9).

It is therefore convenient to feed the heaters of the diodes with a stabilized voltage in order to achieve a stability of the differential positive conductance of the diodes comparable to that obtained for the differential negative conductance of the multigrid tube.

5) The calibration curve of Fig. 3 was found unchanged within instrumental accuracy (1/200) for a few successive operational days and for one month after the circuit was switched off.

The measurements were generally made by means of 2 μs rectangular input pulses.

The discriminator drops in sensitivity with respect to input pulses shorter than 1 μs as per experimental results shown in Fig. 6.

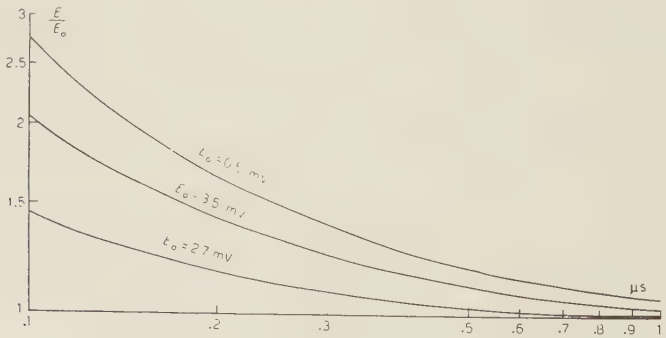

Fig. 6. – Drop of discriminator sensitivity for short input pulses.

The observed behaviour can be theoretically explained along the lines followed by K. KANDIAH.

A similar drop in sensitivity is also observed for input pulses with a rise time larger than .5 μs, due to the 3 μs *RC* coupling between grids g_2 and g_3.

(9) SUKETOSHI, IKEHARA: *Journ. Appl. Phys.*, **25**, 725 (1954).

Input pulses have to be fed to the discriminator from a low impedence source, considering that the 6CS6 tube has no screening electrode between input grid g_1 and screen grid g_2: a non-linear Miller effect is present since the load impedance of g_2 is not linear (retarding field diodes): the capacitive coupling between g_1 and g_2 influences the threshold value unless g_1 is connected to a low impedance source (< 1000 ohm).

An alternative circuit suitable for negative input pulses has been experimented and its scheme is shown in Fig. 7.

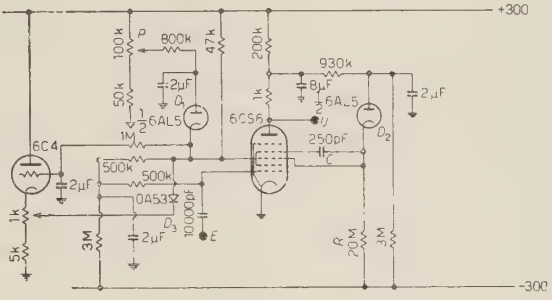

Fig. 7. – Discriminator scheme for negative input pulses.

The results obtained with this instrument practically coincide with those obtained with the described instrument.

A difference in the reset mechanism of the circuit of Fig. 7 made it necessary to introduce diode D_3 in order to limit the positive excursion of g_2 and g_3 at the transition.

4. – Conclusion.

The instrument described seems useful for the purpose of reducing to minimum the number of components the amplification and counting chains which follow the nuclear detectors. In particular, in many instances using photomultipliers of proportional counters the counting chain can be reduced to a decoupling and shaping unit, to the instrument described and to an electronic scaler or rate meter.

The reduction in the number of the components of the amplifier chain does not only offer an economy but is particularly useful when a safe apparatus with minimum possibilities of failure is required.

* * *

The authors are indebted to Prof. MARTIN H. GRAHM for having pointed out some desirable features of the 6CS6 tube.

Appendix

The dependence of the threshold value of the discriminator on the parameters which characterize the circuit is evaluated.

The essential variables are:

Input voltage E applied to grid g_1; voltage V across the retarding field diode which is coincident with the voltage at the electrodes g_2 and g_3.

Current I flowing into the diode, which is coincident with the current at the electrodes g_2 and g_3.

(The variables are defined as the difference between the effective value and the normal value. The difference are not to be considered infinitesimal).

The essential parameters are:

The transconductance S between grid g_1 and g_2.

The negative conductance Y_{neg} which is present across g_2, g_3 and ground.

The normal current I_0 in the diode.

The relationships between the variables can be displayed by the signal flow graph of Fig. 8 ([10,11]) which implies that I is dependent on E and V according to the relation

$$I = -SE + VY_{neg} \tag{4}$$

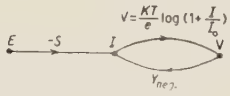

Fig. 8.

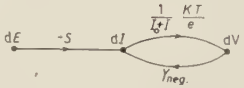

Fig. 9.

and that V is connected to I by the voltage-current characteristic of the retarding field diode

$$V = \frac{kT}{e} \log\left(1 + \frac{I}{I_0}\right). \tag{5}$$

It is further assumed that the negative conductance is constant in all the range of variations of the considered variables.

The differentials of the variables E, I, V are similarly related by the signal flow graph of Fig. 9.

The system is triggered when the amplification dV/dE becomes infinite, which occurs when the feed-back loop gain is 1 i.e.

$$\frac{1}{I + I_0} \frac{kT}{e} Y_{neg} = 1 .$$

([10]) S. J. Mason: *PIRE*, **41**, 1144 (1953).

([11]) S. Barabaschi and E. Gatti: *Energia Nucleare*, **2**, 168 (1955).

If I^* is the critical current $(I + I_0)$ for which the system has feed-back loop gain equal to 1, then

$$I^* = \frac{kT}{e} Y_{neg} . \tag{6}$$

Using this relation we can eliminate I from formula (4) and taking in account (5) have the result sought:

$$E = \frac{kT}{e} \frac{Y_{neg}}{S} \left(\frac{I_0 - I_0^*}{I_0^*} - \log \frac{I_0}{I_0^*} \right) .$$

RIASSUNTO

Si descrive un discriminatore d'ampiezza di impulsi a soglia, ad elevata sensibilità, ottenuto mediante l'impiego di un diodo a campo frenante, e di una resistenza differenziale negativa ad alta stabilità. Detta resistenza negativa si ottiene mediante un tubo multigriglia a ripartizione di corrente tra griglia-schermo ed anodo. La soglia è regolabile tra 1 mV e 30 mV e in questo campo la sua stabilità è dell'ordine dell'1 %.

On the Decay of $^{51}_{24}Cr$.

A. Bisi, E. Germagnoli (*) and L. Zappa

Istituto di Fisica Sperimentale del Politecnico - Milano
(*) *Laboratori CISE - Milano*

(ricevuto il 23 Settembre 1955)

Summary. — From the energy spectrum of γ-rays emitted in the decay $^{51}_{24}Cr \rightarrow {}^{51}_{23}V$ a revised scheme of the levels of $^{51}_{23}V$ is deduced. A direct determination of the energy involved in this transition is described.

1. – Introduction.

The low lying energy levels of $^{51}_{23}V$ have been studied by a number of authors in the last years (1). Two sources of information can be used to build up a level scheme of the above mentioned isotope: the β^- decay of $^{51}_{22}Ti$ (5.79 m) and, in a narrower interval of energy, the orbital electron capture in $^{51}_{24}Cr$ (27.75 d). A comparative investigation of the two decay processes has been recently carried out by Bunker and Starner (1) and the level scheme proposed by these authors is shown in Fig. 1; these schemes are supported by the results of coincidence measurements. The energy associated with the electron capture transition between the ground levels of $^{51}_{24}Cr$ and $^{51}_{23}V$ can be deduced from a measurement of the threshold of the reaction $^{51}_{23}V(p, n)^{51}_{24}Cr$ (2) and turns out to be 750 keV. As far as we know, no investigation of γ-spectra emitted in the internal bremsstrahlung processes associated with the orbital electron capture in $^{51}_{24}Cr$ has been attempted so far and consequently no direct

(1) M. E. Bunker and J. W. Starner: *Phys. Rev.*, **97**, 1272 (1955). In this paper the previous literature is collected.

(2) D. M. Van Patter and W. Whaling: *Rev. Mod. Phys.*, **26**, 402 (1954).

measurement of the energy involved in this decay exists.

The attribution of the orbitals to the energy levels of $^{51}_{23}$V seems to be quite reasonable and is supported by the predictions of nuclear shell theory.

2. – γ-Rays Emitted from $^{51}_{24}$Cr.

a) The γ-rays emitted in the transition $^{51}_{24}\text{Cr} \rightarrow {}^{51}_{23}\text{V}$ have been studied by means of a single crystal scintillation spectrometer, whose output was connected with a conventional chain and with a 20 channel fast pulse analyzer ([3]). A coincidence circuit ([4]) was also used in some cases.

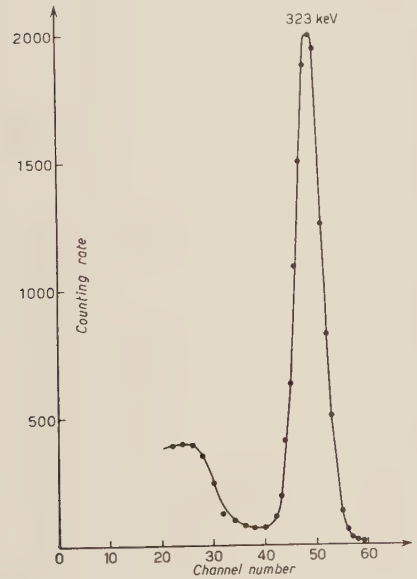

Fig. 2. – γ-spectrum from $^{51}_{24}$Cr (low energy region).

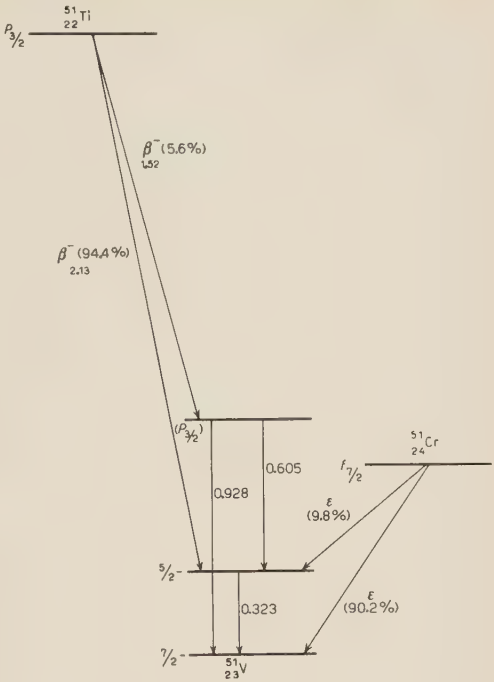

Fig. 1. – Proposed decay schemes of $^{51}_{22}$Ti and $^{51}_{24}$Cr (after Bunker and Starner ([1]).

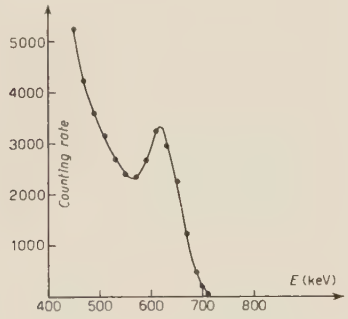

Fig. 3. – γ-spectrum from $^{51}_{24}$Cr (high energy region).

The chromium source has been supplied by AERE (Harwell), after enrichment into $^{51}_{24}$Cr by means of a Szilard-Chalmers process.

([3]) E. Gatti: *Nuovo Cimento*, **11**, 153 (1954).

([1]) E. Germagnoli, A. Malvicini and L. Zappa: *Nuovo Cimento*, **10**, 1388 (1953).

The aim of our measurements was to investigate the above mentioned spectrum of internal bremsstrahlung.

The energy distribution of γ-rays is shown in Fig. 2 and Fig. 3: besides the well known 323 keV line, evidence has been found of a weak γ line, the energy of which resulted to be 624 ± 5 keV after a calibration of the spectrometer with the γ lines of $^{203}_{80}$Hg (279 keV), of $^{22}_{11}$Na (511 keV) and of $^{137}_{55}$Cs (662 keV). After subtraction of the cosmic background this line appeared to be superimposed to a continuous γ spectrum which is to be considered as due to the investigated internal bremsstrahlung.

Actually its end point was in close agreement with the expected value of the energy of the transition $^{51}_{24}\mathrm{Cr} \rightarrow {}^{51}_{23}\mathrm{V}$, as it will be discussed further. However the 624 keV γ line made an accurate investigation of the internal bremsstrahlung spectrum in a sufficiently wide interval of energy impossible.

In order to rule out the possibility that the 624 keV line was due to a small amount of impurity in our source, a measurement of the half life associated to this line was done; the ratio between the counting rates due to the 323 keV and to the 624 keV γ-rays was found to be constant during an interval of about 45 days (almost two half lives of $^{51}_{24}$Cr): it can be therefore concluded that such γ-rays are emitted in the decay of $^{51}_{24}$Cr; in Fig. 4 the results of these measurements are given.

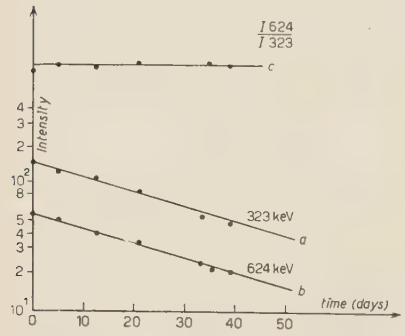

Fig. 4. – Comparison between the decays of the 323 keV γ-line (curve *a*) and of the 624 keV γ-line (curve *b*). The intensity ratio I_{624}/I_{323} is shown in curve *c* (arbitrary units).

To obtain a quantitative determination of the percentage of the disintegration in which the 624 keV γ-rays are emitted, we measured also the probability of emission of the 323 keV γ-rays. For this purpose the intensity of K X-rays emitted in the electron capture process has been measured with the aid of a proportional counter filled with $\mathrm{A} + \mathrm{CH_4}$, the efficiency of which was previously known, and compared with the intensity of the 323 keV γ-rays, as given by a 2.5 cm side NaI(Tl) crystal.

After corrections for the photoelectric efficiency of the crystal and for the multiple Compton scattering in it, and taking into account the fluorescence yield of the K shell ($\omega_K = 0.25$), an intensity ratio $I_{323}/I_K = 0.098$ has been found.

I_{323} is the number of unconverted γ-rays whose energy is 323 keV and I_K is the number of K captures. Such value is very near to the ratio of the probabilities of the two transitions:

$$f_{7/2} \rightarrow f_{7/2} \quad \text{and} \quad f_{7/2} \rightarrow f_{5/2} \qquad \text{(see Fig. 1),}$$

because, as it is well known (1), the 323 keV γ line is only weakly converted and the L-capture probability is likely to be very small owing to the high energy associated with the two electron capture transitions. The value of the branching ratio found here is in complete agreement with the value given by BUNKER and STARNER. A similar comparison has been done between the 624 keV and the 323 keV γ lines, and it can be concluded that the emission of 624 keV γ-rays takes place in every $(2.6 \pm 0.3)10^{-4}$ disintegrations.

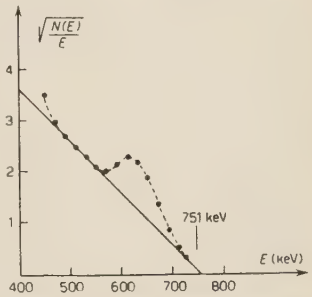

Fig. 5. – Linearized plot of the upper portion of γ spectrum from $^{51}_{24}Cr$.

b) In Fig. 5 a linearized plot of the upper portion of the γ spectrum emitted from $^{51}_{24}Cr$ is given; where the intensity of the 624 keV γ line becomes negligible the linear shape which is peculiar of the internal bremsstrahlung spectrum associated with an allowed transition (5) can be observed. The end point results to be at 751 ± 5 keV, corresponding to a transition energy of 756 ± 5 keV. Owing to the very narrow interval of energy within which the spectrum due to internal bremsstrahlung can be investigated, it did not seem worthwhile to make any correction to the experimental points.

It seems however interesting to point out that a rough estimation of the total probability of the internal bremsstrahlung associated with the 756 keV transition suggests that γ quanta are emitted in every $4 \cdot 10^{-3}$ disintegrations or thereabout. Consequently the internal bremsstrahlung γ-rays seem about ten times more intense than what can be theoretically calculated (6).

c) The consideration of the energy involved in the decay $^{51}_{24}Cr \rightarrow {}^{51}_{23}V$ prevents the identification of the 624 keV γ line the with 605 keV line which has been observed in the decay $^{51}_{22}Ti \rightarrow {}^{51}_{23}V$. γ-γ coincidence measurements have been attempted and a resolving power of about 2 μs has been used. No γ quantum has been found to be coincident with the γ-rays belonging to the 624 keV γ line; conversely it was not possible to draw any definite conclusion from the measurements when the 323 keV line was used to trigger the coincidence circuit because in this case the counting rate was very near to what had to be expected from an evaluation of the number of random coincidences, made with the above resolving power.

At any rate, if the 624 keV line has to be considered as a crossover trans-

---

(5) P. MORRISON and L. SCHIFF: *Phys. Rev.*, **58**, 24 (1940).

(6) C. S. WU in K. SIEGBAHN: *Beta and Gamma Ray Spectroscopy* (Amsterdam, 1955), p. 649.

ition between a level of 624 keV energy and the ground state of $^{51}_{23}$V, the intensity of a possible 301 keV γ line, emitted in the transition between the 624 keV and 323 keV levels would be too weak and its energy too near to 323 keV to make it possible to find a satisfactory evidence of it.

3. – Discussion.

From the above described measurements it can be inferred that a third orbital electron capture process is likely to take place in the decay of $^{51}_{24}$Cr, with a decay energy of about 132 keV and with a relative intensity of $2.6 \cdot 10^{-4}$ or thereabout. From these data, $\log ft$ results to be equal to 7.5. For this transition the two alternative possibilities

$$\Delta I = 0,\ 1; \qquad \text{yes (first forbidden)}$$

$$\Delta I = 2; \qquad \text{yes (first forbidden)}$$

may be considered (7).

From the viewpoint of nuclear shell model and under the hypothesis that the parity of the level at 624 keV should be considered as even, which follows from the above considerations, such a level can be reasonably classified as a $\frac{3}{2}+$.

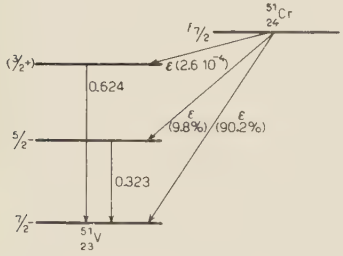

Fig. 6. – Proposed decay scheme of $^{51}_{24}$Cr.

This attribution is also not contradictory with the known data concerning the decay of $^{51}_{22}$Ti (1), because the 624 keV line does not differ too much in energy from the 605 keV line emitted in the decay of $^{51}_{22}$Ti and a possible β^- transition from the ground state of $^{51}_{22}$Ti to the 624 keV level of $^{51}_{23}$V would be rather weak and intermediate in energy between the two much more intense β^- transitions whose energies are 1.52 and 2.13 MeV. It would therefore be rather difficult to find a clear evidence for this transition. The decay scheme of $^{51}_{24}$Cr, given in Fig. 1 should be consequently completed as shown in Fig. 6.

---

(7) M. GOEPPERT-MAYER, S. A. MOSZKOWSKI and L. W. NORDHEIM: *Rev. Mod. Phys.*, **23**, 315 (1951).

* * *

We are grateful to Prof. G. BOLLA for his kind interest.

RIASSUNTO

Dallo spettro di energia dei raggi γ emessi nel decadimento $^{51}_{24}Cr \rightarrow {}^{51}_{23}V$ si ricava uno schema di livelli per il $^{51}_{23}V$. Si descrive inoltre una misura diretta dell'energia associata alla transizione considerata.

Su una formulazione hamiltoniana covariante della teoria classica dei campi.

P. Bocchieri e A. Loinger

Istituto di Fisica dell'Università - Pavia
Istituto Nazionale di Fisica Nucleare - Sezione di Milano

(ricevuto il 30 Settembre 1955)

Riassunto. — Si dà una formulazione covariante della teoria dei campi classici, la quale conduce direttamente, per quantizzazione, alle equazioni di Glauber-Yang-Feldman e, quindi, di Tomonaga-Schwinger.

---

1. – È stata data da Dirac [1,2] una formulazione hamiltoniana, relativisticamente invariante a vista, della teoria classica dei campi, dalla quale si passa direttamente, colle regole ben note, alla teoria quantistica.

Precedentemente a Dirac, una teoria *quantistica* di campo, invariante a vista, è stata sviluppata, come tutti sanno, soprattutto ad opera di Tomonaga e Schwinger. Il metodo di questi autori, pur essendo meno generale di quello di Dirac, dà tuttavia luogo ad un formalismo molto più agile, portando sostanzialmente agli stessi risultati. (La difficoltà relativa alla condizione di Lorentz è aggirata con l'artificio di Gupta e Bleuler [3]).

Per questa ragione, e perchè è sempre interessante indagare i rapporti tra una teoria quantistica e una classica, desideriamo esporre nella presente nota una formulazione hamiltoniana classica, invariante a vista, della teoria dei campi, la quale costituisce l'analogo della teoria di Tomonaga-Schwinger. Più precisamente la nostra formulazione, una volta quantizzata, fornisce le equa-

---

[1] P. A. M. Dirac: *Phys. Rev.*, **73**, 1092 (1948); *Can. Journ. Math.*, **2**, 129 (1950); **3**, 1 (1951); *Nuovo Cimento*, **7**, 925 (1950); **1**, 16 (1955).

[2] R. J. N. Phillips: *Nuovo Cimento*, **12**, 905 (1954).

[3] S. Gupta: *Proc. Phys. Soc.*, **53**, 681 (1950); K. Bleuler: *Helv. Phys. Acta*, **23**, 567 (1950).

zioni di Glauber-Yang-Feldman (4), dalle quali si passa immediatamente a quelle di Tomonaga-Schwinger.

2. – Consideriamo una variabile di campo $\xi[\sigma; x]$, che sia funzione del generico punto x di spazio-tempo e funzionale della generica ipersuperficie σ. Evidentemente una ξ siffatta non ha un significato fisico diretto.

Noi vogliamo dare delle equazioni « di moto » hamiltoniane, le quali descrivano l'« evoluzione » delle variabili di campo rispetto alla σ. A tal fine basterà assegnare una funzione hamiltoniana e le parentesi di Poisson relative alle variabili di campo.

Si noti che questo è il procedimento più diretto: l'introduzione di variabili canoniche è affatto superflua.

Indicando con $\mathcal{H}[\sigma; x]$ la hamiltoniana, l'equazione di moto della ξ rispetto alla σ sarà:

$$\frac{\delta \xi[\sigma; x]}{\delta \sigma(z)} = (\xi[\sigma; x], \mathcal{H}[\sigma; z]) , \tag{1}$$

ove z, qui e nel seguito, designa un punto di spazio-tempo appartenente a σ. Affinchè sia:

$$\frac{\delta^2 \xi}{\delta \sigma(z)\, \delta \sigma(z')} = \frac{\delta^2 \xi}{\delta \sigma(z')\, \delta \sigma(z)} , \tag{2}$$

deve essere, come si deduce immediatamente ricorrendo all'identità di Poisson-Jacobi,

$$\left(\xi[\sigma; x], \frac{\delta \mathcal{H}[\sigma; z]}{\delta \sigma(z')} - \frac{\delta \mathcal{H}[\sigma; z']}{\delta \sigma(z)} + (\mathcal{H}[\sigma; z'], \mathcal{H}[\sigma; z])\right) = 0 ; \tag{3}$$

e poichè questa relazione deve valere qualunque sia ξ, ne segue:

$$(\mathcal{H}[\sigma; z'], \mathcal{H}[\sigma; z]) + \frac{\delta \mathcal{H}[\sigma; z]}{\delta \sigma(z')} - \frac{\delta \mathcal{H}[\sigma; z']}{\delta \sigma(z)} = \text{una costante} . \tag{4}$$

Applichiamo ora questo schema generale al caso di un campo scalare complesso ψ interagente con un campo vettoriale reale Φ_μ, descrivente onde che si propagano con la velocità della luce (5). (Nel seguito si connetteranno queste

---

(4) C. N. Yang e D. Feldman: *Phys. Rev.*, **79**, 972 (1950); vedi anche Z. Koba, Z. Ôisi e M. Sasaki: *Prog. Theor. Phys.*, **3**, 141 (1948).

(5) Le notazioni e le unità di misura assunte sono quelle del lavoro di Yang e Feldman citato in (4).

ψ e Φ_μ col campo mesonico e col campo elettromagnetico, rispettivamente). Parentesi di Poisson:

$$(5) \qquad (\psi[\sigma; x],\ \psi^*[\sigma; x']) = \Delta(x - x') ;$$

$$(5') \qquad (\Phi_\mu[\sigma; x],\ \Phi_\nu[\sigma; x']) = \delta_{\mu\nu} D(x - x') ;$$

e tutte le altre uguali a zero.

Hamiltoniana:

$$(6) \qquad \mathcal{H}[\sigma; z] = ie\Phi_\nu\left(\psi^* \frac{\partial\psi}{\partial z_\nu} - \frac{\partial\psi^*}{\partial z_\nu}\psi\right) + e^2\Phi_\nu\Phi^\nu\psi^*\psi + e^2(\Phi_\nu N^\nu)^2\psi^*\psi ;$$

ove N^ν sono le componenti dei versori della normale a σ in z. La (4) si può soddisfare, per le proprietà delle funzioni D e Δ, solo quando σ è di *tipo spaziale*. In questo caso la costante a secondo membro risulta in particolare nulla.

Equazioni di moto rispetto a σ:

$$(7) \qquad \frac{\delta\psi[\sigma; x]}{\delta\sigma(z)} = ie\left\{\frac{\partial\Delta(x - z)}{\partial x_\nu}\Phi_\nu[\sigma; z]\psi[\sigma; z] + \Delta(x - z)\Phi_\nu[\sigma; z]\frac{\partial\psi[\sigma; z]}{\partial z_\nu}\right\} +$$

$$+ e^2\Phi_\nu[\sigma; z]\Phi^\nu[\sigma; z]\psi[\sigma; z]\Delta(x - z) + e^2(\Phi_\nu[\sigma; z]N^\nu)^2\psi[\sigma; z]\Delta(x - z) ;$$

$$(8) \qquad \frac{\delta\Phi_\mu[\sigma; x]}{\delta\sigma(z)} = ie\left(\psi^*[\sigma; z]\frac{\partial\psi[\sigma; z]}{\partial z^\mu} - \frac{\partial\psi^*[\sigma; z]}{\partial z^\mu}\psi[\sigma; z]\right)D(x - z) + 2e^2\psi^*[\sigma; z]\cdot$$

$$\cdot\psi[\sigma; z]\Phi_\mu[\sigma; z]D(x - z) + 2e^2\psi^*[\sigma; z]\psi[\sigma; z]N_\mu\Phi_\nu[\sigma; z]N^\nu D(x - z);$$

da cui, integrando e designando con E_1 e $E_{2,\mu}$ i secondi membri di (7) e (8) rispettivamente:

$$(9) \qquad \psi[\sigma; x] = \int_{\sigma_0}^{\sigma} E_1[\sigma'; z'; x]\,\mathrm{d}_4 z' + \psi[\sigma_0; x] ;$$

$$(10) \qquad \Phi_\mu[\sigma; x] = \int_{\sigma_0}^{\sigma} E_{2,\mu}[\sigma'; z'; x]\,\mathrm{d}_4 z' + \Phi_\mu[\sigma_0; x] .$$

Dalla (9) e dalla (10) si deduce immediatamente:

$$(11) \qquad (\Box - m^2)\psi[\sigma; x] = 0 ,$$

$$(12) \qquad \Box\Phi_\mu[\sigma; x] = 0 .$$

Valutiamo mediante la (10), la $\partial \Phi_\mu[\sigma; x]/\partial x_\mu$; si ha con qualche calcolo:

$$(13)\qquad \frac{\partial \Phi_\mu[\sigma; x]}{\partial x_\mu} + \int_\sigma \mathrm{d}\sigma' j_\nu[\sigma; z'] N^\nu D(x - z') = \frac{\partial \Phi_\mu[\sigma_0; x]}{\partial x_\mu} + \int_{\sigma_0} \mathrm{d}\sigma' j_\nu[\sigma_0; z'] N^\nu D(x - z') ;$$

ove

$$j_\nu = ie \left\{ \frac{\partial \psi^*}{\partial z^\nu} \psi \quad \psi^* \frac{\partial \psi}{\partial z^\nu} \right\} .$$

L'espressione a primo membro è pertanto indipendente da σ.

Si osservi però che *non* è lecito porre:

$$(14)\qquad \frac{\partial \Phi_\mu[\sigma; x]}{\partial x_\mu} + \int_\sigma \mathrm{d}\sigma' j_\nu[\sigma; z'] N^\nu D(x - z') = 0 ,$$

in quanto si avrebbe incompatibilità colla parentesi di Poisson (5′).

Mediante le posizioni:

$$(15)\qquad \psi(x) = \psi[\sigma; x] - ie \left\{ \frac{\partial}{\partial x_\nu} \int \mathrm{d}_4 x' \, \Delta^\sigma(x, x') \Phi_\nu(x') \psi(x') + \int \mathrm{d}^4 x' \, \Phi_\nu(x') \frac{\partial \psi(x')}{\partial x'_\nu} \Delta^\sigma(x, x') \right\} - e^2 \int \mathrm{d}_4 x' \, \Phi_\nu(x') \Phi^\nu(x') \psi(x') \Delta^\sigma(x, x') ;$$

$$(16)\qquad \Phi_\nu(x) = \Phi_\nu[\sigma; x] + \int \mathrm{d}_4 x' \{ j_\nu(x') - 2e^2 \Phi_\nu(x') \psi^*(x') \psi(x') \} D^\sigma(x, x') ;$$

si trova facilmente che le $\psi(x)$, $\Phi_\nu(x)$ soddisfano le equazioni classiche del campo mesonico e del campo elettromagnetico accoppiati:

$$(17)\qquad (\Box - m^2)\psi(x) = ie \left\{ \frac{\partial}{\partial x_\mu} (\Phi_\mu(x) \psi(x)) + \Phi_\mu(x) \frac{\partial \psi(x)}{\partial x_\mu} \right\} + e^2 \Phi_\mu(x) \Phi^\mu(x) \psi(x) ;$$

$$(18)\qquad \Box \Phi_\nu(x) = - ie \left\{ \frac{\partial \psi^*(x)}{\partial x^\nu} \psi(x) - \psi^*(x) \frac{\partial \psi(x)}{\partial x^\nu} \right\} + 2e^2 \Phi_\nu(x) \psi^*(x) \psi(x) .$$

Non si può però ricavare la condizione di Lorentz $\partial \Phi_\mu(x)/\partial x_\mu = 0$, perchè questa è la trasformata della (14).

In altri termini, la nostra teoria hamiltoniana non è completamente equivalente alle equazioni classiche del campo elettromagnetico accoppiato al campo mesonico. Questa difficoltà è identica a quella che si presenta nella usuale teoria hamiltoniana classica. È però noto che nella corrispondente teoria quantistica

essa può essere aggirata. Il passaggio alla teoria quantistica si esegue formalmente interpretando le equazioni sopra scritte come equazioni operatoriali e sostituendo alle parentesi di Poisson i commutatori divisi per l'unità immaginaria.

Considerando le equazioni in tal modo ottenute come equazioni di moto in una descrizione di Heisenberg *rispetto alla* σ, si possono immediatamente trarre da esse le equazioni della corrispondente descrizione di Schrödinger, le quali vengono a coincidere colle equazioni fondamentali della teoria di Tomonaga-Schwinger, purchè si imponga ulteriormente:

$$\left\{\frac{\partial \Phi_\mu^{(+)}[\sigma; x]}{\partial x_\mu} + \int_\sigma d\sigma' j_\nu[\sigma; z'] N^\nu D^{(+)}(x - z')\right\} \Psi = 0$$

(ove $(+)$ sta ad indicare la parte a frequenze positive) per ogni vettore di stato Ψ del sistema.

Concludendo: si è data una formulazione hamiltoniana, la quale costituisce l'analogo classico della descrizione d'interazione e dalla quale traggono origine direttamente le equazioni di Tomonaga-Schwinger.

SUMMARY

A Hamiltonian covariant formulation of a classical theory of fields is given. Its quantization leads directly to the Glauber-Yang-Feldman equations, which are equivalent to the Tomonaga-Schwinger theory.

IL NUOVO CIMENTO Vol. II, N. 5 1° Novembre 1955

On the Masses and Modes of Decay of Heavy Mesons Produced by Cosmic Radiation.

(G-Stack Collaboration)

J. H. Davies, D. Evans, P. E. Francois, M. W. Friedlander, R. Hillier, P. Iredale, D. Keefe, M. G. K. Menon, D. H. Perkins and C. F. Powell

H. H. Wills Physical Laboratory - Bristol (Br)

J. Bøggild, N. Brene, P. H. Fowler, J. Hooper, W. C. G. Ortel and M. Scharff

Institut för Teoretisk Fysik - København (Ko)

L. Crane, R. H. W. Johnston and C. O'Ceallaigh

Institute for Advanced Studies - Dublin (DuAS)

F. Anderson, G. Lawlor and T. E. Nevin

University College - Dublin (DuUC)

G. Alvial, A. Bonetti, M. di Corato, C. Dilworth, R. Levi Setti, A. Milone (+), G. Occhialini (*), L. Scarsi and G. Tomasini (+)

(+) *Istituto di Fisica dell'Università - Genova*
Istituto di Scienze Fisiche dell'Università - Milano (GeMi)
Istituto Nazionale di Fisica Nucleare - Sezione di Milano
(*) *and of Laboratoire de Physique Nucléaire - Université Libre - Bruxelles*

M. Ceccarelli, M. Grilli, M. Merlin, G. Salandin and B. Sechi

Istituto di Fisica dell'Università - Padova
Istituto Nazionale di Fisica Nucleare - Sezione di Padova (Pd)

(ricevuto il 2 Ottobre 1955)

of measurement. 2) Range measurements on particles stopping in the stack. 3) Scattering and ionisation measurements on particles not coming to rest in the stack. 4) Allocation among different modes of decay. – **4.** *Analysis of measurements on particles decaying in different modes.* 1) The K_μ-mode: (i) Measurements on stopping secondaries; (ii) Measurements on non-stopping secondaries. 2) The χ-mode: (i) Measurements on stopping secondaries; (ii) Measurements on secondary π-mesons which do not come to rest in the stack. 3) The significance of the mass values deduced from the K_μ and χ groups. 4) The $\varkappa$-mode. 5) The K_β-mode. 6) The τ'-mode. 7) Relative frequencies of different modes of decay. – **5.** *Conclusion.* – **6.** *Appendices.* I) Methods of estimating, and correcting for, errors in the measurement of range. II) Conventions on scattering techniques. III) Estimation of Scanning Loss.

1. – Introduction.

In October 1954, a large stack of Ilford G5 emulsion was exposed to the cosmic radiation at a mean altitude of 27000 m over Northern Italy for six hours, by means of a free balloon. The expedition was undertaken as a result of a collaboration between the Universities of Bristol, Milan and Padua.

The stack was made up of 250 sheets each of dimensions 37 cm × 27 cm × 600 μm, which, when packed together with thin paper spacers, made effectively a solid block about 15 cm thick, volume 15 litres and weight 63 kg.

The overall dimensions of the stack were chosen to ensure that about 15% of the μ-meson secondaries of the maximum possible range given by the decay of a K-meson of mass about that of the τ, would be arrested within it; the figure 15% refers to observations on particles decaying in favourable regions of the stack. A larger stack would have been advantageous, but a limit was set by a number of considerations: First, by the size of the individual sheets the manufacturers could produce, and by the capacity of the available processing units in Bristol. Secondly, by the fact that the larger the stack, the greater the load and the attendant difficulties of carrying it to high altitudes. With the stack employed, the total load was already about 140 kg. Using the largest available ballons, the maximum altitude was already limited to 28000 m, and called for novel methods of launching. The difficulties would have been even further increased with greater loads.

Through a failure of the parachute during the descent, about 10% of the emulsion was damaged by impact of the container with the ground; the rest was little affected, and it was processed successfully, the resulting plates being available for scanning and measurement by the end of 1954.

2. – Objectives of the experiments.

A description of the principal objectives of the experiment and preliminary results has been given already; see ref. ([1,2]). Briefly stated, the intention was to make a detailed study of the charged secondary particles formed by the decay of charged heavy mesons produced in the emulsion.

2·1. *Modes of Decay of Heavy Mesons.* – In recent years, observations with photographic emulsions and Wilson chambers have indicated the existence of charged heavy mesons decaying in a variety of modes.

Following the discovery of the τ-meson ([3]), early emulsion work indicated the existence of two other modes of decay of heavy mesons, the $\varkappa$ ([4]) and the χ ([5]):

$$(E) \qquad \varkappa \to \mu + ? + ?$$

$$(D) \qquad \chi \to \pi + ? \qquad \text{(mass of neutral particle} \sim 300\ m_e\text{:}\quad E_\pi = 116 \pm 5\ \text{MeV).}$$

Later work in emulsions confirmed the existence of the $\varkappa$-mode ([5,6]) but left uncertain both the nature of the secondary neutral particles and details of the energy-spectra of the secondaries. Further evidence for the existence of the χ-mode, and for the fact that the transformation involved two π-mesons: $\chi \to \pi + \pi^0$, was obtained in work using both emulsions ([7]) and cloud-chambers ([8,9]).

The cloud-chamber group of École Polytechnique first proposed the exis-

---

([1]) Mimeographed Report — issued 19th May 1955 — of « *G Stack Collaboration Experiment* (1954) »; *Nature*, **175**, 971 (1955).

([2]) *Observations on heavy meson secondaries* (*G-Stack*): Mimeographed Report of the Pisa Conference (June 1955).

([3]) R. H. Brown, U. Camerini, P. H. Fowler, H. Muirhead, C. F. Powell and D. Ritson: *Nature*, **163**, 82 (1949).

([4]) C. O'Ceallaigh: *Phil. Mag.*, **42**, 1032 (1951).

([5]) M. G. K. Menon and C. O'Ceallaigh: *Proc. Roy. Soc.*, A **221**, 292 (1954).

([6]) Report of the Commission on K-particles: *Suppl. Nuovo Cimento*, **12**, 733 (1954).

([7]) M. Baldo, G. Belliboni, M. Ceccarelli, M. Grilli, B. Sechi, B. Vitale and G. T. Zorn: *Nuovo Cimento*, **1**, 1180 (1955).

([8]) H. S. Bridge, H. De Staebler, B. Rossi and B. V. Sreekantan: *Nuovo Cimento*, **1**, 874 (1955).

([9]) A. L. Hodson, T. Ballam, W. H. Arnold, R. D. Harris, R. Rau, G. T. Reynolds and S. B. Treiman: *Phys. Rev.*, **96**, 1089 (1954).

tence of the K_μ-mode ([10]):

$$(C) \qquad K_\mu \to \mu + \nu .$$

Strong supporting evidence for this mode of decay was obtained at the École Polytechnique ([11]) and at Massachussetts Institute of Technology ([8]).

The mode τ', involving the decay into 3 π-mesons, two of them neutral, was first envisaged by PAIS and by DALITZ ([12]). Events compatible with this mode have been observed by the Rochester group ([13]) and later by others. The interpretation of these events in terms of the τ'-mode remains to be confirmed.

The K_β-mode was first observed by the Bristol group ([14]), and confirmed by the Bristol and the Dublin groups ([15]). Only eight examples have been reported hitherto, all of them in emulsions. The situation at present is summarized in Table I.

TABLE I. – *Modes of decay of charged heavy mesons.*

$\tau^\pm \to \pi^\pm + \pi^+ + \pi^-$	(A)
$\tau'^\pm \to \pi^\pm + (\pi^0 + \pi^0)$	(B)
$K_\mu \to \mu + \nu$	(C)
$\chi \to \pi + \pi^0$	(D)
$\varkappa \to \mu$ + 2 or more neutrals	(E)
$K_\beta \to \beta$ + 2 or more neutrals	(F)

2·2. *Importance of Accurate Mass Measurements.* – When the present experiment was begun, the existence of the τ- and $\varkappa$-modes had been finally established, but the evidence for others, χ, K_μ, τ' and K_β, although very strong, was not conclusive. It was anticipated that in the favourable conditions provided by a large stack, there would be a substantial probability of being able to follow a secondary particle to the end of its range. Its nature could thus be established by its observed mode of decay; the observed range would then give the original energy of emission with high precision by an application of

([10]) B. GREGORY, A. LAGARRIGUE, L. LEPRINCE-RINGUET, L. MULLER and C. PEYROU: *Nuovo Cimento*, **11**, 292 (1954).

([11]) R. ARMENTEROS, B. GREGORY, A. HENDEL, A. LAGARRIGUE, L. LEPRINCE-RINGUET, F. MULLER and C. PEYROU: *Nuovo Cimento*, **1**, 915 (1955).

([12]) R. DALITZ: *Proc. Phys. Soc.*, A **77**, 710 (1953); A. PAIS: *Phys. Rev.*, **86**, 663 (1953). See also *Bagneres Report* (1953), p. 229.

([13]) J. CRUSSARD, M. F. KAPLON, J. KLARMANN and J. H. NOON: *Phys. Rev.*, **93**, 253 (1954).

([14]) M. W. FRIEDLANDER, D. KEEFE, M. G. K. MENON and L. VAN ROSSUM: *Phil. Mag.*, **45**, 1043 (1954).

([15]) C. DAHANAYAKE P. E. FRANCOIS, Y. FUJIMOTO, P. IREDALE, C. G. WADDINGTON and M. YASIN: *Phil. Mag.*, **45**, 1219 (1954); R. H. W. JOHNSTON and C. O'CEALLAIGH: *Phil. Mag.*, **46**, 393 (1955).

the range-energy relation. Modes of decay into two particles only would then be distinguished without ambiguity by the homogeneity of the corresponding secondaries, and accurate values of the mass would follow from an application of the conservation laws.

Such accurate mass determinations appeared to be of great importance because of their bearing on the nature of heavy charged mesons decaying in different modes. The existence of a small difference in mass, for example, if it could be established, would exclude the possibility that all the heavy mesons with the same sign of charge represent alternative modes of decay of particles of a single type. The existence of such a small mass-difference had been suggested by experiments with Wilson chambers which indicated that the particles decaying in the mode K_μ were less massive than those transforming in other modes ([10]). It seemed important to test this result by experiments using another method.

Since measurements of the type outlined above were made, a powerful new method has become available following the artificial production of K-mesons in large numbers by the Berkeley 6 GeV proton-accelerator. This allows K-mesons of known momentum to be injected into a stack; their masses are then determined by observations of momentum and range ([16]). It seems certain that this method, which allows a direct comparison to be made between the masses of mesons decaying in different modes, will soon attain a high accuracy. This development, and the considerations which follow, give particular importance to the second objective of the present work, namely the determination of the relative frequency of occurrence in the conditions of the experiment of the different modes of decay.

2·3. *Significance of relative frequencies of occurrence of different modes.* – From very general theoretical considerations, it seems unlikely that all the charged heavy mesons can be attributed to particles of a single type with six modes of decay. The theoretical considerations advanced by DALITZ ([17]), for example, indicate on the basis of the present experimental evidence that the τ and χ-modes cannot be attributed to the decay of particles of a single type. It has been suggested by DALLAPORTA ([18]) that the modes (D),(E),(F) are alternative ways of decay of the same particle, and by GELL-MANN ([19]) that the modes (A), (B), (C) shown in Table I might correspond to the decay of a pseudo-

([16]) S. C. FUNG, N. MOHLER, A. PEVSNER and D. RITSON: *Mimeographed report of the Pisa Conference*, p. 201 (1855); R. W. BIRGE, R. P. HADDOCK, L. T. KERTH, J. R. PETERSON, J. SANDWEISS, D. H. STORK and M. N. WHITEHEAD: *Mimeographed Report of the Pisa Conference* 1955, p. 151.

([17]) R. H. DALITZ: *Proc. of the Rochester Conference* (1955).

([18]) N. DALLAPORTA: *Proc. Pisa Conf.* (1955) to appear in *Suppl. Nuovo Cimento.*

([19]) M. GELL-MANN: *Proc. Pisa Conf.* (1955), to appear in *Suppl. Nuovo Cimento.*

scalar particle, and the modes (D), (E) and (F) to that of a scalar particle. If there are indeed particles of two or more types present, and if they cannot be distinguished by a difference in mass, it becomes of great interest to determine their relative frequencies of occurrence in widely different experimental conditions. Such observations could allow the two types of particles to be distinguished through an observable difference in lifetime. In the experiments on the cosmic radiation using the photographic method, for example, the average time of flight of a K-meson, produced in a nuclear disintegration in the emulsion and arrested within it, is about $3 \cdot 10^{-10}$ s. On the other hand, in experiments with magnetically analysed beams of K-particles from the machines, the time of flight is 10^{-8} s. If there are indeed several types of K-mesons, some with lifetime $\sim 10^{-9}$ s, the relative frequencies of occurrence of different modes of decay will be different in the two experimental conditions.

The relative frequencies of occurrence of different modes of decay are also of great interest in a second connection. If the tentative groupings referred to above are correct, the various modes of decay of particles of a single type must always occur in the same proportions, irrespective of the experimental conditions, and these proportions represent very important constants which any theoretical treatment must seek to explain.

The above considerations emphasize the importance of the measurements of relative frequencies, both for mesons locally produced in a stack, and for those generated outside it which commonly have much longer times of flight. To obtain reliable values will involve very extensive measurements because of the rarity of some modes, and variations in the efficiency with which different modes are detected in some conditions of experiment. A significant result in this field can only be expected if the nature of the secondary decay particles can be established and their energies measured. This requires the favourable conditions provided by a large stack, and the considerable effort involved in finding the heavy mesons and in measuring the tracks. The precautions necessary in such experiments are discussed in the present paper and preliminary results are presented.

2·4. *Energy Spectra of Secondary Particles from modes* $\varkappa$, τ' *and* K_β. – A problem closely associated with the second objective of the investigation is to determine the distribution in energy of the μ- and π-mesons and electrons produced in the modes of decay $\varkappa$, τ' and K_β, in both of which there are two or more neutral particles emitted. The end-points of the spectra have an important bearing on the rest-masses of these neutral particles, and therefore on their nature; and the detailed features of the energy spectra are of great theoretical interest because of the information they would give about the nature and the strengths of the interactions between the different particles involved in the transformations.

In addition to serving these objectives, it was recognised that the stack would provide exceptionally favourable conditions for studying the associated production of heavy mesons and hyperons, their interactions with nuclear particles, the development of high-energy cascades of electrons and γ-rays, the secondary interactions of shower-particles, and many other phenomena of the high-energy region not at present accessible to the machines.

2·5. *Extent of the Collaboration.* – In view of the desirability of obtaining results of great statistical weight, the collaboration was extended to include workers in the Institute for Advanced Studies and University College, Dublin, the Institute of Theoretical Physics, Copenhagen, the University of Genoa and the Laboratoire de Physique Nucléaire, Université Libre, Bruxelles. There would have been advantages in an even wider collaboration, but it was found inexpedient to increase the number of people working in this particular stack, which now amounts to more than thirty physicists and fifty scanners. The division of the stack among different laboratories has the consequence that individual tracks must frequently be followed from plates in one laboratory to those in another, and sometimes on to a third and even a fourth. If the stack is too widely dispersed, the advantages it is designed to exploit may be lost through the complications involved in following tracks.

3. – Experimental Results.

The present report is confined to the results obtained by us on the modes of decay χ and K_μ; on the distribution in energy of the charged secondary particles in the $\varkappa$, K_β and τ' modes; and on the relative frequencies of occurrence of these modes of decay. Within the limits of the present experiment it was not possible to distinguish between the masses of the mesons decaying in the modes χ and K_μ and that of the τ-meson. The mass-values are at present subject to uncertainties in the range-energy relation and other sources of error which are discussed in some detail. Information on the primary particles of these events, their energy-spectra, their origins, and on the particles with which they are associated in production, will be discussed in later publications together with phenomena associated with negative K-mesons, hyperons and heavy unstable fragments.

3·1. *Methods of Measurement.* – After the stack had been processed and distributed among the cooperating laboratories, the first task was to find a large number of decaying K-mesons. In scanning the plates, particular attention was paid to the search for singly charged particles which appeared to decay at rest to a single charged secondary. 324 examples of particles

heavier than a π-meson were thus found, each of which appeared to give rise to a secondary particle lighter than the proton. From the 324 events, those were selected for measurement in which the direction of emission of the secondary particle was such that it had a potential path-length in the stack $\geqslant 5$ cm, with a minimum length in each plate of 2 mm.

Eighty events were studied. Where possible, the track of the primary particle was followed back to the parent star. The mass of the primary was measured in order to show that it was neither a hyperon, nor a proton, with the end of whose path another track happened to coincide.

The information on these 80 secondary particles is contained in Table II which is divided in three sections as follows:

(*A*) Secondary particles which reached the end of their range in the stack;

(*B*) Secondary particles which left the stack after having completed at least two thirds of their potential range, i.e. ~ 14 cm for μ-mesons from the K_μ-decay and ~ 8 cm for π-mesons from the χ-decay. In such events, the residual range of the secondary was small, and its value could be determined with good precision by scattering and ionisation measurements;

(*C*) Secondary particles which, through nuclear interactions, radiation loss, the traversal of damaged plates or bad geometry, produced tracks too short to permit the residual range to be estimated with precision.

3·2. *Range measurements on particles stopping in the stack.* Of the 80 secondary particles selected, 28 came to the end of their range and were observed to decay: 16 as π^+-mesons (π-μ-e-decay), 12 as μ-mesons (μ-e-decay). 7 of the μ-mesons had a range ~ 20 cm; the remaining 5 came to rest with various ranges less than 5 cm. Of the π-meson tracks, 10 had a range of ~ 12 cm; the rest (6) were all shorter than 3 cm. The results are summarized in Table II A_1, A_2, A_3, A_5, and Fig. 1. To these results may be added 2 events showing an apparent decay to ρ-mesons (Table II A_6): these will be dealt with in a later section.

The ranges were measured with calibrated micrometer screws and scales. Before exposure, the thickness of the emulsion strips had been determined by Mr. SWINNERTON and Mr. WALLER of Ilford Ltd using measurements of weight and density.

The main sources of error in determining the range of particles in the stack, together with the magnitude of the errors and the corresponding corrections, are discussed in detail in Appendix I. In describing the results in what follows, the quoted errors include both the statistical errors and the errors on the corrections. The most important systematic corrections arise

from abrasion and from distortion, and the largest statistical error is due to straggling.

When an average value of measured ranges is given, the quoted error includes that due to straggling and gives a measure of the possible departure of the average of our sample from the mean of the population. The errors in measurements of the sample ranges are small compared with this source

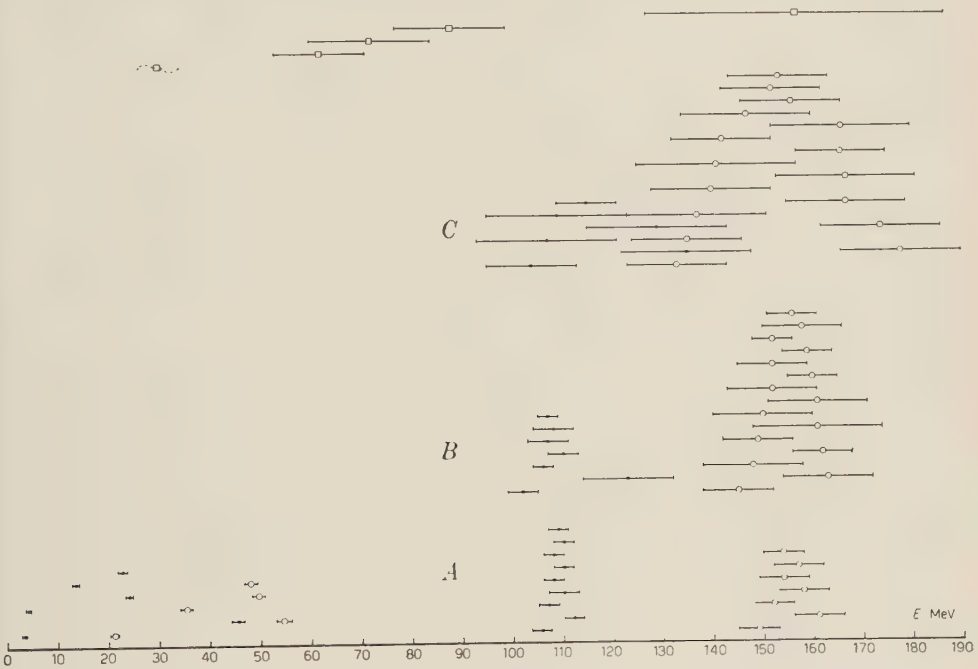

Fig. 1. – Distribution in energy of emission of the K-particle secondaries. (•) identified as π-mesons; (○) identified as μ-mesons; (□) identified as electrons.

of uncertainty in the estimate of the mean range. The range-energy relation used was that calculated for nuclear emulsions by BARONI *et al.* [20], which is in good agreement with the numerous experimental points for proton energies below 40 MeV, and with the two existing points at higher energies.

Using the mass values of the π- and μ-mesons given by SMITH *et al.* [21], the range-energy curve of BARONI *et al.*, gives as the range of the μ-meson arising in the $\pi \to \mu$ decay, (597.7 ± 2.8) μm, the error being due to the uncertainty in the masses. To normalise this curve so that it should be ap-

---

[20] G. BARONI, C. CASTAGNOLI, G. CORTINI, C. FRANZINETTI and A. MANFREDINI: CERN BS/9 (1954).

[21] F. M. SMITH, W. BIRNBAUM and W. H. BARKAS: *Phys. Rev.* **91**, 765 (1953).

TABLE II. – K_{μ}-*mode*, A.1 *stopping*, B.1 *and* C.1 *non stopping secondaries*;

Event	PRIMARY		SECON					Ran
	Range	Parent star	Path available in stack	Length pro plate at emission	Number of plates	Observed length	Fate (stops, out of stack, etc.)	Corra
	cm		cm	cm		cm		c
A.1								
1 Br_{89}	2.77	15+0n	23	0.25	32	—	stops. $\mu \rightarrow e$ decay	20.2
2 $DuUC_{10}$	>0.87	—	26	0.25	51	—	»	21.0
3 Ko_{36}	12.2	—	20	0.70	31	—	»	20.4
4 Pd_{47}	>3.76	—	25	0.25	116	—	»	20.4
5 Pd_{57}	2.40	13+5n	24	0.22	126	—	»	20.9
6 Pd_{74}	6.60	4+0p	25	0.53	59	—	»	19.7
7 Pd_{132}	1.85	8+4n	27	0.5	33	—	»	21.5
B.1								
8 Br_{69}	4.07	3+0K	14	0.65	21	14.2	out of stack	
9 Br_{92}	3.33	10+0p	29	1.9	18	16.2	lost in damaged region	
10 Br_{94}	0.5	10+15p	18	0.11	132	18.3	out of stack	
11 Bx_6 (*)	0.71	8+1n	20	1.15	36	19.8	»	
12 $DuAS_9$	>1.47	—	14.5	6.5	4	14.5	—	
13 $DuUC_7$	1.30	2+0n	17.0	4.0	17	16.2	out of stack	
14 $DuUC_{20}$	3.71	12+0n	15.0	0.8	15	15.0	»	
15 $DuUC_{21}$	>0.6	—	24.4	0.3	66	19.96	»	
16 $GeMi_{70}$	>0.43	—	18.0	0.3	31	17.4	»	

(*) We thank Mr. HIRSCHBERG who supplied this event for measurement in Milan.

pping, B.2 and C.2 non stopping secondaries; χ-mode, A.3; Kβ-mode, C.4; τ'-mode, A.5; Kρ, A.6.

ts	Scattering and ionisation measurements					Attribution	Remarks
n	Section from decay cm	$p\beta$ MeV/c	g^*	Extrapol. total range cm	Energy at emission MeV		
4	—	—	—	—	—	K_μ from range and decay	
5	—	—	—	—	—	»	
4	0-3.0	197 ± 22	1.00 ± 0.03	19.5 ± 3	148 ± 18	»	out of area
5	—	—	—	—	—	»	
5	—	—	—	—	—	»	
4	0-4.5	196 ± 14	—	20.1 ± 2	152 ± 12	»	
5	0-4.5	192 ± 13	—	19.5 ± 1.7	148 ± 10	»	
	0-2.3	226 ± 22	0.95 ± 0.03	23.1 ± 2.9	171 ± 19		
	8.9-11.5	146 ± 15	—	21.2 ± 2	159 ± 13	K_μ from $p\beta$	
	11.5-12.7	118 ± 14		19.7 ± 1.5	149 ± 9		
	12.7-14.1	104 ± 12		19.5 ± 1.3	148 ± 9		
	0-5.1	189 ± 13	1.05 ± 0.04	19.3 ± 1.9	147 ± 12	K_μ from $p\beta$	
	9.3-10.4	137 ± 13	—	19.8 ± 1.7	150 ± 10		
	at 18.33	—	1.89 ± 0.09	20.14 ± 0.2	152 ± 4	K_μ from g^* and range	out of geometry
	0-5.0	188 ± 13	0.90 ± 0.06	19.1 ± 1.7	146 ± 11		
	14.5-15.8	126 ± 15	—	23.7 ± 1.7	174 ± 11		
	15.9-17.1	103 ± 11	—	22.5 ± 1.2	167 ± 9	K_μ from $p\beta$ and range	out of area
	17.1-18.1	76 ± 9	—	21 ± 0.7	157 ± 6		
	18.1-19.2	69 ± 7	—	21.5 ± 0.6	161 ± 6		
	19.2-19.8	55 ± 9	—	21.4 ± 0.5	160 ± 6		
	0-4.5	189 ± 13	0.93 ± 0.4	19.0 ± 1.8	145 ± 12	K_μ from $p\beta$, g^* and range	out at area; extrapolated range based on g^*
	13-13.9	104 ± 15	1.09 ± 0.3	19.5 ± 1.6	148 ± 10	— ——— — ——→	
	at emission	—	0.96 ± 0.11	—	—		
	4.9-6	171 ± 22	—	19.6 ± 2.8	149 ± 18	K_μ from $p\beta$, g^* and range	
	14.3-15.1	—	1.24 ± 0.06	20.2 ± 1.4	152 ± 9		
	14.7-15.2	83 ± 14	—	19.7 ± 1.1	149 ± 8		
	at emission	—	0.80 ± 0.05	—	—		
	4.7-5.7	216 ± 28	—	24.7 ± 2.8	180 ± 17	K_μ from $p\beta$, g^* and range	
	12.5-15.4	—	1.17 ± 0.05	20.5 ± 1.3	155 ± 8		
	13.4-14.4	115 ± 15	-	22.5 ± 1.9	167 ± 13		
	19.15-19.37	—	~ 5.2	21.2 ± .8	159 ± 5	K_μ from ionisation and range	
	0-5.1	231 ± 20	1.00 ± 0.02	25.1 ± 2.1	182 ± 14		
	5.1-9.6	174 ± 13	—	21.8 ± 1.5	163 ± 11	K_μ from $p\beta$ and range	
	9.6-12.6	159 ± 15	—	23.8 ± 2	175 ± 12		
	12.6-15.6	104 ± 9	—	20.2 ± 0.9	152 ± 5		
	15.6-17.4	109 ± 11	—	23.1 ± 1.2	170 ± 7		

TABLE II (*continued*). K_μ-*mode*, A.1 *stopping*, B.1 *and* C.1 *non stopping secondaries*; 7

Event	PRIMARY		SECON					Ra
	Range cm	Parent star	Path available in stack cm	Length pro plate at emission cm	Number of plates	Observed length cm	Fate (stops, out of stack, etc.)	Co
B.1								
17 $GeMi_{72}$	> 1.00	—	28.0	0.55	50	14.1	out of stack	
18 Pd_{81}	> 3.5	—	16	0.5	30	14.6	»	
19 Pd_{82}	3.33	15+0p	17.0	0.45	30	14.1	»	
20 Pd_{90}	4.63	17+6p	20	0.5	67	18.6	»	
21 Pd_{53}	1.93	6+2p	15	0.6	12	14.7	»	
22 Pd_{126}	3.94	7+5p	17	0.4	21	14.5	»	
C.1								
23 Br_{68}	0.9	12+4p	32	0.5	11	5.9	out of stack	
24 $DuAS_1$	> 3.9	—	6	2.0	3	5.6	lost in damaged region	
25 $DuAS_5$	0.73	12+2p	10	0.5	13	4.1	»	
26 $DuAS_{12}$	1.43	1+0n	29	0.3	18	9.5	lost	
27 $DuAS_{15}$	3.94	5+2n	9	0.4	16	6.5	»	
28 $DuAS_{30}$	0.99	11+6p	9	0.3	32	9.1	out of stack	
29 $DuAS_{32}$	> 4.8	—	14	1.0	9	11.6	unknown; following incomplete	
30 $DuUC_1$	> 2.0	—	6	0.35	16	5.5	out of stack	
31 $DuUC_6$	0.95	5+3n	8	0.42	12	5.1	»	
32 $DuUC_{12}$	5.7	2+0n	7	1.00	11	6.2	»	
33 $DuUC_{17}$	> 0.4	—	28	0.6	6	4.5	»	
34 $GeMi_{34}$	> 2.6	—	9.5	0.3	15	7.0	»	
35 $GeMi_{101}$	0.7	6+2n	10	2.4	7	7.5	»	
36 Ko_{32}	0.4	29+8α	9	1.1	5	8.3	»	
37 Ko_{46}	5.8	1+0p	7	0.5	13	6.6	»	
38 Pd_{130}	0.2	1+0p	21	0.31	16	11.8	»	

opping, B.2 *and* C.2 *non stopping secondaries*; $\varkappa$-*mode*, A.3; K_β-*mode*, C.4; τ'-*mode*, A.5; K_ρ, A.6.

ts	Scattering and ionisation measurements					Attribution	Remarks
	Section from decay cm	$p\beta$ MeV/c	g^*	Extrapol. total range cm	Energy at emission MeV		
	0-4.0	201 ± 25	0.95 ± 0.02	18.5 ± 3.4	142 ± 21	K_μ from $p\beta$ and range	
	9.8-12.6	132 ± 13	—	20.8 ± 1.3	157 ± 9		
	12.7-14.1	105 ± 15	—	19.6 ± 1.6	149 ± 11		
	12.3-14.6	121 ± 17	—	21.5 ± 1.9	161 ± 13	K_μ from $p\beta$ and range	
	0-5.4	177 ± 13	—	17.9 ± 1.8	138 ± 11	K_μ from $p\beta$ and range	
	12.9-14.1	121 ± 13	—	21.5 ± 1.5	161 ± 10		(*) from calibration on stopping μ's
	0-5.2	175 ± 11	—	17.4 ± 1.5	135 ± 9	K_μ from $p\beta$, g^* and range	
	at 18.55	—	(*)	20.9 ± 0.8	156 ± 5		
	0-5.1	201 ± 15		21.1 ± 2.1	158 ± 13	K_μ from $p\beta$ and range	
	9.5-13.4	140 ± 10	—	21.8 ± 1.3	163 ± 9		
	0-5.8	168 ± 12	—	16.9 ± 1.6	132 ± 10	K_μ from $p\beta$ and range	
	13.7-14.4	93 ± 8	—	19.1 ± 1.1	145 ± 7		
	0-5.8	180 ± 12	1.00 ± 0.03	18.5 ± 1.7	142 ± 10	K_μ from $p\beta$ and g^*	out of area
	0-5.6	218 ± 15	1.00 ± 0.04	23.7 ± 2	174 ± 12	K_μ from $p\beta$ and g^*	
	0-4.1	184 ± 15	0.94 ± 0.04	18.2 ± 2	140 ± 12	K_μ from $p\beta$ and g^*	
	0-5.0	175 ± 13	0.95 ± 0.05	17.4 ± 1.8	135 ± 11	K_μ from $p\beta$ and g^*	
	0-6.5	220 ± 15	0.93 ± 0.03	24.4 ± 2	178 ± 12	K_μ from $p\beta$ and g^*	»
	0-4.0	165 ± 14	0.94 ± 0.05	15.5 ± 1.8	124 ± 11	K_μ from $p\beta$ and g^* and range	
	8.2-9.1	150 ± 18	1.00 ± 0.05	19.4 ± 2.4	149 ± 13		
	0-4.0	197 ± 16	~ 1	20.0 ± 2.3	151 ± 14	K_μ from $p\beta$, q^* and range	
	10.6-11.6	132 ± 18	1.12 ± 0.05	20.4 ± 2.1	154 ± 14		After 3.7 cm track going through a corner of the stack, distortion too high, measurement and following abandoned.
	0-5.5	188 ± 13	0.90 ± 0.05	19.3 ± 2	147 ± 13	K_μ from $p\beta$ and g^*	
	0-5.0	213 ± 17	0.98 ± 0.04	22.6 ± 2.3	167 ± 14	K_μ from $p\beta$ and g^*	
	0-4.4	214 ± 17	1.06 ± 0.04	22.4 ± 2.3	166 ± 14	K_μ from $p\beta$ and g^*	
	0-3.7	183 ± 15	0.99 ± 0.03	17.7 ± 2.2	137 ± 14	K_μ from $p\beta$ and g^* →	
	0-4.4	192 ± 13	0.99 ± 0.02	19.4 ± 1.8	147 ± 11	K_μ from $p\beta$, g^* and range	
	5.5-7.0	191 ± 20	—	23.3 ± 2.9	171 ± 19		
	0-5.0	212 ± 14	0.86 ± 0.04	22.5 ± 1.8	167 ± 12	K_μ from $p\beta$ and g^*	
	0-7.6	202 ± 12	—	22.3 ± 1.5	166 ± 9	K_μ from $p\beta$ and g^*	out of area
	at 5.7	—	1.00 ± 0.03	—	—		
	0-4.8	183 ± 18	—	18.4 ± 2.5	141 ± 16	K_μ from $p\beta$ and +*	»
	at 4.0	—	0.98 ± 0.03	—	—		
	10.6-11.8	137 ± 15	—	20.9 ± 1.7	156 ± 10	K_μ from $p\beta$ and range	

TABLE II (*continued*). – K_{μ}-*mode*, A.1 *stopping*, B.1 *and* C.1 *non stopping secondaries*; χ

Event	PRIMARY		SECON					Ran
	Range	Parent star	Path available in stack	Length pro plate at emission	Number of plates	Observed length	Fate (stops, out of stack, etc.)	Corr
	cm		cm	cm		cm		
A.2								
39 $DuAS_{24}$	> 3	stress mark	14	0.7	20	—	Stops. $\pi \rightarrow \mu \rightarrow e$ decay	11.
40 $DuAS_{25}$	7.17	17+10n	20	0.25	40	—	»	12.
41 $GeMi_{60}$	1.9	16+7p	15	0.38	40	—	»	12.
42 $GeMi_{106}$	0.14	13+5p	17	0.67	38	—	»	11.
43 $GeMi_{107}$	> 0.65	—	13	0.2	49	—	»	11.
44 Pd_{28}	1.96	12+4p	25	0.12	81	—	»	12.
45 Pd_{52}	1.33	27+29F	17	0.5	36	—	»	12.
46 Pd_{77}	> 3.2	—	13	0.16	55	—	»	11.
47 Pd_{92}	> 8.2	—	19	0.6	17	—	»	11.
48 $GeMi_{29}$	> 2.6	—	22	0.26	28	—	Undergoes elastic collision with a proton, then comes to rest giving $\pi \rightarrow \mu \rightarrow e$ decay	0.4 (10.
B.2								
49 Br_{80}	0.52	23+3n	10	1	9	9.9	out of stack	
50 Br_{96}	4.15	20+1p	9	0.16	54	8.7	»	
51 $DuAS_{27}$	1.66	6+0p	> 12	0.35	29	11.42	»	
52 $DuUC_{3}$	0.98	2+1n	13	0.25	31	7.99	»	
53 $GeMi_{84}$	0.95	3+0p	11.5	1.1	34	10.03	»	
54 $GeMi_{91}$	2.44	10+3p	9	1.5	7	9.02	»	
55 $GeMi_{26}$	> 4.8	—	11.8	0.21	41	9.75	»	

pping, B.2 *and* C.2 *non stopping secondaries*; $\varkappa$ *mode*, A.3; K_β-*mode*, C.4; τ'-*mode*, A.5; K_ρ, A.6.

ts	Scattering and ionization measurements					Attribution	Remarks
n	Section from decay cm	$p\beta$ MeV/c	g^*	Extrapol. total range cm	Energy at emission MeV		
2	0-3	147 ± 14	1.05 ± .05	10.5 ± 1.4	101 ± 9	χ from range and decay	Associated Σ^-. Scattering between 1 and 3 cm from decay unreliable due to visible chopping
2	0-1	154 ± 21	1.23 ± .06	10.3 ± 2.2	100 ± 15	»	
2	0-3.2	150 ± 15	—	11 ± 1.6	104 ± 10	»	
2	0-2.6	178 ± 17	1.12 ± 0.02	13.9 ± 2	122 ± 12	»	
2	2.6-5.9	137 ± 13	—	12.3 ± 1.3	112 ± 8	»	
2	0-3	167 ± 17	1.05 ± 0.02	12.8 ± 1.9	116 ± 13	»	
3	—	—	—	—	—	»	out of geometry
2	0-3.5	147 ± 13	—	10.8 ± 1.3	103 ± 8	»	Associated Y
2	—	—	—	—	—	»	
2	—	—	—	—	—	»	
	Range from collision			Extrapol. range from collision	Energy at the collision		
	0-2.52	163 ± 16	—	12.2 ± 1.9	112 ± 12	χ from range and dynamics of the collision	Energy of emission from the dynamics of the collision $E = (107 \pm 5)$ MeV
	2.5-4.6	136 ± 13	—	11.5 ± 1.3	107 ± 8		
	4.6-7	105 ± 9	—	10.9 ± 0.7	103 ± 5		
2)	7-8.3	68 ± 7	—	10.0 ± 0.4	99 ± 4		
	8.3-9	70 ± 10	—	11.1 ± 0.6	105 ± 5		
	0-2	187 ± 18	120 ± 0.04	14.7 ± 2.3	129 ± 14	χ from ionisation $p\beta$ and range	(*) From calibration on stopping π's
	at 9	72 ± 8	—	11.7 ± 0.7	108 ± 5		
	—	—	(*)	12.2 ± 0.5	112 ± 4		
	at emission	—	1.21 ± 0.05	—	—	χ from g^* and range	out of geometry
	at 7.3	—	1.48 ± 0.07	11.5 ± 0.4	107 ± 4		
	0-3	138 ± 14	1.15 ± 0.05	9,6 ± 1.4	95 ± 9	χ from g^* and range	
	10.85-10.95	—	3.74 ± 0.22	11.42 ± 0.2	106 ± 2		
	0-4	157 ± 15	—	12.1 ± 1.6	111 ± 10	χ from g^*, $p\beta$ and range	Electron pair associated
	7-8	93 ± 8	1.52 ± .08	11.6 ± 0.6	108 ± 4		
	0-3	173 ± 15	1.04 ± 0.02	13.5 ± 1.7	120 ± 10	χ from $p\beta$, g^* and range	
	4.2-4.8	118 ± 23	—	10.7 ± 2	103 ± 12		
	9-10	98 ± 17	—	14.0 ± 1.3	123 ± 9		
	0-3	172 ± 15	1.06 ± 0.03	13.4 ± 1.8	119 ± 11	χ from $p\beta$, g^* and range	
	6.5-7.2	115 ± 18	—	12.8 ± 1.5	116 ± 9		
	7.2-9	70 ± 8	—	10.5 ± 0.5	101 ± 4		
	0-3	152 ± 18	1.00 ± 0.02	11.1 ± 1.9	105 ± 2	χ from $p\beta$, g^* and range	
	3.4-4.8	118 ± 13	—	10.3 ± 1.2	100 ± 7		
	8.6-9.3	71 ± 11	—	11.5 ± 0.7	108 ± 4		
	9.3-9.7	61 ± 9	—	11.4 ± 0.5	107 ± 3		

TABLE II (*continued*). K_μ *mode*, A.1 *stopping*, B.1 *and* C.1 *non stopping secondaries*; 7

Event	PRIMARY		SECON					Ran
	Range	Parent star	Path available in stack	Length pro plate at emission	Number of plates	Observed length	Fate (stops, out of stack, etc.)	Cor r:
	cm		cm	cm		cm		
C. 2								
56 Br_{75}	3.6	18+20α	4	0.9	4	3.9	out of stack	
57 Br_{77}	8.12	5+0p	15	0.1	52	5.3	disappears in flight	
58 Br_{93}	2.6	8+1p	13	0.4	2	0.05	interacts giving 3+0p star	
59 $GeMi_{98}$	> 0.92	—	14	0.7	3	1.8	interacts giving 4+0π star	
60 $GeMi_{105}$	2.94	16+8α	21	0.73	7	2.84	interacts giving 3+0π star	
61 Pd_{44}	1.7	22+2p	13	0.4	4	2	interacts giving 2+0π star	
62 Ko_{37}	2.09	12+1p	5	2	3	5	out of stack	
A. 3								
63 Br_{90}	1.43	4+0p	16	0.45	11	—	stops giving μ-e decay	2.34
64 $DuAS_{29*}$	1.08	2+0n	11.5	0.15	27	—	»	4.03
65 $GeMi_{99}$	> 3.34	—	14	0.3	16	—	»	4.69
66 $GeMi_{108}$	0.95	11+3n	21	0.38	10	—	»	1.04
67 Pd_{30}	1.57	15+3p	20	0.3	12	—	»	3.82
C. 4								
68 $GeMi_{56}$	> 5.5	—	32	0.25	15	5.18	Undergoes rapid increase in scatt. without change in *g*. Becomes impossible to follow	
69 $GeMi_{57}$	> 4	—	24	0.25	1	0.03	Lost into damaged region in the second plate	
70 $GeMi_{93}$	> 2.5	—	18	0.6	2	1.75	Catastrophic energy loss at 1.46 cm. Becomes impossible to follow	

pping, B.2 *and* C.2 *non stopping secondaries*; $\varkappa$-*mode*, A.3; $K\beta$-*mode*, C.4; τ'-*mode*, A.5; K_ρ, A.6.

Scattering and ionisation measurements					Attribution	Remarks
Section from decay cm	$p\beta$ MeV/c	g^*	Extrapol. total range cm	Energy at emission MeV		
0-3.4	180 ± 16	1.19 ± 0.02	17.3 ± 2.2	135 ± 13	χ from g^* and $p\beta$	out of area out of geometry: associated Y
at 5.1	—	1.22 ± 0.06	12.8 ± 0.9	115 ± 6	χ from g^* and interaction	out of geometry
0-0.05	—	1.1 ± 0.14	—	~ 100	χ from g^* and interaction	visible energy of the interaction ~ 40 MeV
0-1.24	163 ± 19	1.08 ± 0.02	11.4 ± 2.4	107 ± 14	χ from $p\beta$ and interaction	visible energy of the interaction ~ 90 MeV
0-2.84	187 ± 18	1.08 ± 0.03	15.1 ± 2.3	129 ± 14	»	visible energy of the interaction ~ 100 MeV
0-2	163 ± 16	—	11.8 ± 2.1	109 ± 14	»	visible energy of the interaction ~ 50 MeV
0-3.6	148 ± 13	1.13 ± 0.04	10.9 ± 1.3	104 ± 9	χ from $p\beta$ and g^*	out of area
1	—	—	—	—	—	$\varkappa$ from range and decay	secondary mass by g^* vs range (210 ± 10) m_e
1.2	—	—	—	—	—	»	out of geometry
1.3	—	—	—	—	—	»	
0.5	—	—	—	—	—	»	
1.3	—	—	—	—	—	»	
0-1.2	88 ± 11	0.94 ± 0.02	—	—	$K\beta$ from $p\beta$, g^* and energy loss	
1.7-3.35	80 ± 8	0.97 ± 0.02	—	—		
4.67-5.27	40 ± 6	1.04 ± 0.03	—	—		
0-0.03	~ 30	—	—	—	»	
0-0.55	72 ± 12	1.04 ± 0.02	—	—		
0.64-1.46	44 ± 5	0.93 ± 0.03	—	—	»	
1.46-1.75	26 ± 5	—	—	—		

TABLE II (*continued*). – Kμ-*mode*, A.1 *stopping*, B.1 *and* C.1 *non stopping secondaries*; χ-

SECOND

Event	PRIMARY		Path available in stack	Length pro plate at emission	Number of plates	Observed length	Fate (stops, out of stack, etc.)	Range
	Range	Parent star						Corre rang
	cm		cm	cm		cm		cm
C.4								
71 $GeMi_{103}$	4.7	—	14	1.6	14	3.91	Catastrophic energy loss at 3.65 cm. Becomes impossible to follow	—
72 Pd_{131}	0.93	3+3π	26	0.5	2	1	lost after 2 plates	—
A.5								
73 Br_1	—	—	3	0.2	2	—	stops giving π-μ-e decay	0.390±
74 Br_2	—	—	5	0.5	7	—	»	2.99±
75 $GeMi_{27}$	6.4	6+5p	5	0.08	12	—	»	1.07±
76 $GeMi_{32}$	>0.24	—	15	0.18	1	—	»	0.047±
77 $GeMi_{90}$	>0.28	—	24	0.11	9	—	»	0.962±
78 Ko	>9	—	—	—	1	—	»	0.028±
A.6								
79 Br_{71}	6.70	17+1p	20	1	10	—	stops giving a blob	5.93±
80 $GeMi_{75}$	—	17+9p	9	0.14	3	—	»	0.28±

plicable to our emulsion, the ranges were measured of 212 μ-mesons from $\pi \to \mu$ transformations recorded in our stack and the mean value was found to be (597.8 ± 2.1) μm. The curve of BARONI *et al.* was therefore employed without modification. An error equal to 0.3% in the energy, corresponding to a given value of range, was assumed, in order to take account of the error ($\pm$ 2.1 μm) in the measured value of the mean range of the μ-mesons used for the normalization and of the uncertainty in the energy of the μ-meson. There are no experimental values for the ranges of protons with energy greater than 342 MeV. The energies deduced for μ-mesons with ranges greater than about 2.7 cm, and π-mesons of range more than 3.5 cm, are therefore given subject to a verification of the range-energy relation.

opping, B.2 *and* C.2 *non stopping secondaries*; *χ-mode*, A.3; K_β*-mode*, C.4; *τ′-mode*, A.5; K_ρ, A.6.

ents	Scattering and ionization measurements					Attribution	Remarks
rgy sion V	Section from decay cm	$p\beta$ MeV/c	g^*	Extrapol. total range cm	Energy at emission MeV		
	0-0.59	157 ± 30	1.04 ± 0.03	—	—	K_β from $p\beta$ and g^*	
	0.59-2.9	101 ± 10	0.98 ± 0.02	—	—		
	2.48-3.65	67 ± 10	1.04 ± 0.02	—	—		
	3.65-3.9	12 ± 4	1.02 ± 0.04	—	—		
	0-1.0	62 ± 9	1.05 ± 0.04			K_β from $p\beta$ and g^*	Possible knock-on electron after 1.2 mm
±0.4	—	—	—	—	—	τ′ from range and decay	out of geometry
±0.5	—	—	—	—	—	»	—
±0.5	—	—	—	—	—	»	out of geometry
±0.1	—	—	—	—	—	»	»
±0.6	—	—	—	—	—	»	»
±0.1	—	—	—	—	—	»	out of area
±1.4	—	—	—	—	—	Secondary mass from range and g^* (281 ± 9) m_e	out of geometry Auger electron at the end of primary range
±0.3	—	—	—	—	—	Secondary probable π from calibration	

3·3. *Scattering and ionisation measurements on particles not coming to rest in the stack: groups B and C.* – Of the remaining 50 secondary tracks which have been analysed, 22 were long enough to belong to the class B, the observed track-lengths being more than 70 % of the total range. From individual or combined ionisation and scattering measurements, the secondary particles could be identified, and appear again to fall into the two more numerous groups: viz. 15 μ-secondaries of *estimated* total range of ~ 20 cm, and 7 π-secondaries of *estimated* total range of 12 cm.

The estimates of range obtained by ionisation measurements depend upon direct calibration only. Different methods have been employed by the collaborating groups for estimating the ionisation in a track. The Bristol and

Dublin groups measured gap-lengths, while the Copenhagen, Genoa-Milan and Padua groups made « gap » or « blob-counts ». In all cases, calibrations using tracks of known range and identity were carried out. The estimate of residual range based on scattering measurements (see following section) depends upon the scattering constant (see Appendix II).

The errors in ionisation and scattering measurements affect only the estimate of the residual range at the point of exit of a particle from the stack. It follows that when this quantity is small compared with the total range, the final precision is comparable with that obtained when the secondaries are actually arrested in the stack. The results are shown in Table II B_1, B_2, and Fig. 1.

(*C*) Amongst those measured, there are 28 secondary tracks in each of which the observed length was less than 70 % of the estimated total range; (class C; see Table II C_1, C_2, C_4 and Fig. 1). Five fall into this class because their path was interrupted by nuclear interactions (π-mesons), 4 because bremsstrahlung loss made further following too difficult (electrons) and the remaining 18 on account of unfavourable geometric conditions.

The secondary particles in these events have been identified by combined ionisation and scattering measurements on the path length available. The value of the extrapolated range so obtained is affected by the uncertainty both of the range-energy relation and of the scattering constant. An estimate of the energy of emission, which depends only slightly on the shape of the range-energy curve, can be obtained by observations of multiple scattering at a point close to the decay. The range energy relation then enters only into the estimate of the energy lost along the track up to the midpoint of the measured section. In order to keep this energy loss a small fraction of the total, the section of the track chosen must be relatively short. This involves a loss of information, and therefore many more tracks would be required to give an accurate mean with which to compare and correct that obtained by range. A discussion of the validity of the constants used in the deduction of the energy of emission from the measured scattering, together with an account of the slightly different techniques employed by the various collaborating groups, and the methods of estimating errors of measurement are contained in Appendix II.

The tracks of class C even when measured in their entirety cannot give as precise information as those of classes A and B, and do not therefore give a good definition of monoenergetic groups of particles. Careful measurement has however made it possible to separate these tracks into 7 π-mesons of energy about 110 MeV; 16 μ-mesons of about 150 MeV; and 5 electrons of various energies, completing the information on the relative frequencies of the various decay modes. The attribution of the high energy π- and μ-mesons of this class

to the monoenergetic groups defined in classes A and B rather than to a continuous spectrum, rests on the absence of π- and μ-mesons in the energy interval 60-100 MeV.

The identification of these short tracks and the possibility of making in the future a significant study of the distribution in energy of the secondary electrons produced in the K_β mode, relies on measurements of scattering. An internal calibration of the validity of these measurements can be obtained from scattering measurements on the first few centimetres of those long tracks of Classes A and B, which are already recognised as belonging to monoenergetic groups of particles. The results of such measurements are given in column 12 of Table II. Fig. 2 shows that the mean energies deduced from the scattering measurements near the point of decay of the class A and B tracks are com-

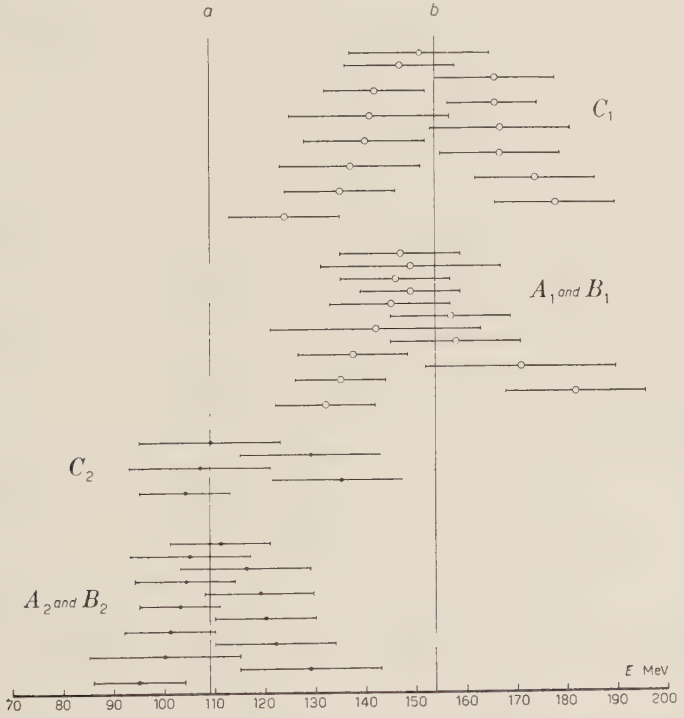

Fig. 2. – Comparison of energies at emission obtained by scattering near the decay point on tracks of classes A and B and those of class C.

Mean energy at emission from scattering near decay point.

	Classes A,B	Class C	All (ABC)	from range
π-meson group	108.7±3.9	114.4±6.1	110.0±3.7	109.2±0.8
μ-meson group	146.4±4.7	152.1±4.6	149.5±4.0	154.8±1.7

(•) K-particle secondaries identified as π-mesons;
(○) K-particle secondaries identified as μ-mesons;
(*a*) and (*b*) indicate the energy obtained from range measurements.

parable within the experimental errors to those of the class C tracks. Further, the experimental spread of the measurements on the C tracks is of the same order as that on the A and B tracks, so that also the former may be considered to represent two unique energy groups.

In addition, within the limits of error there is no disagreement between the values of energy deduced from range measurements, and those from scattering observations near the point of decay. This may indicate, either that range-energy relation and the scattering constant are substantially correct, or that both are wrong in such a way that the energies deduced from them are in error by approximately equal amounts and in the same sense.

3·4. *Allocation among different modes of decay.* – The measurements described above permit an allocation of the measured secondary particles among the 5 decay-modes shown in Table I; Table III gives the total number of particles attributed to each of these groups.

TABLE III.

Characteristic of Group	Assumed Decay Mode	Number of observed events			
		A	*B*	*C*	Total
1) μ-meson of $R \sim 20$ cm	$K_\mu \to \mu + \nu$	7	15	16	38
2) π-meson of $R \sim 12$ cm	$\chi \to \pi + \pi^0$	10	7	7	24
3) electrons of various energies	$K_\beta \to e + ? + ?$	—	—	5	5
4) μ-mesons of various energies	$\varkappa \to \mu + ? + ?$	5	—	—	5
5) π-mesons of various energies	$\tau' \to \pi + \pi^0 + \pi^0$	6	—	—	6
+ 2 examples of K_ρ					

It will be convenient to discuss separately, for each mode of decay, the information provided by the measurements, and finally to try to estimate their true relative frequencies of occurrence in the stack. In the following sections, it should be borne in mind that the errors quoted for the estimated energy of emission of the secondary particles, and the mass value of the primaries deduced from them, correspond only to the experimental uncertainties in range, straggling and scattering; the averages may be displaced when the relations governing the conversion from range or scattering to energy are better known.

4. - Analysis of Measurements on particles decaying in different modes.

4·1. *The* K_μ*-mode.*

(i) Measurements on stopping secondaries (Class A). – The presence of the decay electron in each of the cases in which the secondary

μ-meson was brought to rest does not prove that all of these particles are positive. It is, however, in accord with the strong positive excess reported by the Ecole Polytechnique ([10]) from their Cloud Chamber experiment.

The sharpness of the range distribution (see Fig. 1-*A*) confirms the results of experiments with Wilson Chambers that the transformation is into two particles only, one charged and one neutral, the energy of the former being equal to ~ 150 MeV. We can therefore attribute these particles to the mode K_μ, and assume the transformation

$$(C) \qquad K_\mu \to \mu + \nu \,,$$

the evidence for the probable nature of the neutral particle being based on the results of experiments with Wilson Chambers.

The best estimate of the mean value of the range of the secondary particles is

$$R_\mu = (20.57 \pm 0.24) \text{ cm} \,,$$

($R_\mu = 79 \pm 0.9$ g/cm^2 of emulsion in our stack, density (3.84 ± 0.02) g/cm^3).

The error here is deduced from the individual experimental errors, increased by 3.3% due to straggling (see Appendix I). The spread of the seven determinations leads to an error on the mean of ± 0.24 cm.

The corresponding value of the energy at emission being

$$E_\mu = (154.8 \pm 1.7) \text{ MeV} \,,$$

the value of the mass of the parent particle, assuming the above mode of decay (*C*), is

$$M_{K_\mu} = (976 \pm 7) \text{ m}_e \,.$$

This value may be compared with the Wilson Chamber estimate of the mass of the particles decaying in the K_μ-mode, viz.

E.P. ([11])	(75.7 ± 1.7) g/cm^2	(941 ± 17) m$_e$,
M.I.T. ([8])	(76.5 ± 2.5) g/cm^2	(950 ± 15) m$_e$.

(ii) Measurement on non-stopping secondaries (Classes B and C). – As remarked previously, the value of the residual range at the point of exit of a particle from the stack, when it has been reduced to a comparatively low velocity, can be determined from scattering and ionisation measurements with a precision comparable with that obtained on stopping secondaries.

The mean value of the estimated range for the particles of class B is

$$R_\mu = (20.6 \pm 0.5) \text{ cm} .$$

The corresponding value of the energy at emission is

$$E_\mu = (155.3 \pm 3.1) \text{ MeV}$$

and of the mass of the primary particle,

$$M_{K_\mu} = (978 \pm 13) \text{ m}_e .$$

The information given by the shorter tracks of Class C is, of course, of a poorer quality. For this group, the estimated mean energy at emission is:

$$E_\mu = (153.2 \pm 4.5) \text{ MeV} ,$$

from which the mass of the primary is found to be

$$M_{K_\mu} = (970 \pm 18) \text{ m}_e .$$

The possibility that some of these secondaries are to be attributed to the $\varkappa$-mode is discussed in a later section.

4·2. *The χ-mode.*

(i) Measurements on stopping secondaries (Class A). Of the 10 secondary particles which came to rest in the stack and were identified as positively charged π-mesons by the typical π-μ-e-decay at the end of their range, 9 gave no evidence for nuclear interactions along the path, and one collided elastically with a proton. This last event (No. 48) is discussed in detail in the Pisa Conference Report ([2]).

The procedures used in measuring the ranges of the secondary π-mesons and in estimating errors, were similar to those already discussed; only one feature, peculiar to π-mesons, needs to be mentioned. The range of the π-meson formed in the χ-mode of decay is a considerable fraction of the average path-length traversed before making a nuclear collision. It is therefore to be expected that such collisions will frequently occur; in some cases, however, in which there is only a small angular deflection of the π-meson, and a small loss of energy, they may be difficult to detect. They will then contribute to the straggling to which a homogeneous beam of π-mesons is subject, and should lead to a

skewness in the range distribution of a group of homogeneous particles. Similar effects may occur for protons. For μ-mesons they are much less probable; the relative importance of electromagnetic interactions with nuclei is at present difficult to evaluate and no correction for them has been attempted.

The estimate of the mean range in the present stack of the nine secondary π-mesons of class A is:

$$R_\pi = (11.79 \pm 0.15) \text{ cm}\,; \qquad (R_\pi = 45.3 \text{ g/cm}^2),$$

including $3\,\%$ straggling. The spread of the nine determinations is 0.10 cm. The corresponding value of the energy is

$$E_\pi = (109.2 \pm 0.8) \text{ MeV}$$

and the mass of the parent particle

$$M_\chi = (969 \pm 3)\ m_e\,.$$

An independent estimate of the energy of emission can be obtained from the results of the measurements on event No. 48, already mentioned, for in this event, an evaluation of the energy can be made by two methods which involve very different regions of the range-energy curve. The two estimates of energy are (*a*) (107 ± 2) MeV, using the ranges of both the π-meson and proton; and (*b*) (107 ± 5) MeV, applying dynamical considerations and using only the range of the proton. These two estimates are in very good agreement, which is satisfactory in view of the fact that the value (*b*) depends on the range-energy relation only in a region where it is well established. Including this result, the mean energy at emission for the π-meson is found to be:

$$E_\pi = (109.1 \pm 0.7) \text{ MeV}$$

and the corresponding mass for the primary:

$$M_\chi = (968 \pm 3)\ m_e\,.$$

(ii) Measurements on secondaries π-mesons which do not come to rest in the stack (Classes B and C). – The seven incomplete secondaries for which an accurate estimate of the range could be obtained, all left the stack with a residual range, less than about 4 centimetres. The weighted mean value of the estimated range obtained from these tracks is:

$$R_\pi = (11.4 \pm 0.3) \text{ cm}\,,$$

with a corresponding value of the energy at emission:

$$E_\pi = (106.7 \pm 1.6) \text{ MeV},$$

and of mass,

$$M_\chi = (958 \pm 6)\ m_e .$$

Of the seven secondaries belonging to Class C, five produced nuclear interactions in flight (see Table II, C.2), which makes a total of 6 interactions of the π-meson secondaries in a path length of 205 cm, a result in good agreement with measurements of the interaction length for π-mesons in this energy interval (about 30 cm). In event No. 65, the track of the secondary particle appeared to stop in the central region of the emulsion without producing a star or any ionising particles. It is reasonable to attribute this event to the nuclear scattering of the π-meson with charge-exchange. The average path length of a π-meson in emulsion before such a process occurs, is (2230 ± 1290) cm ([22]). In one event No. 52, a pair of electrons originated at the point of decay of the heavy meson. The observations have been shown to be consistent with the two-body decay of the parent K-particle into a charged and neutral π-meson. The event provides the first evidence from photographic emulsions for the nature of the neutral particle, and it is the first example in which it is possible to identify both the charged and neutral secondary particles ([23]). The mean energy at emission of the particles of class C is found to be:

$$E_\pi = (114.7^{+}_{-} 4.8) \text{ MeV}$$

and the mass of the primary:

$$M_\chi = (989 \pm 20)\ m_e .$$

4·3. *The significance of the mass values deduced from the* K_μ *and* χ *groups.* – In the preceding sections, the masses of the primary particles have been deduced from the estimates of the energies at emission of the secondary particles, these in turn having been based on measurements of range and of multiple-scattering. It follows that the mass determinations are subject to the following uncertainties: 1) straggling in range, 2) undetected interactions, 3) uncertainty in the range-energy relation, and 4) uncertainty in the value of the scattering constant.

([22]) G. Puppi: *Suppl. Nuovo Cimento*, **11**, 438 (1954).
([23]) F. Anderson, G. Lawlor and T. E. Nevin: *Nuovo Cimento*, **2**, 608 (1955).

The uncertainty in the mass-values caused by 1) and 2) will be reduced when a large number of events have been measured, whereas errors due to 3) and 4) are systematic in nature. The extent to which the mass-values may

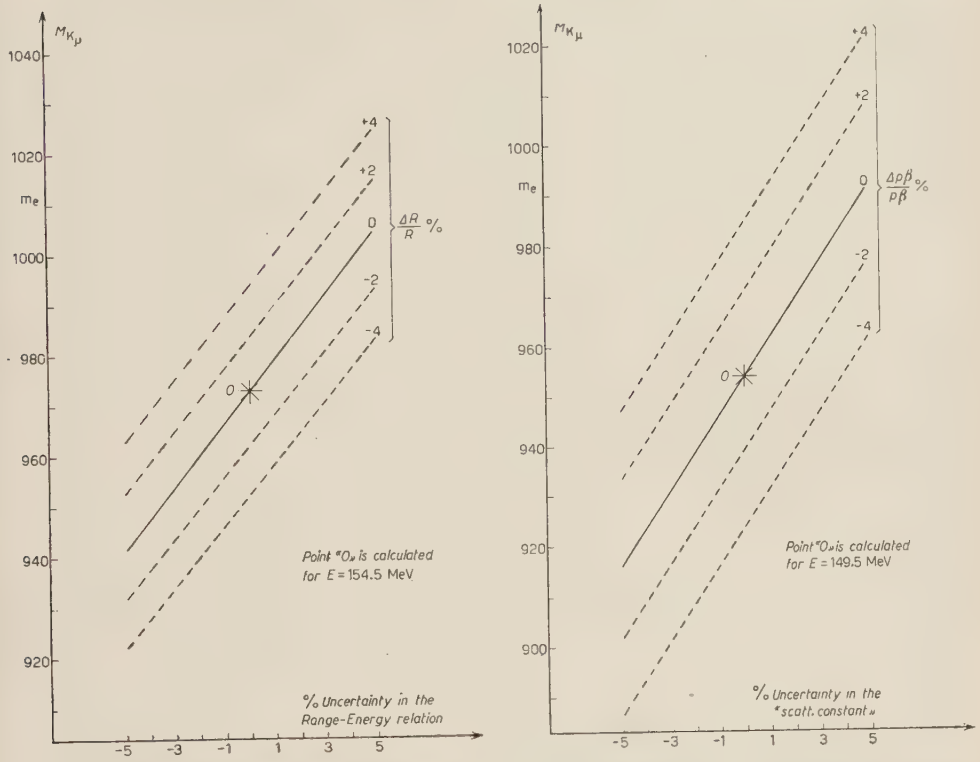

Fig. 3. – Effect on the mass deduced for the K_μ of variation of: *a*) the range-energy relation; *b*) the scattering constant.

change with corrections to the range-energy relation and the scattering constant is shown in Fig. 3 and 4.

4·4. *The χ-mode.* – As stated in [1] and [2], only a small percentage of the heavy mesons found in the stack can be attributed with confidence to the χ-mode of decay. Five unambiguous examples have been observed, in each of which the secondary reaches the end of its range after a few centimetres, and then decays to an electron (see Table II, A_3 and Fig. 1).

The nature of the two or more neutral particles which accompany the charged μ-meson are at present unknown, and the energy corresponding to the end-point of the μ-meson spectrum cannot, yet, be determined. If, for example, there are two neutral particles, both of small rest-mass, and if the mass of the primary particle is equal to that of the τ-meson, the end-point of the

spectrum should be nearly coincident with the unique energy from the K_μ-modet On the other hand, if one of the neutral particles were a π^0-meson, the end-poin. should occur at about 135 MeV. The probability of identifying a heavy meson

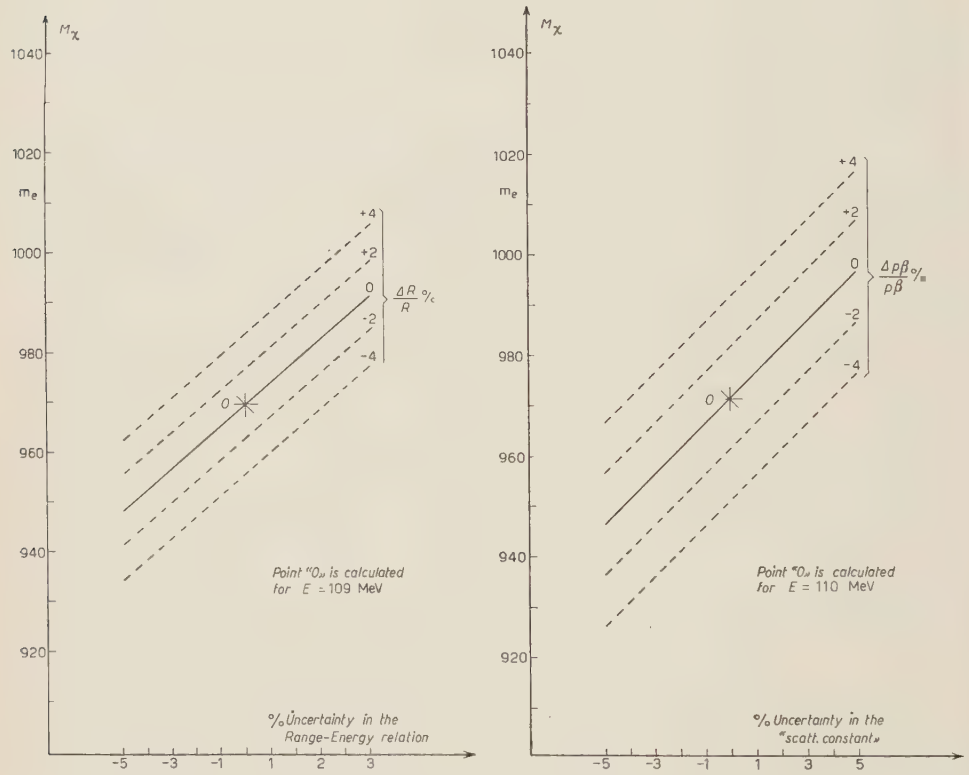

Fig. 4. – Effect on the mass deduced for the χ of variation of: *a*) the range-energy relation; *b*) the scattering constant.

which decays in the $\varkappa$-mode varies with the energy of the secondary μ-meson, and ambiguities can arise when this energy is either high or low.

The particles of class A in our stack, of energy greater than 100 MeV, seem all to belong to the χ- and K_μ-modes. In particular, there is no stopping secondary μ-meson in this energy region which cannot be attributed to the K_μ-mode. On the other hand the spread of the values of $p\beta$ obtained on the short tracks of class C could cover a possible contamination of secondaries other than those of the K_μ or χ. Our results do not therefore give reliable information about the upper limit of the energy-spectrum of the $\varkappa$-mode, except that it is certainly not less than ~ 55 MeV.

The identification of a μ-secondary from the $\varkappa$-mode may also be difficult at the low-energy end of the spectrum, because of the possibility of confusion

with π-mesons arising from the decay or capture of negative K-mesons. Possible sources of ambiguity are:

1) If a π^+-meson secondary arising from the decay of a K-particle dips steeply as it nears the end of its range, its subsequent decay to a μ-meson may pass undetected. The event will then simulate the direct decay of a K-particle to a μ-meson. Event no. 66 offered such an ambiguity. Although at emission, the track was flat, it dipped steeply at a point 5 millimetres from the end of the range. The track was long enough for ionisation measurements to be made on the initial flat portion of the track, and it could be proved that it was in fact due to a μ-meson; in other similar events a decision may not always be possible.

2) A negative K-meson may give rise either through decay or capture to a π^--meson which in its turn suffers nuclear capture without giving a visible star. Such an event would be difficult to distinguish from a $\varkappa$-decay, $\varkappa \to \mu \to e$, in which the track of the final electron escapes observation, or a negative $\varkappa$-decay. Of the two events of this type observed in the G-stack, Table II A6, the track of one secondary (79) was long enough to permit the identification of the particle as a π-meson with certainty; the other (80) is described as a « probable π-meson », the length of the track (2.8 mm) being insufficient for unambiguous identification.

Apart from these difficulties of interpretation, there is a considerable bias inherent in the selection of $\varkappa$-events, the method of search tending to favour the observation of the slower secondaries; a smaller fraction of the faster particles will be arrested in the stack or will produce a track long enough to permit reliable measurements. Furthermore, in principle, the faster secondaries are less likely to be seen because of the lower grain-density in their tracks. Allowing for these features, we may conclude that

1) Particles decaying in the $\varkappa$-mode constitute only a small fraction of the heavy mesons observed in nuclear emulsions, in the present conditions.

2) μ-meson secondaries from the $\varkappa$-mode with energies above 55 MeV are infrequent compared with those of lower energy.

4·5. *The* K_β*-mode.* – The unambiguous identification of the β-decay of a heavy meson may be carried out, if the track of the secondary electron is long enough, either (*a*) by demonstrating that the mass of the secondary particle is less than that of an L- meson; this may be done by ionisation and scattering measurements, if the value of $p\beta c < 80$ MeV; or (*b*), and more securely, by observing the loss of energy of the secondary particle due to bremsstrahlung or « knock-on » processes along the track.

Of the five examples of the K_β mode found in the G-stack, three have been

identified by observing bremsstrahlung loss, the fourth is very slow, and the fifth was identified by ionisation and scattering measurements (Table II, C_4 and Fig. 1-*C*).

In Fig. 5, the values of the energy of the secondary electrons are plotted together with those previously reported.

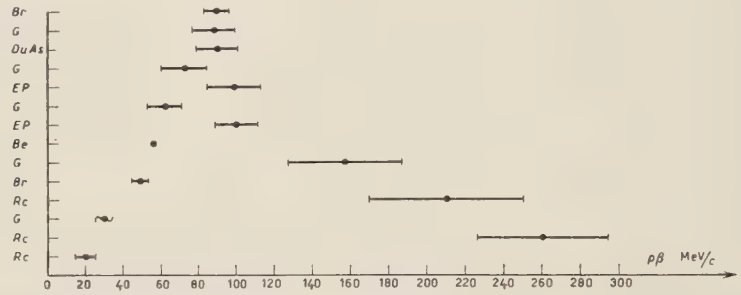

Fig. 5. – Distribution in $p\beta$ of the electron secondaries arising from the K_β decay mode.

Bek: Berkeley group, *5th Annual Rochester Conference* (1955).
Br: Reference (14) and (15).
Du: Reference (14).
EP: J. Crussard, V. Fouché, G. Kayas, L. Leprince Ringuet, D. Morellet, F. Renard and J. Trembley: *Proceedings Pisa Conference* (1955), p. 175.
Rc: M. F. Kaplon, J. Klarmann and G. Yekutieli: *Phys. Rev.*, **99**, 1528 (1955).
G: Present experiment.

The histogram gives only a very rough indication of the energy-spectrum due to this mode of decay. Apart from the fact that the number of events is small, the measured values of the energy will tend to be less than the true values at emission, as a result of bremsstrahlung loss. The problem of determining the energy-spectrum of electrons arising in the K_β-mode is analogous to that already met in experiments on the β-decay of μ-mesons; in the K_β-mode it is more serious because of the higher energies of the decay electrons. The correction for radiation loss can only be made on a large sample of events.

There may also be a considerable bias in the selection of the events. A deficiency of secondary electrons of low energy, for example, may be due to the fact that for very low values of $p\beta c$ (~ 30 MeV), it is frequently difficult to establish the association between the end of the track of the heavy meson and the beginning of that of the electron, due to the usually heavy background of slow electrons. Whenever a possible example of the K_β-mode was observed, the region round the point of decay was carefully examined by different observers before the electron was accepted as coming from that point and from no other. The presence of electron background also increases

the difficulty of following an electron without ambiguity from plate to plate through the stack. For this reason, the fast electron secondaries found in the G-stack were followed three times by different observers in order to be completely sure that no error in following had been made.

An the higher energies, electrons and L-mesons cannot be distinguished by ionisation-scattering measurements. The electronic nature of a particle producing a track must then be established by observing energy-loss due to bremsstrahlung and this requires a relatively long track on which scattering measurements can be made (see e. g. Table II, C4.). Many fast electrons, with shorter tracks, may therefore be overlooked, and there will be a tendency to underestimate the intensity of high-energy electrons in the spectrum.

In experiments with the cosmic radiation, it is possible that an observed heavy meson is in fact negative and that the associated electron is not due to a decay process. In the atomic capture of a K^--meson, for example, Auger electrons may be produced, as in the capture of π^- and μ-mesons; electrons can also arise from the β-decay of a product nucleus following nuclear capture. In such processes, the nuclear interaction of the K^--meson will commonly lead to the ejection of heavy charged particles and the ambiguity then does not arise. Occasionally, however, such heavy particles may all be neutral. It appears very unlikely that electrons produced in such processes could be of energy greater than 10 MeV. Difficulties of this type should not arise in experiments with artificially produced heavy mesons which have been magnetically analyzed.

4·6. *The τ' mode.* – Of the π-meson secondaries of energy distinct from that of the χ group, none has energy greater than 45 MeV (see table II, A_5). These slow π-mesons can therefore all be attributed to the τ'-decay mode.

Since attention was concentrated on the K-particles with a single charged secondary, and small stars were not examined in detail, there was probably a loss of τ-events. Thus no reliable information can be extracted from our results on the ratio of the number of τ' to τ-decays. The value obtained, $N(\tau')/N(\tau) = 6/30$, is presumably an overestimate of the true proportion of mesons decaying in the τ'-mode.

4·7. *Relative frequencies of different modes of decay.* – As remarked in § **1**, studies of the relative frequencies of occurrence of the various modes of decay in different experimental conditions could give an indication of the presence of particles with different lifetimes or different modes of production, and thence provide a proof of the existence of different types of K-mesons. For this purpose, it would be advantageous to employ experimental conditions differing from one another as widely as possible.

At the present time, the three most important types of experiment which

would permit a comparison of relative frequencies would appear to be: (*a*) Studies of S-particles of the cosmic radiation made with Wilson chambers; (*b*) experiments in which K-mesons, generated artificially by bombarding a target with energetic beams of protons, are allowed to enter a stack; and (*c*) experiments with large stacks within which the K-mesons are produced, either by exposure to cosmic radiation, or to beams of artificially accelerated protons or π-mesons.

Of the above experiments, (*b*) and (*c*) both employ the photographic method of detection and appear to give the best conditions for identifying some of the rarer modes of decay. The different times of flight in the two conditions, and the possibility thus provided of detecting a change in relative frequencies if some of the K-mesons have lifetimes shorter than $\sim 5 \cdot 10^{-9}$ s and greater than $\sim 3 \cdot 10^{-10}$ s have already been discussed. In addition, in the cosmic-ray experiments, the parent disintegrations are produced by particles of different types, varying widely in energy, so that the mode of production is substantially different from that in experiments with machines.

The most important disadvantage of the G-stack for such investigations is that the heavy mesons are distributed at random within it and must be distinguished from a background due to large numbers of protons and other particles. In these circumstances, the efficiency with which different modes of decay are detected is not the same.

The first task was to accumulate a sufficient number of K-mesons sufficiently well measured to allow a clear and unbiased separation into the different modes of decay. This involved rapid searching of large areas of the plates, and a corresponding decrease in the efficiency of detecting the less obvious events. It provided tracks in sufficient numbers, however, to allow estimates to be made of the relative frequencies of occurrence of even the rarer modes of decay. In analysing the results, those tracks which were not found in the systematic scanning of the plates—either by following out tracks from parent stars, or by random scanning—and those which failed to obey certain geometrical criteria, were excluded from the statistics. Table IV, col. 1, gives the distribution of the remainder among the various modes of decay. They were found in a total volume of 304 cm^3 of emulsion.

The results show that the K_μ and χ-modes constitute about 80 % of the total, the K_μ being certainly more numerous than the χ. Thus far there is no large discrepancy between these results and those obtained from S-events in the large multi-plate chambers, ([8,11]) and from machine exposures to K-particles ([24]).

([21]) *Mimeographed Report of the Pisa Conference* 1955; p. 161: W. W. Chupp, S. Goldhaber, G. Goldhaber and F. Webb; p. 175: J. Crussard, V. Fouché, G. Kayas, L. Leprince Ringuet, D. Morellet, F. Renard and J. Trembley; p. 195: D. M. Ritson, A. Persner, S. C. Fung, M. Widgoff, G. T. Zorn, S. Goldhaber and G. Goldhaber.

The ratio $N(K_\mu)/N(\chi)$ is low, but, as we shall see, this can be accounted for by the effect of scanning loss.

Although there is no bias in the selection and measurement of the 54 events on which Table IV is based, there was undoubtedly a bias in the recognition of the 324 events, from which they are chosen, owing to differences in the efficiency of finding examples of the different modes of decay.

The method of estimating the extent of the scanning loss, and its effect on the relative frequencies of the decay modes, is described in Appendix III. As can be seen from Table IV, columns 2 and 3, the corrections are considerable. The methods of estimation are only approximate and the corrected values given in Table IV should be taken only as an indication of the extent to which deficiencies in the methods of search can influence the values of the relative frequencies and not as an accurate determination of these values.

Table IV.

Mode	1		2	3	
	No. found	Percentage	Number corrected for loss of secondaries	Number corrected for loss of primaries and secondaries	Percentage
K_μ	27	50	75	105	67 (68) (*)
χ	17	32	22	31	20 (20) (*)
K_β	5	9	10	14	9 (9) (*)
$\varkappa$	4	7	4	5 (4) (*)	3 (2.5) (*)
τ'	1	2	1	2 (1) (*)	1 (0.5) (*)

(*) Supposing χ and τ' unaffected by loss of primaries (see Appendix III).

In spite of these reservations, however, we may conclude that in the conditions of our experiment:

1) more than 50%, and probably not more than 70% of the arrested K-mesons decay in the mode K_μ;

2) the proportion decaying in the χ-mode is less than 30% and probably greater than 15%;

(3) the modes K_β, $\varkappa$ and τ' constitute about 9%, 3% and 1% respectively, of the K-mesons;

4) the ratio $N(K_\mu)/N(\chi)$ is increased from an observed value of 1.6 to 3.4 as a result of corrections for scanning loss. The true value could perhaps be as large as 4.5 but probably not more.

The statistical weight of the present observations is not sufficient to permit us to attempt to detect any variation in the relative frequencies of the various modes in different parts of the stack. Reference to Table II shows that most of the particles which produce the parent stars from which the K-mesons emerge are locally produced in the stack, and of mean energy ~ 100 MeV. A variation in the nature of the K-mesons originating near the outer regions of the stack and those from the interior is not inconceivable if the character of the parent particle is an important determining factor in the mode of production.

5. – Conclusion.

The present results show that a large enough stack of nuclear emulsions is capable of giving unambiguous and rather precise information on the nature of the K-particle secondaries and on the energy with which they are emitted. The G-stack has led to the following conclusions:

1) The existence of two monoenergetic groups of secondaries, one of μ-mesons from the K_μ-mode and one of π-mesons from the χ-mode, has been confirmed. It has further been shown that, in nuclear emulsions as in multiplate cloud chambers, these two groups constitute the greater part of the K-particle secondaries.

2) The estimates of mass of the parent particles, based on the dynamics

TABLE VII.

Decay Mode	Distribution in Energy of the charged secondary	Mass of primary (×)	Frequency
$K_\mu \to \mu + \nu$	line spectrum at $E = \begin{cases} 155 \pm 1.4 & (*) \\ 150 \pm 4 & (+) \end{cases}$	$\begin{cases} 977 \pm 6 (*) \\ 954 \pm 17 (+) \end{cases}$	50-70%
$\chi \to \pi + \pi^0$	line spectrum at $E = \begin{cases} 109 \pm 1 & (*) \\ 110 \pm 4 & (+) \end{cases}$	$\begin{cases} 966 \pm 3 (*) \\ 972 \pm 15 (+) \end{cases}$	15-30%
$K_\beta \to e + ? + ?$	continuous up to ? MeV, highest observed energy in this stack: $(157 \pm \pm 30)$ MeV	—	$\sim$ 9%
$\varkappa \to \mu + ? + ?$	continuous up to ? MeV, highest observed energy in this stack: 55 MeV	—	$\sim$ 3%
$\tau' \to \pi + \pi^0 + \pi^0$	continuous up to ? MeV, highest observed energy in this stack: 45 MeV	—	$\sim$ 1%

(×) Deduced from the energy of the charged secondary.
(*) From range and extrapolated range (classes A, and B),
(+) From scattering measurements near the decay point (classes) A, B and C).

of the two-body decay show a mass value close to that of the τ-meson. The precision is not however such as to exclude differences of as much as 20 m_e.

3) While the energy spectra of the $\varkappa$ and K_β-decay modes are still undefined, the method of their identification having been found satisfactory, their determination remains only a matter of time.

Table VII summarizes the available information on the various modes of decay.

* * *

For the quality of the stack, the care in its preparation, and the important and detailed information concerning its composition, our sincere gratitude is due to Mr. WALLER and his colleagues of Ilford Ltd.

The organisation of the flight and its successful outcome would have been impossible but for the generous and tireless help of the airport authorities and personnel, the meteorological services and the observation posts of the wide visual and radio network. It is therefore with very great pleasure that we take this opportunity of thanking all these who took part in, or made possible, the 1954 flights in the Po Valley. In particular we mention:

the Ispettorato Generale Telecomunicazioni e Assistenza Voli, Ministero Difesa Aeronautica; the Ispettorato Generale Superiore delle Telecomunicazioni, Ministero delle Poste e Telecomunicazioni; the Comando I and II Z.A.T., the Comandi Aeroporti di Linate, Novi Ligure and Padova, the Stazione Radiosonda di Linate, of the Italian Air Force; the Comando Militare Territoriale di Milano, Stato Maggiore, the III Battaglione Trasmissioni Genio Militare Territoriale; the Comandi Dipartimenti Marittimi Alto Tirreno and Alto Adriatico of the Italian Navy; the Direzione O.S.S.M.A., Aeroporto Elmas, the Direzione O.S.S.M.E.A., Verona, the Comando Porto di Genova, the Legione Territoriale C.C. di Parma, the R.A.I. Televisione Monte Penice, S. E. il Vescovo di Bobbio, the Direzione Relazioni Culturali con l'Estero, Ministero degli Affari Esteri, the Centro Francese Studi e Informazioni di Milano, the italian radio-amateurs.

To the scanning teams and technicians of all the collaborating laboratories, we express our gratitude and appreciation of their loyal and enthusiastic cooperation.

Among our Colleagues, who assisted us in various parts of our work and tried to help us improve its quality, we note in particular: Prof. P. CALDIROLA, Prof. N. DALLAPORTA, Dr. H. HEITLER, Prof. C. PEYROU, Prof. G. POLVANI, Prof. A. ROSTAGNI, and Prof. R. W. THOMPSON.

We are indebted for maintenance grant and scholarships of various members of the groups to the Board of the School of Cosmic Physics, Dublin; the De-

partment of Scientific and Industrial Research, the National University of Ireland and the Royal Commission for the Exhibition of 1851.

We are glad to express our warmest thanks to the Gruppo degli Amici dell'Istituto di Scienze Fisiche dell'Università di Milano for financial support, and encouragement.

Appendix I

Methods of estimating, and correcting for, errors in the measurement of range.

(1) *Corrosion and Development Gradient.* – The grains of an emulsion can be eaten away during processing down to a depth of a few microns below the surface. When this occurs, the surface itself remains visible, due to the specks of dirt adhering to it, and dense tracks are thinned down, but still, visible at the surface. On the other hand, tracks of low grain-density may disappear before the surface is reached. Under-development near the glass, and pressure or other markings at the glass-emulsion interface, may result in poor visibility and consequent difficulties of observation. In making measurements on a thin track, its direction as it nears the surface or the glass may be determined and its true length estimated by an extrapolation to the bounding surface

Such extrapolations have been made by several observers in each laboratory, and the reading errors introduced, expressed as a statistical effect, were found to be 0.5%.

(2) *Fluctuations in Thickness of the Emulsion strips.* – After drying, the emulsions were kept in conditions of uniform humidity using as standards the strips which had been weighed before processing. The original average thickness throughout the stack was 605 μm, and the standard deviation of the distribution of thicknesses 1.4 μm. The use of a mean emulsion thickness in computing ranges induces a statistical error which is certainly less than 0.1 %.

(3) *Abrasion.* – After processing, most of the plates had a thin silver layer obscuring the surface. A light abrasive was necessary to remove this and it was possible therefore that a thin layer of emulsion was also removed. Since this would reduce the ranges systematically, an attempt was made to determine its magnitude in the following manner: 212 μ-mesons contained in single emulsions, and 104 crossing from one strip to another,—all of them arising from the decay at rest of positive π-mesons—were chosen and their ranges were measured. From the differences in the two cases it would appear that, during exposure, an amount of material equivalent to 6 or 7 μm of emulsion lay between the surfaces of the emulsions as we see them now. Of this, about 5 μm corresponds to the tissue paper spacers whilst the remainder, 1 or 2 μm, is the amount removed from the emulsion surface during abrasion. The error on this value is ± 2 μm. The effects of abrasion can therefore be neglected.

(4) *Distortion.* – Even if random in direction in the various plates of a stack, distortion will, on the average, produce a small systematic increase in the total range. Measurements made in the present stack show that the distortion is of a fairly regular character and may be represented adequately by means of first and second order distortion vectors. We have measured the magnitude and direction of the second order distortion vectors on a large sample of tracks at various positions in the stack, and have found values ranging from 15 μm in the central regions to 40 μm at about 2 cm from the edge. The spacial distribution of the vectors was found to show a small degree of anisotropy with a preferred direction parallel to the long edges of the strips, the magnitude of the component in this direction being about 10 μm.

The determination of the first order distortion is much more laborious and has been carried out by two independent methods: (i) based on the anisotropy in the angular distribution of α-particles arising from the radioactive decay of thorium nuclei in the emulsion and, (ii) by measuring steep straight tracks passing through several emulsions. The first order distortion vector appears to have a magnitude approximately three times that of the second order and to be in a direction opposite to that of the latter. It follows that the total correction to the range would be of opposite sign to that given by a consideration of the second order distortion alone.

The corrections for distortion and estimation of errors arising from it have been carried out as follows: The ranges have been corrected for the component of the distortion parallel to the long edges of the strips. The geometrical distribution of the stopping secondaries is such that, in our opinion, this is the only correction necessary to avoid systematic errors in the average value of the range. The contribution of distortion to the error on the range is considered to be $(\pm 20n)$ μm where « n » is the number of emulsion strips traversed by the particle. This error takes into account the fact that no correction has been applied for the distortion vector acting in the direction perpendicular to the long edges. We have assumed that this vector acts in the same sense on the various sections of track in the separate emulsion strips. This is certainly not true, since there exists a certain degree of randomness in its distribution through the stack. The error is thus probably an onverestimate for most of the tracks.

(5) *Approximation of the true track profile by a set of chords.* – Because of the numerous small deflections due to multiple Coulomb scattering, the standard method of approximating—for ease in measurement—the trajectory of a charged particle by a succession of chords, results in a slight underestimation of the length of a track. The correction to the measured range is very small; calculation shows it to be about 0.2 %.

(6) *Undetected Interactions.* – Energy losses may occur along the track which are too small to give a detectable change in scattering or ionisation, but will tend to shorten the range. In addition the occurrence of « inner bremsstrahlung », namely, radiation arising from the sudden acceleration of the charged secondary on its creation in the transformation will also make the observed straggling distribution skew towards shorter ranges. No correction can be made until more secondaries have been measured, when we may be able to determine the asymmetrical shape of the distribution.

(7) *Straggling.* – This has been calculated from the curve of BARKAS and YOUNG [25] normalized to fit the emulsion points of HEINZ [26] and of FRY and WHITE [27]. This uncertainty has been included in the error quoted on the mean values of range and on the energy.

APPENDIX II

Conventions on scattering techniques.

1. *Elimination of noise.* – All groups eliminated noise between two cell lengths but the choice of the cells varied between the various laboratories. In some microscopes the noise level could be considered constant for all cell lengths, in others, the variation of noise with cell length had to be taken into account.

2. *Choice of basic and multiple cell-length.* – This depends on the noise-level, distortion level, and the scattering of the track. The same choice was not made by all groups; for example, for the scattering at emission of the K_μ secondaries the cells generally used were:

Group	Basic cell	Multiple cell
Br and Ko	50 μm	150 μm
DuAS	100 μm	200 μm
DuUC	100 μm	300 μm or 200 μm
GeMi and Pd	50 μm	200 μm

3. *Cut-off.* – All used 4× mean cut-off, some simply, the others (Br and DuAS) with replacement, and a suitable correction to the scattering constant found by internal calibration.

4. *Scattering Constant.* – Two theoretical curves were used, that of GOTTSTEIN-MOLIÈRE [28] and that of VOYVODIC-PICKUP [29]. Internal calibration by two of the groups (Br and DuAS) indicated that the Molière curve should be increased by $(2.4 \pm 1.3)\%$ and $(3.4 \pm 1.3)\%$ respectively. An increase of 3.4% of the Molière curve brings it into coincidence with that of VOYVODIC and PICKUP. The final results are all standardised on the latter, and a 2% uncertainty included in the error as indicated by our own calibration, rather than the former 8% recommended by the Bureau of Standards [30].

---

[25] W. H. BARKAS, and L. YOUNG: *Phys. Rev.*, **98**, 605 (1955)

[26] O. HEINZ: *Phys. Rev.*, **94**, 1728 (1954).

[27] W. F. FRY, G. R. WHITE: *Phys. Rev.*, **90**, 207 (1953).

[28] K. GOTTSTEIN, M. G. K. MENON, J. H. MULVEY, C. O'CEALLAIGH and O. ROCHAT: *Phil. Mag.*, **42**, 708 (1951).

[29] L. VOYVODIC and E. PICKUP: *Phys. Rev.*, **85** 91 (1952).

[30] *Recommendations etc.*, in *Suppl. Nuovo Cimento*, **11**, 228 (1954); *Recommendations etc.*, in *Suppl. Nuovo Cimento*, **12**, 474 (1954).

5. *Elimination of Distortion.* – This is a much discussed and delicate problem. The measurements quoted in Appendix I showed the general level of *C*-shaped distortion to be low. There remains however a doubt that the crash of the stack after the parachute failure might have introduced some irregular, possibly wavy distortion. In fact chopping was detected in some parts of the stack. In such a case it may be expected that the third difference should not eliminate completely the distortion.

Some preliminary tests on this point indicated that, while the ratio $D'''/D''\sqrt{\frac{3}{2}}$ on the sections of tracks having dip less than 7° was lower than that found on fast tracks in Sardinia stacks and on glass-backed plates ((1.08 ± 0.01) by DuAS and (1.10 ± 0.01) by GeMi), the ratio $p\beta'''/p\beta''$ on sections of all tracks near the decay, was about one, when a correction factor (1.09 ± 0.01) was applied. The question of the efficiency of third differences to test the presence of irregular distortions is one which will be interesting to investigate in later work. For the time being, it must simply be borne in mind that our results obtained by scattering at the higher energies are subject, not only to the 2% uncertainty in the scattering constant, but also to the validity of the application of the factor (1.09 ± 0.01) in a stack which has been subject to some mechanical stress.

Appendix III

Estimation of scanning loss.

(a) *Events lost because of failure to observe the primary particle.* – Since the observed number of ending proton tracks was the same for all members of one group of observers, it is assumed that the number of K-particles lost through missing the primary is the same for all observers. A frequency distribution of the angles of dip of a random sample of 200 observed heavy mesons, showed a rapid decrease in the efficiency of detection for angles of dip of the primary greater than 53° in the unprocessed emulsion. This leads to a loss of about 30%.

At first sight, one might expect this source of loss to be independent of the nature of the secondary particle. It is possible however, that when a heavily dipping K-particle has a heavily ionizing secondary, as in the $\varkappa$ or τ'-modes, the secondary track may lead to the recognition of the event. These considerations were taken into account in making estimates of loss.

(b) *Events lost because of failure to observe the secondary track.* – Having observed a heavy particle coming to the end of its range, the observer may fail to distinguish the secondary track, especially if this has low grain-density. The observed density of K-particles per cm³ of emulsion varied considerably among different observers of the same group. Since the density of ending proton tracks is nearly constant, this «differential loss» must be attributed to a failure to detect some of the secondary particles.

A value for the efficiency of detection by different observers,—certainly an over-estimation—may be found by supposing the best observers to have

an efficiency of 100 %. The individual values were then found to vary widely, the overall efficiency of different groups varying from 30 to 60 %. It is assumed that this loss is due to a failure to observe the K_μ, χ and K_β modes and is negligible for the $\varkappa$ and τ'-modes.

(c) *Estimate of the effect of loss on the frequency of the groups.* – It is obvious that the lower the grain-density of a track, the easier it will be lost. The actual determining factor may be either the gap distribution or the size of the blobs in the track, but since both of these are functions of the grain-density, we will, for simplicity, take the latter as parameter in the following discussion.

The number of identified K-particle secondaries was too small to permit a significant test as to whether the relative frequency of the decay-modes varied according to the observer, transparency of the plate, and depth in the emulsion, as does the total scanning loss. We have supposed that it must do so, and have tried to estimate the possible magnitude of the effect by the following rough calculation.

The mean g^* of the K_μ, K_β and χ secondaries are respectively 0.96, 1.00, and 1.10. Estimating that, in general, the secondary track is recognized over the diameter of one field of view (300-500 μm), the fluctuations in grain-density over the section observed can be calculated. If we suppose that there exists a certain number of grains such that all sections of track containing more than this number are seen, and all containing less, are lost, then we can calculate, in function of this limiting number, what proportion of the totals is represented by the observed numbers of K_μ, K_β and χ secondaries respectively. Having estimated in (a) and (b) the total number of particles lost, we have clearly a unique value of this limiting number of grains and an estimate of the numbers of K_μ, K_β and χ in our emulsions.

SUMMARY

A large emulsion stack, exposed at high altitude, has been used to study the decay-modes of K-particles which produce a single charged secondary. The 5 decay modes, K_μ, χ, $\varkappa$, K_β and τ' have been recognized from the nature and energy of the charged secondary. The masses of the parent particles of the two-body decay modes, K_μ and χ found from the mean range of the charged secondary are $(976 \pm 7)\ m_e$ and $(969 \pm 3)\ m_e$ respectively. Independent values derived from measurements of the scattering of the secondary track near the decay point are $(954 \pm 17)\ m_e$ and $(972 \pm 15)\ m_e$ respectively. The reliability of these mass values is discussed. An examination of the relative frequency of the decay modes in these experimental conditions indicates that the K_μ- and χ-modes constitute respectively about 67 % and 20 % of all the K-particle decays: the K_β, $\varkappa$- and τ'-modes being present to about 9 %, 3 %, and 1 % respectively.

RIASSUNTO

Un pacco di emulsioni nucleari di grandi dimensioni, esposto ad alta quota alla radiazione cosmica, è stato impiegato per studiare i modi di decadimento delle particelle K che producono un unico secondario carico. I 5 modi di decadimento K_μ, χ, $\varkappa$, K_β e τ' sono stati riconosciuti dalla natura ed energia del secondario carico. I valori della massa delle particelle primarie per i modi di decadimento (in due corpi) K_μ e χ, ottenuti dalla misura del percorso del secondario carico sono $(976 \pm 7)\ m_e$ e $(969 \pm 3)\ m_e$ rispettivamente; valori indipendenti, dedotti dalla misura della diffusione multipla della traccia dei secondari, nelle vicinanze del punto di decadimento, sono rispettivamente $(954 \pm 17)\ m_e$ e $(972 \pm 15)\ m_e$. Viene discussa l'attendibilità di questi valori. Un esame delle frequenze relative dei vari modi di decadimento nelle condizioni sperimentali della presente ricerca indica che i modi K_μ e χ costituiscono rispettivamente circa il 67 % e il 20 % di tutti i decadimenti di particelle K, il K_β, $\varkappa$ e τ' sono presenti per circa il 9 %, 3 % e 1 % rispettivamente.

Observations des émulsions nucléaires en lumière réfléchie.

R. RECHENMANN (*)

Laboratoire de Physique Corpusculaire de l'Université de Strasbourg

(ricevuto il 1° Agosto 1955)

Resumé. — On indique une méthode de coulée et de développement d'émulsions nucléaires sur supports opaques pour l'observation en lumière réfléchie. Cette méthode est utilisée pour l'étude d'un granit du Monte Capanne. Après développement, l'observation au microscope Leitz « Orthoplux » muni d'un dispositif « ultropak » permet de localiser et de compter les trajectoires de particules α émises par les minéraux.

L'utilisation des émulsions nucléaires liquides (émulsion Ilford « in gel form ») présentent un progrès considérable dans les techniques autoradiographiques basées sur l'observation des trajectoires individuelles.

Dans les applications biologiques [1], géologiques [2], ou autres [3], déjà publiées, cette méthode a été limitée à l'étude d'obejts transparents pouvant être observés par transmission au microscope.

Nous avons eu à étudier la distribution des inclusions radioactives et l'estimation de leur activité α sur des sections planes d'échantillons de granit. La surface d'une section étant de plus de 20 cm², il aurait fallu tailler un grand nombre de lames minces pour l'observation en lumière transmise; aussi avons-nous tenté de couler l'émulsion directement sur les blocs de granit et d'observer simultanément la surface du granit et l'émulsion en lumière réfléchie.

Les résultats ayant donné satisfaction, il nous a semblé utile de décrire la technique employée.

(*) En congé de l'Institut de Physique de l'Université de Strasbourg.

(1) P. CÜER, C. M. GROS et R. RECHENMANN: *Journ. de Phys. et Rad.*, **13**, 59 (1952); F. GAVOSTO et A. FICQ: *Ann. Inst. Pasteur*, **86**, n,3, 320 (1954); J. VIVIEN et R. RECHENMANN: *Compt. Rend. Soc. de Biol.*, **168**, 170 (1953).

(2) FORD: *Nature*, **167**, 273 (1951); M. R. PICCIOTTO: *Bull. du Centre de Phys. Nucl. de l'Univ. de Bruxelles*, n. 33 (1952).

(3) A. BONETTI et G. P. S. OCCHIALINI: *Nuovo Cimento*, **8**, 725 (1951); M. REINHARZ et G. VANDERHAEGHE: *Nuovo Cimento*, **12**, 243 (1954).

Fig. 1. – Grande plage active de sphène. Les α sont distribués d'une façon homogène. Objectif à sec Leitz « Ultropak » 11 fois. Échelle = 50 μm.

Fig. 2. – Inclusion active très réfringente dans une plage de quartz. On distingue nettement les α brillants sur fond noir. Objectif à immersion Leitz « Ultropak ». 75 fois. Échelle = 50 μm.

Photographies réalisées au Laboratoire de Physique Corpuscolaire de Strasbourg.

a) *Coulée.* - Pour faciliter l'adhérence de l'émulsion, on commence par recouvrir la surface portée à une température de 30° avec un substratum de gélatine d'une épaisseur de l'ordre du micron par coulée d'une solution composée comme suit:

— 100 cm³ d'eau;

— 0.5 g de gélatine pure;

— 0.2 g d'alun de chrome.

Après séchage, on coule de l'émulsion Ilford C2 « in gel form » refondue à 50 °C sur la roche portée à une température d'environ 26 °C. L'émulsion est ensuite séchée deux heures dans un séchoir à gradient de température et atmosphère d'azote. La couche d'émulsion séchée a une épaisseur de 50 μm.

b) La roche avec sa couche d'émulsion est gardée à une température de 5 °C.

c) *Développement.* - Dure 20 min à une température de 16 °C dans un révélateur à l'amidol ayant la composition suivante (4):

— H_2O 1000 cm³;

— 35 g d'acide borique;

— 18 g de sulfite de sodium;

— solution de bromure de potassium à 10%, 8 cm³;

— 4.5 g d'amidol.

L'échantillon est ensuite lavé à l'eau courante pendant 10 min, puis fixé dans un bain contenant 40% d'hyposulfite de sodium et 5% de sulfate de sodium. Après éclaircissement, on dilue progressivement le bain d'hyposulfite avec une solution aqueuse à 5% de sulfate de soude. La roche après 20 min additionnelles dans cette dernière solution est rincée à l'eau courante. On n'a observé aucun décollement de l'émulsion pendant toute la durée de ces opérations.

Après séchage, l'observation en lumière réfléchie est faite au microscope Leitz-Ortholux, muni de l'équipement « Ultropak ». Des inclusions microscopiques et les traces des particules α et des électrons sont nettement visibles à à des grossissements allant de 100 à 500 fois (voir photos).

On a fait un essai avec deux blocs de granit du Monte Capanne (Ile d'Elbe). L'examen en lumière réfléchie ne permet pas une étude minéralogique détaillée de la roche, mais il a été facile d'identifier les minéraux essentials: quartz, feldspath, biotite, et la plupart des accessoires opaques ou transparents.

D'autre part les particules α émises par les minéraux sont facilement reconnaissables et dénombrables (voir photos).

(4) C. C. Dilworth, G. P. S. Occhialini et L. Vermaesen: *Bull. Centre Phys. Nucl. Uni. Bruxelles*, part I, n. 13*a*, Février 1950).

* * *

Ce travail a été effectué au Laboratoire de Physique Nucléaire de l'Université Libre de Bruxelles sous la direction de M. R. Picciotto.

Je remercie l'Office des Relations Culturelles franco-belges pour la bourse d'études qui m'a permis de mener à bien ce travail. Je tiens également à remercier tous les membres du Laboratoire pour l'aide et les conseils dont ils m'ont toujours fait bénéficier au cours de mon séjour.

RIASSUNTO (*)

Si descrive un metodo per la colata e lo sviluppo di emulsioni nucleari su supporti opachi per l'osservazione in luce riflessa. Si utilizza il metodo per lo studio di un granito del Monte Capanne. Dopo sviluppo, l'osservazione al microscopio Leitz « Ortholux », munito di dispositivo « ultropak » permette di localizzare e contare le traiettorie delle particelle α emesse dai minerali.

(*) *Traduzione a cura della Redazione.*

LETTERE ALLA REDAZIONE

(La responsabilità scientifica degli scritti inseriti in questa rubrica è completamente lasciata dalla Direzione del periodico ai singoli autori)

Disappearence of Adsorbed Gases from Dielectric Surfaces Under Electrodeless Discharge.

S. R. Mohanti

Physico-Chemical Laboratories, Banaras Hindu University, India

(ricevuto il 12 Settembre 1955)

The author [1] has shown that the threshold potential [2,3] V_m of the self-maintained A.C. electrodeless discharge through electronegative gases and vapours is lowered under continued excitation at applied potential $V > V_m$. This has been ascribed to diminution, through disappearence of the adsorbed gas layer(s) by desorption or/and chemical interaction, of the work function φ of the (instantaneous) cathode surface on which the antecedent half cycle had deposited the residual (i.e., unneutralized) electrons [4]. The current i of the self-maintained discharge is given fairly accurately by [5,6]

$$(1) \qquad i = i_0 \frac{(\alpha - \beta) \exp [(\alpha - \beta)x]}{\alpha - \beta \exp [(\alpha - \beta)x]},$$

$$(2) \qquad i = i_0 \frac{\exp [\alpha x]}{1 - \gamma (\exp [\alpha x] - 1)}$$

and

$$(3) \qquad i = i_0 \frac{\alpha \exp [\alpha x]}{\alpha - \eta\theta g \{\exp [(\alpha - \mu)x] - 1\}}$$

where i_0 is the primary current, α and β the (Townsend) coefficients for impact ionization by electrons and positive ions, γ and $\eta\theta g$ those for cathodic electron emission by respectively positive ion and photon bombardment (θ is the number of photons produced by an electron per cm in the field direction, η the fraction of the photons which produce electrons that succeed in leaving the cathode and g a geometrical factor signifying the fraction of photons created in the gas which reach the cathode), μ the absorption coefficient of the photons in the gas, and x the electrode separation. Progressive diminution in φ during discharge would entail an opposite change in the surface dependent γ and the $\eta\theta g$ processes and would therefore enhance i at constant V, as observed.

All-glass Siemens' tubes, chemically cleaned and degassed, contained pure oxygen at different (100-300 mm Hg, 28-30 °C) pressures (pO_2). The high tension and the low tension electrodes consisted, in each case, of a 10 per cent aqueous solution of sodium chloride inside the inner tube, and in a glass jacket

(1) S. R. Mohanty: *Journ. Chim. Phys.* (Under publication).

(2) S. S. Joshi: *Current Sci.*, **8**, 548 (1939).

(3) S. R. Mohanty: *Journ. Chem. Phys.*, **22**, 2095 (1954).

(4) S. R. Mohanty: *Zeits. f. Phys. Chem.* (Neue Folge), **4**, 233 (1955).

(5) L. B. Loeb: *Fundamental Processes of Electrical Discharge in Gases* (New York, 1939).

(6) J. M. Meek and J. D. Craggs: *Electrical Breakdown of Gases* (Oxford, 1953).

surrounding the outer tube (Fig. 1). This assembly was enclosed in another glass jacket through which thermostat water of temperature regulated to ± 0.05 °C was circulated. The gas was subjected to continuous discharge at a fixed V in the range 3-7 kV (r.m.s., 50 Hz) and i was measured at intervals of time (t) with a sensitive galvanometer (G) actuated by a Cambridge vacuum thermocouple (« Vacuo-junction », V.J.).

Fig. 2 which represents a typical set of results, obtained with a certain ozonizer (internal diameter of the outer tube, 17.2 mm; external diameter of the inner tube, 8.5 mm; electrode separation, 4.35 mm; thickness of the glass walls, 1.6 mm; length of the discharge column, 18.0 cm), $pO_2 = 265$ mm, 35.1 °C and 6.67 kV shows that i increases with t at first rapidly and then slowly; a constant maximum i_{max} is obtained on prolonged discharge. Thus, whilst the increase in i over the first 20 minutes of discharge

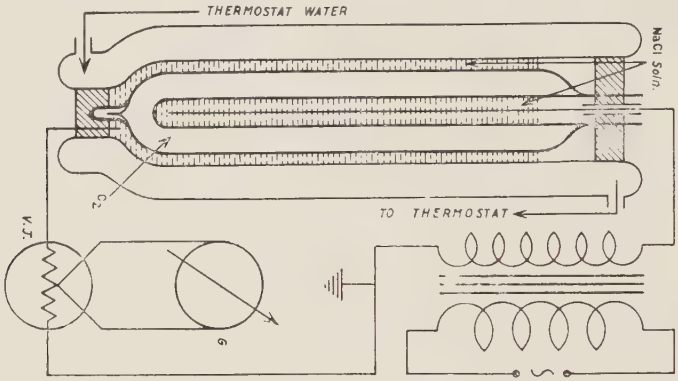

Fig. 1. Measurement of current under ozonizer excitation.

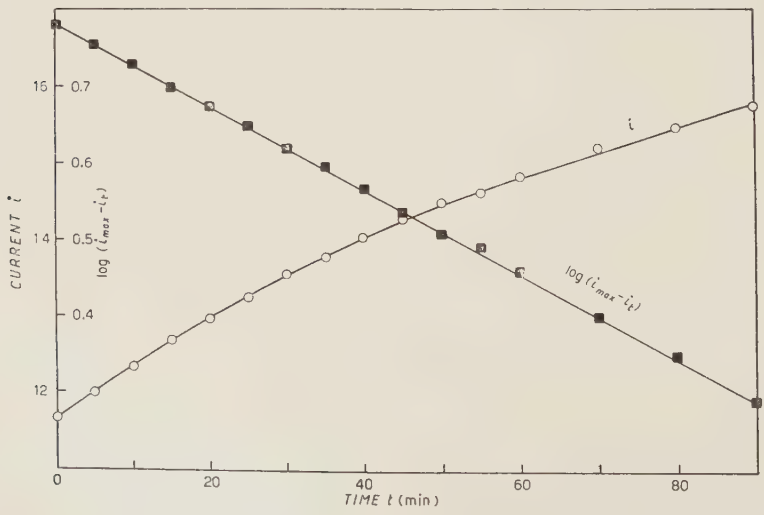

Fig. 2. Current as a function of the duration of discharge.

was 11.1 per cent of the value (11.66, arbitrary units) at initiation, that from 70th to 90th minute was only 3.6 per cent of the value at the lower t; i_{max} (17.66) was recorded in about 4 hours.

The data are representable accurately by the relationship

$$(4) \quad (i_{max} - i_t) = (i_{max} - i^0) \exp[-kt],$$

where i^0 and i_t are the values of i at commencement ($t = 0$) and at time t respectively, and k a constant; this is evident from the linearity of the $\log (i_{max} - i_t) - t$ graph (Fig. 2). The value of k calculated from the slope of the straight line is 0.0126 min^{-1}. It is significant that equation (4) is identical in form to that of the first order chemical reaction ([7,8]).

Further work on the energetics and the mechanism of the process is in progress, and will be published elsewhere.

* * *

Grateful thanks of the author are due to Professor S. S. Joshi for his kind interest in the work.

([7]) Cf. S. R. Mohanty: *Journ. Indian Chem. Soc.*, **28**, 487 (1951); *Journ. Chem. Phys.*, **21**, 1908 (1953).

([8]) Cf. S. R. Mohanty, T. D. Prasada Rao and R. Ramaiah: *Journ. Sci. Industr. Res.*, **13** B, 144 (1954).

Investigation of Magnetic Moments of Atomic Nuclei,

P. S. Faragó, M. Gécs and J. Mertz

Department of Electromagnetic Waves, Central Research Institute of Physics - Budapest

(ricevuto il 23 Settembre 1955)

In a recent review article [1] preliminary results of our measurements of the magnetic moments of ^{23}Na and ^{31}P were reported. Since the publication of those results considerable improvement was achieved as regards the reliability of our experiments.

The results given in our earlier paper are systematically smaller than the accepted values, the discrepancy being greater than the standard error, which itself is not much higher than is usual. The results were obtained by measuring simultaneously the resonance frequency of the unknown nuclei and of protons. Although the half width of the proton signals shows that the inhomogeneity of the magnetic field is very small over the region occupied by *one* sample, it was found, that the difference between the

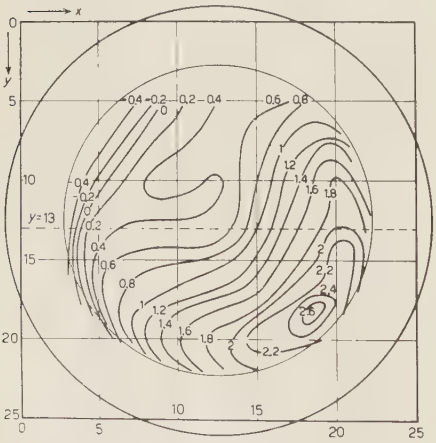

Fig. 1. – Lines of equal magnetic field intensity in a plane parallel to the pole faces of the electromagnet; x and y are measured in cm, parameters mean deviations of magnetic field in gauss from the average value $H_0 \sim 1650$ gauss.

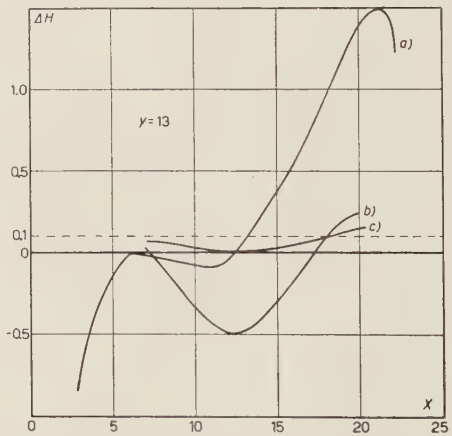

Fig. 2. – Variation of magnetic field along section $y = 13$ (shown in Fig. 1) as explained in the text.

[1] P. S. Faragó: *Suppl. Nuovo Cimento*, **1**, 249 (1955).

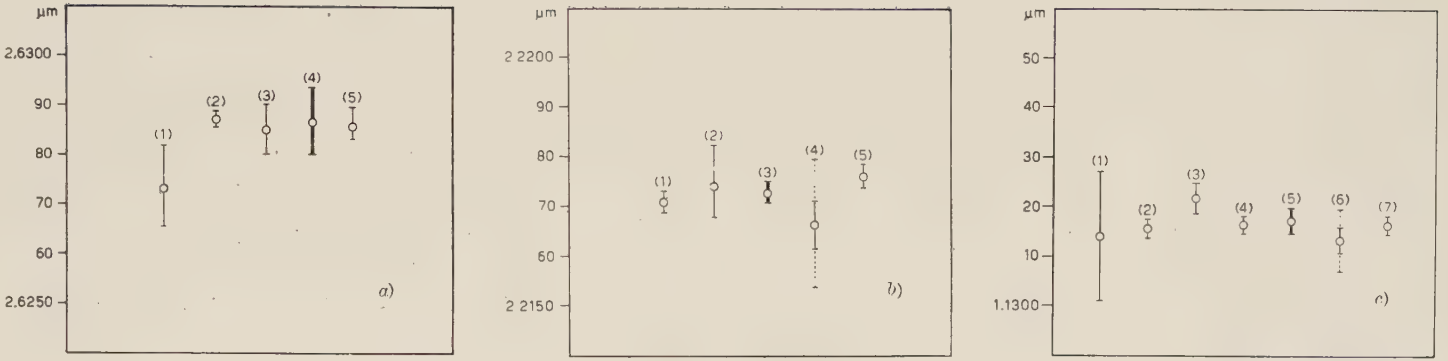

1) Poss, 1949.
2) Siegbahn and Lindström, 1949.
3) Zimmerman and Williams, 1949.
4) Accepted value (Table I).
5) Our result, 1955.

1) Bitter, 1949.
2) Zimmerman and Williams, 1949.
3) Accepted value (Table I).
4) Our result, 1954.
5) Our result, 1955.

1) Pound, 1948.
2) Bitter, 1949.
3) Chambers and Williams, 1949.
4) Sheriff and Williams, 1951.
5) Accepted value (Table I).
6) Our result, 1954.
7) Our result, 1955.

Fig. 3. A comparison of results obtained by various authors. All values are re-evaluated with the magnetic moment of the proton given in ref. ([2]), and corrected for magnetic shielding. *References*: Poss: *Phys. Rev.*, **75**, 600 (1949);. Siegbahn and Lindström: *Nature*, **163**, 211 (1949); Zimmerman and Williams: *Phys. Rev.* **76**, 350 (1949); Bitter: *Phys. Rev.*, **75**, 1326A (1949); Pound: *Phys. Rev.*, **73**, 1112/erratum (1948); **74**, 228 (1948); Chambers and Williams: *Phys. Rev*, **76**, 638 (1949); Sheriff and Williams: *Phys. Rev.*, **82**, 651 (1951).

mean values of the magnetic field in the regions occupied by two samples is considerable, and produces the systematic (and in our early measurements undetermined) error.

With the aid of two twin-tees containing proton samples and fed by the same signal generator, two proton signals were produced on the screen of a two-ray c.r.o. After calibrating the sweep amplitude for differences in magnetic field intensities, the field was mapped (Fig. 1). Curve *a*) in Fig. 2 shows the field intensity variation in a plane section parallel to the field. It is obvious, that a part of the inhomogeneity is caused by the fact that the pole faces are not exactly parallel. After elimination of this error as far as was possible, the variation of field was changed as shown by curve *b*). The remaining inhomogeneity was corrected by shimming the pole faces with the aid of nickel films produced electrolytically, their contours corresponding to the « niveau lines » of the field map. The result in the section specified is shown by curve *c*). Essentially the same improvement was obtained in other sections as well.

In the corrected field we repeated the measurements of the magnetic moments of ^{23}Na and ^{31}P and redetermined that of ^{19}F. Frequencies were measured with a heterodyn frequency meter. Its crystal was calibrated with a primary standard with a relative error of 10^{-7} and the dial of the frequency meter allowed a precision better than 1 part in 10^4 in relative frequency measurements. The samples were placed in the gap so that the difference between the magnetic field in the regions occupied by the two samples was certainly smaller than 10^{-4}-times the mean field intesinty.

^{19}F was measured in a sample of concentrated HF. ^{23}Na was studied in almost concentrated aqueous solution of $Na_2S_2O_3$ and NaCl. The results did not show any deviation for the two kinds of samples. ^{31}P was measured in almost concentrated H_3PO_4.

The results are summarized in Table I. The value used for the magnetic moment of the proton is $\mu_1 = 2.79276 \pm 0.00006$

TABLE I.

		^{19}F	^{23}Na	^{31}P
	ν/ν_{proton}	0.940875 ±0.01%	0.264553 ±0.01%	0.404868 ±0.01%
μ/μ_1	uncorrected	2.62756 ±0.0003	2.21649 ±0.00025	1.130665 ±0.00012
	corrected for diamagnetic shielding (*)	2.62856 ±0.0003	2.21770 ±0.00025	1.131695 ±0.00012
	accepted value (†)	2.6287 ±0.0007	2.21728 ±0.00025	1.13171 ±0.00020

(*) N. F. RAMSEY: *Nulcear Moments* (New York, 1953), Table 2, pp. 86-87.
(†) Values published by RAMSEY (op. cit., Table 1, pp. 78-85) are reevaluated with the of μ_1 given in the text.

nuclear magnetons, as given by HIPPLE, SOMMER and THOMAS (2).

A comparison of our results with those published by others is shown in Fig. 3. « Our result, 1954 » for ^{23}Na and ^{31}P refers to values published in our earlier paper (1). The dotted lines represent the probable errors due to the previously uncontrolled deviation of the original magnetic field in the region occupied by the two samples. « Our result, 1955 » represents values given in the above Table.

A more detailed account will be published shortly in the *Acta Phys. Hung.*

(2) HIPPLE, SOMMER and THOMAS: *Phys. Rev.*, **76**, 1877 (1949); **80**, 487 (1950).

Sullo sviluppo della componente fotonica nell'atmosfera.

G. Poiani

Istituto di Fisica dell'Università - Trieste
Istituto Nazionale di Fisica Nucleare - Gruppo Aggregato di Trieste

(ricevuto il 27 Settembre 1955)

La generazione e lo sviluppo della componente fotonica nell'atmosfera sono assicurati dai tre processi principali: *a*) disintegrazione dei π^0 in 2γ e conseguente cascata elettrofotonica; *b*) disintegrazione dei μ in e $+ 2\nu$ e conseguente cascata elettrofotonica; *c*) collisione dei μ contro gli elettroni del mezzo e cascata generata da questi ultimi. È noto che il primo processo è preponderante alle alte quote, mentre il secondo prevale nella bassa atmosfera ed al l.d.m.

Per la valutazione quantitativa delle varie componenti si può utilmente adoperare il metodo della trasformata di Mellin (T.M.) ([1,2]). Si abbia infatti una radiazione, che chiameremo primaria che, attraverso un qualche processo, ad es. di collisione, decadimento ecc., generi una radiazione secondaria. Indicando con $m_p(s)$ la T.M. dello spettro differenziale della primaria, $m_g(s)$ quella dello spettro di generazione della componente secondaria, e $m_\sigma(s)$ quella dello spettro sorgente secondario, se lo spettro di generazione è una funzione omogenea di grado $m_g = -1$, sussiste la semplice relazione funzionale fra le rispettive T.M.:

$$m_\sigma(s) = m_p(s) \cdot m_g(s) \,. \tag{1}$$

Questa proprietà può estendersi anche al caso in cui lo spettro di generazione sia una funzione omogenea di grado $m \neq -1$; si dimostra in tal caso che la relazione precedente si trasforma nella:

$$m_\sigma(s) = m_p(s + m + 1) m_g(s) \,. \tag{2}$$

Adattando opportunamente questo procedimento ai tre processi sopra elencati, riesce agevole calcolare singolarmente il loro contributo alla componente fotonica nell'atmosfera.

([1]) P. Budini e K. Molière: *Kosmische Strahlung* (Göttingen, 1953), p. 367.
([2]) P. Budini e G. Poiani: *Nuovo Cimento*, **10**, 1288 (1953).

a) La T.M. dello spettro differenziale sorgente dei π^0 nell'atmosfera, alla profondità t (u.d.r.), avendo riguardo alla teoria simmetrica delle forze nucleari, è data da [1]:

$$m_{\pi^0}(s, t) = \tfrac{1}{3} m_\pi(s) m_n(s, 0) m_n^c(s, t) ,$$

dove $m_n(s, 0)$ è la T.M. dello spettro della nucleonica primaria, $m_n^c(s, t)$ quella della cascata nucleonica ed $m_\pi(s)$ quella dello spettro di produzione dei π. Segue subito che la T.M. dello spettro sorgente dei γ nell'atmosfera è data da:

$$m_\gamma(s, t) = m_{\pi^0}(s, t) m_{\pi^0,\gamma}(s) ,$$

dove $m_{\pi^0,\gamma}(s)$ è la T.M. dello spettro di generazione dei fotoni di decadimento dei π^0.

Sia ora $m_\gamma^c(s - 1, t, t')$ la T.M. dello spettro integrale dei fotoni alla profondità t, proveniente da una cascata e.f. generata in t' da una primario fotonico. La T.M. dello spettro integrale fotonico alla profondità t è allora data da:

$$m_{\Gamma,\pi^0}(s - 1, t) = \int_0^t m(s, t') m_\gamma^c(s - 1, t - t')\, \mathrm{d}t' . \tag{3}$$

Le espressioni delle varie T.M. possono esser prese dalla letteratura [1,4]; sostituendole nella (3) si ottiene:

$$m_{\Gamma,\pi^0}(s - 1, t) = 0.407 \frac{\sigma_0 + \lambda_2(s)}{s(s + 1)} \frac{m_n(s, 0) m_\pi(s)}{\lambda_1(s) - \lambda_2(s)} \frac{\exp[-\lambda_1(s)t] - \exp[-k(s)t]}{k(s) - \lambda_1(s)} ,$$

$$k(s) = 0.61[1 - \gamma/\alpha^s] , \qquad \alpha = 2.2 ; \quad \gamma = 0.2 ,$$

da cui, per antitrasformazione col metodo della sella, si arriva agevolmente alla espressione dello spettro fotonico integrale di decadimento dai π^0:

$$\Gamma_{\pi^0}(W, t) = 0.407 \frac{K(s, -s)}{\sqrt{2\pi D'}} (W + \varepsilon)^{-s} \frac{\lambda_2 + \sigma_0}{s(s + 1)} \frac{m_n(s, 0) m_\pi(s)}{\lambda_1(s) - \lambda_2(s)} \frac{\exp[-\lambda_1 t] - \exp[-kt]}{k(s) - \lambda_1(s)}$$

$$D(s) = \frac{m_\pi'(s)}{m_\pi(s)} + \frac{m_n'(s)}{m_n(s)} - \tfrac{1}{2}[k'(s) + \lambda_1'(s)] - \frac{1}{s} - \frac{1}{s + 1} - \lg(W + \varepsilon) + \left(\frac{\lambda_2 + \sigma_0}{\lambda_1 - \lambda_2}\right)' = 0 .$$

In queste formule l'accento indica la derivazione rispetto al parametro s.

Nel calcolo eseguito si è tenuto conto, oltre che dei processi e.m. di alta energia, anche della ionizzazione, sostituendo all'energia del fotone, l'energia $(W + \varepsilon)$ in cui ε è l'energia critica del mezzo attraversato ($\varepsilon = 86$ MeV per u.d.r. per l'aria), e moltiplicando per la funzione $K(s, -s)$ di Rossi. In tal modo si può ritenere che il risultato sia valido con una certa approssimazione sino ad un'energia minima di

---

[3] Rif. [1], p. 418.

[4] B. Rossi: *High Energy Particles* (New York, 1952).

~ 10 MeV. Con tale valore del taglio inferiore energetico, si è calcolata la curva P della fig. 1, rappresentante il contributo del decadimento dei π^0 alla componente fotonica.

b) Lo spettro differenziale mesonico può rappresentarsi, entro l'intervallo energetico 50 MeV — ∞, e da 1033 g·cm^{-2} a ~ 200 g·cm^{-2}, con sufficiente approssimazione, a mezzo della formula empirica:

$$(3) \quad \mu(E, t) = A(t) \frac{E}{[C(t) + E]^3}, \quad E \text{ in MeV},$$

in cui i coefficienti A e C sono funzioni della profondità t, e rappresentati dalle curve della fig. 2. Questo spettro si avvicina con buona approssimazione alle curve

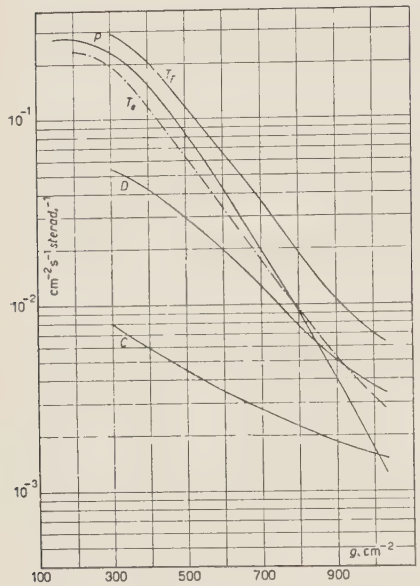

Fig. 1. – Intensità delle componenti fotoniche nell'atmosfera ($W > 10^7$ eV, $\lambda \sim 50°$ N).

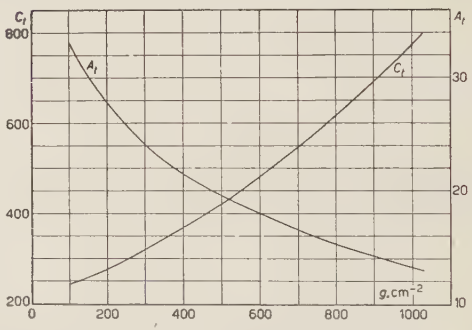

Fig. 2. – Valori dei coefficienti $A(t)$, $C(t)$, in funzione della profondità atmosferica.

sperimentali riportate da Puppi e Dallaporta ([4]), fino ad una quota di 300 g·cm^{-2}, mentre la sua pendenza si adatta ai dati di Wirtz, nell'intervallo energetico $1 \div 10$ GeV. La T.M. di questo spettro è data da:

$$m_\mu(s, t) = A_t C_t^{s-1} \varphi(s); \qquad \varphi(s) = \frac{\Gamma(s+2)\Gamma(1-s)}{\Gamma(3)}.$$

Invece lo spettro differenziale di produzione degli elettroni di energia E' dal decadimento dei mesoni di energia E, si può rappresentare con l'espressione:

$$g(E', E)\,dE' = k \frac{\delta(E' - \alpha E)}{Et}, \qquad k = \frac{\mu c^2 \alpha}{\mathcal{C}_0},$$

(μ — massa del mesone μ; $\mathcal{C}_0$ – vita media del μ) dove si utilizza la formula barometrica usata da Stanton ([7]) e con la funzione δ si esprime l'ipotesi che gli elet-

([6]) *Progress in Cosmic Ray Physics* (Amsterdam, 1952), p. 315.
([8]) Rif. ([1]), p. 296.
([7]) H. E. Stanton: *Phys. Rev.*, **66**, 48 (1944).

troni vengano emessi nel decadimento tutti con un'energia che è una frazione α, relativisticamente invariante, dell'energia massima. Il valore assunto per α è di 0.3. La funzione $g(E', E)$ è omogenea di grado $m = -2$; di essa può facilmente ottenersi la T.M., che viene espressa da

$$m_g(s, t) = \frac{k}{t} \alpha^s .$$

Dalla (2) si ottiene allora la T.M. dello spettro sorgente degli elettroni di decadimento dai μ:

$$m_\sigma(s, t) = m_\mu(s - 1) m_g(s, t) ,$$

e da questa, tramite la cascata e.f., rappresentata con la T.M. dello spettro integrale della cascata $m^c_\gamma(s - 1, t)$, creata questa volta da un primario fotonico, si ottiene la T.M. dello spettro fotonico integrale da decadimento dei μ:

$$m_{\Gamma,d}(s - 1, t) = \int_{t_0}^{t} m_\sigma(s, t') m^c_\gamma(s - 1, t - t')\, \mathrm{d}t' .$$

Eseguendo l'antitrasformazione e tenendo conto delle osservazioni fatte in precedenza, si ottiene:

$$(4) \qquad \Gamma_d(W, t) = \frac{k}{(2\pi)^{\frac{1}{2}}} \int_{t_0}^{t} \Gamma(s) \left(\frac{\alpha}{W + \varepsilon} \right)^s \frac{\varphi(s)}{s} K(s, -s) C_{t'}^{s-2} \frac{A_{t'}}{t'} \frac{\exp\left[\lambda_1 (t - t')\right]}{(D')^{\frac{1}{2}}} \mathrm{d}t' ,$$

con la sella:

$$D(s) = \frac{\varphi'(s)}{\varphi(s)} - \frac{1}{s} + \lg \frac{W + \varepsilon}{\alpha} + \frac{K'(s)}{K(s)} + \lambda_1'(t - t') + \lg C_{t'} = 0 .$$

L'integrazione della (4) è stata eseguita numericamente, per vari valori di t, a partire da $t_0 = 100\ \mathrm{g \cdot cm^{-2}}$, in quanto si può ritenere che intorno a questa quota possa farsi sentire il contributo della disintegrazione dei μ alla formazione della e.f. La curva D in fig. 1 rappresenta il risultato.

c) Con analoga trattazione si può calcolare la componente derivante dagli elettroni di collisione da parte dei mesoni. Poichè però questa componente è di minore entità, eccetto che in prossimità del l.d.m., si è proceduto al suo calcolo usando alcune semplificazioni. Intanto in prima approssimazione il contributo allo spettro integrale fotonico da parte di questa componente, può scriversi:

$$\Gamma_c(W, t) = \int_{E}^{\infty} (\sigma E', t) Z_\gamma(W, E')\, \mathrm{d}E' ,$$

dove $Z_\gamma(W, E')$ è la traccia fotonica integrale e

$$\sigma(E', t) = \int_{E'_{\min}}^{\infty} f(E', E_0) \mu(E_0, t)\, \mathrm{d}E_0 ,$$

è lo spettro sorgente degli elettroni di collisione. In esso $f(E', E)$ è lo spettro di produzione degli elettroni di collisione [4]:

$$f(E', E_0)\,\mathrm{d}E' = \frac{h}{E'^2}\left[1 - \frac{E'}{E_m(E')} + \frac{1}{2}\frac{E'}{E_0}\right], \qquad h = 2\pi \frac{Z}{A} N r_0^2 m_e c^2 ,$$

$E_m(E')$ è l'energia massima che il mesone può trasferire nell'urto all'elettrone, $E_{\min}$ è invece l'energia minima che il mesone deve possedere per poter proiettare un'elettrone di energia E'. Per la traccia fotonica integrale si è scelta l'espressione di Richards e Nordheim [4,8]:

$$Z_\gamma(E', W) = 0.92E' . \qquad W = 10 \text{ MeV}.$$

Con opportune semplificazioni ed approssimazioni, si ottiene:

$$\Gamma(W, t) \approx 0.92h\left[\lg \widehat{\frac{E_m}{E}} - 1\right] \int_{E\,\min}^{\infty} \mu(E_0, t)\,\mathrm{d}E_0 ,$$

in cui $\lg \widehat{E_m/E}$ è un valor medio pesato. Nella fig. 1 la curva C rappresenta la componente derivante dai processi di collisione.

L'andamento delle tre componenti è perfettamente analogo a quello delle corrispondenti elettroniche, calcolate da P. Budini, come era del resto da aspettarsi. In fig. 1 la curva T rappresenta la somma delle tre, e quindi l'andamento della fotonica integrale nell'atmosfera. Essa può paragonarsi alla curva sperimentale riportata da Rossi [9] per la componente elettronica. Il risultato dei calcoli denuncia una prevalenza della componente fotonica su quella elettronica, a tutte le quote. Il rapporto fra le due non è però costante: da un valore poco più del doppio al l.d.m. esso va decrescendo con la quota, come viene rappresentato dalla curva della fig. 3.

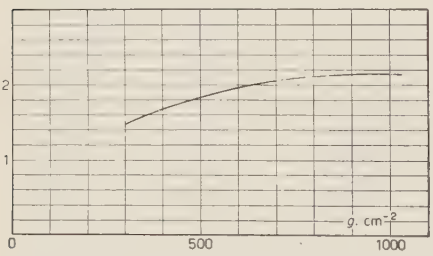

Fig. 3. – Rapporto fotoni su elettroni alle varie quote.

È da sottolineare però che questo risultato è valido entro i limiti posti dalla cosiddetta approssimazione « B » della teoria degli sciami; alle basse energie è da attendersi che il valore del rapporto vada crescendo ancor più, per il prevalere dell'assorbimento degli elettroni sui processi di diffusione dei fotoni.

Indicazioni in tal senso si possono infatti ricavare dalle ricerche di B. Ferretti e G. Bernardini [10], per energie inferiori ai 10 MeV, e dalle recenti esperienze di M. Ageno e coll. [11] per energie inferiori al MeV.

* * *

Mi è gradito ringraziare il prof. P. Budini per le discussioni avute sull'argomento.

[8] J. A. Richards and L. W. Nordheim: *Phys. Rev.*, **74**, 1106 (1948).
[9] B. Rossi: *Rev. Mod. Phys.*, **20**, 537 (1948).
[10] B. Ferretti e G. Bernardini: *Nuovo Cimento*, **16**, 173 (1939).
[11] M. Ageno, G. Cortellessa e R. Querzoli: *Nuovo Cimento*, **1**, 453 (1955).

The α-Particle Model of ^{20}Ne.

A. Gamba and A. Moncassoli
Istituto di Fisica dell'Università - Torino

(ricevuto il 4 Ottobre 1955)

Recently Dennyson [1] has shown that the α-particle model works quite well in predicting spins, parities and energies of the excited states of ^{16}O.

The investigation of the α-particle model of ^{20}Ne was carried out already in 1938 by Teller and Wheeler [2], but the agreement with experiment seemed then rather poor. However, let us consider a slightly modified version of the model. We assume with Teller and Wheeler that in ^{20}Ne the α-particles are arranged at the vertices of a trigonal bipyramid, but, in contrast with them, no assumption is made about the equality of all « bond distances » between two α-particles. In our model two distances are necessary to specify the configuration: the side l of the equilateral triangle of the base and the distance b between the two α-particles at the opposite poles of the bipyramid.

The rotational states of the system are those of the symmetrical top with energy levels

$$(1) \qquad E_{J,K} = \{J(J+1) - K^2\}R + K^2 r$$

where

$$R = \frac{\hbar^2}{2A}, \quad r = \frac{\hbar^2}{2B},$$

A and B being the moments of inertia with respect to the axis in the plane of the base triangle and perpendicular to this plane respectively. The only values of the quantum number J and K ($K \leqslant J$) allowed by the Bose statistics are

J even with $K = 0$,

any J with $K = 3n \neq 0$, n integer.

Identifying the first two excited levels of ^{20}Ne with the first two predicted levels, one is able to predict the next two levels, which happen to be in remarkably close agreement with experiment as shown in Table I.

The next rotational state would be a 5^- state of 7.09 MeV, that is above the 0^+ experimental level at 6.74, which probably corresponds to the first vibrational level. We made calculation of the vibrational spectrum, which turns out to be in complete disagreement with the known data. We think, however, that a simple explanation of the failure of the model for energies higher than the first vibrational level, may be given as follows.

Using the experimental values for the

(1) D. M. Dennison: *Phys. Rev.*, **96**, 378 (1954).

(2) E. Teller and J. Wheeler: *Phys. Rev.*, **53**, 778 (1938).

parameters R and r it is easily found that the distance d is much shorter than l. More precisely, whereas two α-particles at the vertices of the base triangle are separated by a distance, which is somewhat larger than twice the α-particle radius, the two α-particles at the vertices of the pyramids are separated by a distance of the order of the nuclear radius of the α-particle. Therefore, there is a considerable overlapping of the wave function of these two α-particles, which do not preserve any more their individualities and give rise to a substantial exchange energy. However, this energy is accounted for in the ground state, and, being the same for all rotational levels, does not affect the calculations, as far as low rotational states are concerned. But as soon as the first vibrational level is excited, the lack of the individuality of the α-particles causes the model to break down completely.

As a final remark, we suggest the measurement of spins and parities of the 2nd, 3rd, 4th excited states of ^{20}Ne as the most important check of our model.

TABLE I [3].

J, K values	Energies		Spins and Parities	
	Theoretical	Experimental	Theoretical	Experimental
0.0	0	0	0^+	0^+
2.0	1.630	=1.630	2^+	2^+
3.3	2.2	=2.2	3^-	—
4.3	4.373	4.36	4^+	—
4.0	5.43	5.4	4^+	—

The = sign indicates the levels which are identified in order to determine the parameters R and r of formula (1).

[3] The experimental data are taken from F. AJZEMBERG and T. Lauritsen: *Rev. Mod. Phys.* **27**, 77 (1955).

On the Scattering of Neutrons by Alpha Particles.

E. Clementel and C. Villi

Istituti di Fisica dell'Università di Padova e di Trieste
Istituto Nazionale di Fisica Nucleare - Sezione di Padova

(ricevuto il 10 Ottobre 1955)

The knowledge of the phenomenological phaseshifts of neutrons elastically scattered by α-particles provide informations on the ^2P virtual ground state of ^{5}He and on the magnitude and sign of the splitting in energy of the $P_{\frac{3}{2}}$ and $P_{\frac{1}{2}}$ components of the doublet, the characteristics of which are related to specific nucleon-nucleon spin-orbit forces. When the coupling between spin and orbital angular momentum is taken into account, the $(n-\alpha)$ differential cross-section reads [1]

$$(1)\qquad \frac{k^2\,\mathrm{d}\sigma(\vartheta)}{\mathrm{d}\Omega} = \left|\sum\{(l+1)\sin\delta^l_{l+\frac{1}{2}}\exp[i\delta^l_{l+\frac{1}{2}}] + l\sin\delta^l_{l-\frac{1}{2}}\exp[i\delta^l_{l-\frac{1}{2}}]\}P_l(\cos\vartheta)\right|^2 + \\ + \left|\sum\{\sin\delta^l_{l+\frac{1}{2}}\exp[i\delta^l_{l+\frac{1}{2}}] - \sin\delta^l_{l-\frac{1}{2}}\exp[i\delta^l_{l-\frac{1}{2}}]\}\sin\vartheta\cdot P'_l(\cos\vartheta)\right|^2 .$$

If we confine ourselves to neutron energies E_n lower than about 3 MeV in the laboratory system, the interaction of waves associated with angular momenta higher than 1 can be neglected, and Eq. (1) becomes

$$(2)\qquad \frac{k^2\,\mathrm{d}\sigma(\vartheta)}{\mathrm{d}\Omega} = |(1/2i)\boldsymbol{a} + (1/2i)\boldsymbol{b}\cos\vartheta|^2 + |(1/2i)\boldsymbol{c}\sin\vartheta|^2 = A + B\cos\vartheta + C\cos^2\vartheta ,$$

where

$$(3)\qquad A = (1/4)(|\boldsymbol{a}|^2 + |\boldsymbol{c}|^2) , \qquad B = (1/4)(\boldsymbol{a}^*\boldsymbol{b} + \boldsymbol{a}\boldsymbol{b}^*) , \qquad C = (1/4)(|\boldsymbol{b}|^2 - |\boldsymbol{c}|^2) .$$

$$(4)\qquad \begin{cases} \boldsymbol{a} = \exp[2i\delta_0] - 1 , \\ \boldsymbol{b} = 2\exp[2i\delta_{\frac{3}{2}}] + \exp[2i\delta_{\frac{1}{2}}] - 3 , \\ \boldsymbol{c} = \exp[2i\delta_{\frac{3}{2}}] - \exp[2i\delta_{\frac{1}{2}}] . \end{cases}$$

---

[1] F. Bloch: *Phys. Rev.*, **58**, 829 (1940).

In Eqs. (4) we have written $\delta_{\frac{1}{2}}^{0} \equiv \delta_0$, and omitted the index 1 in the two P-phaseshift symbols. Comparing relations (2) (3) (4) with those given in the Appendix [(A.1), (A.4), (A.5)] of a previous paper (2), it is seen that the neutron-alpha elastic differential cross-section has the identical mathematical structure as the differential cross-section for the scattering of positive pions by protons. At author's knowledge, this identity has never been clearly stressed hitherto, and the techniques, used for phaseshift analysis of the experimental data, have been developed independently, like, for example, the LAUBENSTEIN (3) and SEAGRAVE (4) graphical methods, used in the (n-α) case, and the ASHKIN and VOSKO method (5), used for pion-nucleon scattering.

From the structural identity between (π^+-p) and (n-α) cross-sections, follows that what is called the Fermi-Yang ambiguity in the former case, corresponds in the latter, to the inverted respectively to the normal doublet for the $P_{\frac{3}{2}}$ and $P_{\frac{1}{2}}$ states. A mathematical inspection of the scattering equations shows that the « P-state ambiguity », recently shown by CRITCHFIELD and DODDER (6) in the scattering of protons by α-particles and first noted by YANG (7) in the (π^+-p) case, is a peculiar feature of the scattering of fermions by zero spin nuclei; therefore, it should be expected to arise also in the P-state scattering of neutrons by ^{6}Li, ^{8}Be, ^{12}C, etc.

On the basis of this identity, it is natural to take profit of the experience gathered in the enormous amount of work carried out to clear up the behavior of pion nucleon phaseshifts, in order to achieve a better understanding of the (n-α) phaseshift fitting mechanism. The conclusion is immediately reached that the (n-α), P phaseshifts satisfy the relation

$$\delta_{\frac{3}{2}}^{(+)} - \delta_{\frac{1}{2}}^{(+)} = \delta_{\frac{1}{2}}^{(-)} - \delta_{\frac{3}{2}}^{(-)}, \tag{5}$$

where we have labelled with (+) and (—) the phaseshifts concerned with the normal respectively with the inverted doublet and corresponding, in the (π^+-p) case, to Yang and Fermi solutions. Inspection of the values given in Table III of ref. (6) shows that the relation (5) is satisfied (8). The previous notation has been chosen for consistency reasons since, according to the analytical method, developed for the scattering of positive pions, but still valid for (n-α) scattering [Eqs. (1)-(6) of ref. (2)], the normal, respectively the inverted, P-state phaseshifts are bound, for any given value of δ_0, to the two P-state solutions of the scattering equations. The procedure of course, remains unchanged, the phaseshifts α_3, α_{33} and α_{31} being replaced by δ_0, $\delta_{\frac{3}{2}}$, $\delta_{\frac{1}{2}}$, and the numbers A_+, B_+ and C_+ by the new input coefficients A, B and C, obtained by least square fit of Eq. (2) to the measured angular distribution of the elastically scattered neutrons.

For a given neutron energy, eight sets of the three (n-α) phaseshifts are compatible with the data. The attractive nature of the $P_{\frac{3}{2}}$ state eliminates the mirror

(2) E. CLEMENTEL, G. POIANI and C. VILLI: *Nuovo Cimento*, **2**, 389 (1955). The first of Eqs. (4) must be read $\cos 2\alpha_{33}^{(\pm)} = \lambda_+ \pm (\lambda_+^2 - \mu_+)^{\frac{1}{2}}$.

(3) R. A. LAUBENSTEIN and M. J. W. LAUBENSTEIN: *Phys. Rev.*, **84**, 18 (1951).

(4) J. D. SEAGRAVE: *Phys. Rev.*, **92**, 1222 (1953).

(5) J. ASHKIN and H. S. VOSKO: *Phys. Rev.*, **91**, 1248 (1953).

(6) C. L. CRITCHFIELD and D. C. DODDER: *Phys. Rev.*, **76**, 602 (1949).

(7) H. L. ANDERSON *et al.*: *Phys. Rev.*, **91**, 155 (1953).

(8) FERMI *et al.* [*Phys. Rev.*, **95**, 1581 (1954)] first pointed out that the multiplicity of P-phaseshifts is the same in (n-α) and (π^+-p) scattering.

sets with all signs reversed. The remaining four sets are formed by the two P-phaseshifts, corresponding either to a positive or a negative δ_0. The sets associated to a positive δ_0 are not well behaved and can be rejected on continuity grounds. The final selection between the remaining two sets, corresponding, for the same negative value of δ_0, to the normal and inverted doublet, requires the knowledge of the polarization of the scattered neutrons. This circumstance is similar to that arising for pion-nucleon scattering, being the choice between Fermi and Yang solutions in principle possible by measuring the polarization of the recoiling nucleon.

The most straightforward determination of the (n-α) phaseshift and the test of their stability against variations of the input coefficients A, B and C, can be carried out by means of the same phaseshift analyzer, discussed in a previous note (9), with explicit reference to pion-nucleon scattering. The following analysis, performed with a 40 cm ($=OO'$) mechanical analyzer, is intended to be of an illustrative nature only and no attempt has been made to establish how sensitive the phaseshifts are to the uncertainties of the data.

The initial values of the numbers A, B and C were determined by fitting ADAIR's (10) angular distributions at 60°, 90° and 120°; then, the quantities u, v and w were calculated and presented to the analyzer, which, according to Eqs. (8) of ref. (9), « feels » the data in the following way

$$(6) \qquad \begin{cases} u(k) = 4 - (k^2/2\pi)\sigma_T(k)\,, \\ v(k) = \pm 2k\{[\mathrm{d}\sigma(0°)/\mathrm{d}\Omega] - (k/4\pi)^2[\sigma_T(k)]^2\}^{\frac{1}{2}}\,, \\ w(k) = 2\{1 - k^2\,\mathrm{d}\sigma(90°)/\mathrm{d}\Omega\}\,, \end{cases}$$

where $\sigma_T(k)$ is the total (n-α) cross-section. Starting from such initial values a simultaneous variation of all the input coefficients was carried out to accomplisg the extrapolated data also with the phaseshift continuity. In this operation the variation of $v(k)$, for a fixed value of k, was found essential; this is of course a consequence of the fact that the coefficient B, and therefore the forward scattering cross-section, is not well determined by experiments. The results of this analysis are listed in Table I and II. With the new values of A, B and C, the phaseshift continuity is established all over the explored energy interval, the integrated cross-section $k^2\sigma_T(k) = 4\pi(A+C/3)$ is found in good agreement with the experimental one, but the values of the calculated angular distribution at 180° appears, in particular above the resonance energy, larger than Adair's data apparently require.

In Fig. 1 the mechanical analyzer is presented in its resolution position for the scattering energy of 0.4 MeV ($OQ_1Q_2Q_3P_1$) and 2.73 MeV ($OQ'_1Q'_2Q'_3P'_1$). The striking feature of the curve (1), showing the track of the input terminal P_1 for neutron

(9) E. CLEMENTEL and C. VILLI: *Nuovo Cimento*, **2**, 845 (1955). To adequate the description of the analyzer to neutron-alpha scattering, the phaseshifts α_i, α_{i3}, α_{i1}, should be replaced by δ_0, $\delta_{\frac{3}{2}}$, $\delta_{\frac{1}{2}}$. It is worth while to point out that the analogue computer, built by BALDINGER [*Helv. Phys. Acta*, **25**, 446 (1952)] for phaseshift analysis of neutron-alpha cross-sections, could also be used in the analysis of the experimental data of positive and negative pions scattered by protons. Taking into account the mathematical symmetry between positive and negative (elastic and charge-exchange) scattering, in the latter case the analogue computer should operate on the following combination of the experimental cross-sections

$$\frac{\mathrm{d}\sigma'(\vartheta)}{\mathrm{d}\Omega} = \frac{3}{2}\left[\frac{\mathrm{d}\sigma(\pi^-)}{\mathrm{d}\Omega} + \frac{\mathrm{d}\sigma(\pi^0)}{\mathrm{d}\Omega}\right] - \frac{1}{2}\,\frac{\mathrm{d}\sigma(\pi^+)}{\mathrm{d}\Omega}\,.$$

(10) R. K. ADAIR: *Phys. Rev.*, **86**, 155 (1952).

energies ranging from 0.4 to 2.73 MeV, is the spectacular jump between 1.2 and 1.4 MeV, required by the continuity of the phaseshifts versus neutron energy. At approximately 1.3 MeV one finds $v(k)=0$; therefore, at this energy, the cross-section for forward scattering is equal to the square of the total cross-section multiplied by $(k/4\pi)^2$. The qualitative features of this situation are again very similar to those implied by pion-nucleon scattering for isotopic spin $\frac{3}{2}$ [9,11].

TABLE I. – *Input coefficients for* n-α *scattering in S and P waves.*

E_n (MeV)	A	B	C	u	v	w
0.4	0.086	— 0.208	0.166	3.717	0.315	1.828
0.6	0.193	— 0.427	0.567	3.237	0.866	1.614
0.75	0.350	— 0.966	1.158	2.528	1.307	1.300
0.865	0.547	— 0.495	1.606	1.835	1.394	0.906
1.0	0.665	— 0.453	2.646	0.934	1.362	0.670
1.2	1.031	0.195	3.046	— 0.094	0.575	— 0.062
1.4	1.256	1.196	2.845	— 0.408	— 1.323	— 0.512
1.7	1.275	1.407	2.610	— 0.290	— 1.661	— 0.550
2.0	1.315	1.702	2.055	— 0.009	— 2.071	— 0.630
2.4	1.354	1.774	1.867	0.047	— 2.087	— 0.708
2.73	1.393	1.847	1.678	0.095	— 2.102	— 0.786

TABLE II. – *Phaseshifts in S and P waves.*

E_n (MeV)	δ_0	Inverted doublet		Normal doublet	
		$\delta_{\frac{1}{2}}^{(-)}$	$\delta_{\frac{3}{2}}^{(-)}$	$\delta_{\frac{1}{2}}^{(+)}$	$\delta_{\frac{3}{2}}^{(+)}$
0.4	— 15°	3°	10.5°	14.5°	4°
0.6	— 19°	4°	20°	26.5°	10.5°
0.75	— 22°	5°	32°	40.5°	13.5°
0.865	— 24°	6°	41°	52.5°	17.5°
1.0	— 24.5°	7°	54°	72.5°	25.5°
1.2	— 25°	8°	72°	106°	42°
1.4	— 29°	10°	101°	192°	101°
1.7	— 32°	12°	108°	216°	120°
2.0	— 37°	17°	119°	242°	140°
2.4	— 38°	20°	121°	243°	142°
2.73	— 40°	23°	123°	243.5°	143.5°

Inspection of Fig. 1 shows that the analyzer configuration at 2.73 MeV ($OQ_1'Q_2'Q_3'P_1'$) is not obtained by continuous deformation and proper counter-clockwise rotation in the plane xy of the mechanical system ($Q_1Q_2Q_3P_1$) around the junction at Q_1, starting from its initial position at 0.4 MeV. In fact, moving the point P_1 on the « experimental track » (curve 1), it is found that approximately at the energy

(11) H. L. ANDERSON: *Rev. Mod. Phys.*, **27**, 269 (1955).

$E_n = 1.4$ MeV the points Q_2 and Q_3 coincide; then, for higher energies, the phaseshifts related to the inverted doublet are fixed by the arm $Q_1'Q_3'P_1'$, which, because of the phaseshift continuity, is correlated at lower energies to the arm $Q_1Q_3P_1$.

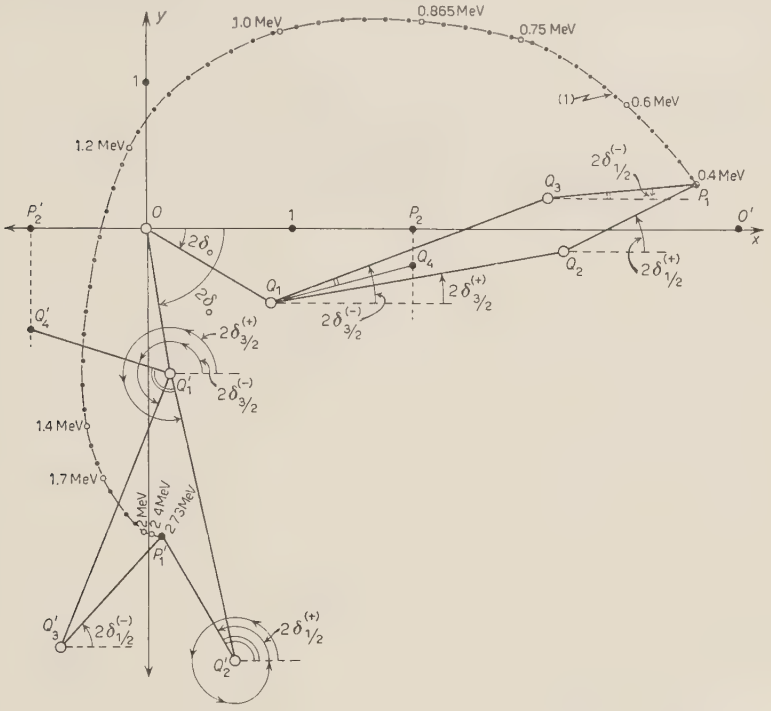

Fig. 1. – Mechanical phaseshift analysis of neutrons elastically scattered by α-particles. Solutions labelled with (+) and (—) correspond to the normal respectively inverted doublet. The curve (1) shows the track of the point P_1 for neutron energies ranging from 0.4 to 2.73 MeV in the laboratory system. The phaseshift analyzer is shown in the two resolution positions for the scattering energies of 0.4 MeV ($OQ_1Q_2Q_3P_1$) and 2.73 MeV ($OQ_1'Q_3'Q_3'P_1'$).

The inversion of the arms $Q_1Q_2P_1$ and $Q_1Q_3P_1$, occurring exactly at the energy satisfying the relation ([2,9]) $\lambda^2(k) = \mu(k)$, follows from the fact that, with increasing neutron energy, the phaseshifts related to the normal doublet (Yang solutions in the (π^+-p) case) vary much faster than those related to the inverted one. In the neutron-alpha scattering this circumstance arises from the weak attraction of the $P_{\frac{1}{2}}$ state compared to that of the $P_{\frac{3}{2}}$ state. Approximately at the energy at which the coefficient B goes from negative to positive values, the analyzer clearly shows that the angle $2\delta_{\frac{1}{2}}^{(+)}$ increases beyond 360°. This fact is completely general and holds also for the scattering of positive pions by protons. It follows that the *continuity* of the phaseshifts labelled with (+) insures the *validity of the « ambiguity relation »* (5) *below and above the resonance energy* ([12]).

([12]) It follows that the conventional definition of Yang solutions at high energies is conflicting with the continuity of these phaseshifts versus pion energy. The relation ([2,9]) $\alpha_{33}^{(+)} - \alpha_{31}^{(+)} = \pi - [\alpha_{33}^{(-)} - \alpha_{31}^{(-)}]$, valid above the $\alpha_{33}^{(-)}$-resonance, becomes $\alpha_{33}^{(+)} - \alpha_{31}^{\prime(+)} = \alpha_{31}^{(-)} - \alpha_{33}^{(-)}$, where we have taken into account the relation $\alpha_{31}^{\prime(+)} - \alpha_{31}^{(+)} = \pi$ between the « real » $\alpha_{31}^{\prime(+)}$ Yang phaseshift and the « conventional » one.

The interest in accurate analyses of (n-α) data has been revived by recent attempts ([13]) to explain the «experimental» phaseshifts in terms of two-body nuclear potentials, containing a spin-orbit term of the $\boldsymbol{L}\cdot\boldsymbol{S}$ type. The results so far obtained, using a resonant group structure wave function for the five body system and solving the collision equation by variational procedures, are very promising.

* * *

A helpful correspondence with Prof. P. HUBER and with Prof. J. D. SEAGRAVE is gratefully acknowledged. We thank Dr. I. GABRIELLI and Dr. G. IERNETTI for the construction of the phaseshift analyzer and for the measurements carried out with it, and Dr. L. BERETTA for several check calculations.

([13]) B. H. BRANSDEN and J. S. C. MCKEE: *Phil. Mag.*, **45**, 869 (1954); S. HOCHBERG, H. S. W. MASSEY and L. H. UNDERHILL: *Proc. Phys. Soc.*, **67**A, 987 (1954); S. HOCHBERG, H. S. W. MASSEY, H. ROBERTSON and L. H. UNDERHILL: *Proc. Phys. Soc.*, **68**A, 746 (1955).

Problems of Film Formation and Flow in Liquid Helium II.

S. Franchetti

Istituto di Fisica dell'Università - Firenze

(ricevuto l'11 Ottobre 1955)

In a previous work [1], a quantum-mechanical model for liquid He was imagined, employing a comparatively simple formalism.

The basis of this model is a « local eigenfunction » $\varphi(\boldsymbol{\rho})$ describing the simplest motion of an atom in the field of its neighbours. It is an essential feature of this function that it has to take account of the *correlations* between the motions of the « central atom » and of its neighbours. (These correlations are strong and result in lowering considerably the effective potential well the atom is moving in, thus leading to a marked spreading of the φ function, which is the fundamental one corresponding to the effective potential well assumed spherically symmetrical). From this function, more general one-particle eigenfunctions are built up which take the form of Bloch waves, i.e. (apart from a normalization factor)

$$(1) \qquad \psi_{\boldsymbol{K}}(\boldsymbol{\rho}) = \sum_n \exp\,(2\pi i \boldsymbol{K}\cdot\boldsymbol{r}_n)\varphi(\boldsymbol{\rho}-\boldsymbol{r}_n)\ .$$

Here the $\boldsymbol{r}_n$ are vectors defining a *lattice* [2] and $\boldsymbol{K}$ a constant vector.

The *fundamental state* corresponds to $\boldsymbol{K}=0$ and fulfils the basic requirements for representing the *superfluid* in the frame of the Einstein condensation theories. (Uniform spreading over macroscopic spaces, « insensitiveness » to boundary conditions). Its energy is the zero-point energy (per atom). It could also be used to build an approximation to Feynman's Φ-function [3], which would read (c^0 a normalization factor)

$$(2) \qquad \Phi = \prod_{\alpha=1}^{N} \sum_n c^0 \varphi(\boldsymbol{\rho}_\alpha - \boldsymbol{r}_n)\ .$$

The *excited states* ($\boldsymbol{K}\neq 0$) can be shown to have kinetic energies larger than that of the fundamental state by an amount proportional to K^2, a property that makes it possible to define an *effective mass*. The φ-function can be so chosen as to give the right amount of zero-point energy and at the same time an effective mass μ in the right range (2 to 3 times the atom mass) [4].

Main aspects neglected by the model — at least at this stage of approxim-

[1] S. Franchetti: *Nuovo Cimento*, **12**, 743 (1954).

[2] One should not fear this assumption is to give the liquid too much order. Indeed there remains plenty of randomness, due to the breadth of the φ-function being of the order of next-neighbour distance. (This peculiarity is shared by no other liquid than the heliums).

[3] See for instance Feynman's article in Gorter: *Progress in Low Temperature Physics* (Amsterdam, 1955).

[4] A tentative evaluation of $\varphi(\boldsymbol{\rho})$ is given in ref. [1]. A self-consistency method is being studied for a more objective evaluation.

ation — are *phonons* (5), as well as their interaction with the Bloch-wave states(1). Phonons could be introduced as done by FEYNMAN (3). On the contrary, the writer thinks that the role now attributed to rotons should largely be taken over by the simpler excitons (1).

The present work was undertaken to see what conclusions could be drawn from the model about films and related problems.

Since in these problems the (attractive Van der Waals) forces are long-range ones, a further simplification of the eigenfunctions can be attempted, consisting in replacing the φ functions in (1) by a *constant* average value. The eigenfunctions with $\boldsymbol{K} \neq 0$ then turn over to simple De Broglie waves, but there still remains an important difference against a mere free-particle approach, and this is the existence of a « uniform » eigenfunction corresponding to $\boldsymbol{K} = 0$. (As a minor consequence, the other eigenfunctions are to be « cosines » instead of the familiar « sines »).

Here are the main points investigated so far.

I) **Film at** 0 °K.

a) Static case. The treatment leads directly to the Schiff-Frenkel-Meyer theory of the film with its characteristic dependance of the thickness t on the inverse cube root of the height z

$$t = \text{const}\, z^{-\frac{1}{3}} . \tag{3}$$

The procedure is to form an expression for the average energy $\bar{\mathcal{E}}$ of an atom at height z (taking as zero the energy of an atom in the bulk of the liquid) and to write down the condition of stability of the profile, namely

$$\bar{\mathcal{E}} + t\frac{\theta\bar{\mathcal{E}}}{\theta t} = 0 . \tag{4}$$

b) Moving film. Spontaneous flow of the film is suggested by the fact that with the law (3) for the profile, an upward gliding of the liquid is accompanied by a *decrease* of potential energy, showing that the system cannot be in equilibrium under the following forces *alone*: i) Van der Waals forces wall-liquid; ii) the same, liquid-liquid; iii) weight.

c) Critical Velocity. As well known, the (superfluid) critical velocity v_c is related to the thickness of the film by the equation

$$v_c t \approx 10^{-4}\ \text{cm}^2\ \text{s}^{-1} . \tag{5}$$

The proposed model suggests that dissipation will set in when the kinetic energy per atom (of the collective, adiabatic, motion) reaches the value of the 1-st standing wave having a $\boldsymbol{K}$-vector perpendicular to the wall ($\lambda = 2t$). (Excitation of phonons is ruled out because for the wavelenghts in question their energy is far greater). Since atoms are not localized within the thickness of the film, the kinetic energy per atom has to be calculated as an *average* over the velocity field (at a given height z in the film). The energy of the wave to be excited is $h^2/8\mu t^2$, from which, with $\mu = 3\ \text{m}_{\text{He}}$ one gets

$$(\overline{v^2})^{\frac{1}{2}} t \approx 3 \cdot 10^{-4}\ \text{cm}^2\ \text{s}^{-1} . \tag{6}$$

A factor of the order 3 is to be expected, since the velocity field is very probably far from uniform, thus giving $v_c = \bar{v} < (\overline{v^2})^{\frac{1}{2}}$. (It is really not a true constant but a slowly varying function of t).

There remains to explain why the moving fluid does not loose momentum by exciting waves (or phonons) with $\boldsymbol{K}$ *parallel* to the wall, whose energies lie as close as we please to the funda-

(5) This restricts applications to temperatures either of 0 °K, or above 1 °K, where phonons are comparatively unimportant.

mental state (their wave-lenghts being unrestricted). It turns out that these transitions are *forbidden*, whereas the former is *allowed*, if we admit that the perturbing potential — i.e. any change in the Van der Waals field encountered by the fluid in its motion — depends solely on a coordinate *normal* to the velocity field. This in turn means that the motion should take place along very nearly equipotential lines, a feature not unlikely, in wiev of the accelerations being so small.

II) « Normal Fluid » in the Film.

a) Static case. To investigate this case the writer has studied the behaviour of a perfect Bose-Einstein gas of material particles [i.e. the excitons (1) (6)] under « laminar » conditions of volume, the smaller dimension t being no longer much larger than $h(8\pi\mu T)^{-\frac{1}{2}}$.

The problem is simple as far as the (Helmholtz) free energy is concerned and recalls the analogous one for rotating molecules at low temperature (7). The following result is found for the free energy per particle (8)

$$(7) \qquad F_{\text{lam}} - F_{\text{bulk}} = -kT \ln\left(1 - \frac{g}{t}\right) = kT\left(\frac{g}{t} + \frac{g^2}{t^2} + \ldots\right), \quad g = \frac{h}{(8\pi\mu kT)^{\frac{1}{2}}}.$$

Any effect of this kind gives small terms $\bar{\epsilon}$ [eq. (4)], which however are important in determining the form of the film. Their effect is to bring the exponent in (3) to values between $-\frac{1}{3}$ and $-\frac{1}{2}$ in better agreement with experiment.

b) Motion of the normal fluid. Although it may perhaps prove not so simple to work it out quantitatively, the model sets a clear difference between the superfluid and the normal fluid as regards the motion in the film. Indeed, whereas the motion of the former is completely adiabatic (for velocities below the critical) the same cannot be true for the latter. In any adiabatic displacement, the wavelenghts [of phonons or of states (1) with $\boldsymbol{K} \neq 0$] would have to change continuosly according to the thickness of the film, and with them the energy. To avoid this, changes in the quantum numbers — i.e. transitions — would have to take place and this can be done only at a rate fixed by the values of the corresponding matrix elements. This suggests also that whenever there is superfluid in non-vanishing concentration, *this alone* will move, the normal fluid forming at the expense of the superfluid while thermal equilibrium is re established with the surroundings.

A fuller account of the present work will be published later.

(6) A similar behaviour is not expected for phonons, since their number is not a constant.

(7) See for instance TER HAAR: *Elements of Statistical Mechanics* (New York, 1954), p. 62.

(8) In addition there should be a similar but smaller effect, due to a slight increase of the average density.

Coefficiente di anelasticità nei getti dei raggi cosmici.

G. Bertolino
Istituto di Fisica dell'Università - Torino

(ricevuto il 12 Ottobre 1955)

In un precedente lavoro [1] si è studiato il valore del coefficiente di anelasticità nei getti, considerato come rapporto fra l'energia totale dei mesoni prodotti e l'energia totale, nel sistema del baricentro, delle particelle primarie che vengono a collisione, dando origine al getto stesso. La formula impiegata, basata sull'angolo limite ϑ_L del getto, porta in alcuni casi a valori del coefficiente di anelasticità superiori all'unità.

Allo scopo di eliminare questi valori del coefficiente di anelasticità, che chiameremo « anomali », si è ristudiato il problema, su una base statistica più larga, comprendente anche eventi trovati e misurati nell'Istituto di Fisica Nucleare dell'Università di Padova, dei quali ho potuto servirmi. Si è osservato che i getti con coefficiente di anelasticità anomalo hanno una distribuzione angolare affatto particolare, colle tracce esterne eccezionalmente allargate rispetto alle tracce che costituiscono la parte centrale del getto. Quest'allargamento delle tracce esterne può essere spiegato se si suppone che, al fenomeno primario — collisione nucleone-nucleone —, si sovrappongano dei fenomeni secondari, nello stesso nucleo cui appartiene il nucleone urtato, come scattering dei mesoni formati entro il nucleo, formazione di mesoni secondari per urto dei nucleoni o mesoni provenienti dall'urto primario contro un altro nucleone. Tutti questi fenomeni secondari daranno come risultato un allargamento del getto.

È ovvio che, volendo calcolare l'energia ed il coefficiente di anelasticità del getto, i valori angolari misurati nel getto da introdurre nei calcoli dovranno essere scelti in modo da prescindere, possibilmente, da questi fenomeni secondari. Questa considerazione ha particolare importanza nel calcolo del coefficiente di anelasticità, in quanto il calcolo del coefficiente stesso si basa sull'angolo limite ϑ_L, vale a dire sull'angolo massimo formato nel sistema del laboratorio da una traccia del getto, quale si origina nella collisione nucleone-nucleone, coll'asse del getto.

Nel presente lavoro si propone di ristudiare il coefficiente di anelasticità con un criterio che cerca di eliminare i fenomeni secondari, escludendo dal getto, nei casi nei quali si presentino le distri-

[1] G. Bertolino e D. Pescetti: *Nuovo Cimento*, **12**, 630 (1954).

buzioni angolari alle quali si è prima accennato, le tracce estreme. Come criterio generale, si escludono dai getti le tracce più esterne, a partire da quella il cui angolo coll'asse del getto è pari ad almeno 1.5 volte l'angolo formato dalla traccia precedente, sempre coll'asse del getto.

In pratica, su 59 getti studiati con 516 tracce complessive, si sono escluse 78 tracce. L'angolo medio delle tracce dei getti considerati risulta pari a 14° circa; il valore medio dell'angolo formato dalle tracce escluse coll'asse risulta pari a 60° circa. È interessante anche considerare il valore medio dell'angolo formato dall'ultima traccia della quale si è tenuto conto, coll'asse del getto, nel caso di getti (40 getti) nei quali si sono escluse le tracce estreme: questo valore medio è pari circa a 27° e, confrontato col valore medio dell'angolo formato dalle tracce escluse coll'asse del getto — 60° —, mette in evidenza l'esistenza di un'effettiva discontinuità nella distribuzione angolare dei getti osservati.

Calcolando il coefficiente di anelasticità dei getti, dopo introdotto come valore di ϑ_L l'angolo corrispondente alla traccia estrema considerata, non si riscontrano più valori del coefficiente di anelasticità superiori all'unità. I coefficienti di anelasticità danno come valore medio

$$K = 0.46 \pm 0.21$$

Mantenendo la distinzione dei getti fatta in un precedente lavoro [1], sulla traccia di altri autori [2,3], troviamo

$$\text{Zona A} \qquad K = 0.52 \pm 0.21$$

$$\text{Zona B} \qquad K = 0.18 \pm 0.12$$

I getti della zona B, la cui energia totale è più elevata dell'energia dei getti della zona A con identico numero di tracce, presentano coefficiente di anelasticità minore; la ragione del valore percentualmente più elevato dello scarto quadratico medio per i getti della zona B, si deve riportare al numero minore di getti della zona B (11 complessivamente) rispetto al numero di getti della zona A (48 complessivamente).

Da calcoli che verranno in seguito pubblicati, si è potuto concludere che esiste ancora una relazione, approssimativamente lineare, fra l'energia totale liberata nella collisione nucleone-nucleone ed il numero di mesoni prodotti. Questa relazione, nel campo a cui si estendono le misure, porta ad un valore dell'energia praticamente costante per ogni nucleone prodotto (nel limite degli errori).

* * *

Ringrazio vivamente il Prof. Rostagni ed il Prof. Dallaporta per avere messo a mia disposizione gli eventi analizzati nell'Istituto di Fisica Nucleare, Sezione di Padova. Ringrazio il Prof. Wataghin per il costante interesse a questo lavoro e per la discussione dei risultati.

(2) C. Dilworth, S. J. Goldsack, T. F. Hoang e L. Scarsi: *Compt. Rend.*, **236**, 1551 (1953).

(3) T. F. Hoang: *Journ. de Phys.*, **14**, 395 (1953).

Su una semplice deduzione delle equazioni di Low dal formalismo di Lehmann - Symanzik - Zimmermann.

F. Duimio, P. Gulmanelli e A. Scotti

Istituto di Scienze Fisiche dell'Università - Milano
Istituto Nazionale di Fisica Nucleare - Sezione di Milano

(ricevuto il 18 Ottobre 1955)

Nel quadro di recenti tentativi [1,5] di trattazione della teoria quantistica dei campi nella rappresentazione di Heisenberg, hanno particolare interesse, anche dal lato applicativo [6], le equazioni integrali non-lineari ottenute da Low [7].

Ci proponiamo di mostrare come tali equazioni siano direttamente deducibili dallo schema sviluppato da Lehmann, Symanzik, Zimmermann [8], nel quale, sulla base delle sole ipotesi di invarianza, causalità e assegnazione delle condizioni asintotiche, viene ricavato un sistema generale di equazioni per i prodotti cronologicamente ordinati di operatori di Heisenberg.

Con una semplice estensione del formalismo di LSZ atto a comprendere, insieme a un campo mesonico φ, un campo nucleonico [5-9], si possono definire i seguenti operatori:

$$(1)\qquad \begin{cases} \varphi^{f\alpha}(t) = i\displaystyle\int_{x_0=t} \left\{ \varphi(x) \frac{\partial f_\lambda(x)}{\partial x_0} - f_\alpha(x) \frac{\partial \varphi(x)}{\partial x_0} \right\} \mathrm{d}^3x \,, \\ \psi^{g\alpha}(t) = \displaystyle\int_{x_0=t} \psi \beta \bar{g}^c_\alpha \, \mathrm{d}^3x \,, \\ \bar{\psi}^{g\alpha}(t) = \displaystyle\int_{x_0=t} \bar{\psi} \beta g_\alpha \, \mathrm{d}^3x \,. \end{cases}$$

(1) C. N. Yang e D. Feldman: *Phys. Rev.*, **79**, 972 (1950).
(2) G. Källen: *Helv. Phys. Acta*, **26**, 755 (1953).
(3) P. T. Matthews e A. Salam: *Proc. Roy. Soc.*, **221** A, 128 (1954).
(4) K. Nishijima: *Proc. Theor. Phys.*, **12**, 279 (1954).
(5) S. S. Schweber: *Nuovo Cimento*, **2**, 397 (1955).
(6) F. Low e S. Chew: *Phys. Rev.*, in corso di pubblicazione.
(7) F. Low: *Phys. Rev.*, **97**, 1392 (1955).
(8) H. Lehmann, E. Symanzik e W. Zimmermann: *Nuovo Cimento*, **1**, 205 (1955).
(9) S. S. Schweber: *Nuovo Cimento*, **2**, 173 (1955).

Definizioni analoghe valgono per i campi φ_{in}, φ_{out}, ψ_{in} e ψ_{out}.

Le funzioni f_α e g_α sono soluzioni a frequenza positiva rispettivamente delle equazioni libere di Klein-Gordon e di Dirac, soddisfacenti alle relazioni di ortonormalità

$$(2)\qquad \begin{cases} -i\int\left\{f_\alpha \frac{\partial f_\beta^*}{\partial x_0} - f_\beta^* \frac{\partial f_\alpha}{\partial x_0}\right\} \mathrm{d}^3x = \delta_{\alpha\beta}\,, \\ \int g_\alpha^* g_\beta \,\mathrm{d}^3x = \delta_{\alpha\beta}\,. \end{cases}$$

Negli sviluppi successivi utilizzeremo le soluzioni d'onda piana

$$f^{\alpha_k}(x) = (\Sigma k_0)^{-\frac{1}{2}} \exp\,[ikx], \qquad g^{\alpha_p} = w(p) \exp\,[ikx]\,.$$

Lo stato generale di n nucleoni, n antinucleoni e k mesoni incidenti si potrà scrivere:

$$(3)\quad \Psi_{\text{in}}(n, m, k) = (n!m!k!)^{-\frac{1}{2}}\, \bar{\psi}_{\text{in}}^{g\alpha_1} \ldots \bar{\psi}_{\text{in}}^{g\alpha_n} \psi_{\text{in}}^{g\alpha_1} \ldots \psi_{\text{in}}^{g\alpha_m} \varphi_{\text{in}}^{f\alpha_1} \ldots \varphi_{\text{in}}^{f\alpha_k} \Psi_0 \quad \text{con } \Psi_0 \equiv \text{vuoto vero.}$$

L'elemento di matrice S per lo scattering mesone-nucleone sarà dato da

$$(4)\qquad (p'q' \,|S\,| pq) = (\bar{\psi}_{\text{out}}^{p'} \varphi_{\text{out}}^{q'} \Psi_0,\ \bar{\psi}_{\text{in}}^{p} \varphi_{\text{in}}^{q} \Psi_0)\,.$$

Utilizzando le formule di riduzione rispetto alle sole variabili mesoniche (che pertanto coincidono con quelle date in LSZ), otteniamo:

$$(5)\qquad (p'q' \,|S\,| pq) = -\iint (\Box_x - \mu^2)(\Box_y - \mu^2)\{\bar{\psi}_{\text{out}}^{p'} \Psi_0,\ T(\varphi(x)\,\varphi(y))\bar{\psi}_{\text{in}}^{p} \Psi_0\} \cdot \cdot (4q_0 q_0')^{-\frac{1}{2}} \exp\,[iqx] \exp\,[-iq'y]\,\mathrm{d}x\,\mathrm{d}y\,,$$

$$(6)\qquad (p'q' \,|S\,| pq) = -i\int (\Box_x - \mu^2)(\bar{\psi}_{\text{out}}^{p'} \varphi_{\text{out}}^{q'} \Psi_0,\, \varphi(x) \bar{\psi}_{\text{in}}^{p} \Psi_0) \cdot (2q_0)^{-\frac{1}{2}} \exp\,[iqx]\,\mathrm{d}x\,.$$

Precisando ora l'interazione, che in LSZ è del tutto indeterminata, assumeremo

$$(7)\qquad (\Box - \mu^2)\varphi(x) = j(x)\,,$$

con (*)

$$(8)\qquad j(x) = ig\bar{\psi}(x)\gamma_5\psi(x) + \lambda\varphi^3(x) - \delta\mu^2\varphi(x)\,.$$

Facendo uso della [3,4]

$$(9)\qquad (\Box_x - \mu^2)T(\varphi(x)\,AB\,\ldots) = T((\Box_x - \mu^2)\varphi(x)\,AB\,\ldots) + i\frac{\delta}{\delta\varphi(x)}\,T(AB\,\ldots)\,,$$

(*) Notiamo qui che già Cini e Fubini [*Nuovo Cimento*, **2**, 860 (1955) e precedenti note], utilizzando alcuni risultati di LSZ avevano sviluppato considerazioni che permettevano di ottenere le equazioni di Low ed altri interessanti risultati, nell'ipotesi più restrittiva della linearità dell'hamiltoniana di interazione rispetto al campo mesonico.

con $AB \ldots$, generici operatori di campo, dalla (5) otteniamo:

$$(10) \qquad (p'q' \mid S \mid pq) = -\iint \left(\bar{\psi}^{p'}_{\text{out}}\Psi_0, \left[T(j(x), j(y)) + 3i\lambda\delta(x-y)\varphi^2(x)\right]\bar{\psi}^{p}_{\text{in}}\Psi_0\right) \cdot$$

$$\cdot (4q_0q'_0)^{-\frac{1}{2}} \exp[iqx] \exp[-iq'y]\,\mathrm{d}x\,\mathrm{d}y\,,$$

che coincide con la (1.11) di Low (*).

È essenziale nella derivazione della (10) l'ipotesi esplicitamente assunta sia da Low sia da LSZ che l'impulso finale q' del mesone sia diverso dall'impulso iniziale q.

La formula (6) esprime, come in Low, la relazione tra la quantità

$$(11) \qquad \left(\bar{\psi}^{p'}_{\text{out}}\varphi^{q'}_{\text{out}}\Psi_0,\ j(x)\bar{\psi}^{p}_{\text{in}}\Psi_0\right),$$

e la matrice S.

Per la quantità (11) si ha, sempre con l'uso delle formule di riduzione:

$$(12) \qquad \left(\bar{\psi}^{p'}_{\text{out}}\varphi^{q'}_{\text{out}}\Psi_0,\ j(x)\bar{\psi}^{p}_{\text{in}}\Psi_0\right) =$$

$$= -i\int (\Box_y - \mu^2)\left(\bar{\psi}^{p'}_{\text{out}}\Psi_0,\ T(j(x), \varphi(y))\bar{\psi}^{p}_{\text{in}}\Psi_0\right)(2q'_0)^{-\frac{1}{2}} \exp[-iq'y]\,\mathrm{d}y =$$

$$= -i\int \left(\bar{\psi}^{p'}_{\text{out}}\Psi_0, \left[T(j(x), j(y)) + 3i\lambda\delta(x-y)\varphi^2(y)\right]\bar{\psi}^{p}_{\text{in}}\Psi_0\right)(2q_0q'_0)^{-\frac{1}{2}} \exp[iqx] \exp[-iq'y]\,\mathrm{d}x\,\mathrm{d}y,$$

che, nell'approssimazione a un solo mesone e zero coppie, si riduce a un'equazione integrale non-lineare per la grandezza (11).

È possibile ottenere facilmente relazioni analoghe alle (12) che intercedono tra quantità di tipo più generale, ad esempio

$$\left(\bar{\psi}^{p'}_{\text{out}}\varphi^{q'}_{\text{out}}\varphi^{q''}_{\text{out}}\Psi_0,\ j(x)\bar{\psi}^{p}_{\text{in}}\Psi_0\right) =$$

$$= -i\int (\Box_y - \mu^2)\left\{\bar{\psi}^{p'}_{\text{out}}\varphi^{q''}_{\text{out}}\Psi_0,\ T(j(x), \varphi(y))\bar{\psi}^{p}_{\text{in}}\Psi_0\right\}(2q'_0)^{-\frac{1}{2}} \exp[-iq'y]\,\mathrm{d}y =$$

$$= -i\iint (\Box_y - \mu^2)(\Box_z - \mu^2)\left(\bar{\psi}^{p'}_{\text{out}}\Psi_0,\ T(j(x), \varphi(y)\varphi(z))\bar{\psi}^{p}_{\text{in}}\Psi_0\right) \cdot$$

$$\cdot (4q_0q'_0)^{-\frac{1}{2}} \exp[-iq'y] \exp[-iq''z]\,\mathrm{d}y\,\mathrm{d}z\,.$$

Ringraziamo il Prof. P. Caldirola per il gentile interessamento.

(*) Alla stessa equazione partendo da diversi punti di vista erano giunti M. L. Goldberger [*Phys. Rev.*, **97**, 508 (1955) e Schweber (5)].

A Neutron Detection Method to be Used with Pulse Accelerators.

F. Ferrero, R. Malvano and C. Tribuno

Istituto Nazionale di Fisica Nucleare - Sezione di Torino

(ricevuto il 30 Ottobre 1955)

In the present paper we describe a method of neutron detection that we are now using in experiments on photoneutron angular distribution, and we point out its principal advantages over other detection systems which may be employed in the same circumstances [1,2].

The method is based on the detection of the β-rays produced in the decaying

$$^{104}\mathrm{Rh} \xrightarrow[42\ \mathrm{s}]{\beta^-} {}^{104}\mathrm{Pd} \qquad (E_{\beta\ \max} = 2.6\ \mathrm{MeV})$$

following the capture of epithermal and fast neutrons—slowed down by a suitable thickness of paraffin—by a thin foil of ^{103}Rh, according to the slow neutron reaction:

$$^{103}\mathrm{Rh} + \mathrm{n} \rightarrow {}^{104}\mathrm{Rh} \qquad (E_\mathrm{n} \leqslant 1.4\ \mathrm{eV}).$$

This type of neutron detector has roughly the same sensitivity for neutrons from a few keV to 4-5 MeV.

Detectors very similar to ours were used recently by G. A. Price [3]. In his experiments, however, in order to measure the β activity of the irradiated Rh foil, he switches, after a definitive irradiation time, the neutron sensible material, from the irradiation place on to a thin mica-window G.M. counting apparatus. In our case, on the contrary, we decided, in order to get better statistics and reproducibility of the measurements, to count the β-activity during the long time interval (~ 20000 μs) between each X-ray pulse that, in our B.B.C. 31 MeV betatron, lasts for no more then 10 μs.

We can, therefore, record the activity for reasonably long time intervals, although we must wait some thousand μs in order that all brief γ-activities from any excited nucleus in (γ, n), (γ, p), (n, p), (n, γ) reactions cease completely; we avoid furthermore to record the γ-rays produced eventually by electrons lost during the acceleration cicle of the betatron. An electronic gate, synchronized to the betatron expansion pulses, (whose frequency is 50 Hz) paralises the counting apparatus for ~ 5000 μs partly before and after each pulse.

The geometrical dimensions of the apparatus are similar to the ones suggested by G. A. Price. The 0.7 g/cm² Rh foil is placed around a thin glass wall beta counter (35 mg/cm²). The system is embedded in paraffin and closed in a 1 mm thick Cd cylinder. Everything is surrounded, except for the front face,

(1) A. O. Hanson and J. L. McKibben: *Phis, Rev.*, **72**, 673 (1947).

(2) J. Halpern, A. K. Mann and R. Nathans: *Rev. Sc. Instr.*, **23**, 678 (1952).

(3) G. A. Price: *Phys. Rev.*, **93**, 1279 (1954).

by a $40 \times 40 \times 40$ cm^3 block of paraffin.

A conventional cathode follower allows to transfer the G.M. pulses from the irradiation room on to the various electronic devices some 20 m distant.

The neutrons produced directly by the accelerator in the walls, screens and collimators, are slowed down by the external paraffin block and captured by the Cd sheet. Those coming instead from the front face, pass through the 74 mm hole in the paraffin external block, are slowed down by the paraffin inside the Cd cylinder and partly are captured by the Rh foil.

We outline in the following the advantages that may be obtained measuring the β-activity between each X-ray pulse compared with the usual method of counting the β-rays after a definite irradiation time t.

The number of active nuclei obtained at the end of that time is:

$$(1) \qquad N_t = \frac{R}{\lambda}(1 - e^{-\lambda t}),$$

being R the production rate and λ the decaying constant.

Relation (1) holds naturally only when the irradiation source is constant during all the time t.

On the other hand, our betatron produces only a pulsed X-ray beam and therefore, being the neutron flux in the (γ, n) reaction not constant, the activity obtained after a definite time $t = \alpha T \gg 1/\lambda$ becomes:

$$(2) \quad N_t = A e^{-\lambda T} \frac{1 - e^{-(\alpha-1)\lambda T}}{1 - e^{-\lambda T}} \simeq \frac{R}{\lambda} \cdot \frac{\tau}{T} = \frac{1}{2\,000} \frac{R}{\lambda},$$

where $A = R/\lambda(1 - e^{-\lambda\tau})$,

T = period between each pulse,

τ = lenght of the X-ray pulse (10 μs),

α = number of pulses during the irradiation time.

The total β-activity that may be recorded is therefore much less than the one obtainable in the case of continuous sources and the relative statistic may result rather poor.

If, on the contrary, we measure the same β-activity between each X-ray beam pulse, the number of counted β-rays is given by:

$$(3) \qquad N_t = A(1 - e^{-\lambda T_c})\, e^{-\lambda(T - T_c)} \cdot \sum_{n=0}^{\alpha} (\alpha - n) e^{-n\lambda T} \simeq \frac{R}{\lambda} \cdot \frac{T_c}{T} \cdot e^{-\lambda(T - T_c)} \cdot \left(\frac{t}{T} - \frac{1}{\lambda T}\right); \qquad \text{for } \alpha T \gg \frac{1}{\lambda},$$

T_c being the counting time interval between each pulse: *this number*, as we may observe in (3), *increases linearly with the time t.*

We measured for comparison, the activity after a definite irradiation time (3 min) in two different ways:

a) for 5 min beginning after 30 s from the starting of the irradiation time;

b) for 2 min beginning after 30 s from end of the irradiation time (without electronic gate).

The results are the following:

	a	*b*
with Pb scatterer	5200	840
without Pb scatterer . .	2 900	490

LIBRI RICEVUTI E RECENSIONI

A. PINCIROLI – *Tubi elettronici*; Ruata Editrice, Torino pp. 265; £ 3800.

Questo libro, come avverte l'Autore nella prefazione alla seconda edizione, deriva da una precedente edizione litografata, che riuniva le lezioni tenute dallo stesso nel corso di « Tubi elettronici » nel Politecnico di Torino.

È dunque un libro scritto e pubblicato essenzialmente per gli studenti e, in un paese come il nostro ove tali libri sono molto rari, l'iniziativa e il necessario sforzo dell'Autore e dell'Editore non possono essere considerati altro che con lode. Invero è noto a tutti quanto sia utile conservare nella vita i testi sui quali si sono compiuti i propri studi e quanto a ciò siano poco adatte le dispense, che per la loro veste editoriale reggono materialmente a mala pena al logorio necessario alla preparazione di un esame.

Il libro del Pinciroli si divide in due parti: la prima, dedicata allo studio del tubo elettronico, la seconda allo studio delle reti che contengono tubi elettronici.

La prima parte si apre con un capitolo dedicato alla cosiddetta fisica del tubo elettronico, cioè allo studio del moto di un elettrone in un campo elettrostatico assegnato. Un paragrafo, inoltre, è dedicato allo studio delle correnti ioniche ed elettroniche nei tubi a gas ed un altro ai fenomeni di emissione di elettroni dai metalli. Nel secondo e terzo capitolo di questa parte è data una descrizione dei modelli di tubo realizzati nella pratica e delle loro caratteristiche di funzionamento.

Occorre dire che questi due ultimi capitoli, specialmente se confrontati con il primo, tenuto tutto in un tono abbastanza elevato, appaiono eccessivamente sbrigativi; inoltre in essi non si fa quasi mai uso delle nozioni generali ricavate nel primo. Chi ha pratica d'insegnamento sa bene che il dare agli studenti dapprima le nozioni più generali e spesso più astratte e poi utilizzarle esclusivamente per dei casi concreti del tutto banali o non utilizzarle affatto, è un costume alquanto diffuso. Tuttavia è facile osservare come questo modo di porgere le questioni finisce quasi sempre per dare al giovane un senso di disagio e spesso di sfiducia nell'utilità di possedere nozioni di carattere generale, conducendolo a ritenere lo studio di tali nozioni un inutile e faticoso esercizio piuttosto che la via per entrare in possesso di strumenti più potenti veramente utili per la soluzione di tutte le questioni particolari.

La seconda parte contiene un breve capitolo introduttivo seguito da un secondo ove si analizzano i casi in cui il tubo elettronico si comporta come un sistema lineare, da un altro dedicato agli oscillatori e, infine, da un ultimo nel quale si studiano i casi in cui il tubo

elettronico deve essere considerato come un sistema non lineare.

Questa seconda parte è indubbiamente compilata con molta chiarezza e benchè in essa venga fatto largo uso di metodi astratti, come quello delle matrici, la sua lettura non lascia perplessità. Peraltro non risulta ben chiaro quale sia la base culturale che l'Autore presuppone nei lettori.

Il volume viene presentato con una veste tipografica molto dignitosa che forse ha sensibilmente inciso sul prezzo col quale l'opera è messa in commercio.

E. PANCINI

J. R. PARTINGTON – *An Advanced Treatise on Physical Chemistry*; 5 volumi. Ediz. Longmans Green & C., London.

Il quinto volume dell'opera del PARTINGTON, recentemente pubblicato, completa il programma che egli stesso si era proposto e forma, con i primi quattro, un grande trattato di consultazione, scritto da un professore emerito della Università di Londra che ha personalmente apportato un notevole contributo alla Chimica Fisica.

L'aggettivo « advanced » incluso nel titolo sta ad indicare, secondo l'Autore, che il libro ha per scopo principale quello di dare informazioni a coloro che le cercano e non quello di servire come testo di studio. Possiamo aggiungere da parte nostra che la trattazione approfondita, anche dal punto di vista matematico, e la straordinaria ricchezza di fonti bibliografiche, giustificano ancor più il nome di « Trattato Superiore di Chimica Fisica » e dànno al lettore una sicura garanzia di completezza e precisione.

Come l'Autore stesso afferma nella prefazione al primo volume, il testo è scritto « un po' alla tedesca », cioè fa prevalere l'esigenza della completezza su quella della semplicità di linea logica, per evitare il pericolo, non infrequente in certe moderne pubblicazioni, di incorrere in eccessive semplificazioni, ingiustificate parzialità o ristrettezza di punti di vista. Naturalmente un trattato scritto con questo criterio richiede, da parte del lettore, un maggiore sforzo di inquadramento, ma, per quanto riguarda l'opera del PARTINGTON, è sempre evidente il profondo lavoro di riordinamento e di valutazione critica da parte dell'Autore, che fa di questi volumi ben più di una semplice raccolta di notizie e di dati.

L'impostazione generale del lavoro pone l'accento prevalentemente sugli aspetti sperimentali e pratici della materia: la teoria, che pure è largamente svolta, è sempre destinata a fornire una spiegazione dei fatti e una guida per la ricerca, piuttosto che mostrata nei suoi aspetti puramente matematici e speculativi.

La necessaria trattazione matematica raggiunge, come si è detto, in molte parti difficoltà di ordine superiore, ma è costante preoccupazione dell'Autore fornire al lettore nel libro stesso tutti gli strumenti di cui può aver bisogno; lo scopo viene raggiunto mediante l'inserzione nel testo di interi capitoli di carattere esclusivamente matematico.

Un'interessante caratteristica di questo trattato è quella di contenere, accanto alle relazioni dedotte dalla teoria, un gran numero di formule empiriche o semiempiriche ed una grande ricchezza di dati quantitativi, di straordinaria utilità per chi cerchi la soluzione di problemi concreti. Non manca per ogni argomento una breve introduzione storica, di cui l'Autore sembra giustamente compiacersi, non volendo lasciare nella dimenticanza le opere dei primi ricercatori, anche se al giorno d'oggi appaiono completamente superate.

Ogni volume è completato da un accurato indice alfabetico e contiene anche un indice analitico abbastanza dettagliato (ad eccezione del 1° volume). Vi

sono liste dei simboli e delle abbreviazioni usate nelle citazioni dei periodici; si sente invece la mancanza di un completo indice dei nomi e di un indice generale. La bibliografia che, come si è detto, è straordinariamente ricca, è riportata in nota e sparsa in tutte le pagine del libro. Sarebbe quindi assai difficile stabilire se e dove sia citata l'opera di un determinato Autore.

Per quanto riguarda la natura della materia svolta, ricordiamo che l'Autore dichiara che il suo libro tratta soltanto di chimica fisica e non di fisico-chimica nè di fisica matematica, intendendo con ciò restringere il campo alla definizione di « Chimica Fisica » data da VAN'T HOFF: « la scienza dedicata alla introduzione di conoscenze fisiche nella chimica, con lo scopo di essere utile a quest'ultima ».

I primi tre volumi trattano successivamente delle proprietà fondamentali dei gas, dei liquidi e dei solidi, dopo alcuni capitoli di carattere generale e introduttivo sulla termodinamica, la teoria cinetica dei gas, la meccanica statistica, la teoria dei quanti, la meccanica ondulatoria, ecc.

Gli ultimi due volumi sono dedicati all'ottica fisico-chimica e allo studio dei dielettrici; alcuni degli argomenti svolti sembrano appartenere alla fisica pura, alla elettrologia e talvolta all'elettrotecnica, ma è chiaro che essi servono a completare il quadro generale.

L'ottica fisico-chimica svolta nel quarto volume comprende capitoli sulla rifrazione, polarizzazione, attività ottica, teoria elettromagnetica della luce, rotazione magnetica, piezoelettricità e piroelettricità.

Il quinto volume continua lo svolgimento dell'ottica affrontando un argomento di straordinario interesse teorico e pratico, lo studio cioè degli spettri molecolari in connessione con la struttura delle molecole. Il modo con cui questi argomenti sono svolti vuol essere « una via di mezzo tra l'esposizione eccessivamente semplificata che si trova in alcuni libri e quella assai dettagliata dai testi scritti per specialisti, forse troppo difficile per studenti di chimica, ma che pure omette un'adeguata considerazione di alcune parti della teoria ».

Sembra a noi che in questo capitolo il PARTINGTON lasci un po' in ombra la parte sperimentale e pratica per dare maggior risalto alla teoria che viene trattata nei suoi vari aspetti in modo notevolmente approfondito.

La sezione undecima, sulle proprietà dei dielettrici è divisa in tre parti: misura di costante dielettrica, momenti dipolari, materiali iperelettrici (ferroelettrici). In questi capitoli anche gli aspetti sperimentali e pratici appaiono largamente considerati.

Osservando il trattato nel suo insieme ci si rende conto di essere di fronte ad un lavoro gigantesco e davvero sorprendente quando si pensi che è opera di un solo Autore; le 3200 pagine complessive contengono un'immensa mole di informazione, coordinata, documentata e messa alla portata di ogni studioso benchè provenga talvolta da fonti difficilmente reperibili.

F. A. LEVI

M. E. ROSE – *Multiple Fields*. John Wiley & Sons, New York; Chapman & Hall, London, 1955, pag. VIII+99.

Lo sviluppo in serie di multipoli è, come è noto, uno strumento necessario per trattare svariati problemi della fisica, ed in particolare della fisica nucleare: in particolare la teoria delle transizioni β e γ, la conversione interna, problemi di correlazioni angolari; più in generale tutti i problemi che trovano la loro naturale descrizione in una rappresentazione caratterizzata dagli autostati del momento angolare.

Il libro del ROSE è una esposizione

sistematica della teoria dei campi di multipolo, con particolare riferimento al campo elettromagnetico.

Sebbene la teoria venga sviluppata a partire dalle proprietà di trasformazione per rotazione, non si fa praticamente uso in questo libro del linguaggio della teoria dei gruppi; la trattazione è più estesa di quella contenuta nell'appendice del libro di BLATT e WEISSKOPF, *Theoretical Nuclear Physics*, ma fondamentalmente dello stesso tipo; la maggiore estensione permette tuttavia una esposizione più chiara e completa. Negli ultimi due capitoli la teoria viene applicata ai problemi menzionati della conversione interna e dell'emissione γ in nuclei.

In definitiva la trattazione del ROSE è adeguata al problema, e lo studio del libro è senz'altro utile a tutti coloro che desiderano impadronirsi di questo necessario strumento di calcolo.

G. MORPURGO

Direttore responsabile: G. POLVANI Tipografia Compositori - Bologna

Questo fascicolo è stato licenziato dai torchi il 27-X-1955